Structure/function studies of C1q interactions with Ig-like receptors : implications in immune tolerance and autoimmunity

Guillaume Fouët

THÈSE

Pour obtenir le grade de

DOCTEUR DE L'UNIVERSITÉ GRENOBLE ALPES

Spécialité : **Biologie structurale et nanobiologie**

Arrêté ministériel : 25 mai 2016

Présentée par

Guillaume FOUËT

Thèse dirigée par **Véronique ROSSI-ECHINARD,**
Et codirigée par **Christine GABORIAUD**

Préparée au sein de **l'Institut de Biologie Structurale**
Dans **l'École Doctorale Chimie et Sciences du Vivant**

Structure/function studies of C1q interactions with Ig-like receptors: implications in immune tolerance and autoimmunity

Etude structure/fonction des interactions de C1q avec des récepteurs de type Immunoglobuline impliqués dans la tolérance immune et l'auto-immunité

Thèse soutenue publiquement le **23 février 2021,**
Devant le jury composé de :

Monsieur Franck FIESCHI
Professeur des Universités, Université Grenoble Alpes, Président

Madame Catherine MOALI
Directeur de Recherche, Université Claude Bernard Lyon I, Rapporteure

Madame Lubka ROUMENINA
Chargé de Recherche, Sorbonne Université, Rapporteure

Monsieur Yves DELNESTE
Directeur de Recherche, Université d'Angers, Examinateur

Madame Véronique ROSSI-ECHINARD
Maître de Conférences, Université Grenoble Alpes, Directrice de thèse

Madame Christine GABORIAUD
Directeur de Recherche, Université Grenoble Alpes, Co-directrice de thèse

ACKNOWLEDGMENTS

Mes remerciements vont tout d'abord à mes directrices de thèse Véronique Rossi et Christine Gaboriaud. Un immense merci pour votre soutien, votre disponibilité, votre patience mais avant tout pour la confiance que vous m'avez accordée. Vous avez su me laisser réaliser ce travail avec beaucoup de liberté tout en gardant un œil attentif sur l'avancement du projet.

Véronique, je te suis extrêmement reconnaissant de m'avoir accepté en stage lorsque je n'étais alors qu'un étudiant de L1, de m'avoir renouvelé ta confiance en master pour ensuite enchainer avec cette thèse. Grâce à toi, j'ai pu faire connaissance avec C1q et découvrir les joies de l'enzymo, des ELISA et de la SPR. Tu as grandement contribué à me donner l'envie d'embrasser la voie de la biochimie et d'aller jusqu'au bout avec cette thèse.

Christine, je te remercie pour tout le temps que tu m'as consacré durant ces trois année (et avant !). Je garderai un très bon souvenir de nos sessions synchrotron où tu m'as toujours accompagné dans la joie et la bonne humeur ! Tes photos de paysages et animaux sauvages vont me manquer mais j'espère en recevoir par mail régulièrement 😉.

Je remercie vivement Nicole Thielens pour sa bienveillance et toute l'attention qu'elle a pu porter sur mes travaux tout au long de ces trois années de thèse.

Merci à toutes les trois pour vos conseils avisés, votre bonne humeur et votre positivité qui ont été de précieux alliés pendant les trois années qui viennent de s'écouler.

Je remercie les membres de mon jury de thèse pour avoir accepté de consacrer de leur temps afin d'évaluer mon travail, Catherine Moali et Lubka Roumenina en tant que rapporteures et Yves Delneste et Franck Fieschi en tant qu'examinateurs.

Je tiens également à remercier affectueusement l'ensemble des membres du groupe IRPAS sans qui cette expérience n'aurait pas été aussi enrichissante.

Un immense merci à Isabelle pour tout ce qu'elle a fait pour moi, que ce soit pour me montrer et m'apprendre la culture cellulaire et la purification de C1q ou pour son aide pour réaliser les dernières manips pendant que j'étais coincé par la rédaction. J'ai passé de très bons moments au labo à tes côtés, merci pour ça.

De la même façon, je remercie Anne pour son aide au lancement du projet pour me montrer la production en bactéries. Merci pour ta bonne humeur permanente qui m'a permis de garder le sourire tout au long de ces trois années.

Merci à Samy, avec qui j'ai partagé le bureau pendant presque la totalité de ma thèse. Il s'en sera dit des choses dans ce bureau… Merci pour les moments que l'on a vécu ensembles (au labo et en dehors), qui m'ont permis de décompresser et relativiser quand les manips ne marchaient pas.

Je remercie également Jean-Baptiste, Jean-Philippe, Pascale, Philippe, Jean-Pierre et Catherine. Vous m'avez tous accueilli avec beaucoup de gentillesse et je garde de très bons souvenir avec chacun d'entre vous.

Merci à Caroline, Aline, Katharina, Daphna, Winnie, Joanna, Michel et Luca avec qui j'ai eu l'occasion d'interagir pour diverses manips.

Merci à nos voisins les SAGAG, Romain, Evelyne, Rabia, Rebekka, Yoann et Thibault pour les bons moments que l'on a passés ensemble au café le matin.

Merci à tous mes amis de l'IBS, notamment Rana, Rida, Lynda, Kévin, Anna, Anne-So, Kaiyao, Thibault, Anas, Wiktor, Laura, Quentin, Elena, Benoit, Romain, Alister, François, Faustine, Amélie et Romy (pour ne citer qu'eux…).

Merci à mes collègues doctorants élus, Marie, Elise, Clarisse, Simon, Baptiste, Damien, Richard et Ghadir. J'ai apprécié cette aventure à vos côtés et je vous souhaite bon courage pour la fin ! Je remercie aussi le bureau et les membres de Globalps pour les supers moments qu'on a passés ensemble lors des nombreux évènements de l'asso.

Je remercie infiniment mes amis Machon et Matthieu, qui ont toujours été là pour me supporter et m'encourager pendant ces trois années. Merci également à Julie, Sarah, Sandrine, Marjo, Antho, Kévin, Cédric et Pierrick pour les nombreux moments que nous avons partagés et qui m'ont permis de déconnecter du labo.

Enfin, un simple merci ne serait pas suffisant pour exprimer ma profonde gratitude envers ma famille et plus particulièrement mes parents qui ont toujours cru en moi et m'ont sans cesse poussé vers l'avant. Merci de m'avoir soutenu pendant ces trois années de thèse, surtout quand la pression était au plus haut !

A ceux que j'aurais oubliés, un grand merci pour ces trois années !

ABBREVIATIONS

ACAMPs – Apoptotic cells-associated molecular patterns

C1-inh – C1 inhibitor

$C1r_2s_2$ – Tetramer of C1r and C1s proteases

C4BP – C4b binding protein

CCP – Complement control protein module

CLR – Collagen-like regions of C1q

CR – Cysteine-rich complement-type repeat

CR1 – Complement receptor 1

CR2 – Complement receptor 2

CR3 – Complement receptor 3

CR4 – Complement receptor 4

CRT – Calreticulin

DAF – Decay accelerating factor

DNA – Deoxyribonucleic acid

ECM – Extracellular matrix

EGF – Epidermal growth factor

ESRF – European synchrotron radiation facility

FACIT – Fibril-associated collagens with interrupted triple helices

FB – Factor B

FD – Factor D

FH – Factor H

FI – Factor I

GAPDH – Glyceraldehyde phosphate dehydrogenase

GAS6 – Growth arrest-specific protein 6

GPI – Glycosylphosphatidylinositol

GPVI – Glycoprotein VI

GR – Globular regions of C1q

HIV – Human immunodeficiency virus

HMGB1 – High-mobility group box 1

HRP – Horseradish peroxidase

HTLV – Human T-lymphotropic virus

IC – Immune complex

IFN – Interferon

IgG – Immunoglobulin G

Ig-like – Immunoglobulin-like

IgM – Immunoglobulin M

IL – Interleukin

IPTG – Isopropyl β-D-thiogalactopyranoside

ITIM – Immune receptor tyrosine-based inhibitory motif

LAIR – Leukocyte-associated immunoglobulin-like receptor

LHR – Long homologous repeat

LILRB1 – Leukocyte immunoglobulin-like receptor B1

LPS – Lipopolysaccharide

LRC – Leukocyte receptor complex

LRP1 – Low density lipoprotein receptor-related protein 1

MAC – Membrane attack complex

MASP – MBL-associated serine protease

MBL – Mannose-binding lectin

MCP – Membrane cofactor protein

MCP-1 – monocyte chemoattractant protein 1

MERTK – Myeloid-epithelial- reproductive tyrosine kinase

nc2 – Non-collagenous domain 2

NF-κB – Nuclear factor- κB

NK – Natural killer

NMR – Nuclear magnetic resonance

OSCAR – Osteoclast-associated receptor

PAMPs – Pathogen-associated molecular patterns

PCR – Polymerase chain reaction

PDB – Protein data bank

pDC – Plasmacytoid dendritic cells

PEG – Polyethylene glycol

PS – Phosphatidyl serine

PTX3 – Pentraxin 3

RA – Rheumatoid arthritis

RAGE – Receptor for advanced glycation end-products

RMSD – Root-mean square deviation

SAXS – Small angle X-ray scattering

SEC-MALLS – Size-exclusion chromatography-multi angle laser light scattering

SLE – Systemic lupus erythematosus

SP-A – Surfactant protein A

SP-D – Surfactant protein D

SPR – Surface plasmon resonance

SR-F1 – Class F scavenger receptor 1

TLR – Toll-like receptor

VWF – Von Willebrand factor

WT – Wild type

TABLE OF CONTENTS

TABLE OF FIGURES

LIST OF TABLES

INTRODUCTION

I. The complement system

1 General overview

The complement system represents a major component of innate immunity and constitutes the fast and efficient first-line host defense against pathogens (Walport 2001a, b). Initially, the complement system was discovered in the 19th century as a heat-labile serum component essential for antibody-mediated bactericidal activity. It is a very efficient part of innate immunity able to opsonize pathogens and apoptotic cells surfaces for their elimination through phagocytosis or lysis. This complex system consists in more than 40 soluble and membrane proteins. The main producer of the circulating soluble complement proteins is the liver (hepatocytes) but local production of complement proteins can be performed by epithelial, endothelial and immune cells (Zhou et al. 2016; Lubbers et al. 2017). Complement proteins are produced in an inactive form and require proteolytic cleavage for activation. After initial activation, they are able to associate and sequentially activate each other, triggering the local generation of fragments playing an important role in pathogens elimination through inflammatory signaling, opsonization and lysis (Merle et al. 2015b).

2 The complement cascade

The complement cascade can be initiated by three different pathways of activation: the classical, lectin and alternative pathways. Each activation pathway leads to the assembly of an enzymatic complex, the C3 convertase able to cleave the central component C3 that leads to the activation of a common amplification loop and terminal pathway (Figure 1).

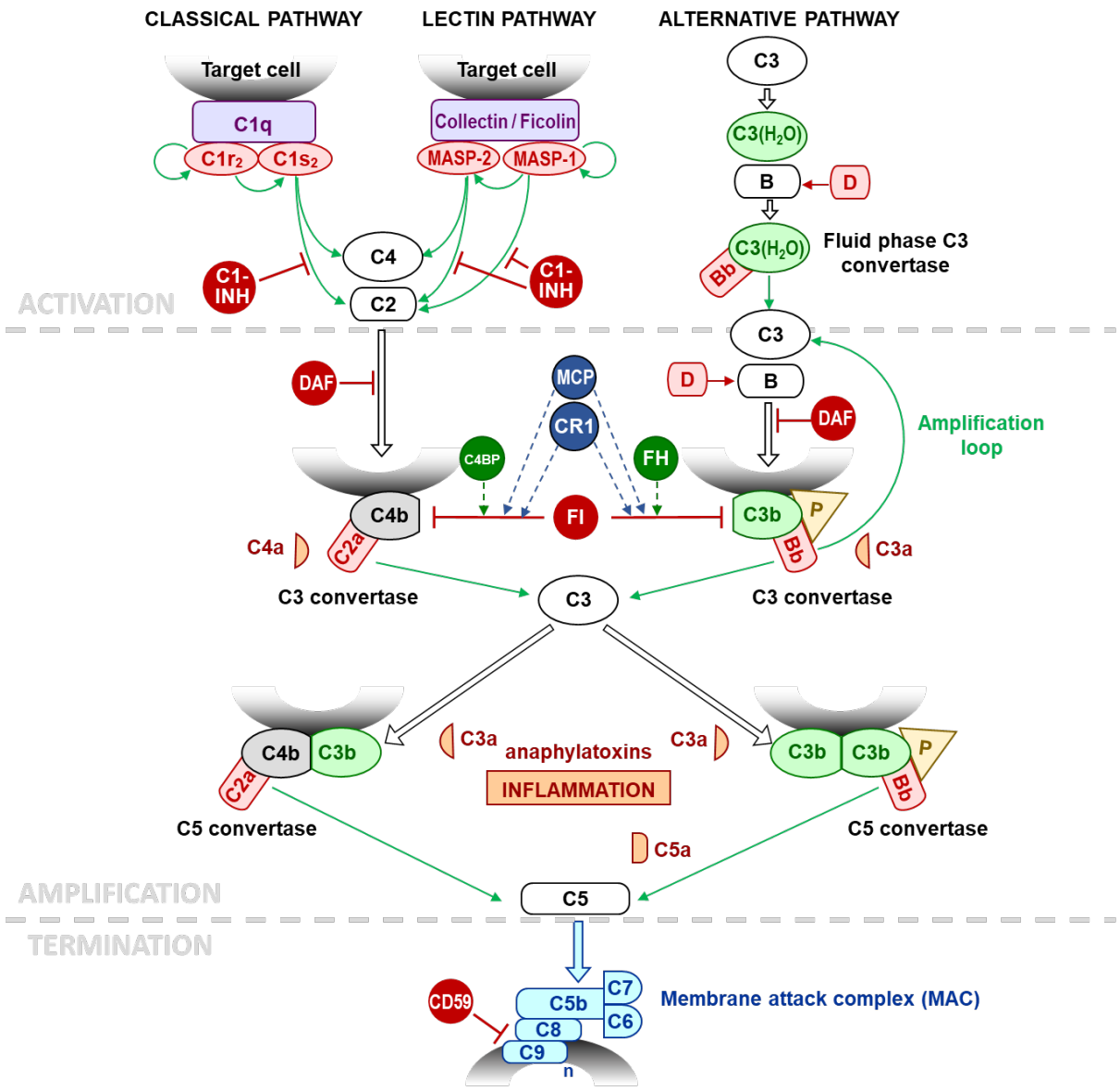

Figure 1: Overview of the complement cascade. *The complement activation can be initiated by the three different classical, lectin or alternative pathways. Each pathway results in the formation of the C3 convertase. The C3 convertase then cleaves the C3 component, generating the C3b that associates with the C3 convertase and forms the C5 convertase, responsible for C5 cleavage. The C5b fragment initiates the formation of the membrane attack complex (MAC). Multiple steps of the complement cascade are under the regulation of soluble or membrane proteins. The C1r/C1s/MASPs proteases are inhibited by the C1-inhibitor (C1-INH) serpin. The convertases are regulated by the factor I (FI) and its cofactors: C4b-binding protein (C4BP), factor H (FH), decay accelerating factor (DAF), complement receptor 1 (CR1), membrane cofactor protein (MCP). Assembly of the MAC is prevented by CD59. Enzymatic activities are represented with green arrows. (Adapted from Defendi et al. 2020).*

3 The three complement activation pathways

3.1 The classical and lectin pathways

Both the classical and lectin activation pathways rely on the recognition of pathogens or altered-self components triggering the activation of proteases and initiating the complement cascade by the cleavage of C4 and C2 complement components, releasing C4a, C4b, C2a and C2b fragments. Association of C4b and C2a fragments generates the membrane-associated

enzymatic assembly [C4bC2a] called C3 convertase that cleaves the C3 component into C3a and C3b (Figure 1). The classical and lectin pathways are initiated by homologous multimolecular complexes composed of a recognition molecule that belongs to the soluble defense collagens family associated with their cognate complement protease.

The soluble defense collagens are a family of proteins gathering complement C1q, mannose-binding lectin (MBL), the collectin CL-LK, ficolins and pulmonary surfactant proteins A and D (SP-A and SP-D). They all contain a C-terminal recognition domain preceded by a collagen-like triple-helical region (Fraser and Tenner 2008; Casals et al. 2019).

Soluble defense collagens are pattern recognition molecules of the innate immune system playing an important role in the sensing and elimination of pathogens and cell debris. Indeed, the defense collagens can recognize pathogens or apoptotic cells-associated molecular patterns through their C-terminal domain and trigger efficient immune reactions such as complement activation, phagocytosis stimulation or immune cells activation (Figure 2) (Casals et al. 2019).

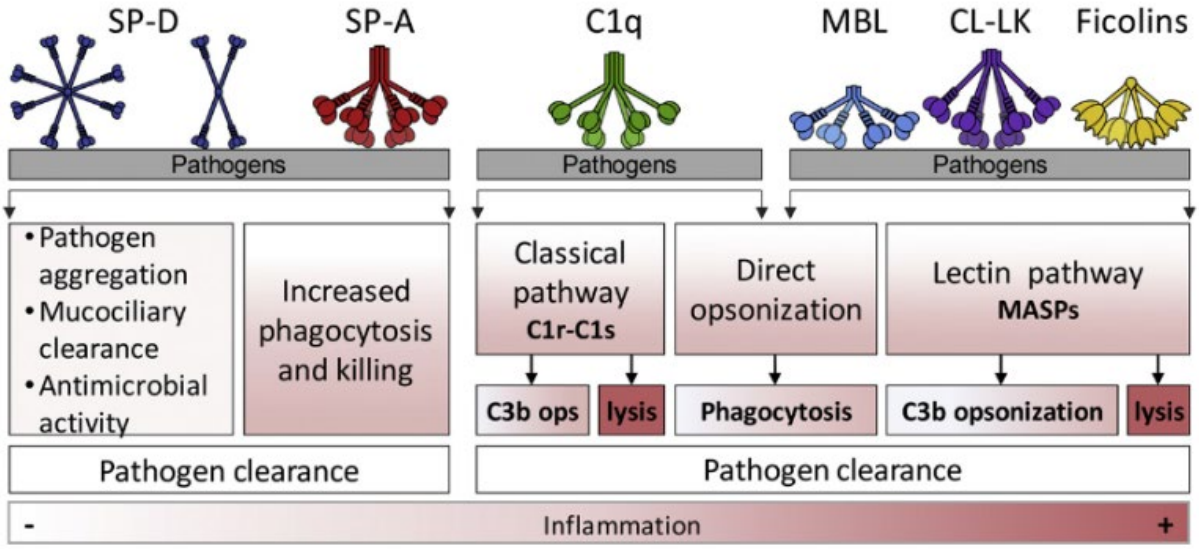

Figure 2: Mechanisms used by soluble defense collagens to respond to infection. *(Taken from Casals et al., 2019).*

The classical pathway recognition molecule is the defense collagen C1q, which is able to interact with antibodies (IgG and IgM) complexed with antigens, pentraxins, pathogen associated molecular patterns (PAMPs) and apoptotic cell associated molecular patterns (ACAMPs). C1q interaction with its ligands triggers the subsequent activation of its associated proteases within the C1 complex: C1r and C1s. Activated C1s then cleaves C4 and C2 components to generate the classical pathway C3 convertase (C4b2a) (Figure 1).

The lectin pathway can be initiated by several defense collagens: MBL, CL-K1, CL-LK and ficolins 1, 2 and 3, able to recognize glycoproteins and glycolipids presents on pathogens surfaces (Walport 2001a; Fujita 2002). Each of these defense collagens is associated with MASP-1 and -2 (MBL-associated serine protease 1 and 2). As for the classical pathway, the defense collagen interaction with its ligands induces the activation of MASP-1 and MASP-2, leading to the C4 and C2 components cleavage and the same C3 convertase as for the classical pathway (Figure 1).

3.2 The alternative pathway and amplification loop

The alternative pathway activation does not rely on pathogen recognition and subsequent proteolytic activity. Indeed, in the plasma, C3 component can spontaneously hydrolyze and generate the C3(H_2O) component which can bind to complement factor B (FB), a structural and functional homolog of C2. FB is then cleaved by factor D (FD), leading to the formation of the alternative fluid phase C3 convertase [C3(H_2O)Bb], able to cleave C3 into C3a and C3b fragments. In addition to the spontaneously produced C3b-like molecule, FB can bind to deposited C3b fragments on pathogens and generate the [C3bBb] alternative C3 convertase. This mechanism of C3 cleavage generating C3b fragments associating with FB and promoting further C3 cleavage leads to a strong complement activity and is called the complement amplification loop (Figure 1).

4 The terminal pathway

Each of the above-described pathway of complement activation leads to the formation of an enzymatic complex called C3 convertase, able to cleave C3 into C3a and C3b fragments. Thanks to the amplification loop, large amounts of C3 fragments can be produced even with a weak initial activation. Once the concentration of C3b deposition on the pathogen surface is high enough, the C3 convertase associates with additional C3b molecules and switches from C3 to C5 substrate specificity (Pangburn and Rawal 2002; Rawal and Pangburn 2003). The resulting C5 convertase then cleaves C5 into C5a and C5b fragments. C5b then sequentially associates with C6, C7, C8 and C9 on the target's membrane. Polymerization of C9 and association to the C5b-8 deposited complex leads to the formation of the final [C5b-9] membrane attack complex (MAC) which consists in a pore inserted in the target's membrane inducing cell lysis and death (Podack 1984; Tegla et al. 2011) (Figure 1).

In addition to cell lysis through the MAC formation, the complement system exhibits diverse biological functions like opsonization and inflammation properties. Indeed, complement

components fragments generated by the activation cascade are not exclusively involved in the terminal MAC formation. For example, C3a and C5a fragments, the by-products of C3 and C5 cleavage, are anaphylatoxins that interact with specific cell receptors, triggering important functions in immune cells recruitment, inflammatory signals generation and maturation of the adaptive immune system (Elsner et al. 1994a, b; Ehrengruber et al. 1994; Schraufstatter et al. 2002; Peng et al. 2009; Merle et al. 2015a). Moreover, complement component fragments deposited on a target surface can be directly recognized by immune cells receptors, thus enhancing targets clearance and phagocytosis. For example, after complement activation, target cells present both C3b and C4b fragments on their surface that can be recognized by several receptors on immune cells surfaces such as CR1, CR2, CR3 or CR4 (Ricklin et al. 2010).

5 Regulation of the complement system

The complement system is a very efficient weapon of innate immunity against pathogens and damaged tissues elimination but it can be very harmful for neighboring cells if the activation cascade is uncontrolled. This highlights the need for a tight regulation of the complement cascade. Such control is performed by several soluble and membrane regulators that operate at different levels of the cascade (Zipfel and Skerka 2009).

The most relevant way of regulation of early complement activation is the inactive proenzyme state of the initiating proteases that are activated only after target recognition by the defense collagens of the initiation complexes. The consecutive activation of the proteases leads to the initiation of the classical and lectin pathways. In addition, the serine protease activity of C1r, C1s and the MASPs is controlled by a soluble inhibitor: C1-inhibitor (C1-inh; SERPING1). C1-inh is a member of the serpin family of serine protease inhibitors that binds to the active site of its target protease and irreversibly blocks its enzymatic activity. This inhibitory process also induces the dissociation of the C1 complex (Sim et al. 1979; Davis et al. 2008). C1-inh is present in the serum at a 7-times higher concentration than the C1 complex, therefore preventing unsuitable activation of the C1-hosted proteases (137 µg/mL (C1-inh) versus 80 µg/mL (C1q); Schumaker et al. 1987).

The next level of regulation of the complement cascade occurs at the level of the central C3 and C5 convertases through several membrane and soluble proteins that inhibit their association. One of the principal regulators is factor I (FI), a soluble serine protease able to cleave C3b and C4b, thereby inducing the convertase inactivation. The activity of FI towards C3b and C4b fragments is dependent on various cofactors such as the soluble factor H (FH), the C4b-binding

protein (C4BP), the membrane complement receptor type 1 (CR1; CD35) or the membrane cofactor protein (MCP; CD46) (Whaley and Ruddy 1976; Fujita et al. 1978; Masaki et al. 1992). In addition, FI and FH also inhibit the alternative C3 and C5 convertases formation by competing with C3b for the binding to FB and C5. Moreover, decay accelerating factor (DAF; CD55), a membrane-associated regulatory protein, inhibits the association and enhances the dissociation of both C3 and C5 convertases (Hourcade et al. 2002).

Conversely to these regulators aiming at dissociating the protein complexes forming the C3 and C5 convertases, the properdin (also known as factor P) is the only positive regulator of the complement cascade. Indeed, properdin stabilizes the alternative C3 and C5 convertases by bridging the C3b and Bb fragments (Alcorlo et al. 2013).

The terminal pathway and formation of the membrane attack complex are also tightly regulated at different levels of control. The complement component C8 plays an important role in the MAC formation. Indeed, if C8 binds to [C5b-7] in the absence of a cell membrane, conformational changes occur and inhibit the pore formation (Nemerow et al. 1979). At another level, the MAC formation is regulated by the GPI-anchored CD59 which inhibits C9 binding to the [C5b-8] membrane complex, as well as C9 polymerization and final assembly of the membrane attack complex (Rollins and Sims 1990; Farkas et al. 2002). Finally, another regulation mechanism implies clusterin and vitronectin that capture the soluble [C5b-7], [C5b-8] and [C5b-9] complexes and prevent their binding to the membrane (Preissner et al. 1989; Tschopp et al. 1993; Hadders et al. 2012).

II. Focus on the C1q molecule (classical pathway)

1 Generalities

C1q is the molecule that activates the classical complement pathway after recognition of various molecular patterns associated with either pathogens or damaged tissues. As the majority of complement components, C1q is a circulating molecule and is present in the plasma at a concentration of around 80 µg/mL in physiological conditions (Reid 2018). However, C1q synthesis is not achieved by the hepatocytes but mostly by monocyte-derived cells and is under the control of various stimuli. For example, C1q production by macrophages and dendritic cells is upregulated by toll-like receptor (TLR) signaling induced by pathogen-associated lipopolysaccharide or lipoteichoic acid (Walker 1998; Baruah et al. 2006). In addition to these exogenous stimuli, C1q synthesis can be regulated by cytokines such as IL-1, IL-6 or IFN-γ (Walker 1998; Lu et al. 2008).

2 Structural and molecular organization of C1q

C1q is a multimeric protein and results from the assembly of 18 polypeptide chains of three different types: A, B and C. C1q chains assemble by 3 into 6 ABC heterotrimers, each containing an N-terminal collagen-like triple helical region of around 81 amino acids (CLR) and a C-terminal globular region of 135 residues (GR). These heterotrimers are maintained together through interchain non-covalent interactions and disulfide bonds between chains A-B and C-C. The N-terminal collagen-like region of each C1q chain contains the characteristic collagen Gly-X-Y repetitive sequence pattern where X is often a proline residue and Y a hydroxyproline. As for every collagen, C1q collagen region undergoes several post-translational modifications such as proline and lysine residues hydroxylation and hydroxylysine O-glycosylation (Reid 1979; Pflieger et al. 2010). Six C1q ABC trimers assemble via their N-terminal CLR into a fiber bundle that splits up at mid-length (due to imperfect collagen repeats) into 6 collagen triple-helices with C-terminal globular heads at their extremity (Reid 2018) (Figure 3).

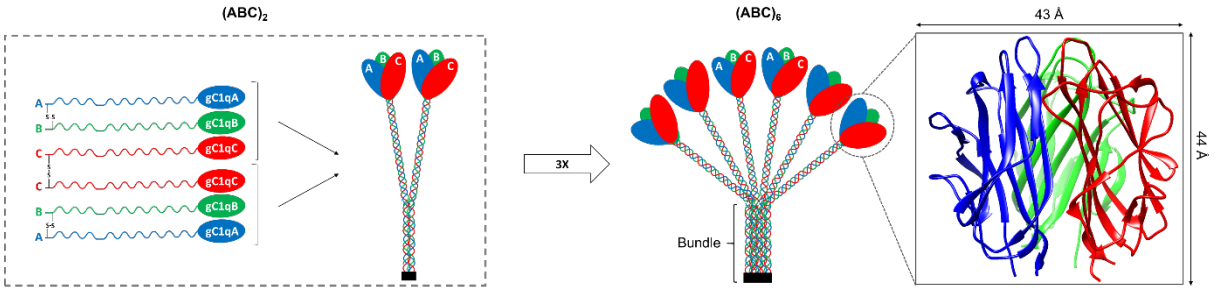

Figure 3: Schematic representation of C1q assembly. *The C1q molecule is assembled from 18 polypeptide chains of three different types (A, B and C) each containing an N-terminal collagen-like sequence and a C-terminal globular domain (gC1q). Six C1q chains assemble into the $(ABC)_2$ sub-unit that then trimerizes into the full-length $(ABC)_6$ C1q exhibiting its characteristic bouquet-like shape with six C-terminal globular regions (GR) linked together through six collagen-stems (CLR) assembled into an N-terminal bundle. The right panel shows the crystal structure of C1q GR (PDB code: 1PK6). (Taken from Fouët et al. 2020a; Article 1).*

These two different C1q regions have been studied thanks to limited proteolysis of the whole C1q purified from human serum. Indeed, digestion of C1q with pepsin results in isolated CLR whereas collagenase digestion of C1q generates the GR (Figure 4) (Reid 1976; Brodsky-Doyle et al. 1976; Hughes-Jones and Gardner 1979). Studies on both isolated CLR and GR revealed that they host distinct functions.

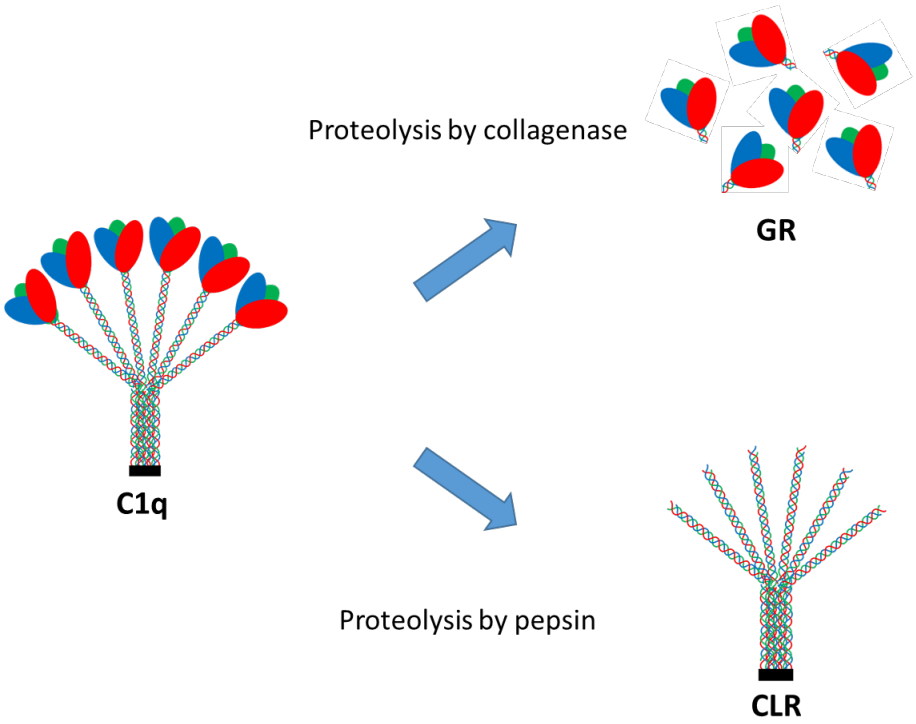

Figure 4: Generation of C1q GR and CLR fragments by limited proteolysis with collagenase and pepsin.

The globular regions of C1q are mostly responsible for the recognition of the multiple targets of C1q such as immunoglobulins, pathogens and apoptotic cells associated molecular patterns (reviewed in Kishore et al. 2004) (Table 1).

Targets	C1q interacting region	References
Endogenous ligands		
IgG/IgM	GR	(Gadjeva et al. 2008; Ugurlar et al. 2018; Sharp et al. 2019)
C-reactive protein	GR	(Kojouharova et al. 2004)
Pentraxin 3 (PTX3)	GR	(Nauta et al. 2003; Bally et al. 2019)
β-amyloid peptide	GR	(Tacnet-Delorme et al. 2001)
fucoidan	CLR	(Tissot et al. 2003)
DNA	GR/CLR	(Jiang et al. 1992)
Phosphatidylserine	GR	(Païdassi et al. 2008)
Annexins	?	(Leffler et al. 2010; Martin et al. 2012)
GAPDH	GR	(Terrasse et al. 2012)
Ceramide transporter proteins	GR	(Bode et al. 2014)
Pathogen-associated ligands		
Lipopolysaccharide (LPS)	GR	(Loos et al. 1990; Roumenina et al. 2008)
gp41 of HIV-1 gp21 of HTLV-1	GR	(Kojouharova et al. 2003)

Table 1: List of C1q targets (non-exhaustive). *The functional region of C1q involved in the target interaction and the associated references are indicated.*

The C1q CLR are involved in immune mechanisms through their interaction with the tetramer of C1r and C1s proteases or membrane receptors (Siegel and Schumaker 1983; Eggleton et al. 2000) (Table 2).

Soluble effectors and membrane receptors	C1q interacting region	References
$C1r_2s_2$	CLR	(Siegel and Schumaker 1983)
gC1qR (P33)	GR	(Ghebrehiwet et al. 1994)
cC1qR (calreticulin)	CLR/GR	(Païdassi et al. 2011)
CR1 (CD35)	CLR/GR	(Klickstein et al. 1997; Jacquet et al. 2018)
LRP1 (CD91)	CLR/GR	(Fouët et al. 2020b)
SR-F1	CLR	(Wicker-Planquart et al. 2020)
Integrin α2β1	CLR	(Zutter and Edelson 2007)
DC-SIGN	GR	(Pednekar et al. 2016)
LAIR-1 (CD305)	CLR	(Son et al. 2012)
LAIR-2 (CD306)	CLR	(Son et al. 2012)
RAGE	GR	(Ma et al. 2012; Son et al. 2016)
Siglec 3 (CD33)	GR	(Son et al. 2017)

Table 2: List of C1q receptors and soluble effectors (non-exhaustive). *The functional region of C1q involved in the receptor interaction and the associated references are indicated.*

3 Complement-associated functions of C1q

The initial and most studied function of C1q is its important role in the elimination of self- and non self-components via the activation of the classical complement pathway. In human serum, C1q is almost exclusively (90%) found associated with the $C1r_2s_2$ tetramer of C1r and C1s, forming the C1 complex.

In order to initiate the complement classical pathway, both C1r and C1s need to be activated by proteolytic cleavage of an arginine-isoleucine bond within the serine protease domain. Even if the exact mechanism underlying C1 activation still remains elusive, it is clearly established that

C1q binding to an activator surface induces C1r autolytic activation. Then, activated C1r cleaves and activates C1s that afterward cleaves C4 and C2, triggering formation of the classical C3 convertase and activation of downstream complement cascade (Gaboriaud et al. 2007).

Both C1r and C1s are serine proteases sharing the same modular architecture with the succession of CUB_1-EGF-CUB_2-CCP_1-CCP_2 modules followed by a C-terminal serine protease domain (Figure 5A) (Gaboriaud et al. 2014). C1r and C1s proteases assemble into a heterodimer via their CUB_1-EGF-CUB_2 modules in a head to tail fashion (Figure 5A). The Ca^{2+}-dependent assembly of $C1r_2s_2$ with C1q in the C1 complex is crucial for complement cascade initiation. Site-directed mutational studies on recombinant C1r, C1s and C1q allowed the precise identification of the C1q binding sites on each protease and the C1q residues involved in the interaction. On the protease C1r CUB_1 and CUB_2 respectively, E49/Y56/D102 and D226/D228/Y235/D273 residues are involved in the C1 complex formation. On C1s CUB_1 module the interaction implicates E45/D98 residues (Bally et al. 2009). The crystal structure of C1r and C1s dimers revealed the association of two C1r/C1s dimers with the two C1r copies in the center (Figure 5B) (Almitairi et al. 2018). On C1q side, the binding of $C1r_2s_2$ involved three lysine residues located in the collagen-like region of C1q: LysB61, LysC58 and LysA59, the latter in a lesser extent (Bally et al. 2013). In addition, a C1q variant containing the substitution of its glycine residue at position 63 in the B chain into a serine, was identified in a patient suffering from lupus and was shown to be unable to interact with the $C1r_2s_2$ tetramer (Roumenina et al. 2011).

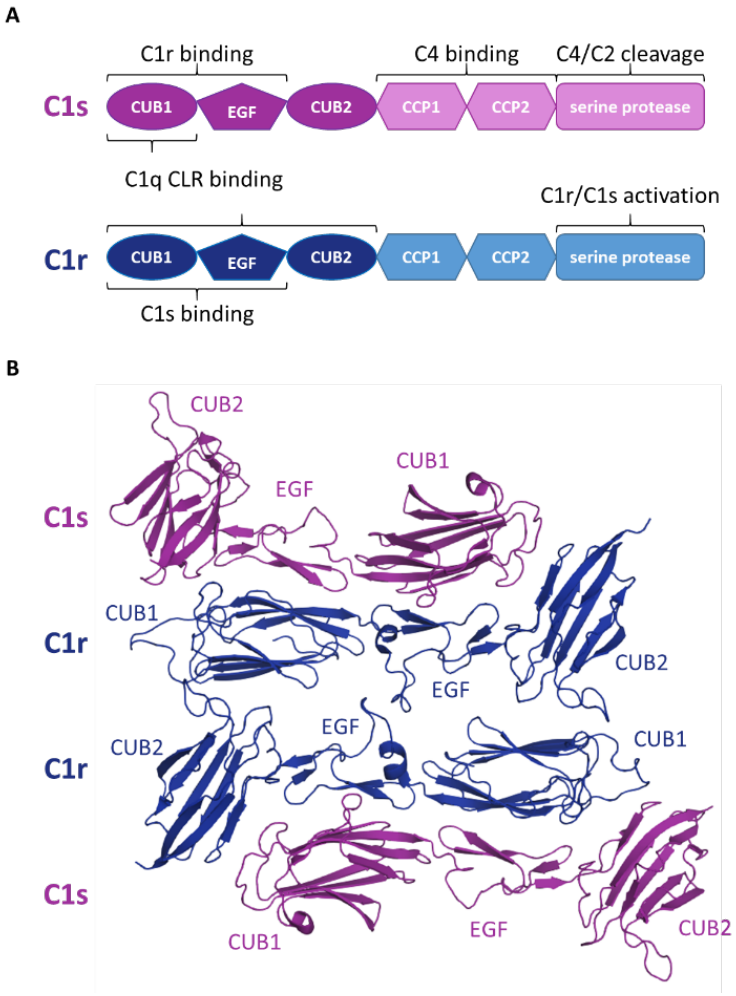

Figure 5: The C1r2s2 complex. *A. Schematic representation of the C1r and C1s modular organization.* ***B****. Crystal structure of the C1r and C1s CUB1-EGF-CUB2 domains forming the core of the* $C1r_2s_2$ *tetramer (PDB code: 6F1C).*

The identification of each partner binding sites coupled with the available structures of C1r and C1s led to the proposal of initial models for the C1 complex (Bally et al. 2009; Venkatraman Girija et al. 2013). Due to the intrinsic flexibility of the C1q molecule, poor structural information is available for the whole C1 complex. However, a recent cryoelectron tomography study provided structural insight into C1 bound to an IgM (Figure 6) (Sharp et al. 2019). Such model confirmed the arrangement of the $C1r_2s_2$ platform in the C1q collagen cone with the two C1r copies in the core of $C1r_2s_2$. However, the two C1r/C1s dimers are not as tightly packed as in the crystal structure (Figure 6).

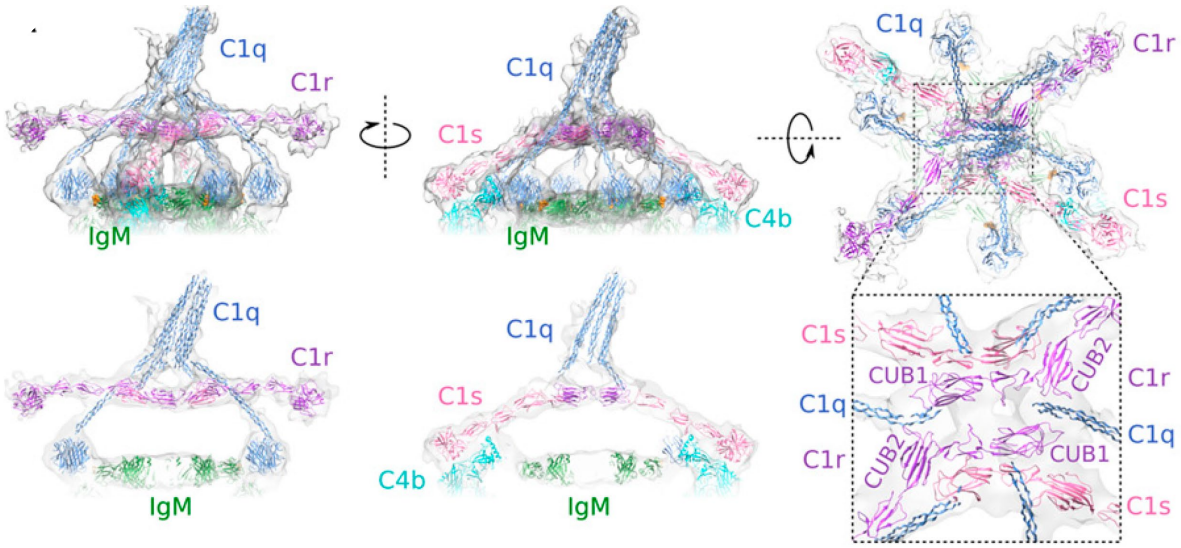

Figure 6: C1 binding to IgM platforms. *Model of C1q and $C1r_2s_2$ bound to an hexameric IgM showing the orientations of C1r and C1s within the C1 complex. Cryoelectron tomography snapshot of C1-mediated cleavage of C4 (Taken from Sharp et al., 2019).*

4 Receptors and complement-independent functions of C1q

C1q interacts with multiple ligands and receptors on a large range of cell types, providing to this molecule a wide variety of functions independent of complement activation (Nayak et al. 2012) (Tables 1 and 2). It is now well established that C1q mostly interacts with danger and "eat-me" signals through its GR while receptors on immune cells recognize C1q-opsonized target via C1q CLR (Eggleton et al. 2000; Gaboriaud et al. 2011) (Table 1). The C1q-mediated immune effector mechanisms will therefore depend on which immune cell senses C1q and which immune receptors are involved in the C1q recognition.

4.1 Involvement of C1q in apoptotic cells phagocytosis

These really distinct functions of C1q GR and CLR are even more evident for the recognition of apoptotic cells by C1q that engages specifically its globular regions (Navratil et al. 2001; Païdassi et al. 2008). Even if few immune receptors interact with the C1q GR, the major contribution is given by the C1q CLR, an interaction that generally results in the engulfment of C1q-labelled targets. C1q engagement in phagocytosis stimulation can be divided in three main mechanisms (Figure 7).

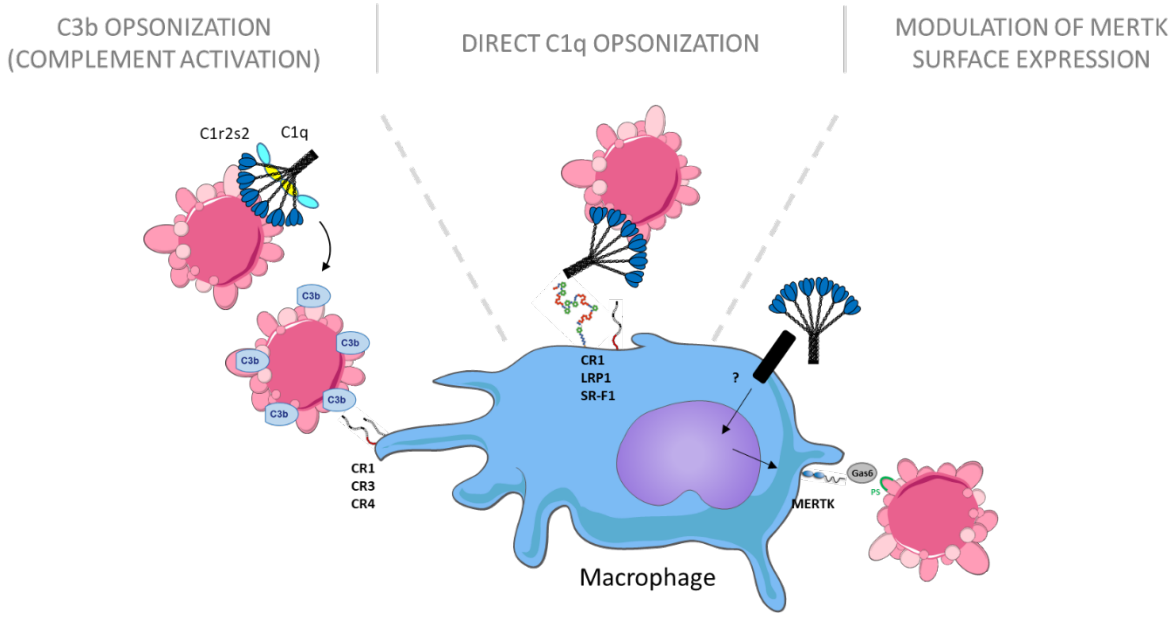

Figure 7: C1q involvement in apoptotic cell clearance. *C1q is involved in apoptotic cells (in pink) engulfment by macrophages (in blue) through three mechanisms. Left: C1q contributes to C3b opsonization generated by the classical complement pathway activation. Middle: C1q directly opsonizes the apoptotic cell for macrophage recognition. Right: C1q interaction with macrophage receptors increases phagocytic Mer tyrosine kinase (MERTK) and Gas6 expressions (Adapted from Galvan et al. 2012b).*

First, C1q is indirectly involved in the phagocytosis of pathogens and apoptotic cells through complement activation after recognition of the Fc region of immunoglobulins associated with antigens (immune complexes, IC) at the surface of target cells. Indeed, C1q-mediated complement activation leads to the deposition of C3b and C4b fragments on target's surface and triggers the engulfment through CR1, CR3 and CR4 (Fearon 1980; Mevorach et al. 1998).

Second, Galvan and colleagues showed that C1q binding to the surface of macrophages positively regulates the expression of several genes coding anti-inflammatory proteins involved in the clearance of apoptotic cells such as the Mer tyrosine kinase (MERTK) and its ligands Growth arrest-specific 6 (Gas6) and protein S (Galvan et al. 2012a). However, the mechanism and the macrophage receptors involved in this genes upregulation still remain elusive. A recent study suggests that the C1q-dependent increase of MERTK expression engages the alarmin HMGB1 and is mediated through two immunoglobulin (Ig)-like receptors RAGE (receptor for advanced glycation end-products) and LAIR-1 (leukocyte-associated immunoglobulin-like receptor 1) (Son et al. 2016).

Third, C1q globular regions are able to directly recognize pathogen- and apoptotic cells-associated molecular patterns such as LPS, lipid A, DNA or phosphatidyl serine (PS) (Table1). C1q can also interact through its CLR with several immune receptors involved in phagocytic functions such as CR1, LRP1 or SR-F1 (Table 2). Because of this dual recognition capacity,

C1q was suggested to act as an opsonin on its own, bridging targets to be eliminated and phagocytic cells.

- **Complement receptor 1 (CR1, CD35)** was initially described for its complement regulatory functions alone or in association with factor I (Fearon 1979; Iida and Nussenzweig 1981; Masaki et al. 1992). CR1 is a multimodular transmembrane receptor with an extracellular part composed of 30 CCP modules organized into 4 long homologous repeats (LHR) A, B, C and D. CR1 is involved in phagocytic mechanisms and is mainly engaged in the elimination of immune complexes and targets opsonized by the complement C3b and C4b fragments (Fearon 1980; Fearon et al. 1989). Surface plasmon resonance experiments reported the *in vitro* interaction of CR1 with the collagen-like region of C1q (Klickstein et al. 1997). Further studies showed that C1q interaction with CR1 enhances erythrocytes adhesion and the uptake of apoptotic cells by dendritic cells and macrophages (Tas et al. 1999; Nauta et al. 2004). During my PhD thesis, I was involved in the investigation of C1q interaction with CR1. Briefly, we demonstrated that C1q interacts with the CR1 CCP 24 and 25 modules in the long homologous repeat D, via its collagen-like regions (Article 3, Jacquet et al. 2018).
- **Low density lipoprotein receptor-related protein 1 (LRP1, CD91)** is a multimodular transmembrane receptor composed of the succession of multiple modules of three different types: β-propeller domains, EGF and CR modules. LRP1 is a scavenger receptor involved in the clearance of apoptotic cells, especially in association with another known C1q receptor: calreticulin (CRT). C1q was described as a ligand for LRP1, suggesting its involvement in LRP1-dependent apoptotic cells removal. This was confirmed in different studies showing that C1q is required for apoptotic cells removal through LRP1/CRT (Ogden et al. 2001; Vandivier et al. 2002). However, another study pointed out that the phagocytosis enhancing capacity of C1q does not engage LRP1 (Lillis et al. 2008). In order to address this question, I took part in the deciphering of C1q interaction with LRP1 that conducted to the identification of C1q collagen-like regions binding sites on LRP1 clusters II and IV (Article 4, Fouët et al. 2020).
- **Class F scavenger receptor 1 (SR-F1, also known as SCARF1)** is a multimodular transmembrane endocytic receptor composed of ten extracellular EGF repeats (Adachi et al. 1997). SR-F1 was initially described as a receptor for multiple non-self and endogenous ligands, therefore mediating a large range of physiological functions (Patten 2018). SR-F1 was reported to be an important actor of the C1q-dependent removal of apoptotic cells and as for LRP1, this process may require the formation of a multimolecular complex with CRT (Berwin et al. 2004; Païdassi et al. 2011; Ramirez-Ortiz et al. 2013; Wicker-Planquart et al. 2020).

4.2 Immune modulation

The elimination of apoptotic cells and immune complexes is a crucial process of immunity homeostasis and needs to be tightly controlled. Indeed, apoptotic cell phagocytosis has to be efficiently performed without inducing an excessive immune response against ingested autoantigens. Disruption of the silent immune complexes and apoptotic cells clearance is an important factor of chronic inflammation and autoimmune diseases onset such as systemic lupus erythematosus (SLE) (Pieterse and van der Vlag 2014; Tsai et al. 2017). As discussed above, C1q appears to play a substantial role in the removal of apoptotic cells. A previous study showed that C1q-deficient mice are prone to lupus-like disease development and carry excess of apoptotic bodies (Botto et al. 1998). Moreover, this hypothesis was supported by the strong association of genetic or acquired C1q deficiencies with SLE (Walport et al. 1998; Botto and Walport 2002). Botto's lab recently reported that aside from the C1q-mediated clearance of apoptotic cells, the main regulatory role of C1q is the modulation of CD8+ T-cells metabolism through its interaction with mitochondrial gC1qR (Ling et al. 2018).

In addition to its involvement in the enhancement of apoptotic cells phagocytosis, C1q was shown to exhibit regulatory properties on immune cells which is consistent with the establishment of a safe removal of self-components. Indeed, several studies report the anti-inflammatory influence of C1q on various immune cells such as macrophages, dendritic cells or microglial cells.

4.2.1 Modulation of cytokine synthesis

C1q alters the level and profile of cytokine synthesis as another way to reduce inflammation and maintain tolerance. Indeed, C1q fixation on peripheral blood monocytes was shown to inhibit the LPS-induced TLR activation signals with the suppression of the pro-inflammatory cytokines IL-1α and IL-1β expression and the stimulation of the anti-inflammatory IL-10 and the IL-1 receptor antagonist (Fraser et al. 2006). Moreover, Nauta et al. showed that apoptotic cells opsonized with C1q induced a cytokine response of dendritic cells with the increase of IL-6, IL-10 and TNF-α expression whereas no effect was observed for apoptotic cells alone (Nauta et al. 2004). This difference was suggested to be associated to different immune receptors such as LRP1, CR1 and calreticulin. Interestingly, C1q was shown to be able to modulate the cytokine profile secreted by endothelial cells. Namely, C1q binding to endothelial cells induces the increase of IL-8, IL-6 and MCP-1 expression (van den Berg et al. 1998). This study can be related to the one of Kang and colleagues who showed the modulation of cytokine expression

by the mannose-binding lectin (another defense collagen, homologous to C1q) on endothelial cells (Kang et al. 2007).

4.2.2 Dendritic, T and B-cells maturation and activation

Cytokines are powerful molecules important for the recruitment and maturation of immune cells at the site of inflammation. It is therefore not surprising that C1q mediates immune tolerance through the modulation of the dendritic cells functions. First, C1q was shown to possess chemotactic properties toward dendritic cells in order to recruit them at the site of inflammation (Vegh et al. 2006). Moreover, C1q was shown to induce dendritic cells with tolerogenic properties in several studies (Yamada et al. 2004; Castellano et al. 2004). However, C1q was also demonstrated to generate dendritic cells activation triggering IFNγ production by T cells (Csomor et al. 2007). The latter study is in agreement with previous studies of Botto's lab who showed that LPS injection in C1q-/- mice induced less IFNγ production by T-cells than wild-type mice in a dendritic cells dependent manner (Cutler et al. 1998; Baruah et al. 2009).

Furthermore, C1q was shown to be involved in the biology of B-cell. Indeed, C1q is able to bind to inactive and activated B lymphocytes to either stimulate IgG or IgM production (Young et al. 1991). In line with this study, C1q-/- mice present a reduced tolerance of B cell to autoantigens displayed by apoptotic cells (Ferry et al. 2007).

However, the above mentioned tolerogenic activities of C1q toward immune cells may certainly engage other specific immune receptors, through unclear mechanisms that await further investigations. Son and colleagues recently proposed receptors from the immunoglobulin (Ig)-like family to play a role in the maintenance of immune cells tolerance (Son et al. 2012, 2016, 2017; Son and Diamond 2015) (Figure 8). The interaction of C1q with these Ig-like receptors RAGE, CD33 and more specifically LAIR-1 is further described in the next section.

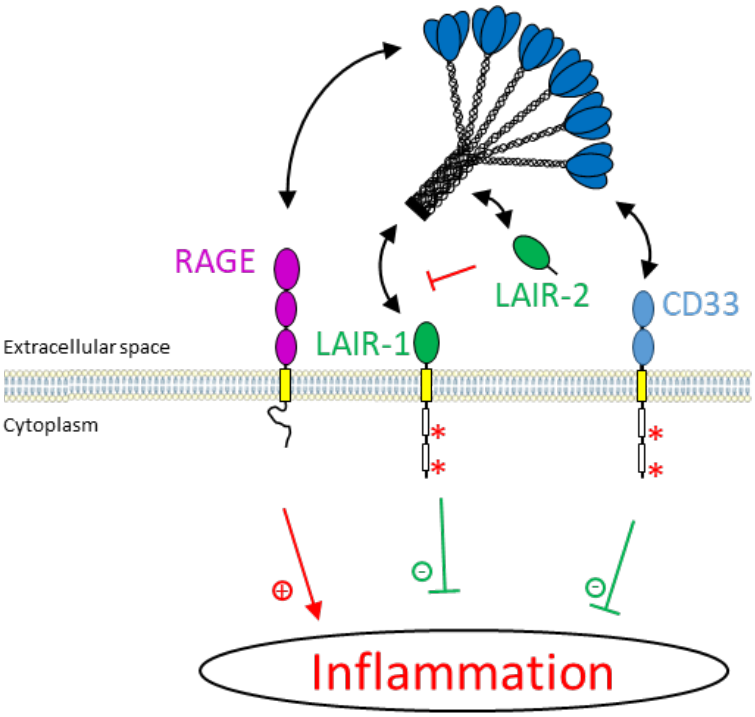

Figure 8: C1q interaction network with the immunoglobulin-like receptors. *C1q interaction with the immunoglobulin-like receptors RAGE, LAIR-1/2 and CD33 induces different inflammatory signals to modulate the immune response.*

III. LAIR-1

1 Generalities

Leukocyte-associated immunoglobulin-like recptor-1 (LAIR-1; CD305) was first identified and characterized in 1997 on human natural killer (NK) cells for its efficient inhibition of NK cells cytotoxicity after cross-linking by the DX26 antibody, suggesting that LAIR-1 is an immune inhibitory receptor. Further investigations revealed that LAIR-1 is expressed on a wide range of human immune cells such as NK cells, T cells, B cells, monocytes, neutrophils, basophils and mast cells (Meyaard et al. 1997, 1999; van der Vuurst de Vries et al. 1999; Saverino et al. 2002; Verbrugge et al. 2006; Florian et al. 2006; Jansen et al. 2007; Zhang et al. 2014). Molecular cloning and biochemical analyses demonstrated that LAIR-1 is a 32 kDa type I transmembrane receptor composed of an extracellular domain of 142 amino acids (aa), a transmembrane domain of 23 aa and an intracellular domain of 101 aa. LAIR-1 belongs to the immunoglobulin (Ig)-like superfamily with a single extracellular C2-type Ig-like domain containing one N-glycosylation site (Figure 9). LAIR-1 is structurally related to other Ig-like superfamily members localized to the leukocyte receptor complex (LRC) on human chromosome 19 (Barrow and Trowsdale 2008). Among these receptors, LAIR-2 (CD306) is a soluble homolog of LAIR-1 lacking the transmembrane and intracellular regions, with an Ig-like domain sharing 84% of sequence homology with the Ig-like domain of LAIR-1.

The cytoplasmic region of LAIR-1 contains two amino acids sequences corresponding to immune receptor tyrosine-based inhibitory motifs (ITIMs), which explains the immune inhibitory activity of LAIR-1 (Figure 9) (Meyaard et al. 1997). As for many receptors, intracellular ITIMs phosphorylation depends on LAIR-1 dimerization. The dimerization of LAIR-1 extracellular domains upon ligand binding results in the recruitment of intracellular Src homology 2-containing protein tyrosine phosphatases leading to a negative regulation of intracellular signaling associated with immune cell maturation, activation and differentiation (Meyaard et al. 1997; Xu et al. 2000; Sathish et al. 2001; Jin et al. 2018).

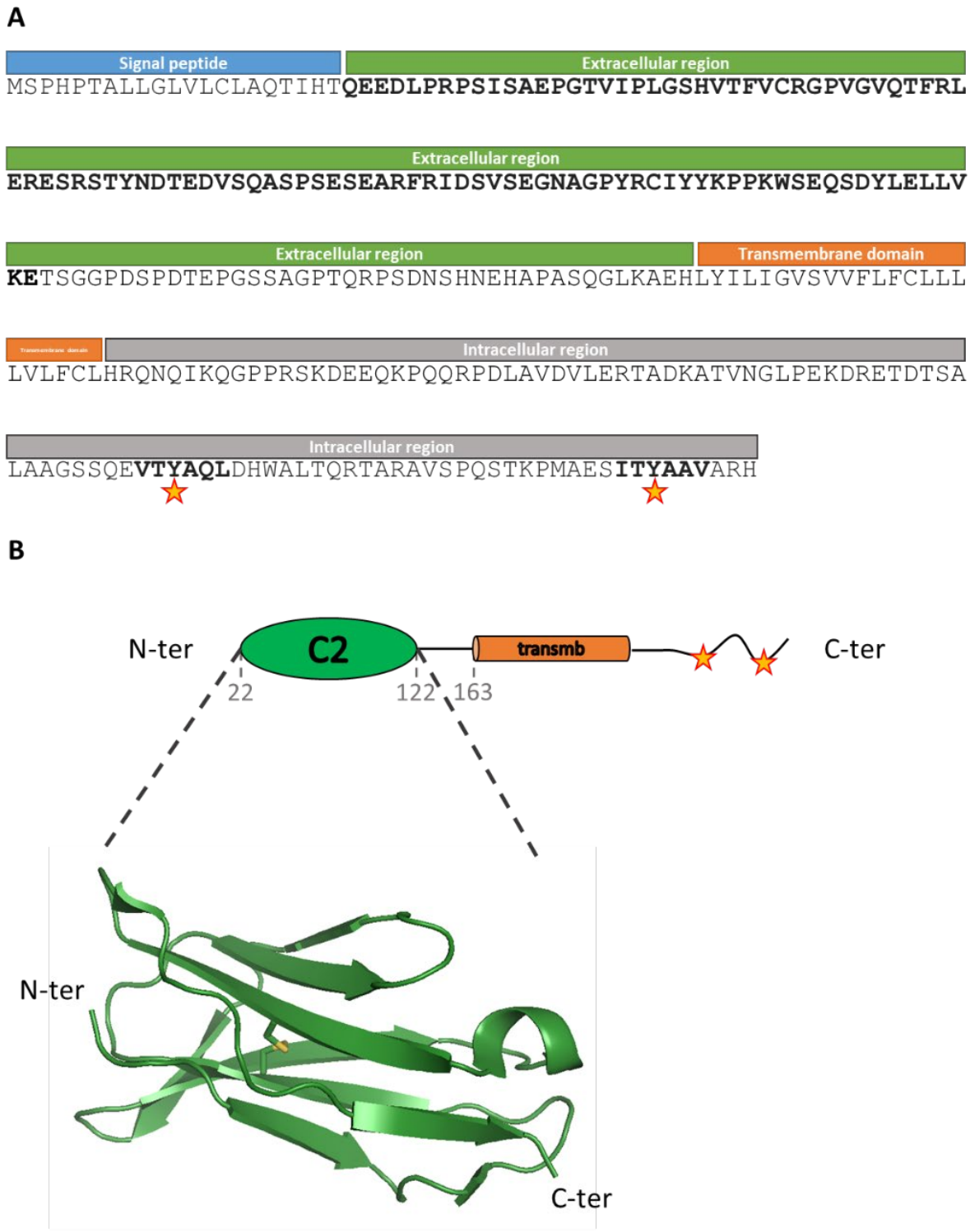

Figure 9: Structural organization of LAIR-1. ***A****. Amino acids sequence of human LAIR-1. Signal peptide, extracellular region, transmembrane domain and intracellular region sequences are labeled with blue, green, orange and grey rectangles, respectively. Phosporylated ITIM tyrosines are labeled with star icons and the extracellular Ig-like domain sequence is indicated in bold.* ***B****. Schematic representation of LAIR-1 with the crystal structure of LAIR-1 Ig-like domain (PDB code 3KGR) cartoon representation is shown in green. The stars represent intracellular phosphorylated tyrosine residues.*

2 LAIR-1: a collagen receptor

Collagens are the most abundant protein family in the human body and constitute up to 30% of the whole animal's proteins (Frantz et al. 2010). Up to now, 28 different collagen family members have been identified and numbered collagens type I to XXVIII. All members of the collagen family are homo- or hetero-trimers composed of three identical or different polypeptide chains (named α chains) and are characterized by the presence of at least one triple-helical domain (Figure 10). This particular structural assembly relies on the presence of repeating Gly-X-Y triplet in the sequence of each collagen chain, X residue is frequently a proline and Y a 4-hydroxyproline generated after post-translational modifications (Ricard-Blum 2011). Within the collagen triple-helical structure, the three collagen chains are not in phase but they are shifted, leading to a registering order with leading, middle and trailing chains (Figure 10).

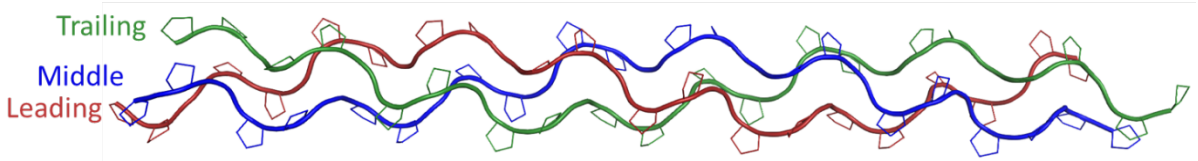

Figure 10: Crystal structure of a [(Pro-Pro-Gly)$_{10}$]$_3$ collagen triple-helix *(PDB code 1K6F, Berisio et al. 2002). The three α-chains are colored in red, blue and green.*

Even if all collagens share a basic triple-helical feature, they can achieve diverse supramolecular assemblies, such as fibrils, hexagonal network or even beaded filaments (Figure 11) (Ricard-Blum 2011). Most of the collagen types assemble into fibrils in a heterotypic manner, meaning that the collagen fibrils are composed of more than one type of collagen. For example, collagen fibrils are made up of collagen types II and III or II, XI and IX in cartilage, I and III in skin or I and V in cornea (Bruckner 2010; Wu et al. 2010). The proportion of triple-helical regions in collagens can vary from 10% in collagen XII to 96% in collagen I (Ricard-Blum 2011). Fibrillar collagens such as collagens I, II, III, V, XI, XXIV and XXVII have a triple helical-region that represents the major part of their sequence. In addition, a subfamily of collagens called fibril-associated collagens with interrupted triple helices (FACIT) gathers collagens that contain several collagen triple-helical regions separated by non-collagenous (nc) regions. The FACITs do not form polymers alone but are associated with fibrils and are suggested to act as molecular bridges playing a major role in the organization and stability of extracellular matrices (Shaw and Olsen 1991).

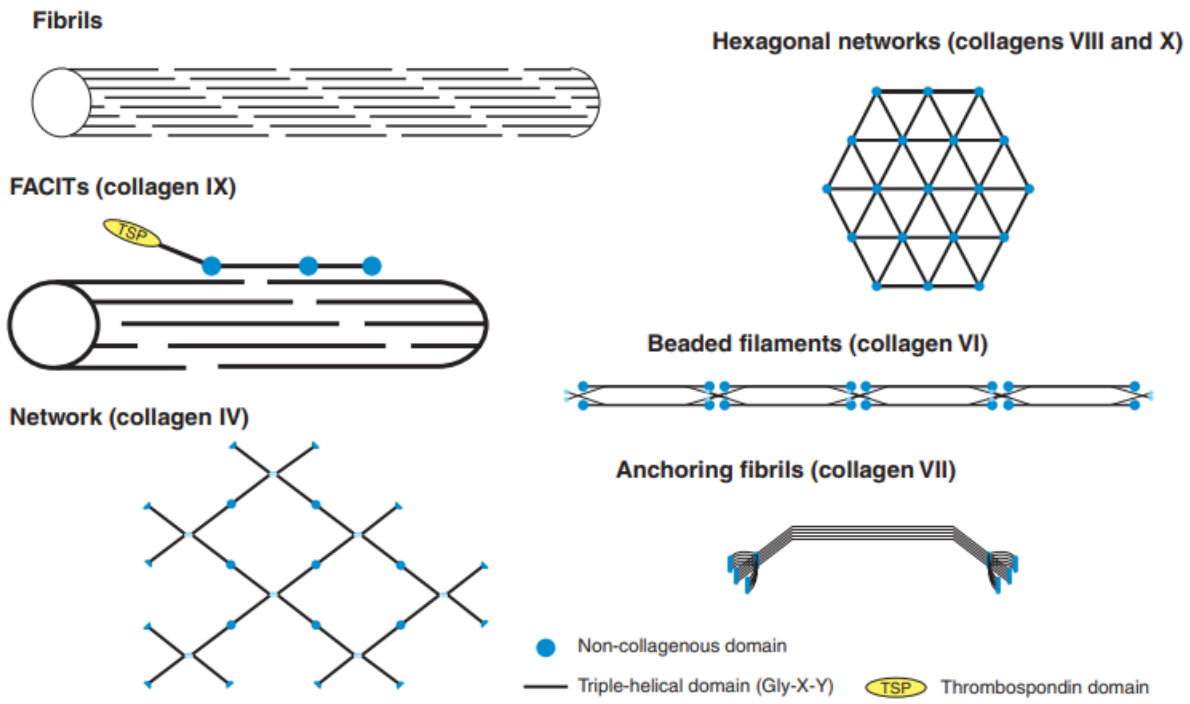

Figure 11: Supramolecular assemblies formed by collagen *(Taken from Ricard-Blum 2011). FACITs: fibril-associated collagens with interrupted triple helices.*

LAIR-1 is a receptor for collagens. Indeed, collagens are able to cross-link LAIR-1 thus inhibiting the immune cell activation *in vitro* (Lebbink et al. 2006, 2009). LAIR-1 interaction with collagen depends on the presence of hydroxyproline residues. Indeed, surface plasmon resonance studies showed that LAIR-1 interacts well with an immobilized $(GPO)_{10}$ peptide but exhibits low binding signal on an immobilized $(GPP)_{10}$ peptide (Lebbink et al. 2006). Because LAIR-1 interacts with a common collagen feature, it was shown to interact with many collagen types such as collagens I, II, III, IV, XIII, XVII or XXIII (Lebbink et al. 2006, 2009; Brondijk et al. 2010b). In addition, several LAIR-1 binding sites were identified on collagens II and III (Lebbink et al. 2009).

3 Molecular and structural aspects of collagen/LAIR-1 interaction

Only few studies report collagen/LAIR-1 interaction from a molecular and structural point of view. In one of them, Tang and colleagues revealed the high importance of one LAIR-1 residue for the interaction with collagens: arginine 65. Indeed, the mutation of this single residue into a lysine (R65K) was tested both *in vitro* and on cell surface, revealing altered interaction properties with collagens and therefore inefficient collagen-mediated LAIR-1 phosphorylation and cellular signaling (Tang et al. 2009).

The first structural information about LAIR-1 was given by Brondijk and colleagues with the crystal structure of LAIR-1 extracellular Ig-like domain (PDB code: 3KGR). This structure revealed that, as expected, LAIR-1 extracellular domain exhibits the characteristic Ig-like domain scaffold with two β-sheets connected by a disulfide bridge (Figure 9B). Nuclear magnetic resonance titration analysis of LAIR-1 interaction with a synthetic collagen III peptide identified the collagen binding region of LAIR-1 (Figure 12BC). Indeed, residues R59-E63, T67-N69, A84-F86, R100-I102, W109-S113, Y115-L116, and L118 displayed important chemical shift perturbations upon collagen interaction (Brondijk et al. 2010b). Some of these residues were mutated on membrane full-length LAIR-1 and tested for their ability to interact with collagen I, III and IV. Mutations of arginine 59 or glutamate 61 into an alanine residue drastically inhibit each collagen interaction with stably transfected cells. In addition, arginine 65 substitution into alanine showed an important decrease of collagens binding, also confirming arginine 65 major involvement in collagen/LAIR-1 interaction. Furthermore, arginine 62 and glutamate 111 mutation into alanine had a lesser impact on LAIR-1 interaction properties. These identified residues are highly conserved in LAIR-1 and LAIR-2 proteins from several species, especially for the residues essential for collagen binding (Figure 12A).

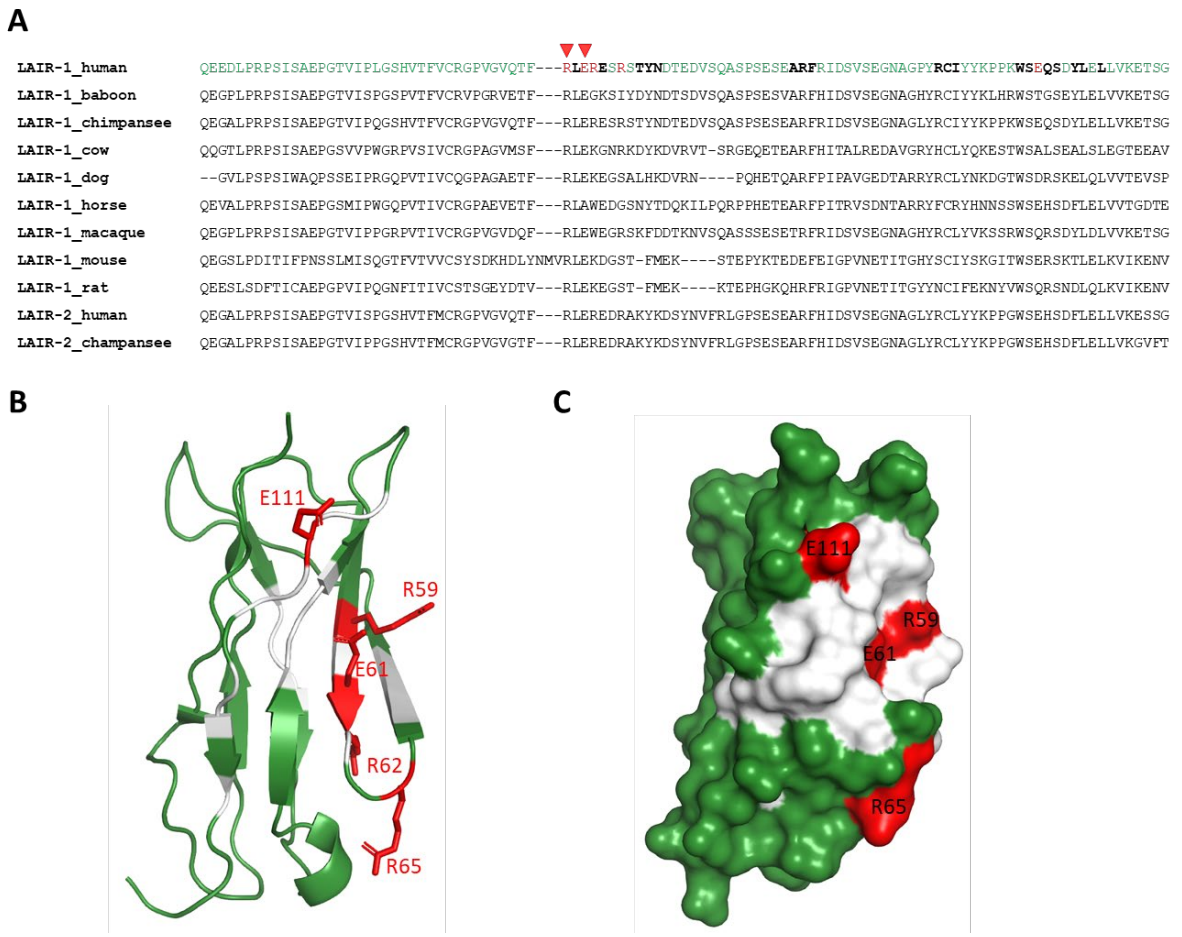

Figure 12: LAIR-1 residues involved in collagen binding. ***A****. Alignment of LAIR-1 sequences from several species. Key residues for human LAIR-1 interaction with collagen III are in red and residues showing NMR chemical shift perturbation in bold. The most conserved residues in LAIR-1 orthologs are labelled with red triangles. Cartoon (****B****) and surface (****C****) representations of LAIR-1 Ig-like domain (PDB code 3KGR). Key residues for human LAIR-1 interaction with collagen III are in red and labelled in black and residues showing NMR chemical shift perturbation in white.*

LAIR-1 is structurally related to another Ig-like family member encoded in the LRC: the glycoprotein VI (GPVI). GPVI is an activating collagen receptor, expressed on platelets and megakaryocytes, playing a major role in thrombosis and hemostasis (Farndale et al. 2004; Horii 2006; Leitinger and Hohenester 2007). Interestingly, GPVI interaction with collagen is dependent on the presence of hydroxyproline residues, as it is the case for LAIR-1 (Knight et al. 1999; Smethurst et al. 2007). This observation highly suggests that GPVI and LAIR-1 interactions with collagen rely on similar molecular mechanisms. Such hypothesis is supported by a study showing that LAIR-1 is able to inhibit collagen-induced GPVI signaling when co-expressed in the same cells (Tomlinson et al. 2007). Moreover, the collagen binding sites of LAIR-1 (i.e., R59 and E61) are present in GPVI sequence and highly conserved in GPVI orthologs (Figure 13).

A

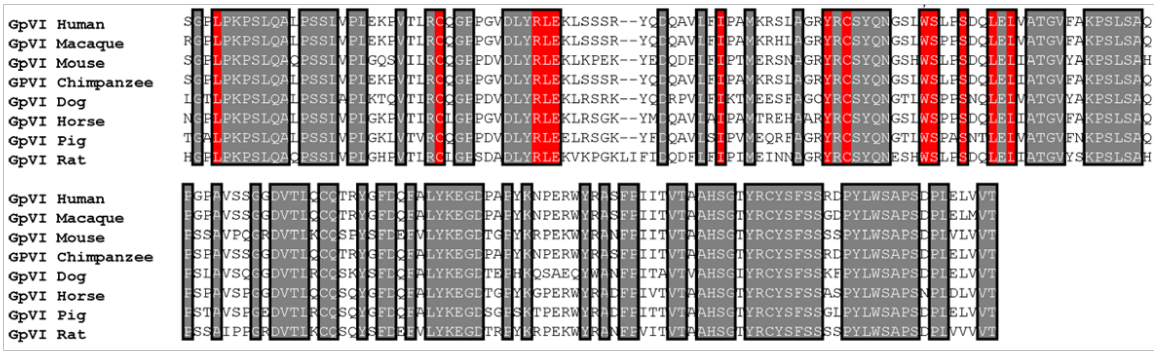

B

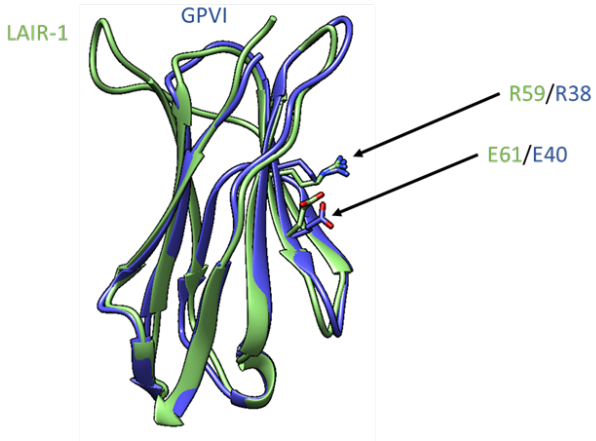

Figure 13: LAIR-1 essential collagen binding residues are conserved in the GPVI. ***A****. Sequence alignment of GPVI from several species. Conserved residues R38 and E40 homologs to LAIR-1 collagen-interacting residues (R59, E61) are shown in red (Taken from Brondijk et al., 2010b).* ***B****. Cartoon representation of LAIR-1, in green, and GPVI, in blue (PDB codes 3KGR and 5OU9, respectively) structure alignment. The homologous collagen-interacting arginine and glutamate residues are labelled with black arrows.*

As opposed to LAIR-1, GPVI structure in complex with a GPO synthetic collagen peptide is available in the protein data bank (PDB code 5OU8). The available crystal structure of GPVI-collagen complex does not support the GPVI collagen binding site previously suggested by computational docking and mutational analyses (Smethurst et al. 2004; Horii 2006). However, the GPVI-collagen complex structure supports a common collagen recognition mechanism with LAIR-1. Indeed, the structure shows that R38 and E40, the respective homologs of LAIR-1 R59 and E61 residues, are directly involved in the interaction of GPVI Ig-like domain with a GPO peptide (Figure 14B). All together, these observations are consistent with a common collagen binding mechanism for LAIR-1 and GPVI.

Furthermore, one additional structural insight into collagen recognition by Ig-like domains could be obtained from the crystal structure of osteoclast associated receptor (OSCAR), another collagen Ig-like receptor encoded in the LRC and involved in osteoclast development, in complex with a collagen peptide (PDB code 5CJB) (Haywood et al. 2016). In this particular case, collagen binding relies on three tyrosine (Y166, Y200 and Y208) and one proline (P204) residues (Figure 14A). Although collagen binding on OSCAR involves residues that are chemically different from the GPVI/LAIR-1 common collagen binding site (hydrophobic versus charged residues in GPVI/LAIR-1), the overall collagen binding region is basically the same on the Ig-like domain surface (Figure 14A).

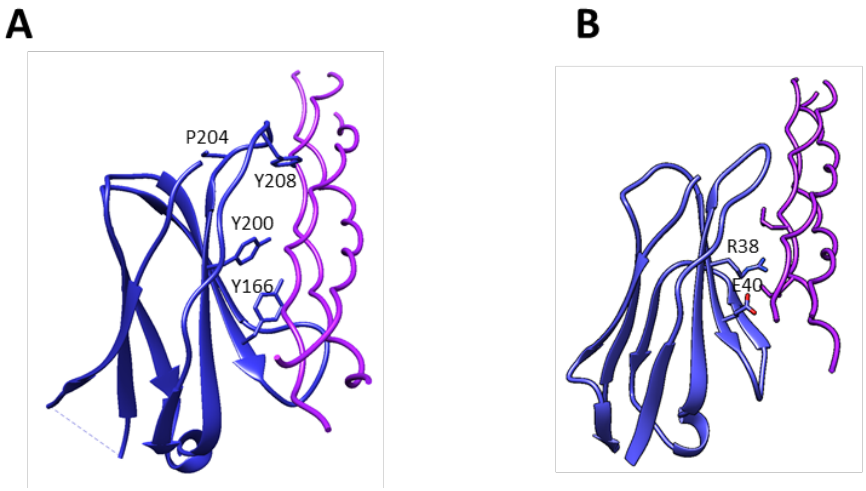

Figure 14: OSCAR (A) and GPVI (B) crystal structures in complex with a collagen peptide (PDB codes 5CJB and 5OU9, respectively). *Receptors Ig-like domains are represented in blue and the collagen peptides in purple. Side chains of the key residues for the interaction are shown and labelled in black.*

4 Regulation of LAIR-1 inhibitory activity

LAIR-1 is broadly expressed on the surface of immune cells and because its ligands (collagens) are very abundant in the human body, the collagen/LAIR-1 interaction needs to be tightly regulated in order to obtain a suitable inhibitory signaling. This regulation can occur by different ways. Indeed, the level of LAIR-1 expression on cell surface can be modulated at different stages of immune cells differentiation or LAIR-1 can be also shed from the cell surface after cell activation, generating soluble LAIR-1 (van der Vuurst de Vries et al. 1999; Ouyang et al. 2004; Verbrugge et al. 2006; Jansen et al. 2007; Zhang et al. 2018). Moreover, a recent study showed that LAIR-1 expression during the inflammation processes is tightly controlled. Indeed, LAIR-1 is over expressed on monocytes and dendritic cells surface during inflammation and its expression comes back to a normal level during the inflammation resolution (Carvalheiro et al. 2020).

The collagen/LAIR-1 interaction can also be regulated by the LAIR-1 soluble homolog: LAIR-2. Indeed, LAIR-2 was shown to interact with the same binding sites as LAIR-1 in collagen molecules. Therefore LAIR-2 acts as a soluble competitor for LAIR-1 interaction with collagens I and III (Lebbink et al. 2006, 2008). This strongly suggests that LAIR-2 may operate as an immunoregulatory molecule by decreasing LAIR-1 inhibitory activity *in vivo*.

5 LAIR-1 involvement in pathologies

Due to its wide expression and important inhibitory activity, it is not surprising that LAIR-1 is involved in a large number of pathologies such as cancer or autoimmune diseases. This part describes selected diseases for which LAIR-1 positive or negative contribution has been reported.

5.1 LAIR-1 in cancer

Due to its wide range of expressing cell types, LAIR-1 has been reported to be involved in many cancer types. Indeed, it was shown that LAIR-1 expression is higher in cancer cells than in healthy cells. For example, LAIR-1 expression is increased in myeloid leukemia cells, epithelial ovarian cancer cells, cervical cancer cells, osteosarcoma and hepatocellular carcinoma cells (Poggi et al. 2000; Zocchi et al. 2001; Cao et al. 2015; Wang et al. 2016; Wu et al. 2019; Zhang et al. 2020). However, the consequences of LAIR-1 activation on tumor development remain elusive. Indeed, LAIR-1 activation in myeloid and lymphocytic leukemia inhibits nuclear factor-κB (NF-κB) signaling, therefore preventing cancer cells proliferation (Poggi et al. 2000, 2008; Zocchi et al. 2001). This inhibitory activity of LAIR-1 upon tumor proliferation was also reported in the cases of ovarian cancer, cervical carcinoma and osteosarcoma (Cao et al. 2015; Wang et al. 2016; Zhang et al. 2020). Only few studies reported a benefic role of LAIR-1 activation in the development of leukemia and hepatocellular carcinoma (Kang et al. 2015; Wu et al. 2019).

Tumors are often associated with enhanced collagens expression that constitutes a suitable microenvironment for tumor growth and migration (Kauppila et al. 1998; Huijbers et al. 2010). These tumor-expressed collagens were shown to be ligands for soluble Fc-fused LAIR-1 and membrane LAIR-1 (Rygiel et al. 2011). This suggests a role for LAIR-1 in tumor strategies to escape immune reactions. Indeed, LAIR-1 crosslinking through tumor-expressed collagens leads to the activation of the downstream suppressive LAIR-1 signaling in T and NK cells, thereby inhibiting their cytotoxic activities against tumor cells (Rygiel et al. 2011).

5.2 LAIR-1 in human malaria

LAIR-1 was recently reported to be involved in malaria. Indeed, a family of broadly reactive antibodies against malaria antigens was identified in individuals living in malaria-endemic regions and characterized (Tan et al. 2016; Pieper et al. 2017). These antibodies present a unique feature with the insertion of an additional DNA sequence between the V and D/J segments, encoding a full Ig-like domain corresponding to the LAIR-1 extracellular domain (Figure 15A). This supplementary domain does not totally fit with LAIR-1 Ig-like domain sequence and displays several mutations. Binding analysis of each mutation revealed that they enhance the binding to *P. falciparum* infected erythrocytes while reducing interaction with its native collagen ligands. These particular antibodies were shown to opsonize infected erythrocytes through interaction with RIFINs, surface-exposed antigens on *P. falciparum* infected erythrocytes (Figure 13B). Structure resolution of one of these antibodies Fab fragment revealed that the entire LAIR-1 Ig-like domain is well folded and exposed at the top of the heavy chain (Hsieh and Higgins 2017) (Figure 15A). This is the first and unique example where the antibody interaction properties with its cognate antigen are owned by an additional domain. In this context, the antibody's Fab domain acts as a link between the antigen-recognizing additional Ig-like domain and the constant fragment of the antibody to induce subsequent immune responses (Figure 15B).

Independently of the broadly reactive antibody reported above, LAIR-1 is involved in the immune evasion of *Plasmodium falciparum.* In this case, wild-type LAIR-1 Ig-like domain interacts directly with a subset of RIFINs at the surface of infected erythrocytes. This finding raises the question of *P. falciparum* infected erythrocytes recognition by transmembrane LAIR-1 on immune cells surface. Indeed, leukocyte immunoglobulin-like receptor B1 (LILRB1), an Ig-like immune receptor structurally related to LAIR-1 was reported to interact with RIFINs, which mimic its natural ligand thus inducing LILRB1 inhibitory activity on immune cell function (Saito et al. 2017; Harrison et al. 2020). It is therefore reasonable to speculate that as for LILRB1, membrane LAIR-1 may be activated by RIFINs binding thereby allowing *P. falciparum* immune evasion (Figure 15C).

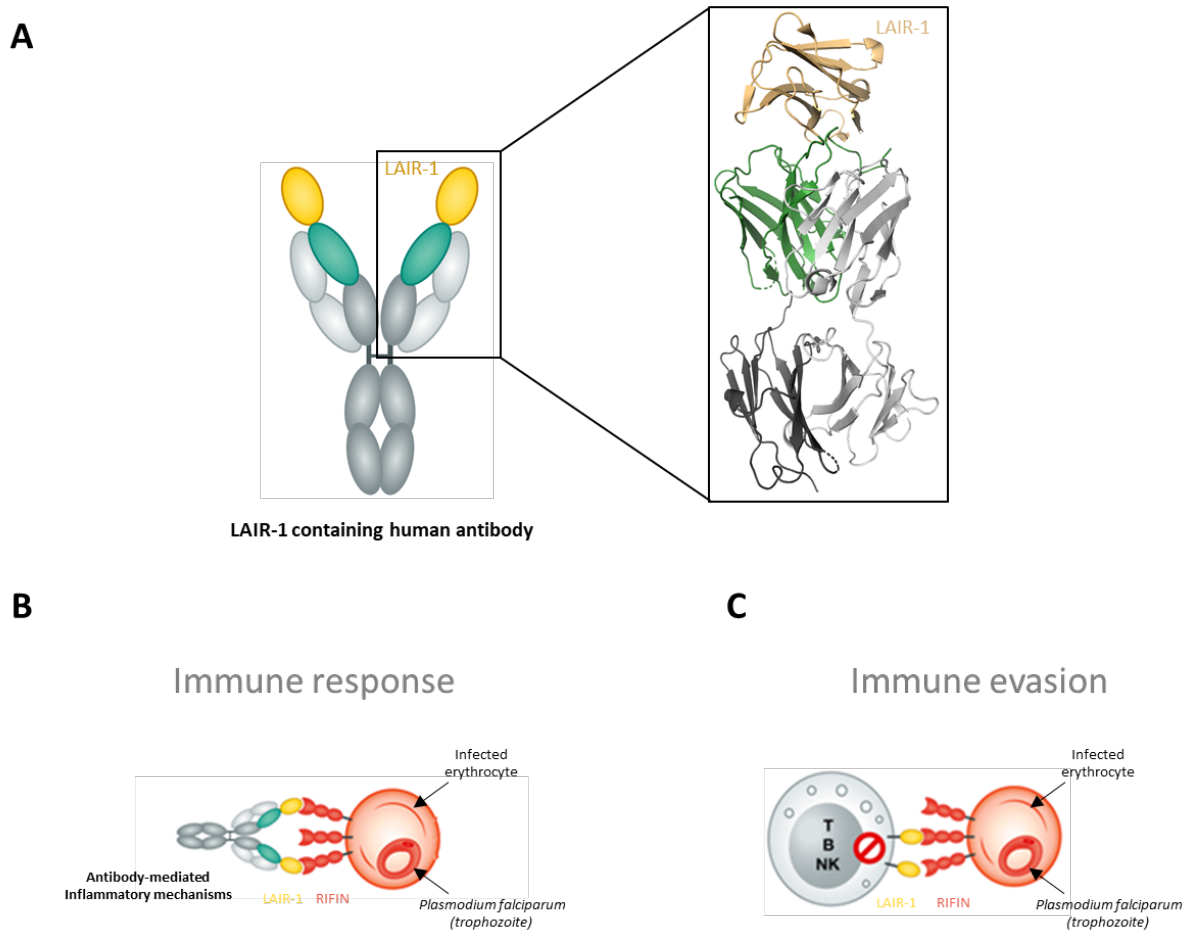

Figure 15: LAIR-1/RIFIN interaction and immune response. ***A****. schematic representation of LAIR-1 containing antibody. The cartoon representation of the crystal structure of the Fab fragment (PDB code 5NST) is shown in the insert.* ***B****. LAIR-1 Ig-like domain insertion in immunoglobulins gives them interaction properties with RIFIN, triggering the Ig-mediated cytotoxic activities.* ***C****. When exposed on immune cells surface, membrane LAIR-1 interaction with RIFIN induces intracellular tolerogenic signals that inhibit T, B and NK-cells cytotoxicity (Adapted from Lanzavecchia 2018).*

5.3 LAIR-1 in autoimmune diseases

Appropriate immune responses rely on a delicate balance between activating and inhibitory signals. Disruption of the immune balance leads to the development of autoimmune diseases like systemic lupus erythematosus (SLE) and rheumatoid arthritis (RA). Because of its broad expression and its important inhibitory role in immune cells phenotype, LAIR-1 is strongly suspected to be involved in the immune imbalance in the cases of SLE and RA.

SLE is a chronic autoimmune disease involving multiple organs and characterized by the presence of a wide variety of auto-antibodies produced by uncontrolled B cells (Rahman and Isenberg 2008; La Cava 2010). SLE etiology remains unclear with multiple endogenous and environmental factors. However, one cytokine seems to have a central role in the development of SLE: interferon alpha (IFNα) (Niewold et al. 2010). Indeed, SLE patients exhibit higher

IFNα serum levels and IFNα-inducible genes expression that correlate with disease activity (Hooks et al. 1979; Ytterberg and Schnitzer 1982; Bengtsson et al. 2000; Kirou et al. 2004). Plasmacytoid dendritic cells (pDC) are a type of immune cells known to be important IFNα producers, especially after stimulation through TLR (Kadowaki et al. 2001; Colonna et al. 2004). Interestingly, crosslinking of LAIR-1 by anti-LAIR-1 antibodies or C1q strongly inhibits TLR-dependent IFNα production by pDC revealing a putative implication of LAIR-1 in SLE (Bonaccorsi et al. 2010; Son and Diamond 2015). This hypothesis is supported by studies reporting lower LAIR-1 expression on pDC in SLE patients than healthy controls (Bonaccorsi et al. 2010; Kanakoudi-Tsakalidou et al. 2014).

RA is characterized by bone erosion in patients' joints as the consequence of excessive osteoclasts activation (Takayanagi et al. 1997). Osteoclasts express LAIR-1 on their surface and a study showed that LAIR-1 activation via anti-LAIR-1 antibodies inhibits osteoclastogenesis (Zhang et al. 2013). These observations suggest that LAIR-1 may be involved in RA pathology. This hypothesis is supported by reports which demonstrate lower membrane LAIR-1 expression on osteoclasts surface and higher levels of soluble LAIR-1 and LAIR-2 in serum, urine and synovial fluids of RA patients in comparison with healthy controls (Nordkamp et al. 2011; Zhang et al. 2013). These findings revealed that LAIR-1 inhibitory activity on osteoclasts is down-regulated in RA patients and may directly contribute to bone destruction.

Several studies demonstrate association of the above-mentioned pathologies with complement proteins and especially C1q or C1q-related receptors disturbance, therefore raising the question of a possible role of C1q interaction with LAIR-1 (Botto and Walport 2002; Dembitzer et al. 2012; Tettey et al. 2015; Son et al. 2015; Bulla et al. 2016; Mangogna et al. 2019).

6 C1q/LAIR-1 interaction

Collagenous regions are not an exclusive feature of the collagen family members and are present in various soluble proteins such as collectins, C1q, adiponectin and ficolins (Myllyharju and Kivirikko 2004) (Figure 2). Because LAIR-1 interacts with a generic collagenous scaffold, it would likely interact with these proteins containing collagen-like regions. Up to now, SP-D, MBL and C1q have been identified as LAIR-1 and LAIR-2 ligands *in vitro*, conferring them a putative role in the modulation of the immune system (Son et al. 2012; Olde Nordkamp et al. 2014a, b).

Furthermore, functional studies of C1q interaction with LAIR-1 on immune cells surface revealed that C1q directly crosslinks LAIR-1, triggering its ITIMs phosphorylation which consequently inhibits monocyte to dendritic cell differentiation and suppresses INF-α production by plasmacytoid dendritic cells (Son et al. 2012). In addition, similar tolerogenic properties were identified for C1q/LAIR-1 interaction on monocytes surface. Indeed, this interaction inhibits toll-like receptor activating signals and maintains monocyte tolerance (Son and Diamond 2015) .

C1q interaction with LAIR-1 engages its collagen-like regions thus leaving its globular regions free to interact with other immune receptors (Son et al. 2012). In this context, initial studies identified and characterized two Ig-like immune receptors for their interaction with C1q globular regions: the receptor for advanced glycation end products (RAGE) and siglec-3 (CD33) (Ma et al. 2012; Son et al. 2016, 2017).

RAGE is a 45 kDa activating transmembrane receptor expressed on monocytes, macrophages and dendritic cells surface with an extracellular region composed of three Ig-like domains: one V-type and two C2-types. This receptor triggers inflammatory reaction cascades when it interacts with several ligands such as AGEs (advanced glycation end products), HMGB1 (high mobility group box 1), LPS or DNA (Sorci et al. 2013; Wang et al. 2017) (Figure 16A). In addition, reports demonstrated RAGE interaction with phosphatidylserine, revealing its putative implication in apoptotic cells phagocytosis (He et al. 2011). Son and colleagues showed that C1q is able to interact simultaneously with RAGE and LAIR-1, thus modulating the immune response. Indeed, in inflammatory conditions, RAGE pro inflammatory signals induced by high HMGB1 levels are suppressed by SHP-1 phosphatase recruited by activated LAIR-1 via C1q interaction (Son et al. 2016) (Figure 16BC).

CD33 receptor belongs to the siglecs receptor family (sialic acid immunoglobulin-like lectins), a family of receptors engaged in sialic acid dependent cell adhesion. CD33 is the shortest siglec member with two extracellular Ig-like domains: a V-type domain responsible for sialic acid interaction and a C2-type domain (Crocker et al. 2007). The cytoplasmic region of CD33 contains two ITIMs, conferring CD33 inhibitory properties regarding inflammation signals. C1q was the first physiological ligand of CD33 identified inducing ITIMs phosphorylation (Son et al. 2017). In addition, this study revealed that C1q crosslinks CD33 and LAIR-1 and generates a large CD33-C1q-LAIR-1 inhibitory complex on monocyte surface inhibiting dendritic cell differentiation and activation (Figure 16D).

These studies of Son and colleagues put C1q-mediated immune regulation in a whole new perspective. Indeed, thanks to its multivalence and different functional regions, C1q could likely simultaneously interact with LAIR-1/2, RAGE and CD33, thus regulating the immune response via a complex local aggregation of pro and anti-inflammatory signals (Figures 8 and 16).

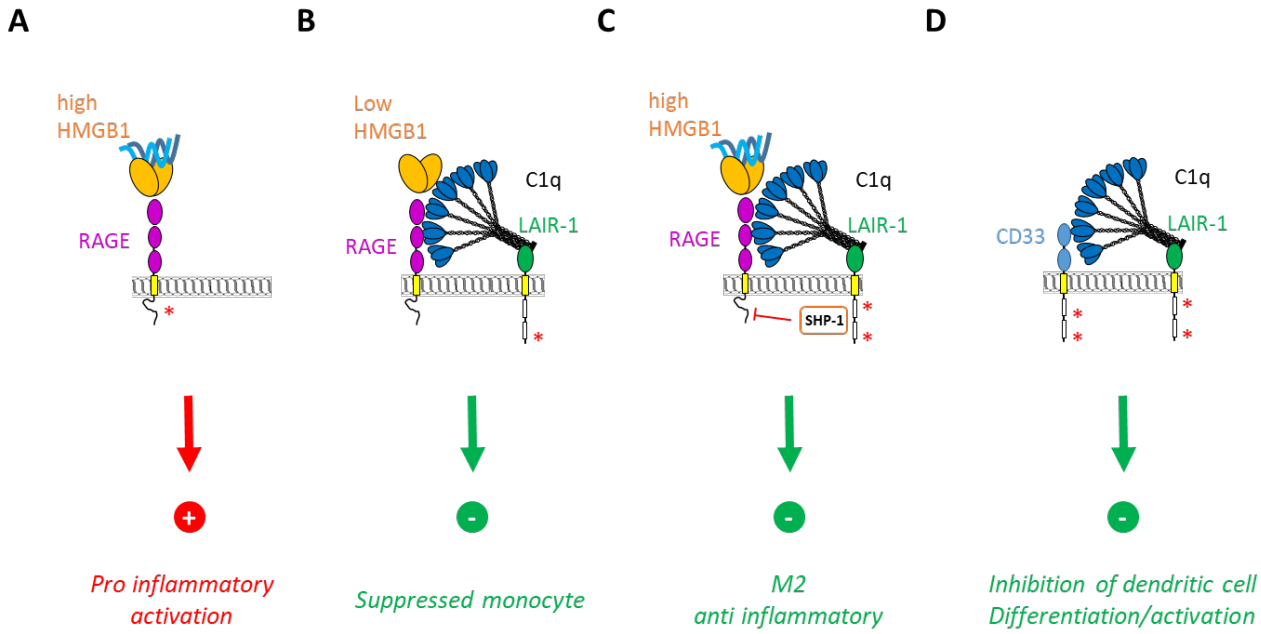

Figure 16: Modulation of immune signals by C1q interaction with the Ig-like receptors RAGE, LAIR-1 and CD33. *Schematic representation of RAGE activation by HMGB1 (**A**) and C1q-mediated immune modulation through RAGE and LAIR-1 in normal (**B**) and inflammatory (**C**) conditions. **D**. Schematic representation of C1q crosslinking of LAIR-1 and CD33. The intracellular phosphorylations are represented with red asterisks.*

IV. Aim of the project

The defense collagen C1q plays a critical role in various immune mechanisms and their control. The impressive versatility of C1q functions relies on its wide range of ligands but above all, on a constantly increasing number of newly discovered C1q receptors triggering different signals upon C1q recognition. Thanks to its multivalence, C1q is likely able to interact with several copies of the same or different receptors and therefore modulates the immune response depending on the receptors engaged. However, how C1q is implicated in these processes remains unclear and awaits further investigations in order to understand the C1q-mediated immune modulation and tolerance mechanisms.

Recently, the first elements clarifying this question were provided by Son and colleagues who reported that C1q-mediated immune modulation was dependent on its interaction with immune receptors from the immunoglobulin-like family: RAGE, CD33 and LAIR-1/2 (Son et al. 2012, 2016, 2017) (Figure 8). These first studies suggest that LAIR-1 and LAIR-2 interact with the C1q CLR while RAGE and CD33 interaction with C1q engages its GR. These different binding regions on the C1q molecule enable the bridging of the receptors through C1q to congregate pro- and anti-inflammatory signals, thus modulating the immune response (Figure 16).

However, the fine details dictating these interactions are fundamental for the understanding of C1q-mediated immune modulation and remain to be identified. In this line, my PhD project initially aimed at identifying the molecular and structural determinants underlying the C1q interaction with its recently identified Ig-like receptors RAGE, CD33 and LAIR-1/2.

We first focused on the analysis of C1q interaction with the Ig-like receptor LAIR-1. As a collagen receptor, LAIR-1 was previously described to interact with the collagen-like regions of C1q. In order to investigate the interaction properties of LAIR-1 with C1q CLR, we took up the challenge of C1q collagen chains registering and developed the first reported recombinant production of C1q collagen-like regions (Article 1).

Then, we combined molecular dissection and mutagenesis strategies to identify the LAIR-1 binding region on C1q and vice versa. This approach allowed us to propose a model for C1q interaction with the inhibitory receptor LAIR-1 (Article 2).

We attempted to investigate the dimerization effect of LAIR-1 on its interaction with C1q. For that part of the project, we also developed two LAIR-1 variants exclusively monomeric or

dimeric in solution (S92K and S92C mutations, respectively). These two LAIR-1 constructs will be of real benefit for that purpose (Results section, III).

In order to expand our project to the study of C1q interaction with LAIR-2 and CD33, we did preliminary trials to express their Ig-like domains (Results section, IV).

Finally, during my PhD, I contributed to the deciphering of C1q interaction with two other receptors: CR1 and LRP1 (Articles 3 and 4).

RESULTS

I. **Article 1:** Headless C1q: a new molecular tool to decipher its collagen-like functions

In order to better understand the challenge of controlling the collagen chain registering in the C1q collagen-like regions, I will introduce the specificities of collagens structure and assembly.

1 The critical role of trimerization domains

Every collagen triplet containing sequence has the intrinsic tendency to assemble in an uncontrolled manner leading to the formation of a gel called gelatin. In order to prevent such molecular aggregates, every collagen holds a C-terminal non-triple helical trimerization domain (Boudko et al. 2012). Four structural classes of trimerization domain have been identified so far: the nc1 domain of collagen IV, the C1q-type domain of collagens VIII and X, the multiplexin trimerization domain of collagens XV and XVIII and the C-propeptide of fibrillar collagens I, II, III, V and XI (Figure 17) (Bogin et al. 2002; Than et al. 2002; Sundaramoorthy et al. 2002; Kvansakul et al. 2003; Vanacore et al. 2004; Boudko et al. 2009; Wirz et al. 2011; Bourhis et al. 2012).

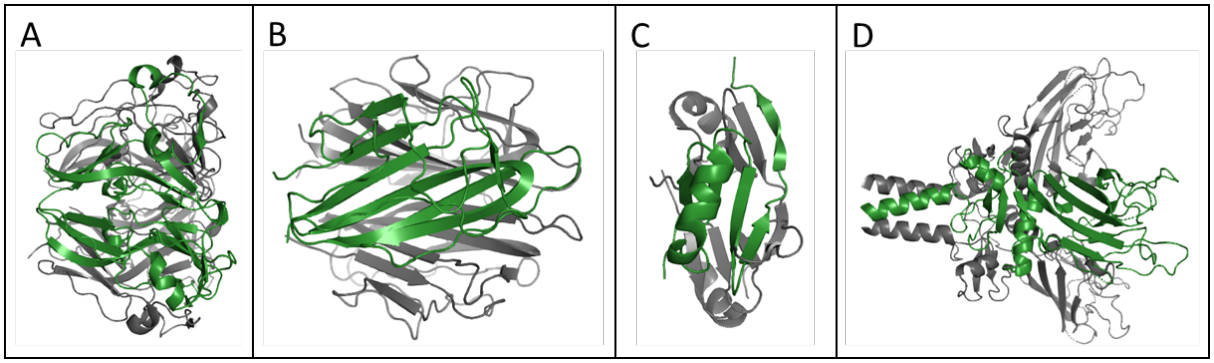

Figure 17: The four structural classes of collagen C-terminal trimerization domains. ***A****. crystal structure of collagen IV nc1 domain (PDB code 1M3D).* ***B****. crystal structure of the collagen X C1q-type domain (PDB code 1GR3).* ***C****. crystal structure of the collagen XVIII multiplexin trimerization domain (PDB code 3HSH).* ***D****. Crystal structure of the collagen III C-propeptide (PDB code 4AK3). Each crystal structure is shown as a cartoon representation with one chain subunit colored in green and the two others in grey. The four crystal structures are oriented in the same direction with the N-terminal extremities on the left of the structure.*

These trimerization domains were demonstrated to correctly align and register the three α-chains at their C-terminal extremities, thus initiating collagen triple-helix folding that proceeds to the N-terminus in a zipper like fashion (Engel and Prockop 1991). The presence of a trimerization domain to selectively align the three collagen α-chains is even more important in the case of heterotrimeric collagens because wrong chain registering into the triple-helix could induce the shedding of ligands binding sites, especially in the cases where the collagen ligand binding involves more than one collagen chain. For example, previous studies revealed that

collagen I recognition by the von Willebrand factor (VWF) A3 domain is mediated through a binding site that depends on the relative position of the three collagen chains in the triple-helix. Indeed, the VWF-A3 binding site on collagen I imposes the trailing position of the α2 chain and any other chain register induces a drastic reduction of the interaction (Brondijk et al. 2012; Jalan et al. 2020).

Type IX collagen belongs to the FACIT family and is encountered within collagens II and XI fibrils mostly found in cartilage. It is composed of three triple-helical collagen domains called COL1, COL2 and COL3 and four non-collagenous domains called nc1, nc2, nc3 and nc4 (Figure 18). In the case of collagen IX, as for most of the FACIT members, the correct trimerization of the triple helix is controlled by the second non-collagenous domain (nc2) (Boudko and Bächinger 2012). Type IX collagen is composed of three different α-chains and is the only heterotrimeric FACIT member. It is demonstrated that the collagen IX nc2 domain, beyond playing a role in collagen chains trimerization, is the leading domain for the selective registering of the three different α-chains (Boudko et al. 2010; Boudko and Bächinger 2016). Indeed, the nc2 domain consists in three different alpha helices that selectively assemble in a heterotrimeric manner, thus registering the upstream and downstream neighboring collagen sequences. Structural study of the nc2 domain of collagen IX revealed that α2, α1 and α3 chains correspond to the leading, middle and trailing chains, respectively (Boudko and Bächinger 2016).

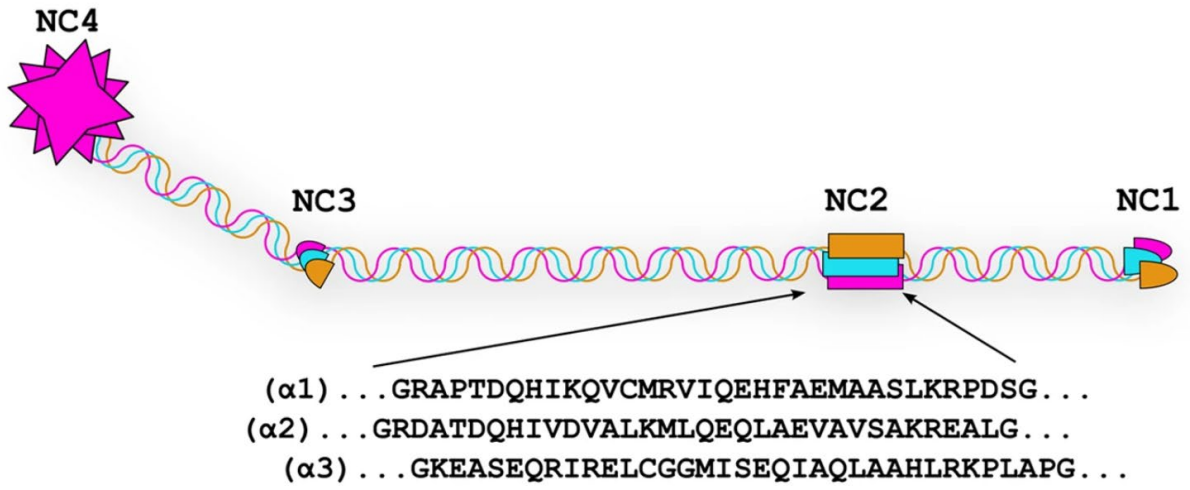

Figure 18: Domain organization of collagen IX. *The four non-collagenous domains (NC) are labeled in black. Three different collagen chains are colored in magenta, cyan and orange. (Taken from Boudko and Bächinger 2016a)*

2 Scientific context and relevance of the article

C1q is composed of 18 polypeptide chains of three different types (A, B and C) that assemble in six ABC heterotrimers. Each heterotrimer contains an N-terminal Gly-X-Y rich triple-helical region (CLR) and a C-terminal globular region (GR). The six heterotrimers are maintained together via N-terminal interchain disulfide bonds, resulting in the whole C1q molecule exhibiting a "bouquet-like" structure with an N-terminal collagen bundle and C-terminal globular "heads" at the end of diverging collagen stems. As mentioned in the introduction (section II), the two C1q functional GR and CLR regions have distinct functions with the GR harboring the versatile interaction properties of the molecule and the CLR triggering the immune signals through interaction with membrane or soluble partners (Eggleton et al. 2000; Gaboriaud et al. 2011).

Historically, studies used C1q purified from human serum and derived fragments generated by limited proteolysis. The digestion of C1q with collagenase or pepsin results in GR or CLR fragments, respectively (Figure 4). Use of these serum-derived C1q CLR and GR allowed analysis of both C1q fragments functions (Reid 1976; Hughes-Jones and Gardner 1979). One drawback of the serum-derived C1q and fragments is that the CLR and GR fragments obtained after enzymatic digestion have C-terminal and N-terminal extremities that are directed by the pepsin and collagenase specificity. This is not fully convenient since after C1q digestion with collagenase, the resulting GR still have a short remaining N-terminal collagen sequence. The same problem is also encountered with serum-derived CLR that contains a short C-terminal non-collagen like sequence (Thielens et al. 1993) (Figure 19).

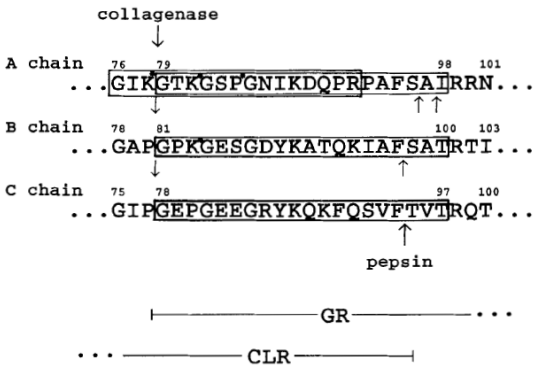

Figure 19: Location of the sites of limited cleavage by collagenase and pepsin in C1q A, B and C chains. *(Taken from Thielens et al., 1993).*

Therefore, serum-derived CLR and GR both share an overlapping sequence (residues 79-98, 81-100 and 78-97 of A, B and C chains respectively) that could hold a putative binding site for

C1q partners, leading to difficult deconvolution of each fragment's contribution to the interaction. To avoid the presence of common remaining binding sites, recombinant production of C1q fragments would allow to restrict the sequence extremities to the region of interest.

Moreover, serum-derived C1q fragments only provide wild-type proteins. This problem has been solved with the development of recombinant production of the entire C1q molecule and the globular region. Such development allowed the production of C1q variants containing point mutations in a view to identify C1q residues involved in the interaction with ligands such as $C1r_2s_2$, pentraxin 3 or IgM (Bally et al. 2013, 2019; Moreau et al. 2016). Up to now, only the globular regions of C1q were available in a recombinant form and the only tool to study the CLR was the pepsin-digested serum-derived CLR. This highlights the need of recombinant CLR for which the N and C-terminal extremities could be defined precisely.

As mentioned above, collagen triple-helix formation implies the proper alignment and positioning of the three collagen chains by a trimerization domain. In the case of C1q, this requirement is controlled by the C-terminal GR that specifically associate to initiate the collagen triple-helix formation (Kishore and Reid 1999). The correct phasing of the C1q collagen chains is even more important because of its heterotrimeric nature. Indeed, the collagen-like region of C1q is composed of three different chains and if the chain order is not respected, some C1q partners' binding sites could be shed. Because of the intrinsic major structural role of the GR for collagen chains assembly and folding, their removal from the C1q sequence would result in the uncontrolled association of the CLR chains. Therefore, the GR cannot be simply removed but need to be replaced by another trimerization domain in order to specifically control the collagen chains registering.

We decided to use the collagen IX nc2 domain to control the CLR chains positioning and phasing. The nc2 domain was really suitable for GR substitution because it is a heterotrimeric domain with the unique structural function of collagen chains specific registering and alignment. The key step of the design of the CLR fusion with the nc2 domain (CLR_nc2) is the choice of which CLR and nc2 chains need to be fused together in order to achieve the same assembly as C1q. To do so, we used the structural information available in the literature and a model of a C1q collagen stem built from the GR crystal structure (PDB code 1PK6, Gaboriaud et al. 2003) was aligned with the crystal structure of the collagen IX nc2 domain with a collagen I fragment on their C-terminal Gly-Pro motifs (PDB code 5CTI, Boudko and Bächinger 2016a). As shown in Figure 20, the GR A, B and C chains were superimposed on the nc2 α2, α1 and α3 chains, respectively. We thus decided to proceed to these chain combinations.

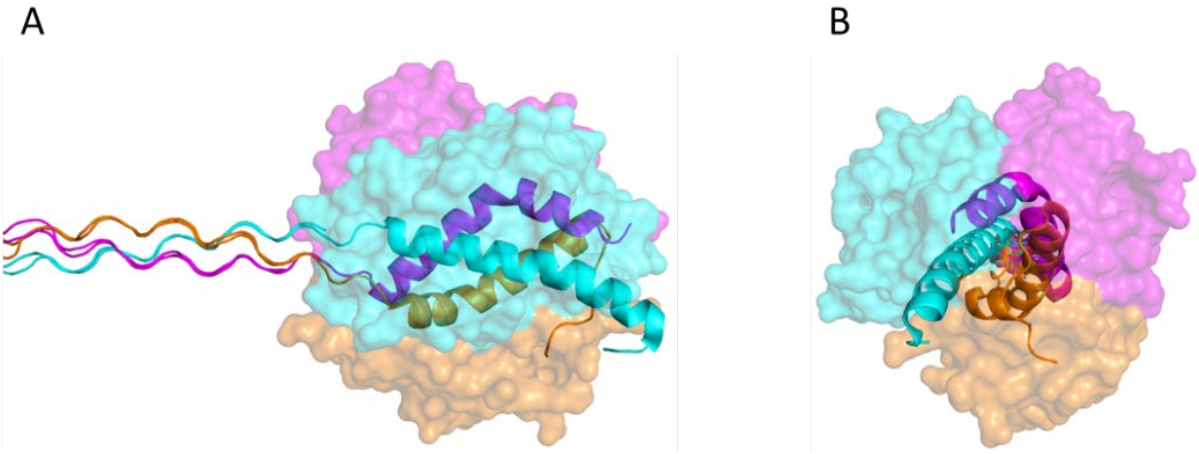

Figure 20: Choice of the CLR_nc2 chains combination. *Side (**A**) and top (**B**) views of the alignment of the crystal structure of the collagen IX nc2 domain with an N-terminal collagen I guest sequence (PDB code 5CTI) with the C1q model built from GR crystal structure (PDB code 1PK6). The nc2 domain is represented in cartoon and superimposed to the GR surface representation. The collagen chains are shown with a cartoon representation. C1q CLR and GR A, B and C chains are colored in cyan, magenta and orange, respectively. The nc2 α1, α2 and α3 chains are colored in magenta, cyan and orange, respectively.*

The following manuscript reports the production, purification and characterization of the resulting CLR_nc2 recombinant protein.

The FEBS Journal

FEBS PRESS science publishing by scientists

Headless C1q: a new molecular tool to decipher its collagen-like functions

Guillaume Fouët[1], Isabelle Bally[1], Luca Signor[1], Katharina Häußermann[2], Nicole M. Thielens[1], Véronique Rossi[1] and Christine Gaboriaud[1]

1 CEA, CNRS, IBS, Université Grenoble Alpes, Grenoble, France
2 Refeyn Ltd., Oxford, UK

Keywords
complement defense collagen; collagen chains registering; surface plasmon resonance; mass spectrometry; mass photometry

Correspondence
V. Rossi, Institut de Biologie Structurale, UMR 5075-Université Grenoble Alpes, CNRS, CEA, CAMPUS EPN, 71, avenue des Martyrs, CS 10090, 38044 Grenoble CEDEX 9, France
Tel: +33 (0)4 57 42 85 38
E-mail: veronique.rossi@ibs.fr
C. Gaboriaud, Institut de Biologie Structurale, UMR 5075-Université Grenoble Alpes, CNRS, CEA, CAMPUS EPN, 71, avenue des Martyrs, CS 10090, 38044 Grenoble CEDEX 9, France
Tel: +33 (0)4 57 42 85 99
E-mail: christine.gaboriaud@ibs.fr

(Received 18 May 2020, revised 20 July 2020, accepted 25 August 2020)

doi:10.1111/febs.15543

Complement component C1q, a soluble defense collagen, is the recognition protein of the classical complement pathway. C1q is able to recognize and interact with multiple targets and, via the subsequent activation of its cognate serine proteases C1r and C1s, initiates the complement cascade. C1q is made up of six ABC heterotrimers each containing two different functional regions, an N-terminal collagen-like region (CLR) and a C-terminal globular region (GR). These heterotrimers assemble via their N-terminal regions, resulting in the characteristic 'bouquet-like' shape of C1q with an N-terminal bundle of collagen fibers with six diverging stems each exhibiting a C-terminal globular head. The GRs are responsible for the versatile recognition of multiple C1q targets, whereas the CLRs trigger immune response through interacting with several cellular or soluble partners. We report here the generation of the first recombinant form of human C1q without its recognition globular heads. The noncollagenous domain 2 (nc2) of type IX collagen has been substituted for the C1q GR in order to control the correct registering of the collagen triple helices of C1q chains A, B, and C. The resulting CLR_nc2 recombinant protein produced in stably transfected EXPI293 mammalian cells was correctly assembled and folded, as demonstrated by mass spectrometry, mass photometry, and electron microscopy experiments. Its interaction properties were investigated using surface plasmon resonance analysis with known CLR ligands: the tetramer of C1r and C1s dimers and MBL-associated protein MAp44. Comparison with the interaction properties of native serum-derived C1q and CLR revealed that recombinant CLR_nc2 retains C1q CLR functional properties.

Introduction

The complement system is a major component of innate immunity, thereby acting as the first line of host defense against pathogens. C1q, the recognition protein of the classical complement pathway, is composed of six ABC heterotrimers, a content abbreviated as $(ABC)_6$. Each heterotrimer consists of an N-

Abbreviations
$C1r_2s_2$, tetramer of C1r and C1s dimers; CLR, C1q collagen-like region; EM, electron microscopy; GR, C1q globular region/head; HPLC, high-performance liquid chromatography; LC/ESI, liquid chromatography/electrospray ionization; MALDI-TOF, matrix-assisted laser desorption ionization-time of flight; MAp44, MBL-associated protein 44; MBL, mannose-binding lectin; MP, mass photometry; MS, mass spectrometry; nc2, noncollagenous domain 2 of type IX collagen; PTX3, pentraxin 3; SPR, surface plasmon resonance; TFA, trifluoroacetic acid.

terminal collagen-like region (CLR) followed by a C-terminal globular region (GR). Two heterotrimers assemble into $(ABC)_2$ due to disulfide bonds between chains A-B and C-C (Fig. 1A). The assembly of three $(ABC)_2$ units results in the formation of the full-length $(ABC)_6$ C1q protein exhibiting a 'bouquet-like' structure, with six C-terminal globular heads connected via six collagen stems assembled in an N-terminal fiber bundle (Fig. 1A) [1,2]. Over the past decades, proteolysis of C1q with either collagenase or pepsin allowed the first molecular dissection of C1q and identification of the distinct GR and CLR functions [3–6]. The GRs of C1q are mostly involved in the recognition of several targets like antibodies Fc regions, pentraxins, pathogen-, and apoptotic cell-associated molecular patterns [7,8]. The CLRs are engaged in immune response effector mechanisms through interaction with a tetramer of C1r and C1s serine proteases (C1 complex formation and classical complement pathway activation) or receptors on surfaces of immune cells [6,9]. Development of C1q and GR production in a recombinant manner gave the opportunity to investigate the molecular basis of C1q interaction with several partners, especially by introducing point mutations [10–13]. Several C1q receptors have been described as interacting with the CLRs of C1q (reviewed in Ref. [3]), raising the interest in recombinant production of C1q CLRs. Such tool would be of real benefit for investigating the specific CLR contribution in the case of C1q partners for which interaction engages both CLRs and GRs such as calreticulin and complement receptor 1 [14,15]. A major obstacle for C1q CLRs recombinant production is the need for control of the folding and the correct phasing of the three different collagen chains. It is admitted that the GRs of C1q play a major role for the CLRs registering [16,17]. Therefore, simple removal of the GRs may result in uncontrolled assembly of the collagen chains. Due to the heterotrimeric nature of the C1q CLR, we decided to replace the C1q GR by another heterotrimeric collagen registering domain: the noncollagenous domain 2 (nc2) of type IX collagen. Indeed, this particular heterotrimeric domain, consisting in three different α-helices (named α1, α2, and α3), has been recently described for its collagen chains registering function [18–20]. In contrast with the C1q GRs that recognize many ligands, the nc2 domains have no other known properties than the function of heterotrimerization. It is therefore particularly suitable to get a correctly folded recombinant headless C1q.

The resulting recombinant protein named CLR_nc2 was produced in stably transfected mammalian cells. Biochemical, biophysical, and functional analyses showed that it is correctly folded and that it retains the capacity of native serum-derived C1q (sC1q) to interact with ligands of CLRs.

Results and Discussion

Design, expression, and purification of recombinant CLR_nc2

CLR_nc2 fusion chains were designed to achieve the same assembly as the C1q protein (Fig. 1). In order to determine which CLR and nc2 chains need to be fused together, the crystal structure of type IX collagen nc2 heterotrimerization domain with a guest fragment of type I collagen (PDB Code: 5CVA, [20]) was superimposed on the C1q model built from the crystal structure of C1q GR (PDB Code: 1PK6, [21]) over their common C-terminal collagen Gly-Pro residues. Visual analysis indicated that nc2 α2, α1, and α3 chains were superimposed on C1q GR A, B, and C chains, respectively. Therefore, the following registering fusion order was used for the design of CLR_nc2: A_ α2: leading chain; B_ α1: middle chain; and C_ α3: trailing chain. The basic unit of CLR_nc2 assembly thus consists of a covalently linked $(ABC)_2$ hexamer that forms trimers to get the full-length CLR_nc2 $(ABC)_6$ protein, as it is the case for C1q (Fig. 1A,B). Three additional Gly-Pro-Pro collagen triplets were inserted between the CLR C-terminal part and nc2 chain sequence in order to enhance the collagen triple-helix formation (Fig. 1C). Of note, a FLAG epitope was added at the C-terminal extremity of the nc2 α3 chain for purification purpose.

Stable EXPI293 cell lines expressing recombinant CLR_nc2 were generated by triple transfection with three different pcDNA3.1 vectors containing each CLR_nc2 chain sequence. Western blot analysis of the culture supernatant revealed that the resulting transfectants expressed recombinant CLR_nc2 (data not shown). The recombinant material was purified by chromatography on an anti-FLAG affinity column, and the bound proteins were eluted by a FLAG peptide. In order to separate properly assembled CLR_nc2 from contaminant single and not well-assembled chains, a second step of purification by size-exclusion chromatography was performed. The overall procedure allowed purification of about 0.1 mg of CLR_nc2 from 1 L of culture supernatant.

Biochemical and structural analyses of CLR_nc2

SDS/PAGE analysis of purified CLR_nc2 revealed a band pattern consistent with the expected assembly of A, B, and C chains. Indeed, under nonreducing conditions, a unique protein band is revealed with an apparent molecular weight of about 120 kDa. This unique band is consistent with the $(ABC)_2$ unit, corresponding to six covalently linked chains (2×A, 2×B, and 2×C)

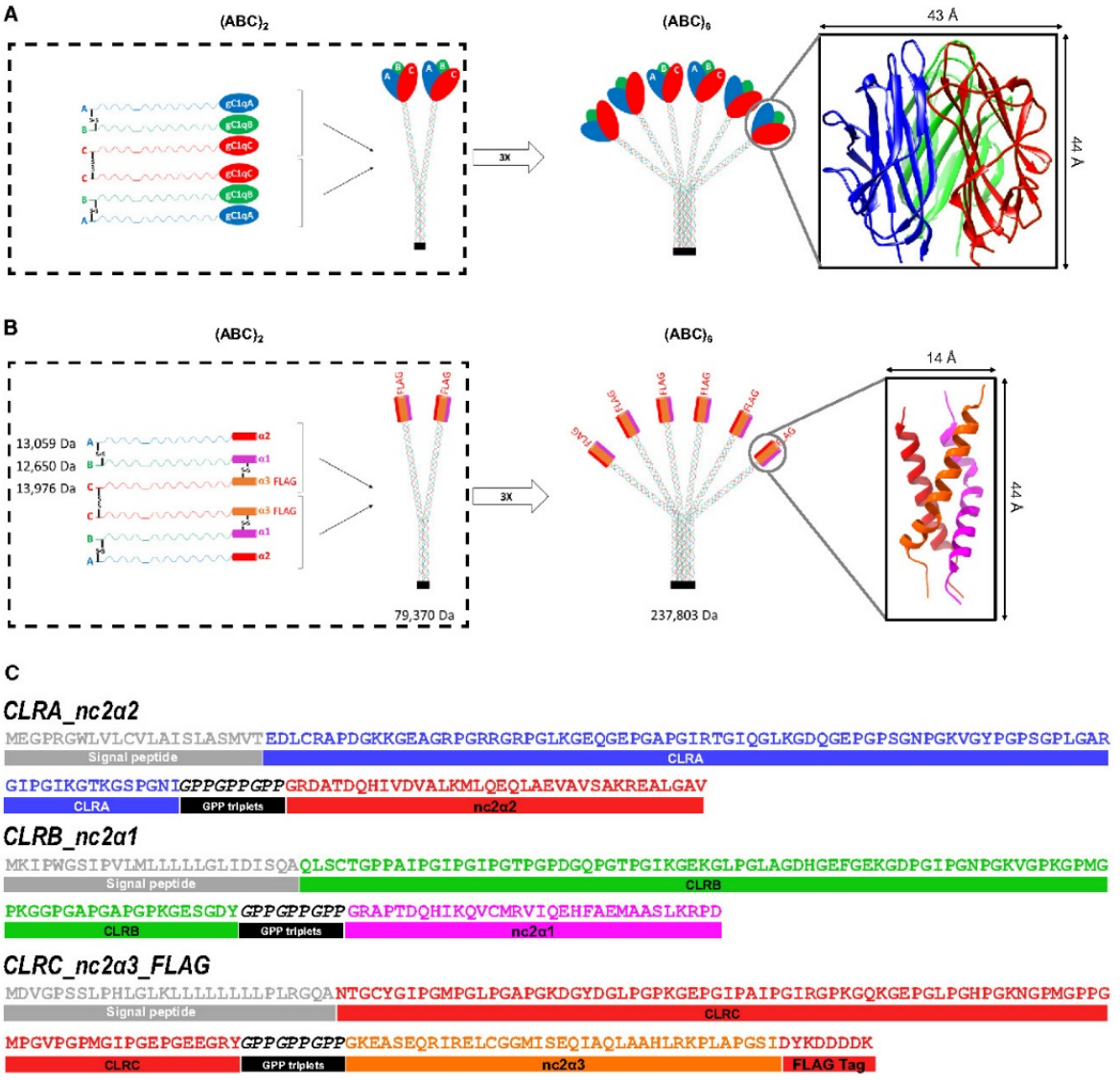

Fig. 1. Schematic representation of C1q and CLR_nc2 assemblies. (A) C1q molecule is assembled from 18 polypeptide chains of three types (A, B, and C) each containing an N-terminal collagen-like sequence and a C-terminal globular gC1q domain. A particular interchain disulfide bond pattern results in a basic unit $(ABC)_2$ comprised of two heterotrimeric collagen-like stalks (CLR) with a C-terminal GR. The association of three $(ABC)_2$ units leads to the full-length C1q $(ABC)_6$ with its characteristic bouquet-like shape. The right panel shows the crystal structure of C1q GR (PDB Code: 1PK6). (B) CLR_nc2 fusion protein assembly is similar to C1q with an additional interchain disulfide bond between α1 and α3 nc2 chains. The right panel shows the crystal structure of nc2 domains (PDB code: 5CVA). Masses calculated from amino acid sequences of CLR_nc2 isolated chains, $(ABC)_2$ and $(ABC)_6$ are given in Dalton. Interchain disulfide bonds and domain sizes are represented in black, and the FLAG epitopes are shown in red. (C) Amino acid sequences of CLR_nc2 fusion chains. CLRA, B, and C chains with their native signal peptides were fused to C-terminal nc2 α2, α1, and α3 chains, respectively. Three GPP collagen triplets were inserted between CLR and nc2 sequences, and a FLAG tag was added at the C-terminal extremity of CLRC_nc2α3 fusion.

with a calculated polypeptide mass of about 79 kDa (Figs 1B and 2A) and additional post-translational modifications (see below). Under reducing conditions, this protein band disappeared and gave lower protein bands around 20 kDa corresponding to the individual CLR_nc2 chains (Figs 1B and 2A). Western blot

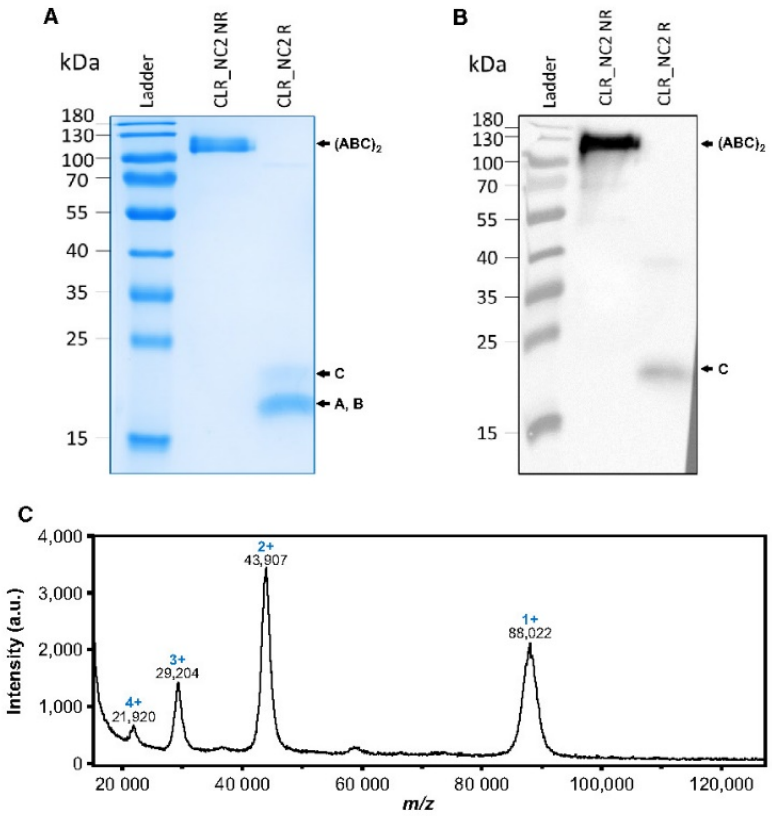

Fig. 2. Characterization of CLR_nc2 by SDS/PAGE and MALDI-TOF MS. (A) SDS/PAGE (12.5% acrylamide) analysis of CLR_nc2 under nonreducing (NR) and reducing (R) conditions. (B) Western blot analysis of CLR_nc2 using a monoclonal anti-FLAG antibody coupled to HRP under nonreducing (NR) or reducing (R) conditions. The results shown are representative of three independent experiments (C) MALDI-TOF mass spectrum of CLR_nc2. Analyses were performed on nonreduced samples as described in Materials and methods. Ionization states and observed masses in Dalton (Da) are indicated in blue and black, respectively.

analysis using a monoclonal anti-FLAG antibody allowed the identification of the C chain in both the unreduced basic unit and the upper band under reducing conditions (Fig. 2B).

Mass spectrometry (MS) experiments were then performed on CLR_nc2 using matrix-assisted laser desorption ionization-time of flight (MALDI-TOF) and liquid chromatography/electrospray ionization (LC/ESI). MALDI-TOF MS under nonreducing conditions yielded a mass value of 88 022 Da for the $(ABC)_2$ unit corresponding to its singly charged ion (Fig. 2C). The observed mass shift of about 8600 Da compared to the expected mass calculated from the amino acid sequence (79 370 Da) accounts for post-translational modifications. Indeed, it is well known that CLR undergo several proline and lysine residue hydroxylations and hydroxylysines O-glycosylations [10,22,23].

Under reducing conditions, the LC/MS chromatogram showed three major peaks, corresponding to the three different CLR_nc2 polypeptide chains (labeled 1, 2, and 3 in Fig. 3A). As illustrated in the lower part of Fig. 3, the LC/ESI-MS analysis of each chromatographic peak allowed the identification of the type of post-translational modifications. Indeed, for peaks 1 and 3, species with a 340 Da mass shift were observed. This mass difference corresponds to a glucosylgalactosyl disaccharide unit O-linked to hydroxylysine residues (Fig. 3B,D) [23]. Moreover, a regular 16 Da mass shift corresponding to the addition of several hydroxyl groups (as indicated in Fig. 3B-D) was observed as second post-translational modification. This revealed a high level of post-translational modifications heterogeneity and did not allow attribution of these three polypeptide chains to A, B, or C CLR_nc2 chains. Of note, similar hydroxylation and O-glycosylation diversity have been reported in both serum-derived and recombinant C1q [10,22].

Furthermore, in order to assess its proper assembly, CLR_nc2 was analyzed using mass photometry (MP), an emerging technique that enables accurate native mass measurements of single molecules in solution [24,25]. MP experiments on CLR_nc2 protein allowed determination of a native mass of 259 ± 8 kDa (mean $\pm$ SD, $n = 4$; Fig. 4A). This native mass of the $(ABC)_6$ assembly is in agreement with the calculated mass of 240 kDa without post-translational modifications (Fig. 1B) and also with the assembly of three

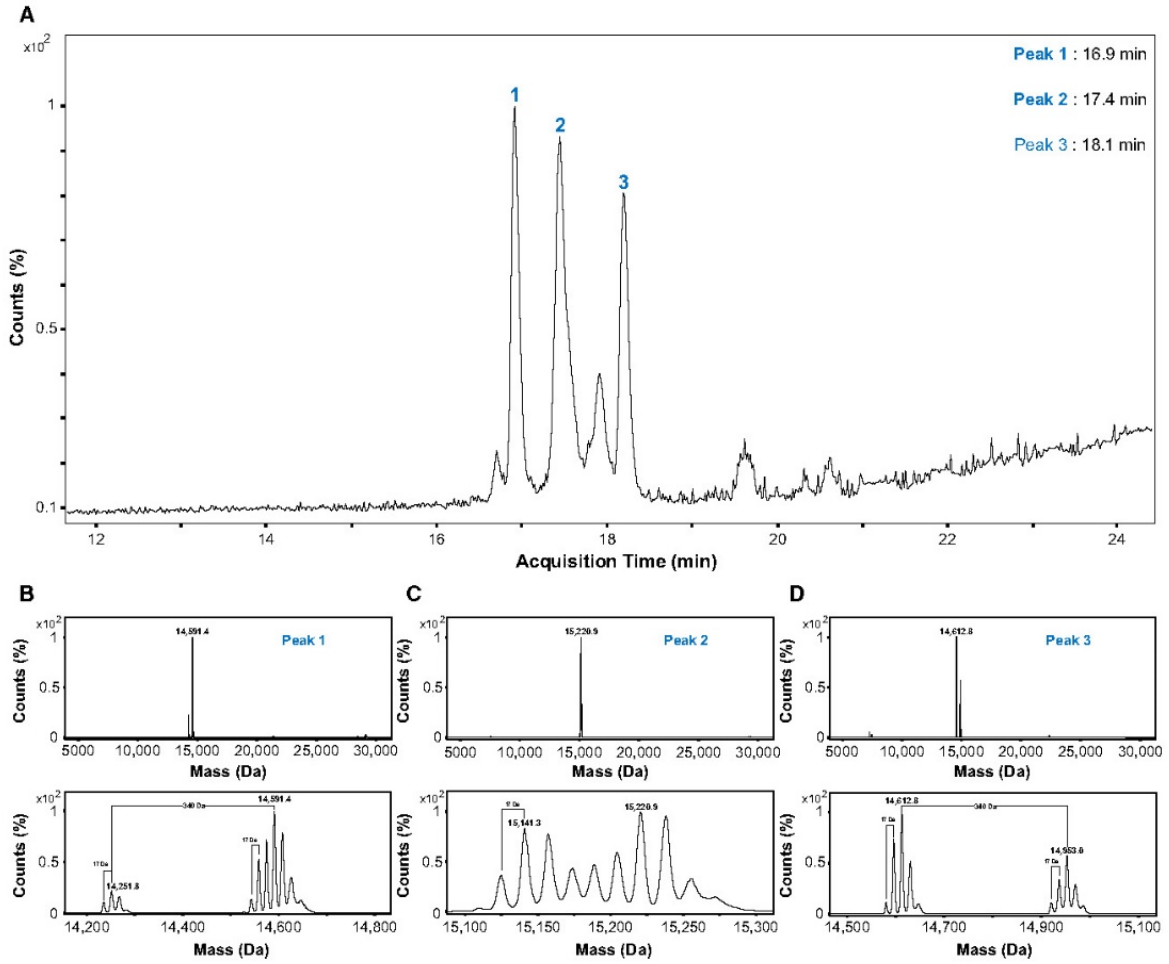

Fig. 3. LC/ESI MS analysis of CLR_nc2. (A) LC/MS chromatogram of reduced CLR_nc2 showing three major peaks. (B-D) Deconvoluted ESI TOF mass spectra (top panels) corresponding to the three main species labeled 1, 2, and 3 (from the A chromatogram), respectively. The bottom panels are more detailed views of each peak content. Observed masses of the major peaks are indicated in black, and regular mass shifts of 16 Da are indicated.

$(ABC)_2$ units of 88 kDa, as determined by MALDI-MS (Fig. 2C). Moreover, MP experiments demonstrated the high sample homogeneity with 80% of the molecules yielding a native mass of 260 kDa (Fig. 4A).

Negative-stain electron microscopy (EM) was then performed to visualize CLR_nc2 protein using sodium silicotungstate as stain. As shown in Fig. 4B-E, well-defined oligomeric particles exhibiting the C1q characteristic bouquet shape were clearly observed. Indeed, negative-stain EM allowed identifying isolated particles with high-contrast central bundle of collagen fibers and divergent flexible stalks. These images are comparable to previous EM analyses of pepsin-digested sC1q [26].

Altogether, these results reveal that GRs substitution by nc2 domains leads to the correct assembly of C1q collagen-like chains.

Functional properties of CLR_nc2

The interaction properties of CLR_nc2 were analyzed by surface plasmon resonance (SPR) and compared to those of serum-derived C1q and CLR (sCLR), using known physiological ligands of C1q CLRs and GRs. Serum-derived and recombinant fragments of C1q

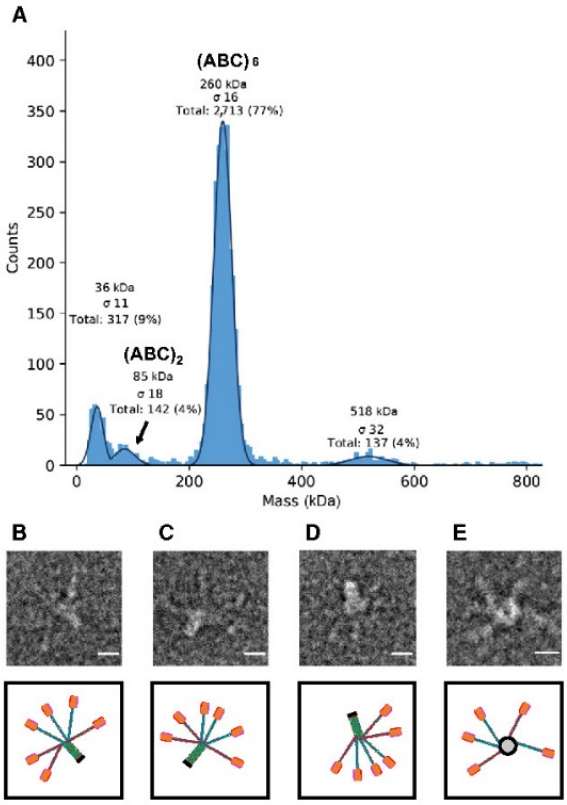

Fig. 4. Characterization of CLR_nc2 assembly and folding. (A) MP analysis of CLR_nc2 and native mass determination. Histogram of one representative experiment is shown. (B-E) Negative-stain EM analysis of CLR_nc2. Representative side views (B, C, and D) and top view (E) of well-contrasted CLR_nc2 particles are shown in the top panels. Bottom panels show schematic representations of CLR_nc2 in the same orientations as in the top panels. Scale bars representing 10 μm are shown in white in the right-bottom corners.

were immobilized on the surface of a sensor chip, and C1q ligands were used as soluble analytes. The tetramer of C1r and C1s serine proteases ($C1r_2s_2$) and MBL-associated protein MAp44 (also called MAP-1), a truncated form of MBL-associated serine protease 3 including the N-terminal CUB1-EGF-CUB2 interaction region, were first tested. These two C1q ligands have been described for their interaction on the same binding site in the CLRs [10]. As illustrated in Fig. 5A, $C1r_2s_2$ bound to both sC1q and recombinant CLR_nc2. Interestingly, our experimental settings did not allow detection of $C1r_2s_2$ binding to sCLR. However, others described $C1r_2s_2$ interaction with sCLR in solution and this difference may be explained by experimental bias due to the immobilization procedure [6]. Nevertheless, MAp44 bound to each C1q derivative (Fig. 5B). Kinetic analysis of $C1r_2s_2$ and MAp44 interaction with sC1q, sCLR, and CLR_nc2 showed a dose-dependent binding response allowing determination of their kinetic interaction constants. The tetramer $C1r_2s_2$ bound recombinant CLR_nc2 with less but still high affinity compared to sC1q with apparent K_D values of 50.3 ± 8.6 nM and 3.43 ± 0.05 nM, respectively (Fig. 6A and Table 1). Moreover, concerning MAp44, we could observe comparable apparent K_D values in the nM range for binding to sC1q, sCLR, and recombinant CLR_nc2 with similar association and dissociation rate constants (Fig. 6B and Table 1). These results indicate that CLR_nc2 retains the binding properties of sC1q and is therefore fully functional.

In addition to immobilization bias, the differences observed regarding $C1r_2s_2$ interaction properties suggest an indirect contribution of the GR domains. Indeed, in sC1q, electrostatic repulsions between the globular heads may restrict the opening and closing of the CLR bouquet structure and somehow guide the appropriate accessibility of the $C1r_2s_2$ binding sites. Therefore, removing the GRs may result in more flexible sCLR with a too close or too open bouquet structure that cannot accommodate $C1r_2s_2$ binding (Fig. 6A, middle panel). Replacement of the GRs by the nc2 domains nevertheless allows partial recovery of the appropriate accessibility of $C1r_2s_2$ binding sites, explaining why we observe less affinity for $C1r_2s_2$ binding to CLR_nc2 than to sC1q (Fig. 6A and Table 1). Indeed, even if an nc2 domain has a similar length as a C1q GR, it has a three times smaller width and should induce less steric hindrance of the C-terminal nc2 domains within the CLR_nc2 protein (Fig. 1). This would certainly lead to a less efficient control of the bouquet structure opening and therefore to a reduced affinity for $C1r_2s_2$. Conversely, in the case of MAp44, which assembles in a less bulky oligomer than $C1r_2s_2$, we can observe comparable apparent K_D values for binding to sC1q, sCLR, and recombinant CLR_nc2 (Fig. 6B and Table 1). This could be explained by the smaller conformational rearrangement of the CLRs likely required for MAp44 binding compared to $C1r_2s_2$. Indeed, MAp44 assembles as a homodimer with a smaller size than $C1r_2s_2$ (88 and 340 kDa, respectively) and also with a lower number of CLR binding sites compared to $C1r_2s_2$ (4 versus 6 binding sites, respectively) [27,28].

Finally, pentraxin 3 (PTX3) and IgM, two known C1q GR ligands, were tested [11]. As expected, both bound to sC1q but did not interact either with sCLR or recombinant CLR_nc2 (Fig. 5C,D). This fully demonstrates that the recombinant CLR_nc2 fusion

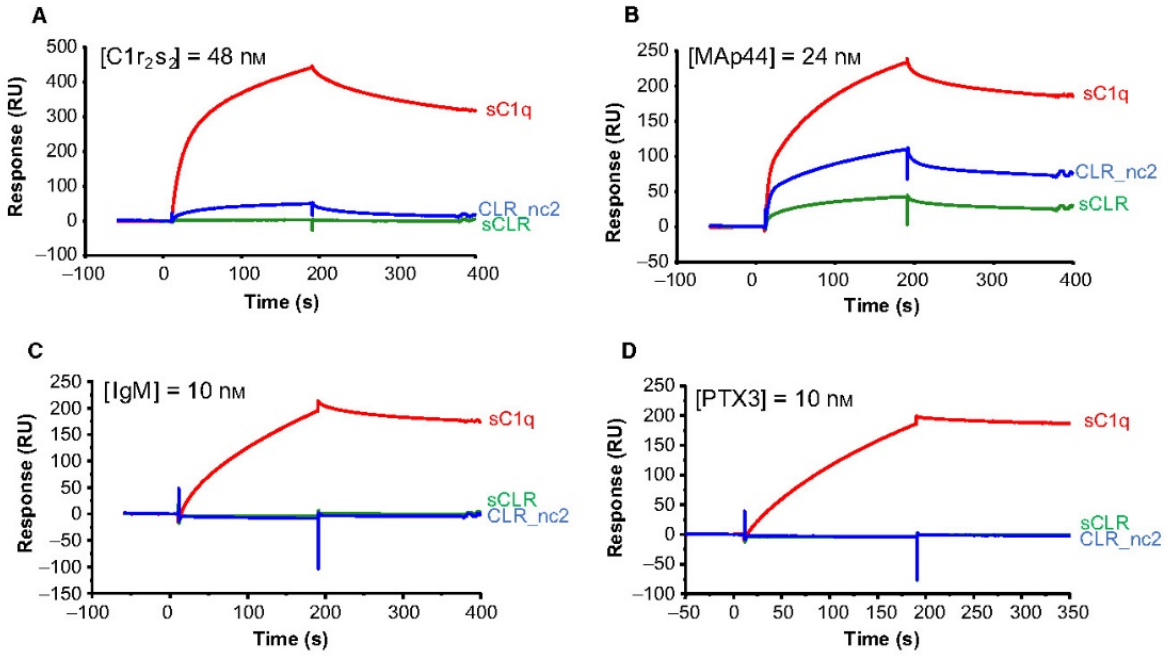

Fig. 5. Interaction of $C1r_2s_2$, MAp44, IgM, and PTX3 with immobilized serum C1q, serum CLR, and CLR_nc2. $C1r_2s_2$ at 48 nM (A), MAp44 at 48 nM (B), IgM at 10 nM (C), and PTX3 at 10 nM (D) were injected at a flow rate of 30 $\mu L \cdot min^{-1}$ in 50 mM Tris/HCl, 150 mM NaCl, 2 mM $CaCl_2$, 0.05% surfactant P20 (pH 7.5) on 14 000 RU, 6200 RU, and 7100 RU of immobilized serum C1q (sC1q), serum CLR (sCLR), and CLR_nc2, respectively.

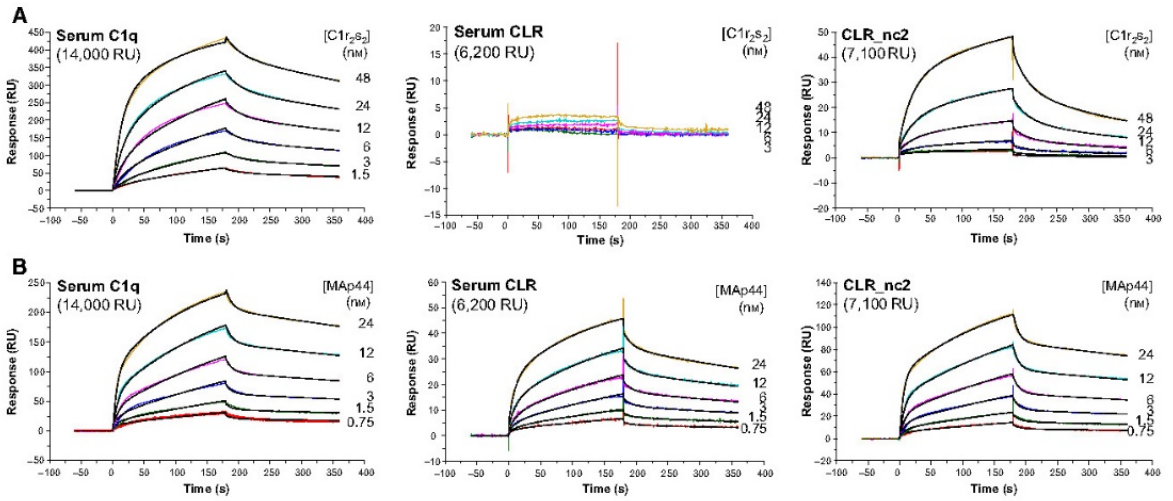

Fig. 6. Kinetic analysis of the interaction of $C1r_2s_2$ and MAp44 with immobilized serum C1q, serum CLR and CLR_nc2. $C1r_2s_2$ (A) and MAp44 (B) were injected at the indicated concentrations over immobilized serum C1q (14 000 RU) (left), serum CLR (6200 RU) (middle), and CLR_nc2 (7100 RU) (right) at a flow rate of 30 $\mu L \cdot min^{-1}$ in 50 mM Tris/HCl, 150 mM NaCl, 2 mM $CaCl_2$, 0.05% surfactant P20 (pH 7.5). Fits obtained by a global fitting of the data to a two-state reaction model are shown in black. The results shown are representative of four ($C1r_2s_2$) or two (MAp44) experiments (Table 1).

Table 1. Kinetic and dissociation constants for binding of $C1r_2s_2$ and MAp44 to immobilized serum C1q, serum CLR, and recombinant CLR_nc2. Values are means ± SD of 4 and 2 separate experiments for $C1r_2s_2$ and MAp44 kinetics, respectively. The association (k_{a1}, k_{a2}) and dissociation (k_{d1}, k_{d2}) rate constants were determined by global fitting of the data using a two-state reaction binding model. The resulting dissociation constant was determined from the rate constants: $K_D = 1/[(k_{a1}/k_{d1})\ (1 + k_{a2}/k_{d2})]$. ND, Not determined.

		Immobilized C1q fragments		
Soluble C1q partners	Constants	sC1q	sCLR	CLR_nc2
$C1r_2s_2$	k_{a1} ($M^{-1}\cdot s^{-1}$)	$9.37 \pm 0.08 \times 10^5$	ND	$3.89 \pm 0.50 \times 10^5$
	k_{a2} ($M^{-1}\cdot s^{-1}$)	$1.49 \pm 0.03 \times 10^{-2}$	ND	$8.02 \pm 0.63 \times 10^{-3}$
	k_{d1} (s^{-1})	$3.01 \pm 0.13 \times 10^{-2}$	ND	$5.58 \pm 1.52 \times 10^{-2}$
	k_{d2} (s^{-1})	$1.78 \pm 0.03 \times 10^{-3}$	ND	$4.39 \pm 0.23 \times 10^{-3}$
	K_D (nM)	3.43 ± 0.05	ND	50.3 ± 8.6
MAp44	k_{a1} ($M^{-1}\cdot s^{-1}$)	$2.13 \pm 0.37 \times 10^6$	$1.32 \pm 0.17 \times 10^6$	$2.81 \pm 0.85 \times 10^6$
	k_{a2} ($M^{-1}\cdot s^{-1}$)	$1.81 \pm 0.12 \times 10^{-2}$	$1.67 \pm 0.04 \times 10^{-2}$	$1.27 \pm 0.04 \times 10^{-2}$
	k_{d1} (s^{-1})	$8.16 \pm 0.38 \times 10^{-2}$	$5.64 \pm 0.22 \times 10^{-2}$	$1.09 \pm 0.14 \times 10^{-1}$
	k_{d2} (s^{-1})	$1.03 \pm 0.02 \times 10^{-3}$	$1.85 \pm 0.09 \times 10^{-3}$	$1.01 \pm 0.03 \times 10^{-3}$
	K_D (nM)	2.1 ± 0.37	4.30 ± 0.64	2.32 ± 0.51

protein is devoid of the C1q GR functions and only retains the binding properties of its CLRs.

Conclusion

The substitution of C1q GR by the nc2 domain of type IX collagen allowed recombinant production of well-folded and functional CLRs of C1q. Such advancement yields to the first recombinant production of CLRs and opens the way for investigating the molecular basis for C1q interaction with CLR receptors such as leukocyte-associated Ig-like receptor 1 or CD91 [29,30]. Indeed, it is now possible to assess effects of point mutations on the binding properties of the isolated C1q CLRs. Of note, the achievement of the proper assembly, folding, and binding functions of CLR_nc2 fusion protein validated the model-based choice of C1q collagen chains registering (A: Leading, B: Middle and C: Trailing).

Interest in trimerization domains was first revealed in a study using an α-helical coiled coil to facilitate and stabilize homotrimeric collagen triple-helix folding [31]. However, register-specific control of heterotrimeric collagen assembly is challenging and only few examples of chains registering strategies have been reported [20,32,33]. This study is the first reported application of type IX collagen nc2 domains for protein engineering, and the strategy of recognition domains replacement by nc2 domains could be easily transferable to other collagen-containing proteins such as soluble defense collagens.

Up to now, generation of the CLRs of C1q was only possible by its peptic digestion. A major issue of this technical approach is that only native CLRs with C-terminal extremities defined by the protease specificity could be obtained. Thanks to the recombinant production of the CLR_nc2 protein, it is now possible to overpass this issue and generate the CLRs of C1q with a tight control of the N- and C-terminal extremities. This will give the opportunity to produce individual heterotrimeric C1q collagen stems with user-defined extremities. Such C1q collagen stems will represent interesting tools for structural and functional investigations of C1q/receptor complexes. For instance, a short C1q heterotrimeric helix containing the $C1r_2s_2$ binding site could be used to obtain structural insights into C1 complex assembly as it has been previously performed with a synthetic homotrimeric MBL-like collagen peptide [34]. Moreover, previous studies revealed that sCLR was able to act as C1 hemolytic activity inhibitor [35]. Therefore, C1q heterotrimeric helix fragments containing the $C1r_2s_2$ binding site may constitute an interesting classical pathway inhibitor by avoiding C1 complex formation and subsequent complement activation.

Materials and methods

Proteins and reagents

C1q was purified from human serum and quantified as described previously [36]. The CLR of C1q were prepared by pepsin digestion of C1q, according to Tacnet-Delorme *et al.* [37], and their molar concentration estimated using a mass value of 189 900 Da and an absorption coefficient ($A_{1\%,\ 1\ cm}$) at 280 nm of 2.1. $C1r_2s_2$ tetramer (C1s, C1rS637A) and MAp44 recombinant proteins were purified and quantified according to published procedures [11,38].

IgM, purchased from Sigma-Aldrich (St Quentin Fallavier, France) and PTX3, kindly provided by B. Bottazzi, was quantified as described previously with mass values of 833 000 and 340 000 Da, respectively [11].

Expression vectors and stably transfected cell lines

The coding sequences of C1q native signal peptides followed by CLRA fused to nc2α2, CLRB fused to nc2α1, and CLRC fused to nc2α3 with a C-terminal FLAG epitope were synthesized and cloned in pcDNA3.1/Neo(+), pcDNA3.1/Hygro(+), and pcDNA3.1/Zeo(+) vectors, respectively (Thermo Fisher Scientific, Illkirch, France).

EXPI293 cells grown in EXPI293 expression medium were cotransfected with CLR_nc2 fusions containing pcDNA3.1 vectors according to the manufacturer's protocol (Thermo Fisher Scientific). Stable transfectants expressing the three chains were selected using 400 μg·mL $^{-1}$ neomycin (Thermo Fisher Scientific), 100 μg·mL $^{-1}$ hygromycin (Sigma-Aldrich), and 10 μg·mL $^{-1}$ zeocin (Thermo Fisher Scientific).

Production of CLR_nc2 in eukaryotic cells and protein purification

The CLR_nc2 stably expressing cells were expanded in EXPI293 expression medium containing 100 μg·mL $^{-1}$ L-ascorbic acid (Sigma-Aldrich) in addition to the three selection antibiotics. The culture medium was harvested and replaced every 72 h of growth. CLR_nc2 containing culture medium was loaded on a 2 mL anti-FLAG M2 affinity column (Sigma-Aldrich) equilibrated in a 50 mM Tris/HCl, 150 mM NaCl (pH 7.4) buffer. After washing with 10 mL of equilibrating buffer, the bound material was eluted with 3 mL of a 100 μg·mL $^{-1}$ FLAG peptide solution in the same buffer. The elution fractions were concentrated and injected on a Superose 6 increase 10/300 GL column (GE Healthcare, Chicago, IL, USA). Pure CLR_nc2 containing fractions were concentrated to 0.4 mg·mL $^{-1}$. The concentration of purified CLR_nc2 was estimated using an absorption coefficient ($A_{1\%,\ 1\ cm}$) at 280 nm of 2.0 and a mass value of 260 000 Da, as determined by both MS and MP.

SDS/PAGE and western blot analyses

Recombinant CLR_nc2 was analyzed by SDS/PAGE under nonreducing and reducing conditions using 12.5% polyacrylamide Tris/HCl gels and then colored using InstantBlue (Expedeon, Abcam, Paris, France) or transferred on nitrocellulose membranes for western blot analysis using Trans-Blot turbo transfer system according to manufacturer's protocol (Bio-Rad, Marnes-la-Coquette, France). CLR_nc2 protein was detected using monoclonal ANTI-FLAG® M2-Peroxidase antibody (Sigma-Aldrich) or rabbit polyclonal anti-C1q serum (in house production) with HRP-conjugated secondary anti-rabbit antibody produced in mouse (Sigma-Aldrich).

MALDI-TOF mass spectrometry

MALDI-TOF mass spectra of protein samples were acquired with an Autoflex maX TOF/TOF mass spectrometer (Bruker Daltonics, Bremen, Germany) operated in linear positive ion mode. External mass calibration of the instrument was done using protein calibration standards from Bruker Daltonics providing mass accuracy < 1000 p.p.m. The protein samples were mixed in a ratio 1 : 20 (v/v) with sinapinic acid matrix [Sigma-Aldrich; 10 mg·mL $^{-1}$ in water/acetonitrile/trifluoroacetic acid (TFA), 50/50/0.1, v/v/v], and 0.5–1 μL of this mixture was deposited on the target and allowed to air dry. Mass spectra data were processed with FLEXANALYSIS software (v.3.4; Bruker Daltonics).

LC/ESI mass spectrometry

Liquid Chromatography Electrospray Ionization Mass Spectrometry (LC/ESI-MS) analyses were performed on a 6210 LC-TOF spectrometer coupled to a high-performance liquid chromatography (HPLC) system (Agilent Technologies, Les Ulis, France). All solvents used were HPLC grade (Chromasolv; Sigma-Aldrich), TFA was from Acros Organics. Solvent A was 0.03% TFA in water, solvent B was 95% acetonitrile-5% water-0.03% TFA.

Before analysis, protein samples were treated with 50 mM dithiothreitol (DTT) at 56 °C for 30 min and then diluted in acidic denaturing conditions to a final concentration of 10 μM with solvent A. Protein samples were firstly desalted on a reverse phase-C8 cartridge (Zorbax 300SB-C8, 5 μm, 300 Å 5 × 0.3 mm; Agilent Technologies) and then separated on a RP-HPLC column (Jupiter C4, 5 μm, 300 Å, 50 × 1 mm; Phenomenex, Le Pecq, France) with a linear gradient from 5% to 95% solvent B in 15 min.

MS spectra were recorded in the positive ion mode in the 300–3200 *m/z* range and the data processed with MASSHUNTER workstation software (v. B.02.00; Agilent Technologies).

Mass photometry

Preparation of sample carrier

Coverslips (high precision glass coverslips, 24 × 50 mm^2, No. 1.5H; Marienfeld, Lauda-Königshofen, Germany) were cleaned by sequential sonication in Milli-Q H_2O, 50% isopropanol (HPLC grade)/Milli-Q H_2O, and Milli-Q H_2O (5 min each), followed by drying with a clean nitrogen

stream. To keep the sample droplet in shape, reusable self-adhesive silicone culture wells (Grace Bio-Labs reusable CultureWell™ gaskets) were cut in segments of 4. To ensure proper adhesion to the coverslips, the gaskets were dried well by using a clean nitrogen stream. To prepare a sample carrier, gaskets were placed in the center of the cleaned coverslip and fixed tightly by applying light pressure with the back of a pipette tip.

Measurement and data acquisition

Protein landing was recorded using a Refeyn One^{MP} (Refeyn Ltd., Oxford, UK) MP system by adding 0.5 µL of the protein stock solution (1.7 µM) directly into a 19.5 µL drop of 50 mM Tris, 150 mM NaCl (pH 7.5) solution. The sample final concentration was 85 nM. Movies were acquired for 120 s (12 000 frames) with Acquire^{MP} (Refeyn Ltd., v2.1.1) software using standard settings.

Image processing

Data were analyzed using Discover^{MP} (Refeyn LTD, v2.1.1). A detailed description of the data processing was previously reported [24].

Discover^{MP} analysis parameters were set to T1 = 1.2 for threshold 1. The values for number of binned frames (nf = 8), threshold 2 (T2 = 0.25), and median filter kernel (=15) remained constant.

Calibration procedure

Contrast-to-mass (C2M) calibration was performed using a mix of proteins with molecular weight of 66, 146, 500, and 1046 kDa. The calibration experiment was analyzed using Discover^{MP} default settings (T1 = 1.5, T2 = 0.25, nf = 5, median filter kernel = 15). The mean peak contrasts were determined in the software using Gaussian fitting. The mean contrast values were then plotted and fitted to a line.

Electron microscopy

CLR_nc2 samples (2 µg·mL^{-1}) were adsorbed to the clean side of a carbon film on mica, negatively stained with 1% (w/v) sodium silicotungstate, and transferred to a 400-mesh copper grid. The images were taken under low dose conditions (< 10 $e^-/Å^2$) with defocus values between 1.2 and 2.5 µm on a Tecnai 12 LaB6 electron microscope at 120 kV accelerating voltage using CCD Camera Gatan Orius 1000.

Surface Plasmon resonance analysis and evaluation

All experiments were performed at 25 °C on a BIAcore T200 instrument (GE Healthcare). Serum C1q and CLR derivatives were diluted to 35 and 25 µg·mL^{-1} in 10 mM sodium acetate (pH 5), respectively, and immobilized on CM5 sensor chips (GE Healthcare) using the amine coupling chemistry in 10 mM HEPES, 150 mM NaCl, 3 mM EDTA, 0.05% (v/v) surfactant P20 (pH 7.4). Binding of $C1r_2s_2$ tetramer, MAp44, PTX3, and IgM was measured at a flow rate of 30 µL·min^{-1} in 50 mM Tris/HCl, 150 mM NaCl, 2 mM $CaCl_2$, 0.05% surfactant P20 (pH 7.5) over 14 000 resonance unit (RU) of immobilized serum C1q, 6200 RU of serum CLR, and 7100 RU of recombinant CLR_nc2. The specific binding signal was obtained by subtracting the background signal over the reference surface submitted to the coupling steps without immobilized protein. Regeneration of the surfaces was achieved by injection of 15 µL of 1 M NaCl, 10 mM EDTA (pH 7.5).

Data were analyzed by global fitting to a two-state reaction binding model of both the association and dissociation phases for at least six analyte concentrations simultaneously, using the T200 BIAEVALUATION 3.1 software (GE Healthcare). Buffer blanks were subtracted from the data sets used for kinetic analysis (double referencing). The apparent dissociation constants were calculated from the rate constants: $K_D = 1/[(k_{a1}/k_{d1})(1 + k_{a2}/k_{d2})]$.

Acknowledgements

This work used the SPR, EM, and MS facilities at the Grenoble Instruct-ERIC Center (ISBG; UMS 3518 CNRS CEA-UGA-EMBL) with support from the French Infrastructure for Integrated Structural Biology (FRISBI; ANR-10-INSB-05-02) and GRAL, a project of the University Grenoble Alpes graduate school (Ecoles Universitaires de Recherche) CBH-EUR-GS (ANR-17-EURE-0003) within the Grenoble Partnership for Structural Biology. We thank Daphna Fenel and Wai Li Ling for the EM experiments and Anne Chouquet and Jean-Baptiste Reiser for access to the SPR platform. We acknowledge Pascale Tacnet-Delorme, Barbara Bottazzi, and Fabien Dalonneau for providing sC1q, PTX3, and $C1r_2s_2$ samples, respectively. Research reported in this manuscript was supported by the French National Research Agency (grant ANR-16-CE11-0019). IBS acknowledges integration into the Interdisciplinary Research Institute of Grenoble (IRIG, CEA).

Conflict of interest

The authors declare no conflict of interest.

Author contributions

GF, NMT, VR, and CG conceptualized the study. GF, NMT, VR, and CG were involved in methodology,

validation, and formal analysis. GF, IB, LS, and KH investigated the study. GF wrote the original draft. GF, NMT, VR, and CG wrote, reviewed and edited the manuscript. NMT contributed to funding acquisition. NMT, VR, and CG supervised the study. All authors read and approved the manuscript.

References

1 Shelton E, Yonemasu K & Stroud RM (1972) Ultrastructure of the human complement component, Clq. *Proc Natl Acad Sci USA* **69**, 65–68.
2 Thielens NM, Tedesco F, Bohlson SS, Gaboriaud C & Tenner AJ (2017) C1q: a fresh look upon an old molecule. *Mol Immunol* **89**, 73–83.
3 Reid KBM, Lowe DM & Porter RR (1972) Isolation and characterization of C1q, a subcomponent of the first component of complement, from human and rabbit sera. *Biochem J* **130**, 749–763.
4 Reid KBM (1976) Isolation, by partial pepsin digestion, of the three collagen-like regions present in subcomponent Clq of the first component of human complement. *Biochem J* **155**, 5–17.
5 Hughes-Jones NC & Gardner B (1979) Reaction between the isolated globular sub-units of the complement component C1q and IgG-complexes. *Mol Immunol* **16**, 697–701.
6 Siegel RC & Schumaker VN (1983) Measurement of the association constants of the complexes formed between intact C1q or pepsin-treated C1q stalks and the unactivated or activated C1r2C1s2 tetramers. *Mol Immunol* **20**, 53–66.
7 Gaboriaud C, Frachet P, Thielens NM & Arlaud GJ (2011) The human c1q globular domain: structure and recognition of non-immune self ligands. *Front Immunol* **2**, 92.
8 Ugurlar D, Howes SC, de Kreuk B-J, Koning RI, de Jong RN, Beurskens FJ, Schuurman J, Koster AJ, Sharp TH, Parren PWHI *et al.* (2018) Structures of C1-IgG1 provide insights into how danger pattern recognition activates complement. *Science* **359**, 794–797.
9 Eggleton P, Tenner AJ & Reid KBM (2000) C1q receptors. *Clin Exp Immunol* **120**, 406–412.
10 Bally I, Ancelet S, Moriscot C, Gonnet F, Mantovani A, Daniel R, Schoehn G, Arlaud GJ & Thielens NM (2013) Expression of recombinant human complement C1q allows identification of the C1r/C1s-binding sites. *Proc Natl Acad Sci USA* **110**, 8650–8655.
11 Bally I, Inforzato A, Dalonneau F, Stravalaci M, Bottazzi B, Gaboriaud C & Thielens NM (2019) Interaction of C1q With pentraxin 3 and IgM revisited: mutational studies with recombinant C1q variants. *Front Immunol* **10**, 461.
12 Moreau C, Bally I, Chouquet A, Bottazzi B, Ghebrehiwet B, Gaboriaud C & Thielens N (2016) Structural and functional characterization of a single-chain form of the recognition domain of complement protein C1q. *Front Immunol* **7**, 79.
13 Espericueta V, Manughian-Peter AO, Bally I, Thielens NM & Fraser DA (2020) Recombinant C1q variants modulate macrophage responses but do not activate the classical complement pathway. *Mol Immunol* **117**, 65–72.
14 Païdassi H, Tacnet-Delorme P, Verneret M, Gaboriaud C, Houen G, Duus K, Ling WL, Arlaud GJ & Frachet P (2011) Investigations on the C1q–calreticulin–phosphatidylserine interactions yield new insights into apoptotic cell recognition. *J Mol Biol* **408**, 277–290.
15 Jacquet M, Cioci G, Fouet G, Bally I, Thielens NM, Gaboriaud C & Rossi V (2018) C1q and mannose-binding lectin interact with CR1 in the same region on CCP24-25 modules. *Front Immunol* **9**, 24–25.
16 Kishore U & Reid KB (1999) Modular organization of proteins containing C1q-like globular domain. *Immunopharmacology* **42**, 15–21.
17 Boudko SP, Engel J & Bächinger HP (2012) The crucial role of trimerization domains in collagen folding. *Int J Biochem Cell Biol* **44**, 21–32.
18 Boudko SP, Zientek KD, Vance J, Hacker JL, Engel J & Bächinger HP (2010) The NC2 domain of collagen IX provides chain selection and heterotrimerization. *J Biol Chem* **285**, 23721–23731.
19 Boudko SP & Bächinger HP (2012) The NC2 domain of type IX collagen determines the chain register of the triple helix. *J Biol Chem* **287**, 44536–44545.
20 Boudko SP & Bächinger HP (2016) Structural insight for chain selection and stagger control in collagen. *Sci Rep* **6**, 37831.
21 Gaboriaud C, Juanhuix J, Gruez A, Lacroix M, Darnault C, Pignol D, Verger D, Fontecilla-Camps JC & Arlaud GJ (2003) The crystal structure of the globular head of complement protein C1q provides a basis for its versatile recognition properties. *J Biol Chem* **278**, 46974–46982.
22 Pflieger D, Przybylski C, Gonnet F, Le Caer J-P, Lunardi T, Arlaud GJ & Daniel R (2010) Analysis of human C1q by combined bottom-up and top-down mass spectrometry. *Mol Cell Proteomics* **9**, 593–610.
23 Shinkai H & Yonemasu K (1979) Hydroxylysine-linked glycosides of human complement subcomponent C1q and various collagens. *Biochem J* **177**, 847–852.
24 Sonn-Segev A, Belacic K, Bodrug T, Young G, VanderLinden RT, Schulman BA, Schimpf J, Friedrich T, Dip PV, Schwartz TU *et al.* (2019) Quantifying the heterogeneity of macromolecular machines by mass photometry *bioRxiv*, 864553. "[PREPRINT]"
25 Young G, Hundt N, Cole D, Fineberg A, Andrecka J, Tyler A, Olerinyova A, Ansari A, Marklund EG, Collier MP *et al.* (2018) Quantitative mass imaging of single biological macromolecules. *Science* **360**, 423–427.

26 Brodsky-Doyle B, Leonard KR & Reid KB (1976) Circular-dichroism and electron-microscopy studies of human subcomponent C1q before and after limited proteolysis by pepsin. *Biochem J* **159**, 279–286.
27 Skjoedt M-O, Roversi P, Hummelshøj T, Palarasah Y, Rosbjerg A, Johnson S, Lea SM & Garred P (2012) Crystal structure and functional characterization of the complement regulator mannose-binding lectin (MBL)/ficolin-associated protein-1 (MAP-1). *J Biol Chem* **287**, 32913–32921.
28 Bally I, Rossi V, Lunardi T, Thielens NM, Gaboriaud C & Arlaud GJ (2009) Identification of the C1q-binding sites of human C1r and C1s a refined three-dimensional model of the C1 complex of complement. *J Biol Chem* **284**, 19340–19348.
29 Son M, Santiago-Schwarz F, Al-Abed Y & Diamond B (2012) C1q limits dendritic cell differentiation and activation by engaging LAIR-1. *Proc Natl Acad Sci USA* **109**, E3160–E3167.
30 Duus K, Hansen EW, Tacnet P, Frachet P, Arlaud GJ, Thielens NM & Houen G (2010) Direct interaction between CD91 and C1q. *FEBS J* **277**, 3526–3537.
31 Yoshizumi A, Fletcher JM, Yu Z, Persikov AV, Bartlett GJ, Boyle AL, Vincent TL, Woolfson DN & Brodsky B (2011) Designed coiled coils promote folding of a recombinant bacterial collagen. *J Biol Chem* **286**, 17512–17520.
32 Hentzen NB, Islami V, Köhler M, Zenobi R & Wennemers H (2020) A lateral salt bridge for the specific assembly of an ABC-type collagen heterotrimer. *J Am Chem Soc* **142**, 2208–2212.
33 Fallas JA, Gauba V & Hartgerink JD (2009) Solution structure of an ABC collagen heterotrimer reveals a single-register helix stabilized by electrostatic interactions. *J Biol Chem* **284**, 26851–26859.
34 Venkatraman Girija U, Gingras AR, Marshall JE, Panchal R, Sheikh MA, Harper JAJ, Gál P, Schwaeble WJ, Mitchell DA, Moody PCE *et al.* (2013) Structural basis of the C1q/C1s interaction and its central role in assembly of the C1 complex of complement activation. *Proc Natl Acad Sci USA* **110**, 13916–13920.
35 Reid KB, Sim RB & Faiers AP (1977) Inhibition of the reconstitution of the haemolytic activity of the first component of human complement by a pepsin-derived fragment of subcomponent C1q. *Biochem J* **161**, 239–245.
36 Arlaud J, Sim B & Colomb G (1979) Differential elution of Clq, Clr and Cls from human Cl bound to immune aggregates. Use in the rapid purification of Cl subcomponents. *Mol Immunol* **16**, 445–450.
37 Tacnet-Delorme P, Chevallier S & Arlaud GJ (2001) Amyloid fibrils activate the C1 complex of complement under physiological conditions: evidence for a binding site for A on the C1q globular regions. *J Immunol* **167**, 6374–6381.
38 Henriksen ML, Brandt J, Andrieu J-P, Nielsen C, Jensen PH, Holmskov U, Jorgensen TJD, Palarasah Y, Thielens NM & Hansen S (2013) Heteromeric complexes of native collectin kidney 1 and collectin liver 1 are found in the circulation with MASPs and activate the complement system. *J Immunol* **191**, 6117–6127.

II. Article 2: Molecular basis of complement C1q collagen-like region interaction with the immunoglobulin-like receptor LAIR-1

1 Scientific context and relevance of the article

LAIR-1 has been mostly described in the literature for its interaction with collagens and it was therefore reasonably suggested that its interaction with C1q was performed via its collagen-like regions. However, this question was addressed in only few studies and further investigations were needed. The use of the CLR_nc2 protein described in Article 1 unambiguously validated the CLR engagement into C1q interaction with LAIR-1. However, we had to slightly modify the recombinant CLR_nc2 protein before using it for the study with LAIR-1. Indeed, when we first designed the CLR_nc2 protein, we introduced three additional collagen GPP triplets between the CLR and nc2 sequences in order to facilitate the collagen triple-helix formation (Article 1). These GPP triplets are likely modified into GPO triplets during the CLR_nc2 processing. There is no doubt in the literature that GPO triplets are high affinity ligands for LAIR-1 and these additional triplets could have introduced artifactual supplementary binding sites in the molecule (Lebbink et al. 2006, 2009). Therefore, we had to remove these collagen triplets from the CLR_nc2 in order to avoid non C1q-specific binding of LAIR-1 to the CLR_nc2. Fortunately, the removal of these additional collagen triplets did not hamper the correct assembly and folding of the C1q collagen-like regions. In order to distinguish this new generation of the CLR_nc2 without the GPP triplets, we decided to rename it C1qCLR_nc2. Moreover, we also generated the first recombinant C1q collagen stem by deleting the N-terminal bundle from the C1qCLR_nc2 that we called C1qstem_nc2. The three different CLR_nc2 fusion constructs used in the following manuscript are shown in Figure 21.

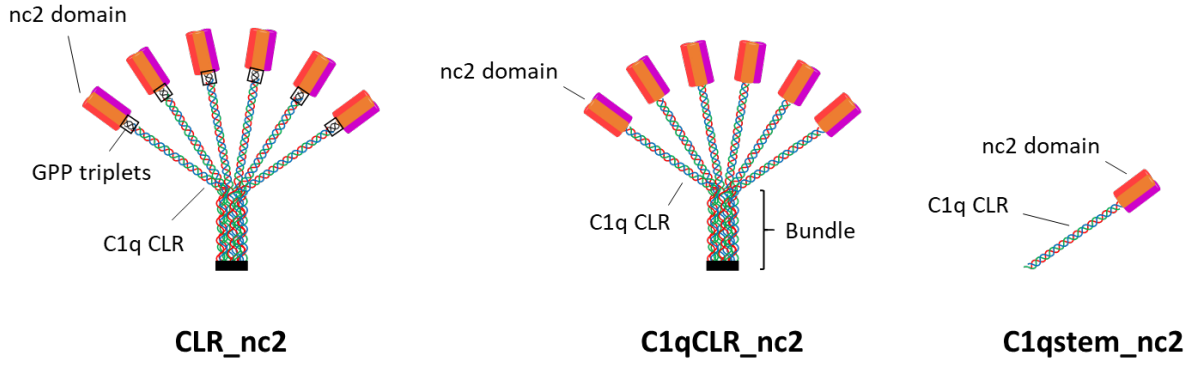

Figure 21: Schematic representation of the CLR_nc2 (left), C1qCLR_nc2 (middle) and C1qstem_nc2 (right). *The nc2 domains are represented as red, orange and purple cylinders, the additional GPP triplets inserted into the CLR_nc2 are colored in black and the C1q collagen chains are shown in red, blue and green.*

Moreover, we investigated C1q/LAIR-1 interaction on the side of LAIR-1. To our knowledge, only one published study aimed at identifying the LAIR-1 amino acid residues involved in the interaction with collagen peptides (Brondijk et al. 2010b). In this study, Brondijk and colleagues performed nuclear magnetic resonance (NMR) experiments to map LAIR-1 residues involved in the interaction with a collagen III peptide. Binding assays using flow cytometry with cells transfected with wild-type or mutated membrane LAIR-1 allowed them to determine the essential role of the two highly conserved arginine 59 (R59) and glutamate 61 (E61) LAIR-1 residues. Interestingly, these two residues are also highly conserved in the glycoprotein VI, another Ig-like collagen receptor, homologous to LAIR-1. This strongly suggests that both LAIR-1 and GPVI interact with collagens using a common mechanism.

To our great surprise, we found a crystal structure of the GPVI Ig-like domain in complex with a collagen peptide deposited in the protein data bank, with no publication associated (PDB code 5OU8) (Figure 22). This structure revealed the central position of the GPVI R38 and E40 residues, homologous to the LAIR-1 R59 and E61, in the binding of the collagen peptide. Moreover, analysis of this structure revealed that the collagen motif recognized by the GPVI mainly corresponds to the hydroxyproline residues of two consecutive GPO triplets (GP**OG**P**O**) (Figure 22). By homology, we made the assumption that this specific collagen motif is also likely recognized by LAIR-1 through it R59 and E61 residues in collagens in general and in our case in C1q CLR sequence.

Interestingly, the GPVI Ig-like domain contains one tryptophan residue (W76) that recognizes the neighboring collagen chain (Figure 22). This tryptophan residue is conserved in LAIR-1 sequence (W109). This particular residue may therefore be involved in the collagen recognition by LAIR-1.

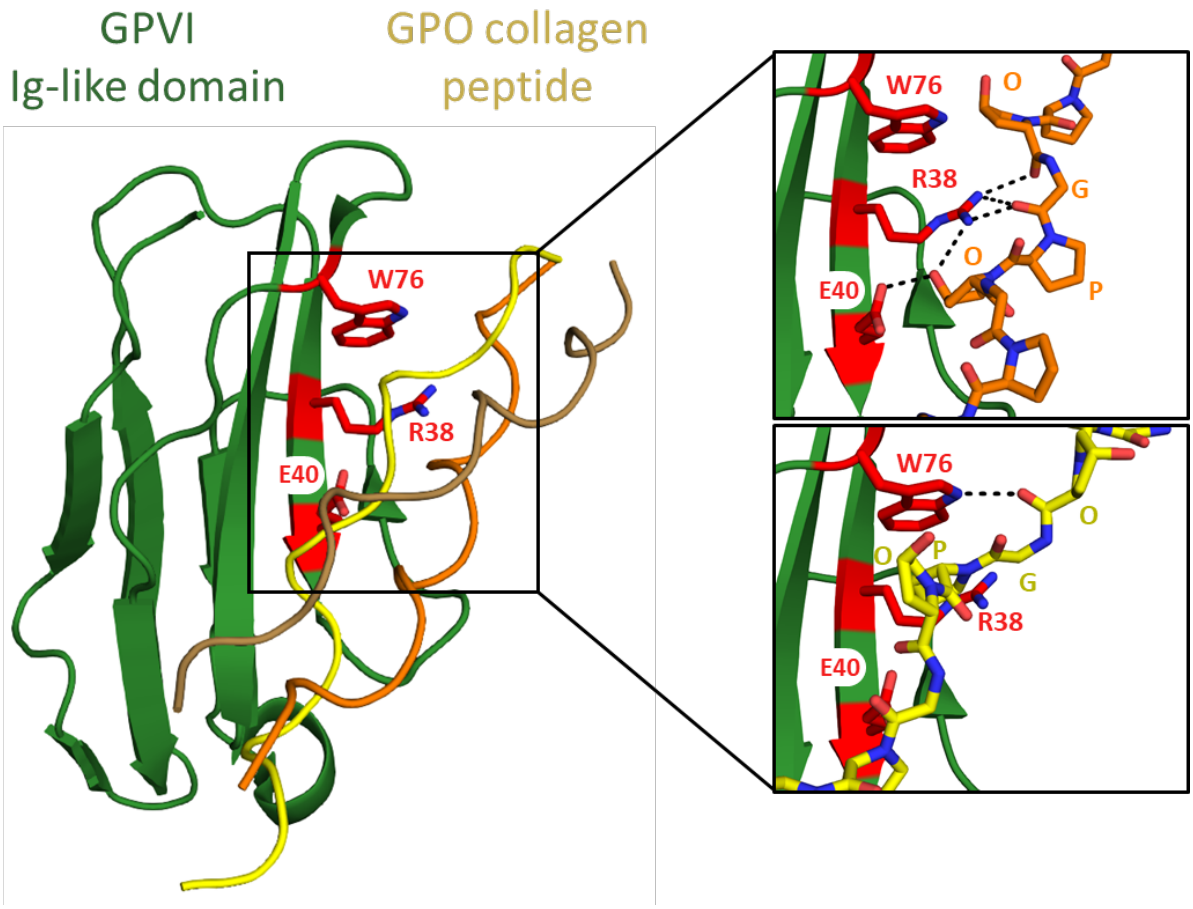

Figure 22: Molecular and structural determinants of collagen recognition by the glycoprotein VI. *Cartoon representation of the crystal structure of the glycoprotein VI (GPVI) (in green) in complex with a GPO collagen peptide (in yellow) (PDB code 5OU8). The two central arginine 38 (R38) and glutamate 40 (E40) as well as the tryptophan 76 (W76) are labeled in red. The inserts show a close view of the GPVI-collagen interface. The side chains of the residues involved in the interaction are shown with a stick representation. The hydrogen bonds between the GPVI and collagen amino acids are represented with black dashed lines.*

By cross-checking these literature-based and structural data with our own experiments, we proposed a model for LAIR-1 Ig-like domain interaction with the C1q collagen-like region. The following manuscript (in preparation) reports our work on the detailed molecular deciphering of C1q interaction with LAIR-1 Ig-like domain.

Molecular basis of complement C1q collagen-like region interaction with the immunoglobulin-like receptor LAIR-1

Guillaume Fouët[1], Isabelle Bally[1], Anne Chouquet[1], Jean-Baptiste Reiser[1], Nicole M. Thielens[1], Christine Gaboriaud[1*] and Véronique Rossi[1*]

[1]Univ. Grenoble Alpes, CEA, CNRS, IBS, F-38000 Grenoble, France.

[*] Correspondence: Christine Gaboriaud christine.gaboriaud@ibs.fr

Véronique Rossi veronique.rossi@ibs.fr

Abstract

The immune system homeostasis relies on a tight equilibrium of interconnected stimulatory and inhibitory signals. Disruption of this balance is characteristic of autoimmune diseases such as systemic lupus erythematosus (SLE). Aside from activating the classical complement pathway and enhancing pathogens and apoptotic cells phagocytosis, C1q has been recently shown to play an important role in immune modulation and tolerance by interacting with several inhibitory and stimulatory immune receptors. Due to its functional organization into collagen-like (CLR) and globular (GR) regions and its multimeric nature, C1q is able to interact simultaneously with several of these receptors and locally congregate pro- and anti-inflammatory signals, thus modulating the immune response. Leukocyte associated immunoglobulin-like (Ig-like) receptor 1 (LAIR-1), an ubiquitous collagen receptor expressed in many immune cell types, has been reported to interact with the CLR of C1q. In this study, we provide new insights into the molecular and structural determinants underlying C1q/LAIR-1 interaction. Recombinant LAIR-1 extracellular Ig-like domain was produced and tested for its interaction with C1q. A molecular dissection of C1q combined with competition assays reveals that LAIR-1 interacts with C1q's CLR through a binding site close but different from the one of its associated $C1r_2s_2$ proteases tetramer. On the other side, we identified LAIR-1 residues involved in C1q interaction by site-directed mutational analysis. All together, these results lead to propose a possible model for C1q interaction with LAIR-1 and will contribute to the fundamental understanding of C1q-mediated immune tolerance.

Introduction

The ability of the immune system to provide an efficient response against pathogens without hyper reacting against host tissues relies on a tight balance between pro- and anti-inflammatory signals. Disruption of this equilibrium can lead to autoimmunity. C1q, a protein initially identified as the recognition protein that triggers the classical pathway of the

complement system, has been shown to play a major role in the maintenance of immune tolerance (Nayak et al. 2012). Indeed, homozygous deficiencies in C1q are strongly associated with severe autoimmune inflammatory diseases such as systemic lupus erythematosus (SLE) (>90% prevalence) (Walport et al. 1998). C1q is a multimeric protein composed of 18 polypeptide chains of type A, B and C. Assembled in 6 heterotrimers maintained by both non-covalent and covalent interactions, these chains are composed of a short N-terminal part containing interchain disulfide bonds (between A-B and C-C), followed by a collagen-like region (CLR) containing the collagen-characteristic repeating G-X-Y sequence (X being any amino acid and Y a proline or hydroxyproline residue) and a C-terminal globular region (GR) (Kishore et al. 2004). This complex assembly leads to the formation of a 460 kDa C1q protein with a "bouquet-like" structure, where 6 C-terminal globular domains are connected via 6 collagen stems gathered in an N-terminal fiber bundle (Shelton et al. 1972; Thielens et al. 2017). Functional studies revealed distinct activities for the GR and CLR of C1q. On one hand, the globular regions are mostly involved the recognition of several targets like antibodies Fc region, molecules on pathogens surfaces or altered-self components (Gaboriaud et al. 2011; Ugurlar et al. 2018). On the other hand, the collagen-like regions of C1q are engaged in immune response effector mechanisms through their interaction with a tetramer of complement C1r and C1s proteases ($C1r_2s_2$) or receptors on immune cells surface (Siegel and Schumaker 1983; Eggleton et al. 2000).

Leukocyte associated immunoglobulin-like receptor 1 (LAIR-1; CD305) is an inhibitory receptor of 32 kDa expressed on many types of immune cells and composed of an extracellular C2-type immunoglobulin-like (Ig-like) domain, a single transmembrane segment and a cytoplasmic tail containing two immunoreceptor tyrosine inhibitory motifs (ITIMs) (Meyaard et al. 1997; Meyaard 2008). It is well established that LAIR-1 is a receptor for a large range of collagen types, from extra cellular matrix and transmembrane collagens (such as collagens I, II, III, IV, XIII, XVII or XXIII) to collagen-containing proteins such as surfactant protein D (SP-D), mannose-binding lectin (MBL) or C1q. LAIR-1 activation by one of these identified ligands leads to its ITIMs phosphorylation, recruitment of SHP-1 tyrosine phosphatase and inhibition of pro-inflammatory signals (Lebbink et al. 2006, 2009; Son et al. 2012; Olde Nordkamp et al. 2014b; Son and Diamond 2015). Human LAIR-1 has a soluble homologue LAIR-2 shown to interact with the same ligands and supposed to control LAIR-1 inhibitory activity by competing for collagen binding (Lebbink et al. 2006, 2008, 2009). LAIR-1 is the only known inhibitory receptor of C1q CLR and Son and colleagues have reported that it is an important mediator of C1q-mediated immune tolerance, together with other immune receptors such as CD33 and the receptor for advanced-glycation end-products (RAGE) (Son et al. 2012, 2016, 2017). Due to its multimeric nature, C1q would likely interact with several of these receptors simultaneously,

thus generating local gathering of pro- and anti-inflammatory signals. However, these processes remain unclear and the molecular and structural determinants of C1q interaction with these receptors have not yet been identified.

In the present study, we aimed at deciphering the molecular basis of C1q/LAIR-1 interaction. To do so, we produced recombinant soluble LAIR-1 Ig-like domain and tested its interaction properties for C1q by surface plasmon resonance (SPR). We showed that C1q interacts with LAIR-1 via its CLR on a binding site close to, but different from the one of $C1r_2s_2$. On LAIR1, mutational analyses allowed the identification of several key residues involved in C1q interaction. Taken together, these results lead us to propose a model for the C1q/LAIR-1 interaction.

Results

Recombinant LAIR-1 Ig-like domain interacts with serum-derived C1q

The recombinant soluble Ig-like domain of wild-type LAIR-1 (WT) and all the variants used in the present study were expressed in bacteria and purified as described in *Materials and Methods*. LAIR-1 extracellular domain contains one N-glycosylation site at the asparagine residue 69. For that reason, LAIR-1 extracellular region was also produced in HEK293F cells to assess the importance of the LAIR-1 glycosylation. Since LAIR-1 Ig-like domain produced in *E. coli* or HEK293F cells showed similar interaction properties with C1q (Figure S1), the results presented in this study were then obtained using LAIR-1 produced in bacteria.

The quality of each LAIR-1 variant was analyzed by ESI-MS and SDS-PAGE (Figure 1). As illustrated in Figure 1A, each LAIR-1 Ig-like domain variant exhibited an ESI-measured mass in agreement with the theoretical mass calculated from the amino acid sequence. Of note, a difference of 2 Da is observed between the theoretical and measured masses accounting for the presence of an intact disulfide bond, thus supporting the correct folding of the Ig-like domain. As expected, SDS-PAGE analysis of LAIR-1 WT and mutated samples reveals a unique protein band with an apparent molecular weight of about 15 kDa, consistent with masses determined by mass spectrometry (Figure 1).

We first assessed the interaction of the recombinant LAIR-1 Ig-like domain with C1q by surface plasmon resonance (SPR). LAIR-1 interacts with serum-derived C1q (sC1q) in the two SPR configurations, i.e. soluble LAIR-1 on immobilized sC1q or soluble sC1q on immobilized LAIR-1 (red curves in Figure 2A and B, respectively). It is noteworthy that the shape of the curves obtained with both configurations is different, suggesting avidity effects in the interaction of

C1q with immobilized LAIR-1, which is absent in the other configuration, when C1q is immobilized. This likely reflects the presence of multiple LAIR-1 binding sites on the sC1q molecule. In order to avoid avidity constraints in SPR analyses, we decided to perform all SPR experiments using immobilized C1q fragments, with the exception of the $C1r_2s_2$ competition assay for which the injection of soluble sC1q is required.

LAIR-1 interacts with C1q collagen stems through a site in close proximity but different from the $C1r_2s_2$ tetramer binding site

In order to identify which C1q functional region is involved in LAIR-1 interaction, soluble LAIR-1 Ig-like domain was injected over immobilized serum-derived GR or CLR. As illustrated in Figure 2A, LAIR-1 interacts with both sC1q and sCLR but no interaction signal was detected on immobilized sGR. This result reveals that LAIR-1 Ig-like domain interacts with C1q exclusively through its collagen-like regions.

With a view to locate more precisely the LAIR-1 binding site in the C1q collagen-like regions, a competition experiment was then performed with a C1q ligand known to interact with the CLR within the C1 complex: the $C1r_2s_2$ tetramer. For that purpose, the C1 complex was reconstituted by incubation of sC1q with recombinant $C1r_2s_2$ at increasing molar ratios before injection over immobilized LAIR-1. C1q was no more able to interact with LAIR-1 when it is fully associated with $C1r_2s_2$ (above 1:3 tetramer versus C1q molar ratio), revealing that the LAIR-1 binding site on C1q CLR is the same or located in close proximity of the $C1r_2s_2$ binding site. Of note, the need of a higher than 1:1 molar ratio to fully inhibit C1q interaction with LAIR-1 can be explained by the concentration used (1 nM) which is almost ten-times lower than the previously determined K_D of C1q interaction with $C1r_2s_2$ (around 13 nM; Bally et al. 2013). Importantly, such a total inhibition of LAIR-1 interaction with C1q when associated with $C1r_2s_2$ suggests that no other LAIR-1 binding site, distant from the $C1r_2s_2$ binding region, is present on C1q CLR (Figure 2B).

As mentioned above, the $C1r_2s_2$ tetramer is known to interact with the collagen-like regions of C1q and C1q lysine residues are involved in this binding (Bally et al. 2013). To assess if LAIR-1 binding to C1q CLRs also requires these lysine residues, we used a recombinant C1q mutant with an alanine substitution of LysA59, LysB61 and LysC58 (rC1q ABC) with recombinant wild-type C1q (rC1q WT) as a control. LAIR-1 binding to these two rC1q variants was assessed using SPR. Although rC1q ABC does not interact with $C1r_2s_2$, this variant retains its interaction properties with LAIR-1 with a K_D similar to that of rC1q WT and sC1q (Figure 3 and Table 1). This reveals that $C1r_2s_2$ and LAIR-1 interact with C1q through different but neighboring binding sites.

As LAIR-1 interaction with C1q involves its collagen-like regions, we used a new C1qCLR_nc2 construct derived from the CLR_nc2 fusion protein recently developed in our laboratory to investigate the collagen-like functions of C1q (Fouët et al. 2020a). We needed to delete the GPP triplets initially added between the CLR and nc2 sequences in order to avoid addition of artifactual LAIR-1 binding sites into the molecule (see discussion section). The ability of LAIR-1 Ig-like domain to interact with wild-type C1qCLR_nc2 was assessed by SPR. As expected, LAIR-1 WT interaction with C1qCLR_nc2 exhibited a K_D value in the same range as with sC1q (Figure 4B and Table 1), therefore confirming that C1q interacts with LAIR-1 via its CLR.

We went further in engineering the C1qstem_nc2 fusion fragment, obtained by deleting the N-terminal part of C1qCLR_nc2 until the CLR hinge region. This C1qstem_nc2 truncated fragment contains a single heterotrimeric C1q collagen stem comprising the $C1r_2s_2$ and LAIR-1 binding sites with one C-terminal nc2 domain (Figure 4A). The C1qstem_nc2 construction was tested for its interaction with LAIR-1 Ig-like domain using SPR and the results indicated that it interacts in a dose-dependent manner (Figure 4C). Kinetic analysis of this interaction reveals a K_D value similar to the one obtained with the full length C1qCLR_nc2. This confirms that the LAIR-1 binding site might not be located in the N-terminal collagen bundle.

All together, these results highlight that LAIR-1 interacts with C1q stems through a binding site close but different from the binding site for the $C1r_2s_2$ tetramer.

A central binding groove in LAIR-1 common for C1q and generic collagen recognition

LAIR-1 is known to be a collagen receptor and previous studies identified a three-stranded β-sheet as the surface involved in the interaction of LAIR-1 Ig-like domain with collagens (in grey in Figure 5A,B). Among the residues forming this interaction groove, two LAIR-1 central amino acids, arginine 59 (R59) and glutamate 61 (E61) are essential for its binding to collagen I, III and IV (Brondijk et al. 2010). Interestingly, these two important residues for collagen interaction are conserved in the homologous glycoprotein VI receptor (GPVI) involved in collagen-induced activation and aggregation of platelets (Figure 5AB; Moroi and Jung 2004). Based on the assumption that LAIR-1 interaction with C1q CLR could be similar to the one with collagens I, III and IV, we produced LAIR-1 Ig-like domain variants with an alanine residue at positions 59 and 61 (R59A and E61A, respectively).

In order to investigate the mutation effects on the interaction of LAIR-1 with a generic collagen used as a positive control, we tested LAIR-1 interaction with a synthetic homotrimeric collagen peptide containing a central stabilizing GPKGEQ motif, found in several defense collagen sequences, surrounded by GPO triplets (Persikov et al. 2005b, a). To do so, we took

advantage of the fact that the collagen binding groove in LAIR-1 contains a unique exposed tryptophan residue (W109) (Figure 5B). This allowed us to set up a test to assess collagen peptide binding to LAIR-1 using nano differential scanning fluorimetry (nanoDSF). Indeed, the interaction of the collagen peptide with LAIR-1 changes the tryptophan environment and thus induces a transition in its fluorescence properties that can be detected using nanoDSF. As illustrated in Figure 5C, nanoDSF measurements showed that both independent substitutions of R59 or E61 strongly impact LAIR-1 binding to the collagen peptide, with a higher effect for the R59A mutation.

SPR experiments on immobilized sC1q, C1qCLR_nc2 and C1qstem_nc2 showed that these substitutions of arginine 59 or glutamate 61 into an alanine residue almost completely abolish LAIR-1 interaction with C1q, pointing out that, as for the positive collagen peptide control, these two residues are essential for C1q interaction (Figures 6 and 7B). The E61A mutation effect on LAIR-1 interaction with C1q fragments is slightly weaker than for the R59A mutation, which is in line with the nanoDSF experiments with a collagen peptide (Figures 5C 6 and 7B). Circular dichroism (CD) experiments confirmed that these mutations do not affect folding, since both R59A and E61A variants displayed similar CD spectra than the WT LAIR-1 Ig-like domain (figure S2).

These results unveil that C1q interaction with LAIR-1 is based on a generic collagen recognition by the two central arginine 59 and glutamate 61 LAIR-1 residues.

Previous reports showed that LAIR-1 and its soluble homologue LAIR-2 have different affinities for C1q (Son et al. 2012; Olde Nordkamp et al. 2014a) and comparison of LAIR-1 and LAIR-2 sequences highlights only few differences in the amino acids exposed on the β-sheet forming the interaction groove for collagen binding (Figure 5A). Among them, the isoleucine 102 of LAIR-1, which is in a central position in the interaction groove, corresponds to a leucine residue in LAIR-2 sequence. Such substitution might induce a slight steric hindrance on the interaction surface so we decided to introduce it in LAIR-1 (I102L) in order to investigate possible steric impact at that position. Isoleucine 102 was also replaced by a bulkier tyrosine residue (I102Y) in order to enhance the steric effect on collagen interaction. Interaction studies using SPR showed that, when isoleucine 102 is replaced by a slightly longer residue (I102L), the interaction with C1q is partially hampered and it is abolished in the case of the larger I102Y substitution (Figure 7B). However, the interaction with the control collagen peptide is only affected by the I102Y mutation (Figure 7B, lower part). This highlights that the isoleucine 102 position is prone to steric conflict for collagen binding, revealing that the collagen residue placed in front of the I102 of LAIR-1 should be small enough to accommodate LAIR-1 binding without introducing steric conflict.

Building of a C1q/LAIR-1 interaction model

As mentioned above, the central LAIR-1 arginine 59 and glutamate 61 residues are essential for C1q but also generic collagen backbone binding. Nevertheless, we showed that LAIR-1 recognition of C1q does not randomly occur along the CLR but is located on a specific binding site close to the $C1r_2s_2$ interaction region. Therefore, we investigated the binding specificity of C1q interaction with LAIR-1. For that purpose, we designed a model based on the structural literature and the results presented above. One crystal structure of GPVI in complex with a GPO-containing collagen peptide is available in the protein data bank (PDB code: 5OU8). Analysis of this structure reveals that the GPVI R38 and E40 residues (homologues of LAIR-1 R59 and E61, respectively) are central in collagen interaction and recognize the OGXO motif of two consecutive GPO triplets of a single chain. LAIR-1 R59 and E61 residues should likely recognize similar motifs on C1q. We identified three similar motifs in the C1q B and C chain sequences in close proximity to the $C1r_2s_2$ binding site that could be recognized by LAIR-1 (underlined in Figure 8A). We performed a structure alignment of the LAIR-1 Ig-like domain (PDB code 3RP1) with the GPVI collagen-binding domain and aligned the GPVI-associated collagen peptide with a model of one C1q collagen stem, in the region of the putative LAIR-1 binding sites on their common hydroxyproline residues. Such alignment led to the generation of three putative model of LAIR-1 in interaction with one C1q stem (Figures 8 and S3). In the different models, we identified three residues facing the LAIR-1 I102 residue: A71 on C1q A chain, P73 and I76 on C1q C chain (represented in black in Figures 8 and S3). Considering the constraint that a small C1q residue must face LAIR-1 I102, together with the close proximity to the $C1r_2s_2$ and the presence of two possible electrostatic interactions at side of the central R59 and E61, the model represented in Figure 8B with an alanine residue at this position on C1q A chain (A_A71) was selected as the most consistent one.

Exploring the distal LAIR-1 residues involved in C1q binding.

Interestingly, in the selected model shown in Figure 8B, two glutamate residues at position 72 and 111 of LAIR-1 (E72 and E111) are facing two positively charged C1q residues: lysine 65 of C1q B chain (B_K65) and arginine 72 of C1q A chain (A_R72), respectively. These four residues might likely lock the specific recognition of the central C1q hydroxyproline residues by LAIR-1 R59 and E61. Indeed, these two pairs of charge-opposed residues are located at each side of the collagen binding groove of LAIR-1 and could introduce more specificity toward C1q than generic collagen recognition (Figure 7A and 8B). In order to test the engagement of the two LAIR-1 glutamate residues, we generated two LAIR-1 variants. The SPR results show that both mutations reduce LAIR-1 binding to C1q and CLR_nc2 constructions, with a stronger effect for E72K than for E111K mutation (Figure 7B). However, these two mutations on LAIR-1 have no effect on LAIR-1 interaction with the control collagen peptide (Figure 7B, lower part).

This strongly suggests that these two LAIR-1 glutamate residues are involved in the specific recognition of C1q by LAIR-1.

In order to test the engagement of the two C1q residues in the interaction with LAIR-1, we generated two C1qCLR_nc2 variants containing the substitution of lysine 65 on C1q B chain and arginine 72 on C1q A chain into glutamate residues (B_K65E and A_R72E, respectively). SPR analyses showed that the B_K65E mutation did not have any effect on LAIR-1 interaction in comparison with the C1qCLR_nc2 WT (Figure 9A and Table 1). Regarding the C1qCLR_nc2 A_R72E variant, the K_D value obtained for LAIR-1 interaction was slightly higher than for C1qCLR_nc2 WT, suggesting that the arginine 72 on C1q A chain, albeit not essential, is likely involved in LAIR-1 interaction (Figure 9B and Table 1). These results can be related to the interaction behavior of LAIR-1 mutants of the two E72 and E111 residues. Indeed, the LAIR-1 E72K and E111K mutations exhibited weaker inhibitory effect on C1q interaction than the mutations in the central LAIR-1 binding site (i.e. R59 and E61; Figure 7AB). It is therefore consistent that the mutation of the suggested CLR residues facing the E72 and E111 residues of LAIR-1 triggers a weak effect on the global affinity of C1qCLR_nc2/LAIR-1 interaction, explained by their distal position from the central binding site of LAIR-1 (Figure 7B). We suggest that these two residues are not involved in the direct binding with LAIR-1 but lock and give the specificity of the interaction after initial LAIR-1 docking through its R59 and E61 residues.

Moreover, in order to go further in the deciphering of the LAIR-1 and C1q interaction, we studied the implication of residues that were described as important for the interaction with collagen in a family of broadly reactive antibodies against malaria antigens containing LAIR-1 Ig-like domain (Tan et al. 2015; Pieper et al. 2017). Indeed, these antibodies present a unique feature with the insertion of a full additional LAIR-1 Ig-like domain displaying several mutations that all together enhance the binding to *P. falciparum* infected erythrocytes while reducing the interaction with collagen. Interestingly, in almost all identified mutation profiles, arginine 59 and glutamate 61 constituting the LAIR-1 main collagen-binding site are conserved in the inserted LAIR-1 domain. One could wonder why these Ig-like domains do not interact with collagens, although they contain key residues for their recognition. Among all mutations, we paid attention to the substitution of proline 107 by an arginine residue (P107R). Indeed, this unique mutation leads to a LAIR-1 Ig-like domain devoid of its collagen binding properties (Tan et al. 2016). We thus decided to produce this LAIR-1 Ig-like domain variant and assess its interaction either with C1q, C1qCLR_nc2 fragments or the control collagen peptide. As expected, this mutation reduced the interaction of LAIR-1 with C1q but had almost no effect with the positive control synthetic peptide (Figure 7B). This can be explained by the fact that the P107R mutation introduces a steric hindrance at the extremity of the collagen-binding groove of LAIR-1 Ig-like

domain, which does not allow any longer the proper positioning of large collagen molecules like C1q, but retains the main central region for the binding to a smaller collagen peptide.

Discussion

Besides its major role in the initiation of the classical pathway of the complement cascade, C1q achieves many complement-independent functions such as the opsonization of apoptotic cells and pathogens or maintenance of immune tolerance. Therefore, C1q interaction network on immune cells surface is highly complex and the underlying molecular mechanisms need to be explored. In this study, we investigated the molecular basis of C1q interaction with LAIR-1, an inhibitory immune receptor present on various immune cells.

Molecular dissection of C1q unambiguously showed that LAIR-1 Ig-like domain interacts with the C1q collagen-like regions on a binding site located close to the one of $C1r_2s_2$ as shown by SPR competition assays. In addition, the interactions of LAIR-1 with recombinant C1q with a wild-type sequence or mutated at the $C1r_2s_2$ binding site were similar, revealing that LAIR-1 binding does not engage the same C1q CLR residues as $C1r_2s_2$. Interestingly, we showed that LAIR-1 interaction with C1q is only possible when it is devoid of its associated proteases. This result is in line with previous studies on C1q receptors showing that CR1 and LRP1 can interact with C1q but not with the C1 complex (i.e. C1q in complex with the $C1r_2s_2$ tetramer), showing that these three receptors share the same conditional rule for C1q binding and might share a common binding region on the C1q collagen stems (Jacquet et al. 2018; Fouët et al. 2020b).

This highlights the dual role of C1q in complement related function when associated with $C1r_2s_2$ and complement independent functions when devoid of its cognate proteases, through the interaction with cellular receptors. Even if serum C1q is almost exclusively found associated with $C1r_2s_2$ within the C1 complex, it is not unusual to find C1q alone in physiological conditions. Namely, single C1q can be locally expressed by several cell types or remain after C1-inhibitor mediated C1 complex dissociation (Sim et al. 1979; Kouser et al. 2015).

Our study used C1qCLR_nc2, a variant of the CLR_nc2 recombinant fusion protein designed in our lab, previously reported to retain the $C1r_2s_2$ interaction properties of C1q CLR (Fouët et al. 2020a). In the particular case of LAIR-1 study, we had to remove the three additional GPP collagen triplets initially introduced between the CLR and non-collagenous domain to improve the C1qCLR_nc2 folding. This GPP removal was done in order to avoid introducing artificial interaction sites for LAIR-1. It is likely that during processing and maturation, these additional GPP triplets undergo proline hydroxylation as post-translational modification, resulting in GPO collagen triplets. It is well established that GPO triplets are high-affinity ligands of LAIR-1 and such additional putative binding sites would have introduced nonspecific signal of LAIR-1

312 binding to CLR_nc2 (Lebbink et al. 2006, 2009). Indeed, kinetics SPR experiments using the
313 previously published CLR_nc2 protein containing the additional GPP triplets displayed a lower
314 K_D value and a higher surface binding capacity (Rmax) substantiating the presence of
315 additional binding sites and an increased avidity (Figure S4). Therefore, all experiments
316 presented in this study were done using the C1qCLR_nc2 devoid of additional GPP triplets.

317 We report here that LAIR-1 interacts similarly with C1qCLR_nc2 and sC1q, thus validating the
318 use of C1qCLR_nc2 in the context of studies on C1q collagen-like regions receptors. By
319 deleting the N-terminal portion of each C1q collagen chain until the hinge region, we managed
320 to produce one isolated heterotrimeric C1q collagen stem (called C1qstem_nc2). We showed
321 that the affinity constants of LAIR-1 Ig-like domain interaction with C1qstem_nc2 and the LAIR-
322 1 mutations effects are similar to those obtained with full length C1qCLR_nc2 (Figures 4B,C,
323 8 and Table 1). This unambiguously excludes putative LAIR-1 binding sites in the C1q N-
324 terminal collagen bundle even though recently reported results suggested the opposite.
325 Indeed, Liu and colleagues showed that a molecular mimic combining short sequences of
326 HMGB1 and the N-terminal region of C1q A chain was able to interact simultaneously with
327 RAGE and LAIR-1 and efficiently polarize monocytes to an anti-inflammatory phenotype (Liu
328 et al. 2019). We suggest that this C1q A chain sequence, containing one **PG**X**P** motif, can be
329 recognized by LAIR-1 in the context of the minimal structure of this mimic but is not accessible
330 in the complex C1q architecture, probably hidden by the other C1q collagen stems forming the
331 bundle. Furthermore, the generation of a short and functional heterotrimeric C1q collagen stem
332 opens the way for various applications. For example, C1qstem_nc2 could be used for structural
333 studies of C1q CLR ligands. This approach could be enlarged to other collagen containing
334 proteins such as the soluble defense collagens family.

335 Moreover, a directed mutational analysis of LAIR-1 Ig-like domain based on the literature
336 knowledge on LAIR-1 interaction with collagens, allowed a precise mapping of LAIR-1 residues
337 involved in the interaction with C1q CLR. Indeed, we identified a C1q binding groove in LAIR-
338 1 where the central residues (R59 and E61) directly interact with the collagen backbone and
339 more distal residues (I102, E72, E111 and P107) are likely involved in the recognition
340 specificity and the correct positioning of the C1q CLR in front of the LAIR-1 binding region. Our
341 results are in agreement with a previous study identifying LAIR-1 key residues for collagen
342 interaction (Brondijk et al. 2010). The crystal structure of the GPVI in complex with a collagen
343 peptide recently deposited in the PDB (code 5OU8) reveals that GPVI recognition of the
344 collagen GPO motifs relies on two central arginine and glutamate residues homologous to the
345 R59 and E61 of LAIR-1. Therefore, LAIR-1 and GPVI may share a common interaction
346 mechanism with collagens, based on the direct recognition of the collagen through their central
347 arginine and glutamate residues.

LAIR-2 is a soluble collagen receptor that interacts with the same ligands as LAIR-1 and is suggested to act as a competitor to regulate LAIR-1 collagen-induced inhibitory activity. However, the comparison of the affinity values of LAIR-1 and LAIR-2 interaction with C1q still deserves further investigations. Indeed, Son and colleagues previously reported that LAIR-1 exhibits more affinity for C1q than LAIR-2 while Olde Nordkamp et al. showed the opposite (Son et al. 2012; Olde Nordkamp et al. 2014a). One explanation for the difference could be that the results of these two studies were obtained using LAIR proteins in different oligomeric states. Indeed, the first team used monomeric Ig-like domains whereas the latter used Fc-fused dimeric Ig-like domains. In order to answer this elusive question, we generated the LAIR-1 I102L variant containing a LAIR-2 like collagen binding groove. We showed that C1q interaction with the LAIR-1 I102L variant is decreased, supporting the C1q lower affinity for LAIR-2 than for LAIR-1. Our results are in line with the study of Son et al., both obtained using monomeric LAIR-1. It is noteworthy that within the GPVI, the corresponding residue of I102 is a serine, which is quite smaller. This suggests that the specific steric binding constraint for the residue facing I102 in LAIR-1 is likely missing for GPVI binding (Figure 5A), even if LAIR-1 and GPVI share a common collagen recognition mechanism.

The likely similar mechanism of collagen backbone recognition by LAIR-1 and GPVI allowed us to identify three putative LAIR-1 binding motifs on one C1q collagen stem (underlined in Figure 8A). We generated three different models of LAIR-1 interaction with one C1q collagen stem (Figure 8B and S3). Based on our results and the constraint of a small enough residue in front of the LAIR-1 I102, the most relevant model is the one represented in Figure 8B. This model unveils two C1q residues potentially engaged in LAIR-1 docking: arginine 72 and lysine 65 on C1q A and B chains respectively. These two CLR residues were mutated with a view to confirm their involvement in LAIR-1 binding. However, the generated C1qCLR_nc2 fusion protein variants exhibited no or slight inhibitory effect on LAIR-1 interaction, which could be expected. Indeed, as mentioned above, the A_R72 and B_K65 CLR residues, in association with the respective E111 and E72 LAIR-1 residues, are not involved in generic collagen backbone recognition of C1q by LAIR-1 but are suggested to play a role in the recognition specificity and the correct positioning of both partners. Interestingly, the collagen sequence of C1qC chain recognized in our model is exposed on the same side as the two most important lysine residues of C1q for the interaction with the $C1r_2s_2$ tetramer (Figure 8B). This suggests that the LAIR-1 Ig-like domain may interact with one C1q collagen stem close to and with the same orientation as $C1r_2s_2$, therefore explaining the strong competition effects observed in Figure 2B.

However, we cannot exclude that LAIR-1 might interact with C1q through the two other putative binding sites (Figure S3). These two sites are located on the C1q B chain, far enough from the

motif in the C chain to accommodate the binding of one LAIR-1 Ig-like domain on each site at the same time. Such simultaneous binding of two LAIR-1 copies on C1q collagen stem could be consistent with the required dimerization of LAIR-1 to trigger its inhibitory activity. Indeed, the dimerization of LAIR-1 upon ligand binding results in the phosphorylation of its ITIMs motifs, leading to a negative regulation of intracellular signaling associated with immune cell maturation, activation and differentiation (Meyaard et al. 1997; Xu et al. 2000; Sathish et al. 2001; Jin et al. 2018). Therefore, the dimerization of LAIR-1 might be mediated by the binding of two copies on either the same site on two different C1q collagen stems or two different sites on the same C1q collagen stem.

Materials and Methods

Proteins, cells and reagents

C1q was purified from human serum as described previously (Arlaud et al. 1979). C1q collagen-like and globular regions were prepared as described in Tacnet-Delorme et al. (Tacnet-Delorme et al. 2001). Recombinant $C1r_2s_2$ tetramer (C1s, C1rS637A) was purified and quantified according to published procedures (Bally et al. 2019). Recombinant C1q variants were produced and purified as reported in Bally et al. (Bally et al. 2013).

Oligonucleotides were purchased from Eurogentec, restriction and modification enzymes from New England Biolabs.

Construction of the C1qCLR_nc2 protein

Recombinant C1qCLR_nc2 (WT and mutants) was produced and purified as previously reported (Fouët et al. 2020a) with the difference that L-ascorbic acid 2-phosphate was added during the production step in the EXPI culture medium at a final concentration of 450 µM. Previous reports showed that L-ascorbic acid 2-phosphate is more stable than L-ascorbic acid and enhances production yields for some collagen types (Koch et al. 2006). The DNA sequences corresponding to the GPP triplets present between the C1qCLR and nc2 sequences were removed by site-directed mutagenesis with the Quickchange II XL kit (Agilent technologies).

Construction and purification of the C1qstem_nc2 protein

The coding sequences of C1q native signal peptides followed by CLRA (40-87, mature numbering) fused to nc2α2, CLRB (42-89, mature numbering) fused to nc2α1, and CLRC (39-86, mature numbering) fused to nc2α3 with a C-terminal FLAG epitope were synthesized and cloned in pcDNA3.1/Neo(+), pcDNA3.1/Hygro(+), and pcDNA3.1/Zeo(+) vectors, respectively (Thermo Fisher Scientific, Illkirch, France). The C1qstem_nc2 fragment (WT and mutants) was

produced in expi293 cells (Thermo Fisher Scientific) and first purified on an anti-FLAG M2 affinity column (Sigma-Aldrich) as described for the full length CLR_nc2 (Fouët et al. 2020a). The second purification step was performed on a Superdex 75 10/300 column (GE Healthcare).

LAIR-1 Ig-like domain expression and purification

The C2-type Ig-like domain sequence of LAIR-1 from residues 22 to 122 was inserted in a pET28a plasmid for bacterial expression with a polyhistidine tag at the C-terminal extremity to allow protein purification. Soluble LAIR-1 Ig-like domain was overexpressed by pET28a-LAIR-1 transformed *E. coli* BL21(DE3) cells using an autoinduction protocol (Studier 2005). LAIR-1 Ig-like domain was purified in a two-step process. First, it was affinity purified on a nickel-loaded hitrap chelating HP column (GE Healthcare), washed by a 35 mM imidazole step followed a 35-500 mM imidazole gradient in 25 mM Tris, 150 mM NaCl (pH 8.2). Then a gel filtration step was performed using a Superdex 75 column (GE Healthcare) in 25 mM Tris, 150 mM NaCl (pH 8.2). The LAIR-1 mutants were expressed and purified with the same experimental procedures than for the wild-type. At each purification step, LAIR-1 concentration was estimated using an $A_{1\%,1cm}$ of 10.3 and the molecular masses presented in Figure 1A.

SDS/PAGE, circular dichroism and LC/ESI Mass spectrometry

SDS/PAGE

Recombinant LAIR-1 was analyzed by SDS/PAGE under reducing conditions using 14% poly-acrylamide Tris/HCl gels and then colored using Instant-Blue (Expedeon, Abcam, Paris, France).

Circular dichroism

The far-UV circular dichroism (CD) spectra (from 204 to 260 nm) was collected on a JACSO J-810 CD spectrophotometer. LAIR-1 variants samples at a concentration of 4 µM in 5 mM Trizma, 150 mM NaF (pH 8.2) were scanned ten times at 20°C in a 1 mm path-length cuvette. After subtraction of baseline buffer values, the CD signal was converted to mean molar residue ellipticity ($deg.cm^2.dmol^{-1}$).

LC/ESI mass spectrometry

Liquid Chromatography Electrospray Ionization Mass Spectrometry (LC/ESI-MS) analyses were performed on a 6210 LC-TOF spectrometer coupled to a HPLC system (Agilent Technologies).

All solvents used were HPLC grade (Chromasolv, Sigma-Aldrich), trifluoroacetic acid (TFA) was from Acros Organics. Solvent A was 0.03% TFA in water, solvent B was 95% acetonitrile-5% water-0.03% TFA. Before analysis, protein samples were diluted in acidic denaturing

conditions to a final concentration of 10 µM with solvent A. Protein samples were firstly desalted on a reverse phase-C8 cartridge (Zorbax 300SB-C8, 5 mm, 300 Å 5*0.3 mm, Agilent Technologies) and then eluted with 95% solvent B.

MS spectra were recorded in the positive ion mode in the 300-3200 m/z range and the data processed with MassHunter workstation software (v. B.02.00, Agilent Technologies).

Surface plasmon resonance analyses and evaluation

All SPR experiments were done at 25°C on a BIAcore T200 instrument (GE Healthcare). Each ligand was immobilized on a CM5 sensor chip using the amine coupling chemistry at a flowrate of 10 µL/min in 10 mM HEPES, 150 mM NaCl, 3 mM EDTA, 0.05% (v/v) surfactant P20 (pH 7.4) according to the manufacturer's protocol (GE Healthcare). sC1q or LAIR-1 were diluted at 35 µg/mL in 10 mM sodium acetate (pH 5) or 5 µg/mL in 10 mM sodium acetate (pH 4.5) respectively for the immobilization procedure. All others ligands were immobilized at a concentration of 25 µg/mL in 10 mM sodium acetate (pH 5). All SPR interaction experiments were performed at a flowrate of 30 µL/min in 50 mM Tris, 150 mM NaCl, 2 mM $CaCl_2$, 0.05% surfactant P20 (pH 7.5). All data were analyzed using the T200 Biaevaluation 3.1 software (GE Healthcare).

LAIR-1 interaction with sC1q, sCLR and sGR and competition assay with $C1r_2s_2$

LAIR-1 Ig-like domain was injected at a concentration of 10 µM on immobilized sC1q (14,000 RU), sCLR (6,000 RU) or sGR (1,500 RU) with an association step of 180 s.

For the competition assay, sC1q (1 nM) was pre-incubated with $C1r_2s_2$ at different molar ratios in 50 mM Tris, 150 mM NaCl, 2 mM $CaCl_2$, 0.05% surfactant P20 (pH 7.5) (15 min at 25°C) before injection over immobilized LAIR-1 Ig-like domain (330 RU) with an association step of 180 s.

Interaction of LAIR-1 variants with immobilized serum-derived C1q

Wild-type and mutated LAIR-1 Ig-like domains were injected at a concentration of 10 µM over immobilized sC1q (14,000 RU) with an association step of 180 s. The responses obtained at the equilibrium for each LAIR-1 mutant were normalized as a percentage of the WT interaction signal.

Kinetics of LAIR-1 interaction with sC1q, rC1q variants and CLR_nc2 variants

Soluble LAIR-1 Ig-like domain was injected at increasing concentrations (4-128 µM) over immobilized sC1q (14,000 RU), rC1q WT (12,000 RU) and rC1q ABC (12,000 RU) with an association step of 180 s. The equilibrium dissociation constant (K_D) values were calculated from measured responses at equilibrium (Req) by fitting plots Req versus concentration using steady state analysis (Biaevaluation software).

Soluble LAIR-1 was injected at increasing concentrations (4-256 µM) over immobilized C1qCLR_nc2 WT (6,800 RU), C1qCLR_nc2 A_R72E (6,800 RU) and C1qCLR_nc2 B_K65E (6,400 RU) with an association step of 60 s. LAIR-1 was injected at different concentrations (3.125-400 µM) over immobilized C1qstem_nc2 (2,600 RU) with an association step of 30 s.

The equilibrium dissociation constant (K_D) values were calculated from measured responses at equilibrium (Req) by fitting plots of Req versus concentration using steady state analysis (Biaevaluation software).

NanoDSF experiments

NanoDSF experiments were performed using a Prometheus NT.48 instrument (Nanotemper Technologies) and the provided software PR.thermocontrol v2.0.4. Up to 48 capillaries containing 10 µL of sample were sequentially illuminated at 280 nm, and fluorescence intensity at 350 (F350) and 330 (F330) nm was measured at increasing temperatures (20-95°C, 1°C/min). The F350/F330 ratio and its first derivative were then plotted versus temperature.

NanoDSF analyses were performed on wild-type and mutated LAIR-1 Ig-like domain at a concentration of 80 µM alone or in presence of 80 µM of a synthetic triple helical collagen peptide in order to detect the collagen peptide binding to LAIR-1. The synthetic collagen peptide with the sequence Ac-GPOGPOGPOGPKGEQGPOGPO-NH2 was purchased from GL Biochem (Shanghai).

Acknowledgments

This work used platforms of the Grenoble Instruct-ERIC center (ISBG; UMS 3518 CNRS-CEA-UGA-EMBL) within the Grenoble Partnership for Structural Biology (PSB), supported by FRISBI (ANR-10-INBS-05-02) and GRAL, financed within the University Grenoble Alpes graduate school (Ecoles Universitaires de Recherche) CBH-EUR-GS (ANR-17-EURE-0003). We acknowledge Aline Le Roy for access to the NanoDSF device, Caroline Mas for the CD experiments and Luca Signor for the MS experiments. We acknowledge Pascale Tacnet-Delorme and Fabien Dalonneau for preparing sC1q and $C1r_2s_2$ samples, respectively. Research reported in this manuscript was supported by the French National Research Agency (grant ANR-16-CE11-0019). IBS acknowledges integration into the Interdisciplinary Research Institute of Grenoble (IRIG, CEA).

Author contributions

GF, NMT, CG and VR designed the study. GF, IB and AC performed the research. GF, IB, AC, JBR, NMT, CG and VR analyzed the data. GF, NMT, CG and VR wrote the manuscript draft. All authors contributed to the article and approved the submitted version.

Declarations of interest

The authors declare that the research was conducted in the absence of any commercial or financial relationships that could be construed as a potential conflict of interest.

References

Arlaud J, Sim B, Colomb G (1979) Differential elution of Clq, Clr and Cls from human Cl bound to immune aggregates. Use in the rapid purification of Cl subcomponents. Mol Immunol 16:445–450. https://doi.org/10.1016/0161-5890(79)90069-5

Bally I, Ancelet S, Moriscot C, et al (2013) Expression of recombinant human complement C1q allows identification of the C1r/C1s-binding sites. Proc Natl Acad Sci U S A 110:8650–8655. https://doi.org/10.1073/pnas.1304894110

Bally I, Inforzato A, Dalonneau F, et al (2019) Interaction of C1q With Pentraxin 3 and IgM Revisited: Mutational Studies With Recombinant C1q Variants. Front Immunol 10:. https://doi.org/10.3389/fimmu.2019.00461

Brondijk THC, de Ruiter T, Ballering J, et al (2010) Crystal structure and collagen-binding site of immune inhibitory receptor LAIR-1: unexpected implications for collagen binding by platelet receptor GPVI. Blood 115:1364–1373

Eggleton P, Tenner AJ, Reid KBM (2000) C1q receptors. Clin Exp Immunol 120:406–412. https://doi.org/10.1046/j.1365-2249.2000.01218.x

Fouët G, Bally I, Signor L, et al (2020a) Headless C1q: a new molecular tool to decipher its collagen-like functions. FEBS J. https://doi.org/10.1111/febs.15543

Fouët G, Gout E, Wicker-Planquart C, et al (2020b) Complement C1q Interacts With LRP1 Clusters II and IV Through a Site Close but Different From the Binding Site of Its C1r and C1s-Associated Proteases. Front Immunol 11:. https://doi.org/10.3389/fimmu.2020.583754

Gaboriaud C, Frachet P, Thielens NM, Arlaud GJ (2011) The human c1q globular domain: structure and recognition of non-immune self ligands. Front Immunol 2:92. https://doi.org/10.3389/fimmu.2011.00092

Jacquet M, Cioci G, Fouet G, et al (2018) C1q and Mannose-Binding Lectin Interact with CR1 in the Same Region on CCP24-25 Modules. Front Immunol 9:. https://doi.org/10.3389/fimmu.2018.00453

Jin J, Wang Y, Ma Q, et al (2018) LAIR-1 activation inhibits inflammatory macrophage phenotype in vitro. Cell Immunol 331:78–84. https://doi.org/10.1016/j.cellimm.2018.05.011

Kishore U, Gaboriaud C, Waters P, et al (2004) C1q and tumor necrosis factor superfamily: modularity and versatility. Trends Immunol 25:551–561. https://doi.org/10.1016/j.it.2004.08.006

Koch M, Veit G, Stricker S, et al (2006) Expression of type XXIII collagen mRNA and protein. J Biol Chem 281:21546–21557. https://doi.org/10.1074/jbc.M604131200

Kouser L, Madhukaran SP, Shastri A, et al (2015) Emerging and Novel Functions of Complement Protein C1q. Front Immunol 6:. https://doi.org/10.3389/fimmu.2015.00317

Lebbink RJ, de Ruiter T, Adelmeijer J, et al (2006) Collagens are functional, high affinity ligands for the inhibitory immune receptor LAIR-1. J Exp Med 203:1419–1425. https://doi.org/10.1084/jem.20052554

562 Lebbink RJ, Raynal N, de Ruiter T, et al (2009) Identification of multiple potent binding sites
563 for human leukocyte associated Ig-like receptor LAIR on collagens II and III. Matrix Biol
564 28:202–210. https://doi.org/10.1016/j.matbio.2009.03.005

565 Lebbink RJ, van den Berg MCW, de Ruiter T, et al (2008) The soluble leukocyte-associated
566 Ig-like receptor (LAIR)-2 antagonizes the collagen/LAIR-1 inhibitory immune
567 interaction. J Immunol Baltim Md 1950 180:1662–1669.
568 https://doi.org/10.4049/jimmunol.180.3.1662

569 Liu T, Xiang A, Peng T, et al (2019) HMGB1-C1q complexes regulate macrophage function by
570 switching between leukotriene and specialized proresolving mediator biosynthesis.
571 Proc Natl Acad Sci U S A 116:23254–23263. https://doi.org/10.1073/pnas.1907490116

572 Meyaard L (2008) The inhibitory collagen receptor LAIR-1 (CD305). J Leukoc Biol 83:799–
573 803. https://doi.org/10.1189/jlb.0907609

574 Meyaard L, Adema GJ, Chang C, et al (1997) LAIR-1, a Novel Inhibitory Receptor Expressed
575 on Human Mononuclear Leukocytes. Immunity 7:283–290.
576 https://doi.org/10.1016/S1074-7613(00)80530-0

577 Moroi M, Jung SM (2004) Platelet glycoprotein VI: its structure and function. Thromb Res
578 114:221–233. https://doi.org/10.1016/j.thromres.2004.06.046

579 Nayak A, Pednekar L, Reid KB, Kishore U (2012) Complement and non-complement activating
580 functions of C1q: A prototypical innate immune molecule. Innate Immun 18:350–363.
581 https://doi.org/10.1177/1753425910396252

582 Olde Nordkamp MJM, Boross P, Yildiz C, et al (2014a) Inhibition of the classical and lectin
583 pathway of the complement system by recombinant LAIR-2. J Innate Immun 6:284–
584 292. https://doi.org/10.1159/000354976

585 Olde Nordkamp MJM, van Eijk M, Urbanus RT, et al (2014b) Leukocyte-associated Ig-like
586 receptor-1 is a novel inhibitory receptor for surfactant protein D. J Leukoc Biol 96:105–
587 111. https://doi.org/10.1189/jlb.3AB0213-092RR

588 Persikov AV, Ramshaw JAM, Brodsky B (2005a) Prediction of collagen stability from amino
589 acid sequence. J Biol Chem 280:19343–19349.
590 https://doi.org/10.1074/jbc.M501657200

591 Persikov AV, Ramshaw JAM, Kirkpatrick A, Brodsky B (2005b) Electrostatic interactions
592 involving lysine make major contributions to collagen triple-helix stability. Biochemistry
593 44:1414–1422. https://doi.org/10.1021/bi048216r

594 Pflieger D, Przybylski C, Gonnet F, et al (2010) Analysis of Human C1q by Combined Bottom-
595 up and Top-down Mass Spectrometry. Mol Cell Proteomics MCP 9:593–610.
596 https://doi.org/10.1074/mcp.M900350-MCP200

597 Pieper K, Tan J, Piccoli L, et al (2017) Public antibodies to malaria antigens generated by two
598 LAIR1 insertion modalities. Nature 548:597–601. https://doi.org/10.1038/nature23670

599 Reid KB (1979) Complete amino acid sequences of the three collagen-like regions present in
600 subcomponent C1q of the first component of human complement. Biochem J 179:367–
601 371

602 Sathish JG, Johnson KG, Fuller KJ, et al (2001) Constitutive Association of SHP-1 with
603 Leukocyte-Associated Ig-Like Receptor-1 in Human T Cells. J Immunol 166:1763–
604 1770. https://doi.org/10.4049/jimmunol.166.3.1763

605 Shelton E, Yonemasu K, Stroud RM (1972) Ultrastructure of the Human Complement
606 Component, Clq. Proc Natl Acad Sci U S A 69:65–68

607 Siegel RC, Schumaker VN (1983) Measurement of the association constants of the complexes
608 formed between intact C1q or pepsin-treated C1q stalks and the unactivated or
609 activated C1r2C1s2 tetramers. Mol Immunol 20:53–66

610 Sim RB, Arlaud GJ, Colomb MG (1979) C1 inhibitor-dependent dissociation of human
611 complement component C1 bound to immune complexes. Biochem J 179:449–457

612 Son M, Diamond B (2015) C1q-Mediated Repression of Human Monocytes Is Regulated by
613 Leukocyte-Associated Ig-Like Receptor 1 (LAIR-1). Mol Med 20:559–568.
614 https://doi.org/10.2119/molmed.2014.00185

615 Son M, Diamond B, Volpe BT, et al (2017) Evidence for C1q-mediated crosslinking of
616 CD33/LAIR-1 inhibitory immunoreceptors and biological control of CD33/LAIR-1
617 expression. Sci Rep 7:. https://doi.org/10.1038/s41598-017-00290-w

618 Son M, Porat A, He M, et al (2016) C1q and HMGB1 reciprocally regulate human macrophage
619 polarization. Blood 128:2218–2228. https://doi.org/10.1182/blood-2016-05-719757

620 Son M, Santiago-Schwarz F, Al-Abed Y, Diamond B (2012) C1q limits dendritic cell
621 differentiation and activation by engaging LAIR-1. Proc Natl Acad Sci U S A 109:E3160-
622 3167. https://doi.org/10.1073/pnas.1212753109

623 Studier FW (2005) Protein production by auto-induction in high-density shaking cultures.
624 Protein Expr Purif 41:207–234. https://doi.org/10.1016/j.pep.2005.01.016

625 Tacnet-Delorme P, Chevallier S, Arlaud GJ (2001) β-Amyloid Fibrils Activate the C1 Complex
626 of Complement Under Physiological Conditions: Evidence for a Binding Site for Aβ on
627 the C1q Globular Regions. J Immunol 167:6374–6381.
628 https://doi.org/10.4049/jimmunol.167.11.6374

629 Tan J, Pieper K, Piccoli L, et al (2015) A LAIR1 insertion generates broadly reactive antibodies
630 against malaria variant antigens. Nature 529:105–109.
631 https://doi.org/10.1038/nature16450

632 Tan J, Pieper K, Piccoli L, et al (2016) A LAIR-1 insertion generates broadly reactive antibodies
633 against malaria variant antigens. Nature 529:105–109.
634 https://doi.org/10.1038/nature16450

635 Thielens NM, Tedesco F, Bohlson SS, et al (2017) C1q: A fresh look upon an old molecule.
636 Mol Immunol 89:73–83. https://doi.org/10.1016/j.molimm.2017.05.025

637 Ugurlar D, Howes SC, de Kreuk B-J, et al (2018) Structures of C1-IgG1 provide insights into
638 how danger pattern recognition activates complement. Science 359:794–797.
639 https://doi.org/10.1126/science.aao4988

640 Walport MJ, Davies KA, Botto M (1998) C1q and Systemic Lupus Erythematosus.
641 Immunobiology 199:265–285. https://doi.org/10.1016/S0171-2985(98)80032-6

642 Xu M j, Zhao R, Zhao ZJ (2000) Identification and characterization of leukocyte-associated Ig-
643 like receptor-1 as a major anchor protein of tyrosine phosphatase SHP-1 in
644 hematopoietic cells. J Biol Chem 275:17440–17446.
645 https://doi.org/10.1074/jbc.M001313200

Figure legends

Figure 1. Quality control of the LAIR-1 Ig-like domain variants. (A) Summary table of the theoretical masses calculated from the amino acid sequences and the measured masses by ESI-MS experiments of the LAIR-1 variants produced. (B) SDS-PAGE analysis of the LAIR-1 variants on a 14% polyacrylamide gel under reducing condition.

Figure 2. Identification of the C1q functional region interacting with LAIR-1 and competition assay with the $C1r_2s_2$ tetramer. (A) LAIR-1 (10 µM) was injected over immobilized serum-derived C1q (sC1q, red curve), sCLR (green curve) or sGR (blue curve). (B) sC1q (1 nM) was preincubated with $C1r_2s_2$ at increasing molar ratios (1-5) and injected over immobilized LAIR-1. The grey dashed line represents the $C1r_2s_2$ tetramer injection at a concentration of 10 nM as a control.

Figure 3. Kinetic analysis of LAIR-1 interaction with immobilized serum-derived C1q, rC1q WT and rC1q ABC. LAIR-1 was injected at increasing concentrations (4-128 µM, 2-fold serial dilution) on immobilized sC1q (A), rC1q WT (B) and rC1q ABC (C). Fits obtained by a global fitting of the data to a steady-state model are shown in the top right corner of each panel. The results shown are representative of three (sC1q) or two (rC1q WT and ABC) experiments (see Table 1).

Figure 4. Analysis of LAIR-1 interaction with C1qCLR_nc2 and C1qstem_nc2. (A) Schematic representation of the full length C1qCLR_nc2 protein (left part) and C1qstem_nc2 fragment (right part), the $C1r_2s_2$ binding site is represented with an orange star. (B, C) Soluble LAIR-1 Ig-like domain was injected at increasing concentrations over immobilized C1qCLR_nc2 (B) and C1qstem_nc2 (C). Fits obtained by a global fitting of the data to a steady-state model are shown in the top right corner of each panel. The results shown are representative of three experiments.

Figure 5. LAIR-1 R59 and E61 are central collagen binding residues, conserved in LAIR-2 and GPVI. (A) Sequence alignment of LAIR-1, LAIR-2 and GPVI Ig-like domains. The β-strands forming the collagen interaction groove in LAIR-1 are indicated with grey arrows and the N-glycosylation site (N69) is indicated with a purple star. The LAIR-1 mutated residues are colored in red for the central collagen binding site and in green and orange for the identified distal residues. LAIR-1 conserved and different residues in LAIR-2 and GPVI sequences are colored in light orange and black, respectively. (B) Alignment of the crystal structure of the Ig-like domains of LAIR-1 (in blue, PDB code: 3KGR) and GPVI (in green) in complex with a collagen peptide (in yellow) (PDB code: 5OU8). LAIR-1 R59 and E61 and the GPVI homologous residues are colored in red. LAIR-1 N69 is labelled in purple. The remarkable W109 in LAIR-1, close to the collagen ligand, is labelled in cyan. (C) NanoDSF experiments of LAIR-1 WT (in blue), R59A (in green) and E61A (in red), alone (dashed lines) or in the presence of a positive collagen peptide control (solid lines).

Figure 6. LAIR-1 R59A and E61A mutations abrogate the interaction with C1q and its variants. LAIR-1 WT (blue curves), R59A (green curves) and E61A (red curves) were injected at a concentration of 10 µM over immobilized sC1q (A), C1qCLR_nc2 (B) and C1qstem_nc2 (C).

Figure 7. Mutational analysis of LAIR-1 interaction with C1q. (A) Crystal structure of LAIR-1 Ig-like domain (PDB code: 3KGR). The side chains of the mutated residues are shown and labelled. The central binding residues are colored in red and the distal residues are shown in green and orange (as in Figure 5). (B) SPR measurements of the interaction of LAIR-1 WT and mutants with sC1q, C1qCLR_nc2 and C1qstem_nc2. Results are expressed as the percentage of the LAIR-1 WT response and error bars represent the SD of three different experiments. The detection of a binding signal of LAIR-1 variants with the positive collagen peptide control measured with the nanoDSF method is reported at the bottom. The presence or absence of the characteristic binding signal is reported with + or - symbols, respectively. The cases where a weak binding signal remains are indicated with a ± symbol.

Figure 8. Model of LAIR-1 Ig-like domain in complex with a C1q collagen stem. (A) Sequences of C1q A, B and C chains corresponding to the C1q collagen-like region shown in B. The three lysine residues constituting the $C1r_2s_2$ binding site (A_K59, B_K61 and C_K58) are in bold and the two essential lysines are surrounded with a dashed orange ellipse. The putative LAIR-1 binding OGXO motifs in this region are underlined. The remarkable residues are labelled with their position numbers. The three residues facing the LAIR-1 I102 in each alternative model are labelled in black. The "O" in the sequences stands for proline residues modified into hydroxyprolines, as determined in the literature (Reid 1979; Pflieger et al. 2010). (B) Model of LAIR-1 Ig-like domain (blue, PDB code: 3KGR) in interaction with the C1q CLR triple helix (A chain in cyan, B chain in pink and C chain in green). The collagen-binding groove of LAIR-1 is shown in grey and the side chains of the identified key binding residues are shown and labelled. Mutated lysine 65 and arginine 72 of C1q B and A chains respectively are labelled. The residues facing LAIR-1 I102 in each model are colored in black. The side chains of the identified OGXO motifs are shown in lines.

Figure 9. Kinetic analysis of LAIR-1 interaction with immobilized C1qCLR_nc2 variants. LAIR-1 was injected at increasing concentrations (4-256 µM, 2-fold serial dilution) over immobilized C1qCLR_nc2 B_K65E (A) and C1qCLR_nc2 A_R72E (B). Fits obtained by a global fitting of the data to a steady-state model are shown in the top right corner of each panel. The results shown are representative of three separate experiments (see Table 1).

Figure S1. Comparison of bacterial and mammalian recombinant LAIR-1 extracellular region. LAIR-1 produced in *E. coli* (A) or in HEK293F cells (B) was injected at increasing concentrations (1-16 µM, 2-fold serial dilution) over immobilized sC1q (14,000 RU). Fits obtained by a global fitting of the data to a Langmuir binding model are shown in black. (C) Summary table of the kinetic constants from (A) and (B).

Figure S2. Far-UV circular dichroism spectra (from 204 to 260 nm) of LAIR-1 WT (in blue), R59A (in green) and E61A (in red).

Figure S3. Alternative models of LAIR-1 Ig-like domain in complex with C1q collagen stem. Models of LAIR-1 Ig-like domain (blue, PDB code: 3KGR) in interaction with the C1q CLR triple helix (A chain in cyan, B chain in pink and C chain in green). The collagen-binding groove of LAIR-1 is shown in grey and the side chains of the identified key binding residues

737 are shown and labelled. Remarkable lysine 65 and arginine 72 of C1q B and A chains
738 respectively are labelled. The residues facing the I102 of LAIR-1 in each model are labelled in
739 black. The side chains of the identified OGXO motifs are shown in lines.

740 **Figure S4. Supplementary GPP triplets introduce additional LAIR-1 binding sites within**
741 **CLR_nc2.** (A) LAIR-1 was injected at increasing concentrations (4-128 µM, 2-fold serial
742 dilution) over immobilized CLR_nc2 containing the GPP triplets between the CLR and nc2
743 sequences. Fits obtained by a global fitting of the data to a steady-state model are shown in
744 the top right corner. The result shown is representative of separate experiments (see B). (B)
745 Summary table of the Rmax and K_D values derived from the SPR kinetic analyses obtained
746 with the old (with GPP) and new (without GPP) generation of the CLR_nc2 fusion protein.

Figure 1

A

LAIR-1 variants	WT	R59A	E61A	I102L	I102Y	E72K	E111K	P107R
Theoretical mass (Da) *Calculated from the amino acid sequence*	12,678	12,593	12,620	12,678	12,728	12,677	12,677	12,719
Measured mass (Da) (ESI-MS)	12,676	12,591	12,618	12,676	12,726	12,675	12,675	12,717

B

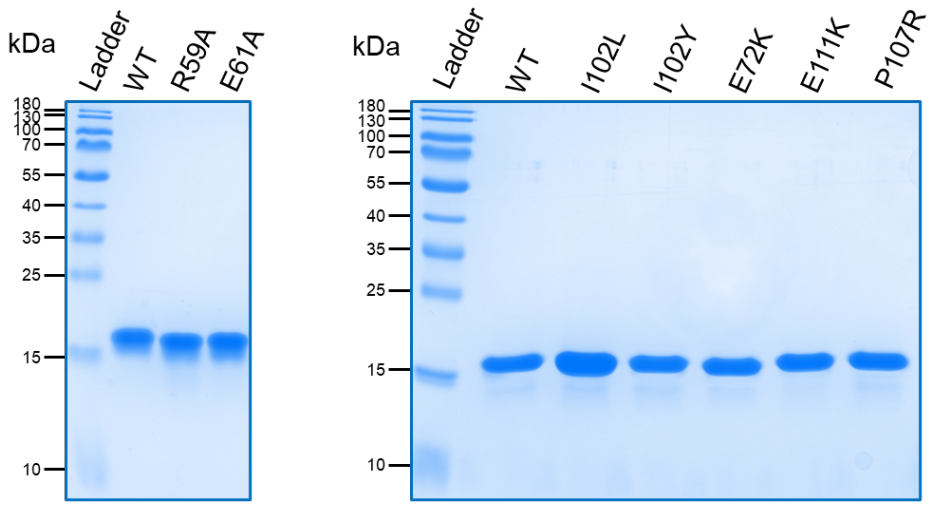

Figure 2

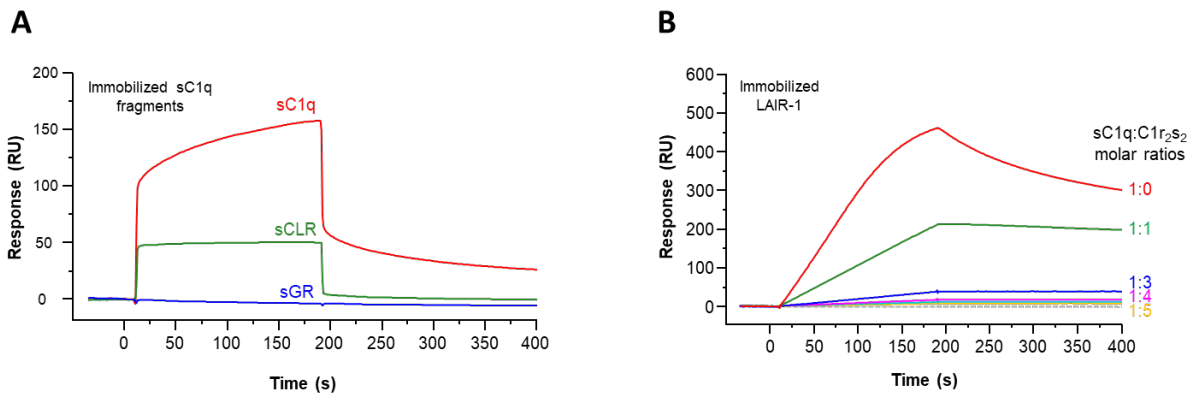

Figure 3

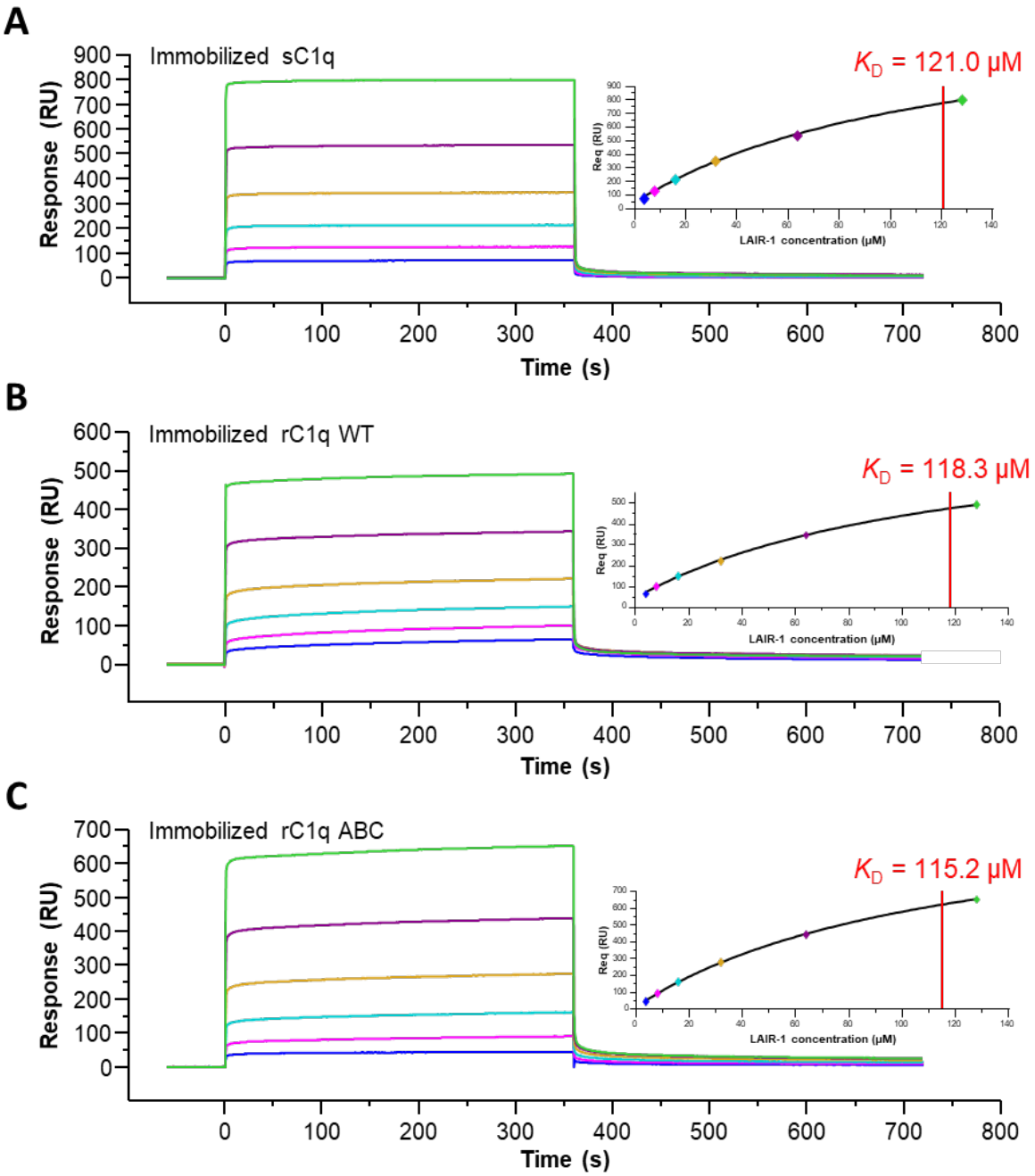
A
Immobilized sC1q
K_D = 121.0 µM
Response (RU)
Time (s)
Req (RU)
LAIR-1 concentration (µM)
B
Immobilized rC1q WT
K_D = 118.3 µM
Response (RU)
Time (s)
Req (RU)
LAIR-1 concentration (µM)
C
Immobilized rC1q ABC
K_D = 115.2 µM
Response (RU)
Time (s)
Req (RU)
LAIR-1 concentration (µM)

Figure 4

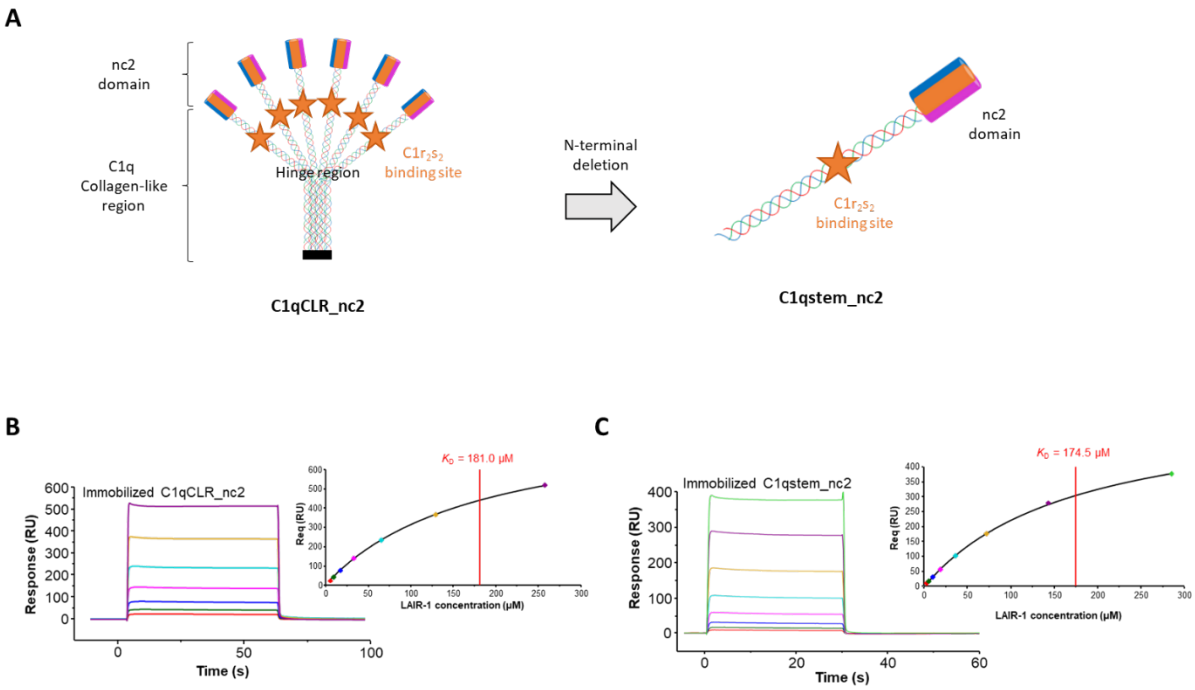

Figure 5

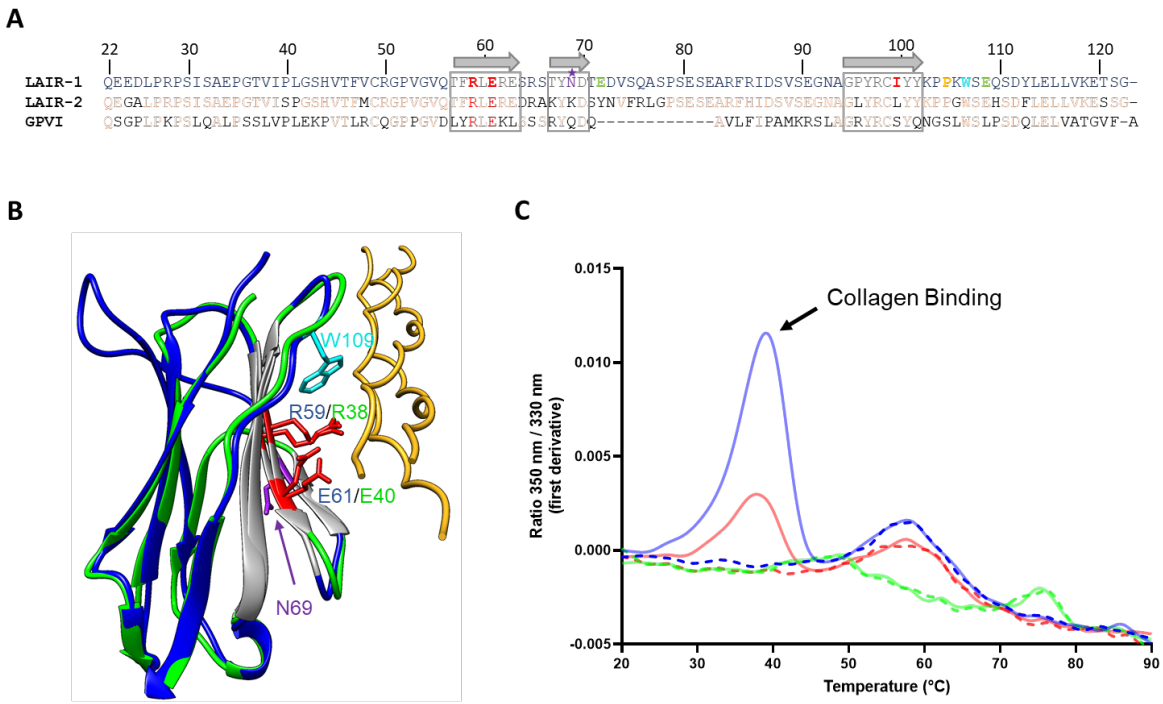

Figure 6

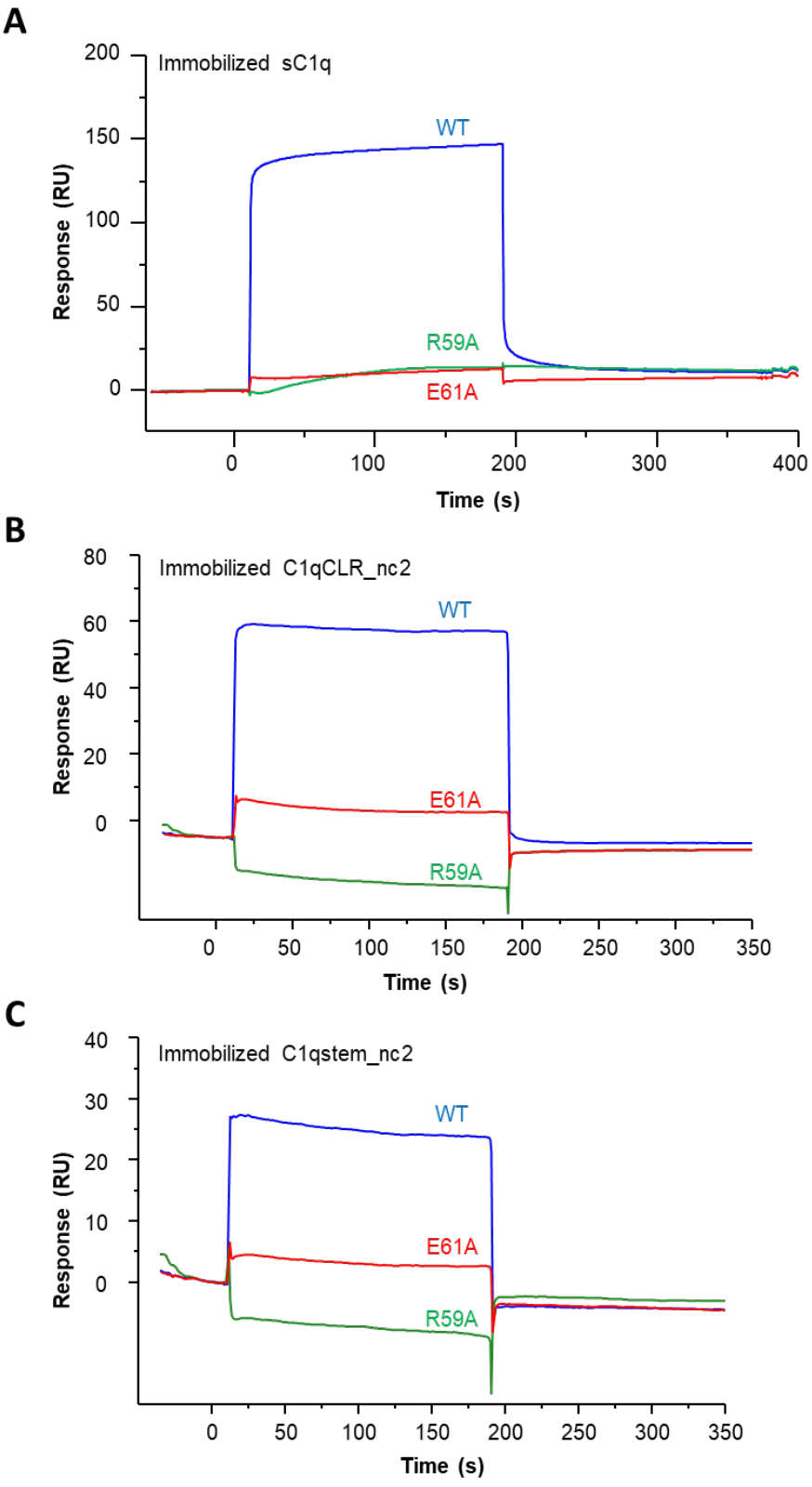
A
Immobilized sC1q
WT
R59A
E61A
Response (RU)
Time (s)
B
Immobilized C1qCLR_nc2
WT
E61A
R59A
Response (RU)
Time (s)
C
Immobilized C1qstem_nc2
WT
E61A
R59A
Response (RU)
Time (s)

Figure 7

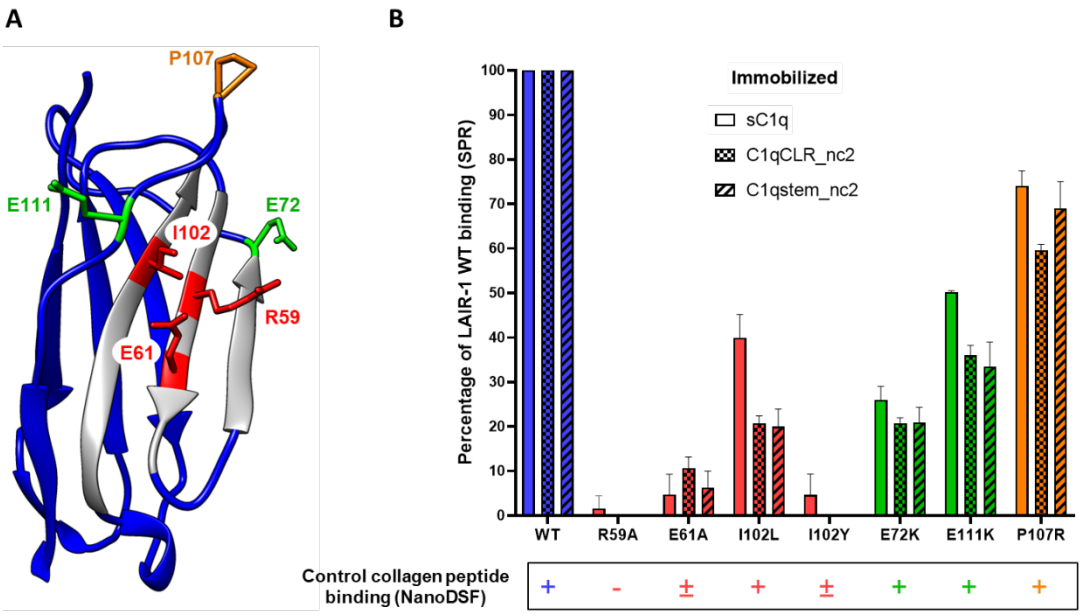

Figure 8

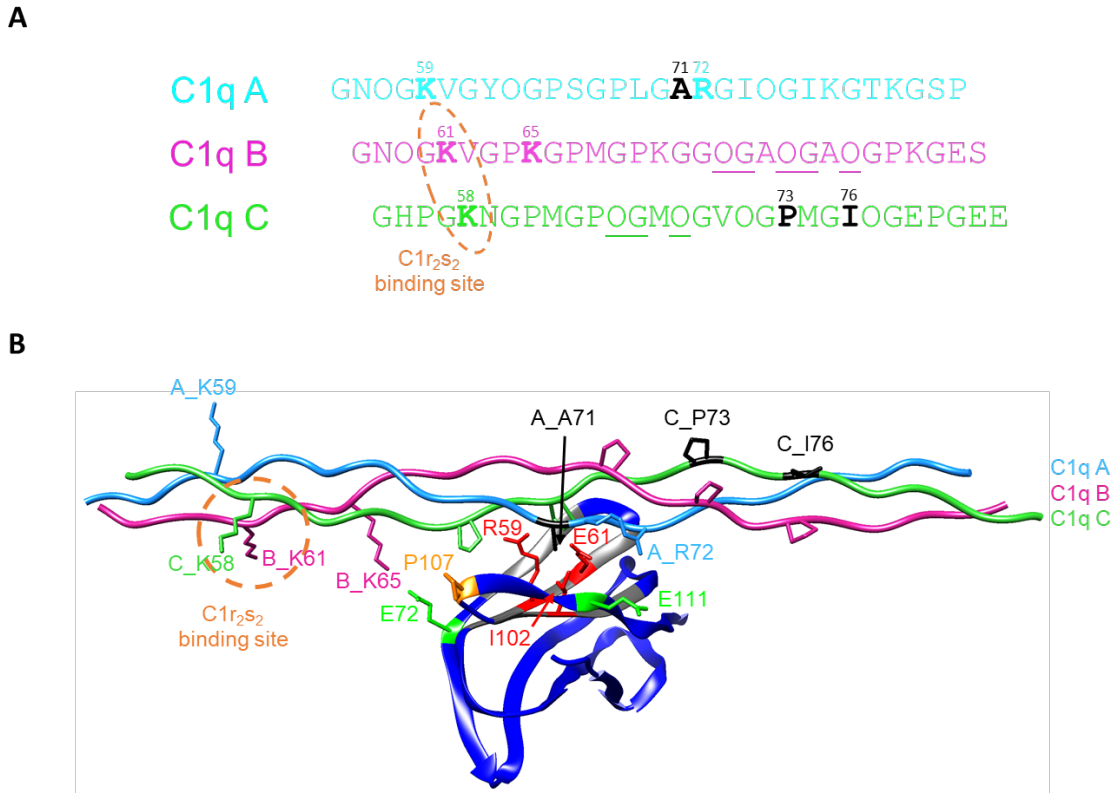

Figure 9

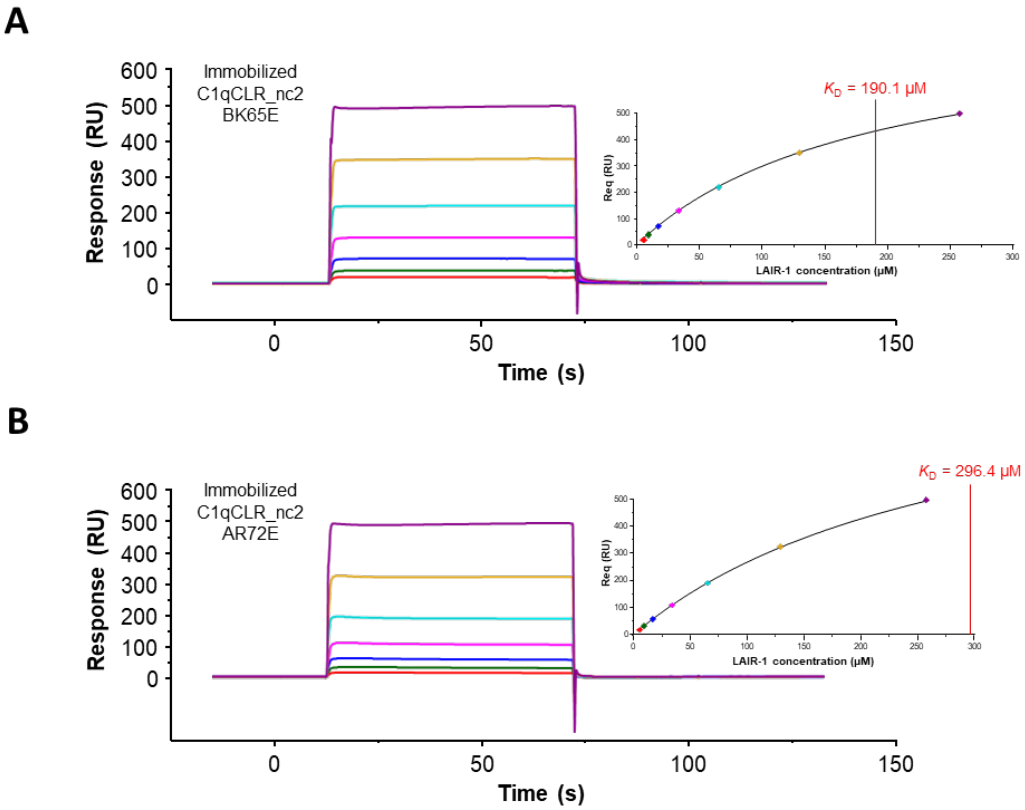

Table 1

Immobilized ligands	LAIR-1 WT K_D (µM)
sC1q	112.3 ± 6.2 *(n=4)*
rC1q WT	99.5 ± 26.6 *(n=2)*
rC1q ABC	131.8 ± 23.5 *(n=2)*
C1qCLR_nc2	179.3 ± 4.8 *(n=3)*
C1qCLR_nc2 AR72E	295.0 ± 10.6 *(n=3)*
C1qCLR_nc2 BK65E	188.8 ± 5.3 *(n=3)*
C1qstem_nc2 DelNter	174.9 ± 0.6 *(n=2)*

Values are means ± SD from separate experiments. The number of replicates (n) are indicated next to the K_D values
The dissociation constant K_D was determined by global fitting of the data using a steady-state binding model.

Supplementary 1

A

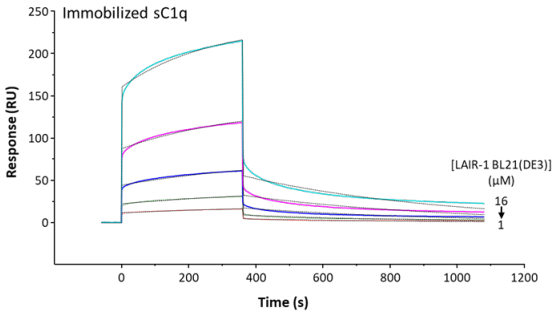

B

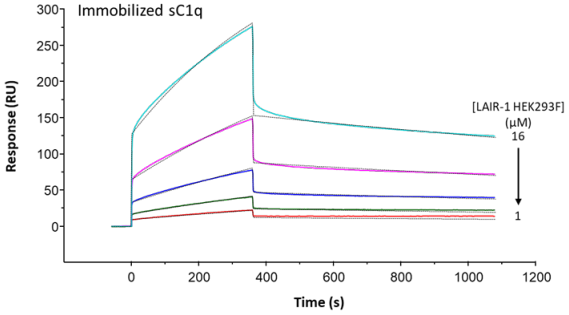

C

Analyte	Serum-derived C1q		
	k_a	k_d	K_D
	$M^{-1}.s^{-1}$	s^{-1} (x 10^{-4})	µM
LAIR-1 BL21(DE3)	132.0	16.8	12.7
LAIR-1 HEK293F	105.2	3.1	2.9

Values are from one experiment. The association (*ka*) and dissociation (*kd*) rate constants were determined by global fitting of the data using a Langmuir binding model.
The resulting dissociation constate K_D was determined by the ratio *kd*/*ka*

Supplementary 2

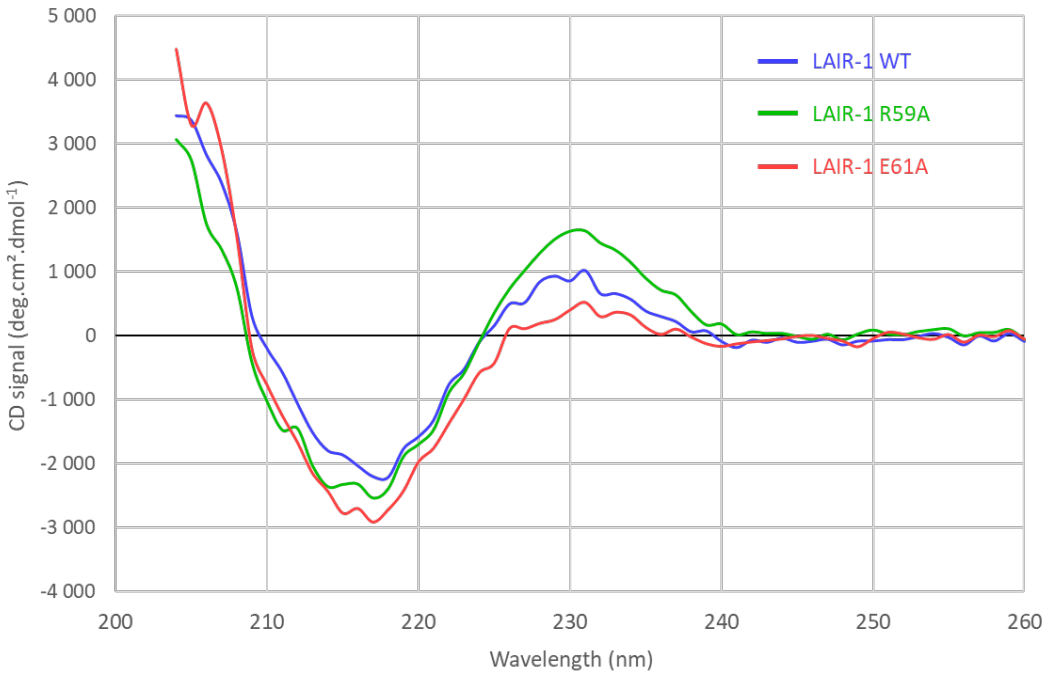

Supplementary 3

A

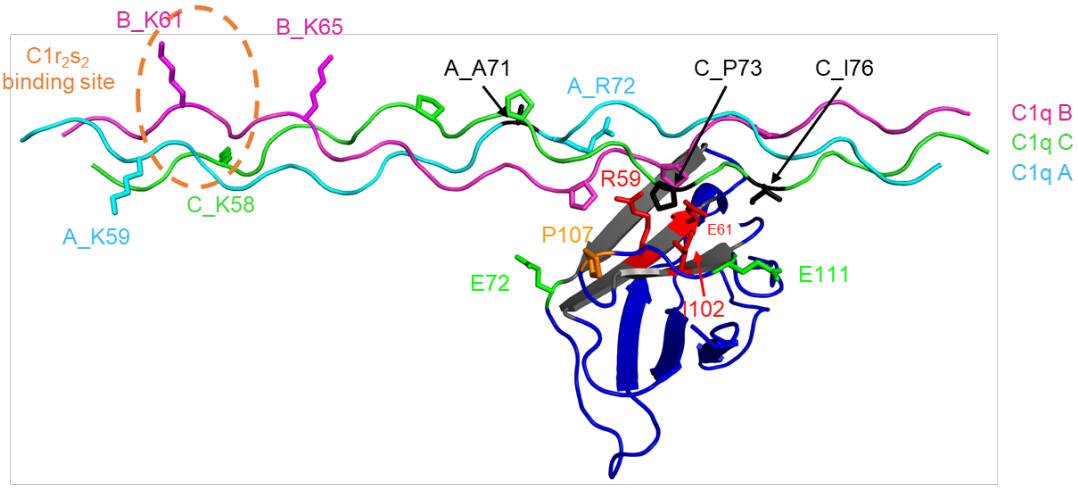

B

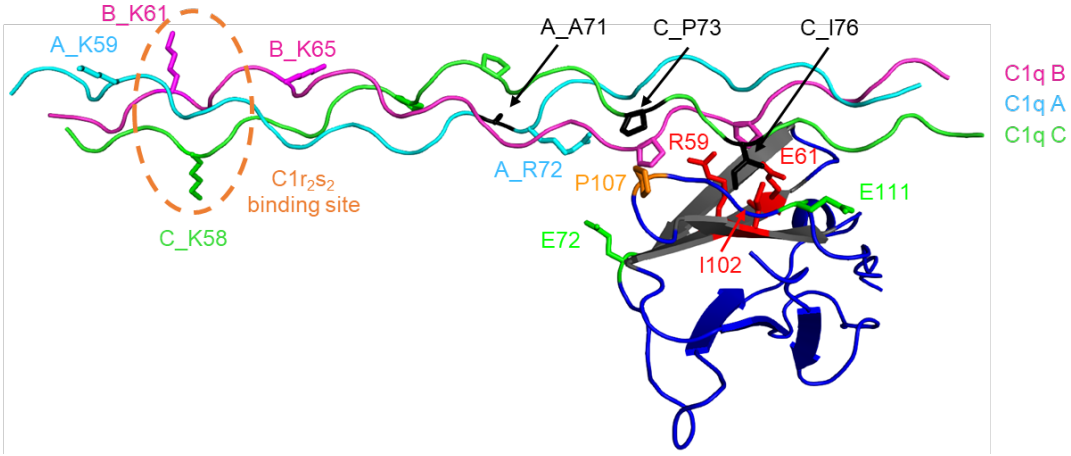

Supplementary 4

A

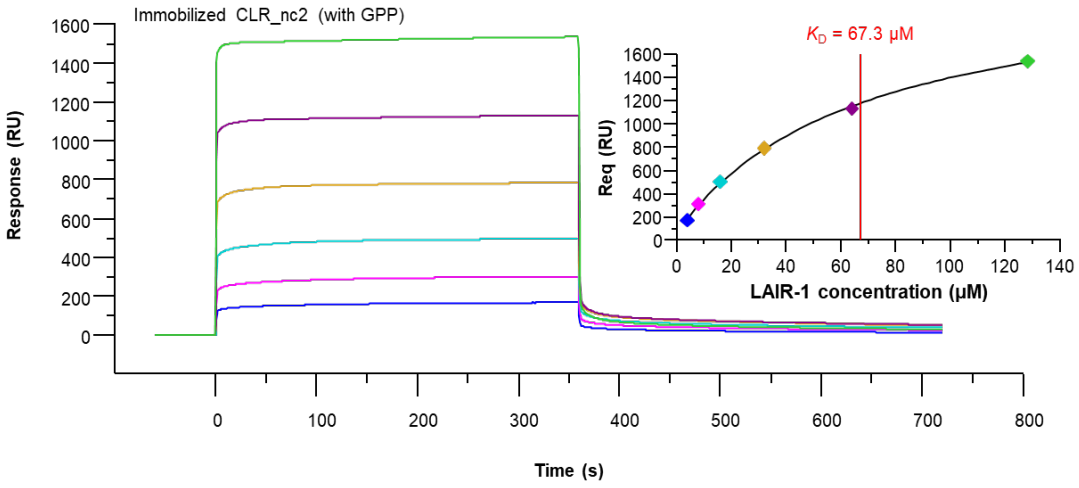

B

Ligand	LAIR-1	
	Rmax (RU)	K_D (µM)
sC1q	1443 ± 31	112.3 ± 6.2 *(n=4)*
CLR_nc2 (with GPP)	2325 ± 168	79.5 ± 11.6 *(n=3)*
C1qCLR_nc2 (without GPP)	871 ± 18	179.3 ± 4.8 *(n=3)*

Values are means ± SD from separate experiments. The number of replicates (n) are indicated next to the K_D values
The dissociation constant K_D was determined by global fitting of the data using a steady-state binding model.

III. **Unpublished Data:** LAIR-1 dimerization effects on C1q interaction

1 Scientific context

As for most of the transmembrane receptors, signal transduction via LAIR-1 relies on its dimerization on the cell surface. It has been previously reported that LAIR-1 intracellular ITIMs phosphorylation is induced by antibody-mediated LAIR-1 dimerization on immune cells, thus recruiting phosphatase and inhibiting positive immune signals induced by other receptors (Meyaard et al. 1997; Xu et al. 2000). Collagens, the natural ligands of LAIR-1 were shown to induce ITIMs phosphorylation upon binding to LAIR-1 (Lebbink et al. 2006, 2009). Based on the fact that LAIR-1 recognizes the collagen Gly-X-Y backbone and that collagen molecules contain multiple collagen triplets, it is likely that one collagen molecule could bind and aggregate several LAIR-1, thus transducing the inhibitory signal. In this context, several analyses of soluble LAIR-1 interaction with collagens used antibody Fc region fusions in order to induce the LAIR-1 Ig-like domain dimerization (Lebbink et al. 2006, 2009; Rygiel et al. 2011; Olde Nordkamp et al. 2014a; Agashe et al. 2018; Kumawat et al. 2019). In our particular case of the study of LAIR-1 interaction with C1q, such Fc fused LAIR-1 Ig-like domain cannot be considered because C1q is known to interact with the Fc region of antibodies through its globular regions (Hughes-Jones and Gardner 1979). This rises the need for an alternative approach to obtain a dimeric LAIR-1 Ig-like domain.

Several crystal structures of the LAIR-1 Ig-like domain are available in the PDB and by analyzing them, we found one (PDB code: 3RP1) with two monomers presenting a possible dimeric-like association in the crystal packing. This association of two LAIR-1 Ig-like domains would be possible on the cell membrane. Indeed, the C-terminal extremities (membrane side) are oriented in the same direction, close to each other (12 Å distance) and the two collagen binding sites are exposed on the other side of the domain (Figure 23A). However, the interaction surface between the two LAIR-1 Ig-like domain is narrow and not favorable for the dimer formation, since PISA (proteins, interfaces, structures and assemblies, Krissinel and Henrick 2007) interface analysis gives a null score. This suggests that LAIR-1 Ig-like domain dimerization on the cell surface should be induced by ligand binding. We tried to detect the binding of LAIR-1 Ig-like domain on itself by SPR and did not detect any binding signal, therefore supporting the ligand-induced dimerization of LAIR-1. As illustrated in Figure 23B,

this association of Ig-like domains could likely accommodate the binding of a collagen triple helix between the two monomers collagen binding surfaces which are perfectly aligned.

Interestingly, a remarkable serine residue (S92; in red in Figure 23) is located in the contact zone of the two LAIR-1 domains. We decided to mutate this serine into a cysteine residue (S92C) in order to block the dimer via disulfide bond for functional and structural studies. We first checked that the S92C mutation would properly position the two cysteines to accommodate an inter-monomer disulfide bridge by using two predictive softwares: modip and DdB2 (Thangudu et al. 2005; Dombkowski et al. 2014). This hypothesis was supported by the two theoretical approaches.

In addition, the serine 92 was also mutated into a bulkier lysine residue (S92K) in order to introduce steric hindrance and avoid formation of such a dimer.

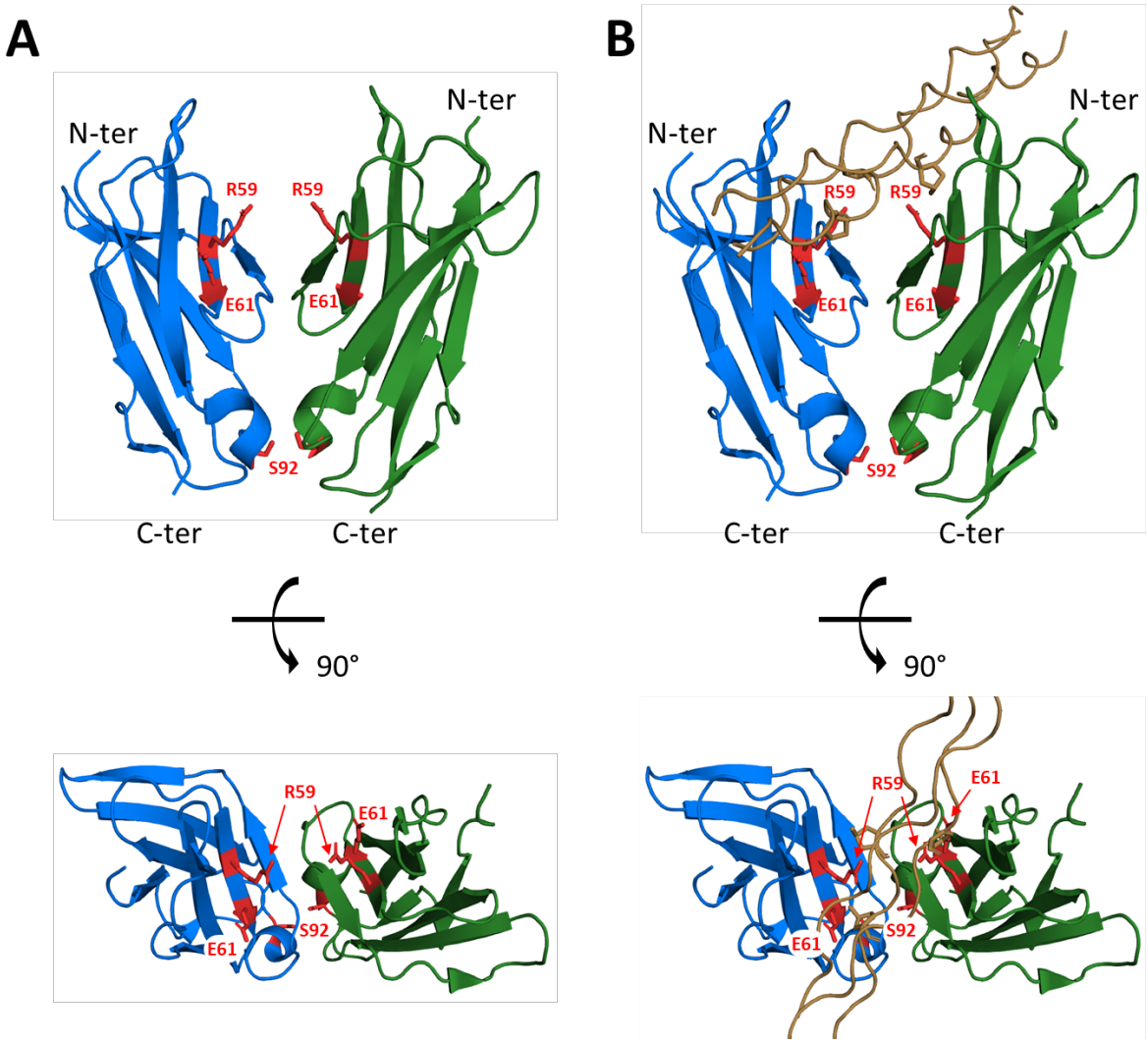

Figure 23: Parallel LAIR-1 subunits association observed in the crystal packing of LAIR-1 Ig-like domain structure. *A. Side view (upper part) and top view (lower part) of A and C subunits in the crystal packing of one LAIR-1 Ig-like domain structure (PDB code: 3RP1). The two essential LAIR-1 residues (R59 and E61) for the collagen interaction and the remarkable serine 92 (S92) residue are labelled in red. The C-terminal and N-terminal extremities are labelled in black.* ***B****. Model illustrating that the collagen binding-sites in these two subunits (in blue and green) are perfectly aligned, and thus possibly offering an extended binding site for a GPO collagen peptide (in brown, extracted from PDB 5OU8). The side chains of the hydroxyproline residues at the interaction surface are shown as sticks.*

2 Results

2.1 SEC-MALLS comparative analysis of LAIR-1 WT, S92K and S92C

In order to validate our strategy and investigate the oligomeric state of the two LAIR-1 S92K and S92C variants, we performed size-exclusion chromatography multi angle laser light scattering (SEC-MALLS) experiments on the purified samples. As shown in Figure 24A, the LAIR-1 WT Ig-like domain (blue curve) is mostly present in a monomeric form with a small portion of dimer. As opposed to LAIR-1 WT, the S92C variant presents a majority of dimers and SDS-PAGE analysis of the dimer fraction under non-reducing and reducing conditions

revealed that the S92C dimer is covalently linked thanks to a disulfide bond between the two Ig-like domains (Figure 24B). As expected, the presence of a lysine residue at position 92 leads to a LAIR-1 variant exclusively monomeric in solution (Figure 24A, red curve).

We managed, with the mutations of the serine 92 of LAIR-1 Ig-like domain, to generate LAIR-1 variants that are exclusively monomeric (S92K) or dimeric (S92C) that will constitute useful tools for the study of LAIR-1 dimerization effects on C1q interaction.

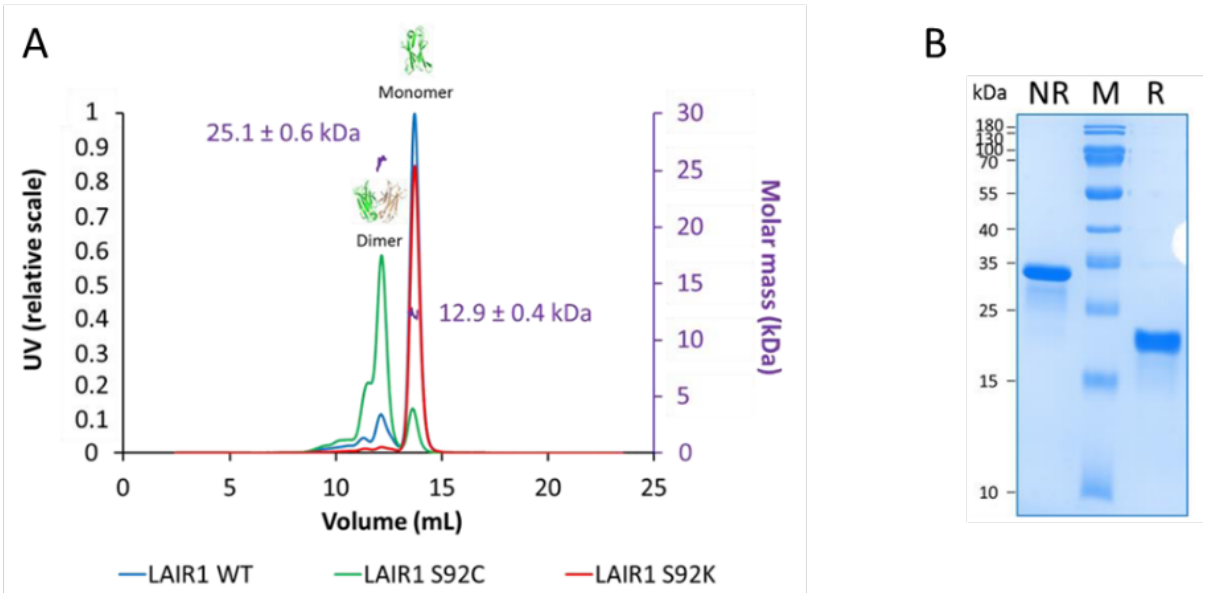

Figure 24: Oligomeric states of LAIR-1 WT, S92C and S92K. *A. SEC-MALLS analysis of LAIR-1 WT, S92C and S92K injected on Superdex 75-10/300 column at concentrations of 5, 4.5 and 4 mg/ml respectively.* ***B****. SDS-PAGE (14% acrylamide) analysis of LAIR-1 S92C covalent dimer under non-reducing (NR) and reducing (R) conditions.*

2.2 Structural characterization of LAIR-1 S92C variant

In order to obtain information about the conformation of the LAIR-1 S92C covalent dimer, we performed X-ray crystallography to solve its structure (Appendix 2). As shown in Figure 25A, our crystal structure reveals that the covalent S92C dimer structure does not exhibit the expected conformation of the initial dimeric model and presented two Ig-like domains rotated around the disulfide bond to get a different orientation from the one presented in Figure 23A. In fact, it is not surprising that a unique disulfide bond at the molecular edge might not rigidly maintain the two monomers and likely allows free rotation around it. This highlights the fact that LAIR-1 extracellular Ig-like domains might not spontaneously dimerize at the cell surface. Thus, the dimerization of LAIR-1could possibly be dependent on the interaction of both monomers with the same collagen, acting as a bridging molecule.

In order to get information about the conformation of the S92C dimer in solution, we performed small angle X-ray scattering (SAXS) experiments and compared the experimental data to the theoretical data generated by both the dimeric model and our solved crystal structure (Figure 25B). The experimental data do not fit with the simulated curves of either the model or the crystal structure (Figure 25B, red and blue curve, respectively). The intermediate conformation observed in the SAXS experiment can be explained by the dynamic rotation of the two monomers at each side of the disulfide bond. This again suggests that the parallel association shown in figure 27 is not stable and likely occurs only transiently.

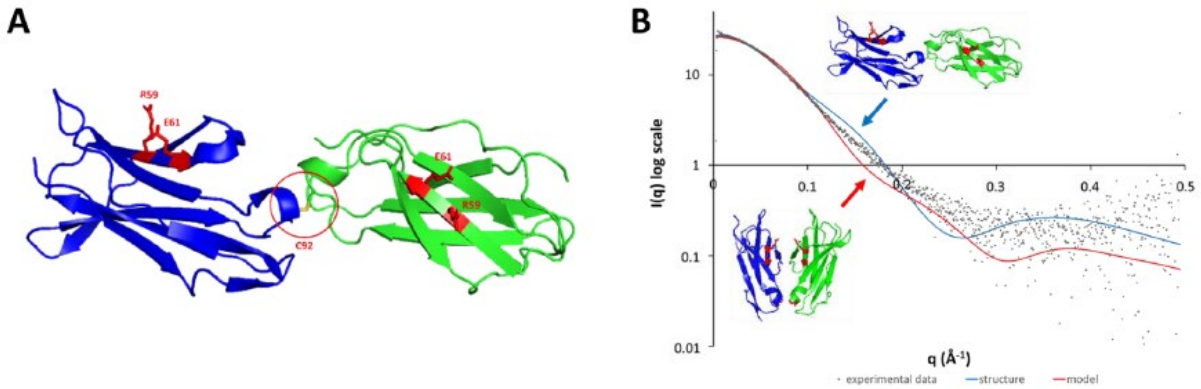

Figure 25: Structural characterization of LAIR-1 S92C covalent dimer. ***A****. Crystal structure of LAIR-1 covalent dimer.* ***B****. SAXS analysis of LAIR-1 S92C covalent dimer. Experimental data (black dots) are compared to theoretical scattering profiles of the model of parallel association (red curve) or our crystal structure (blue curve).*

2.3 Surface plasmon resonance analysis of LAIR-1 S92K and S92C interaction with C1q

The interaction of the LAIR-1 S92C dimer and S92K monomer with serum-derived C1q (sC1q) was investigated using surface plasmon resonance (SPR) and compared to the LAIR-1 WT. As shown in Figure 30A, LAIR-1 S92C dimer kinetic analysis of the interaction with immobilized sC1q reveals that the dissociation constant K_D is 4 times lower than the one obtained with LAIR-1 WT (27 µM instead of 112 µM). Conversely, preliminary SPR experiments highlight that the LAIR-1 interaction is slightly decreased by the S92K mutations (20% decrease of the response, Figure 30B). However, this lower binding efficiency needs to be confirmed by kinetics experiments and K_D value determination. These preliminary binding assays show the positive effect of LAIR-1 dimerization on the affinity of the interaction with C1q that could be attributed to an increase in avidity.

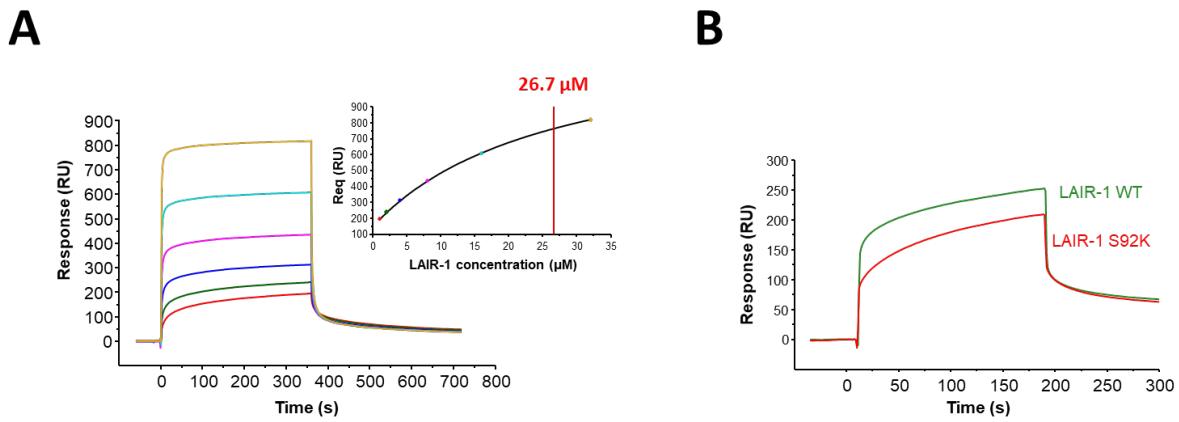

Figure 26: SPR analysis of LAIR-1 S92C and S92K interaction with C1q. ***A****. LAIR-1 S92C was injected at increasing concentrations (1-32 µM) over immobilized sC1q (14,000 RU). Fits obtained by a global fitting of the data to a steady-state model are shown in the top right corner.* ***B****. LAIR-1 WT (green curve) and S92K (red curve) were injected at a concentration of 10 µM on immobilized sC1q (14,000 RU).*

In order to block the LAIR-1 S92C dimer in the conformation were the two Ig-like domains are oriented in the same orientation (Figure 23), we performed crystallization assays in the presence of the synthetic collagen peptide used in Article 2. As LAIR-1 S92C interacts with C1q, we also performed crystallization assays in the presence of the C1qstem_nc2 (Figure 21). Unfortunately, we did not find conditions prone to crystal formation and further screenings of crystallogenesis conditions are needed.

IV. **Preliminary data:** expression of LAIR-2 and CD33 Ig-like domains

1 Design of the constructs

In order to extend the study with the two other Ig-like receptors LAIR-2 and CD33, we tried to produce their soluble Ig-like domains. To do so, we initially planned to use two different expression systems: a bacterial expression system (BL21(DE3)) for structural studies purposes and an eukaryotic expression system (HEK293F) for the functional interaction studies. Therefore, we cloned the Ig-like domain sequences in two different expression vectors: pET28a(+) for expression in bacteria and pcDNA3.1(+) for eukaryotic expression. On one hand, for structural studies, we restricted the sequences cloned in pET28a to the Ig-like domain sequence (i.e., LAIR-2: 22-122 and CD33: 142-232; immature protein amino acids numbering). One the other hand, the sequences cloned into the pcDNA3.1(+) vector were chosen to code for the entire extracellular region of each receptor (i.e. LAIR-2: 1-152 and CD33: 1-232; immature amino acids numbering) (Figure 27; Appendix 1).

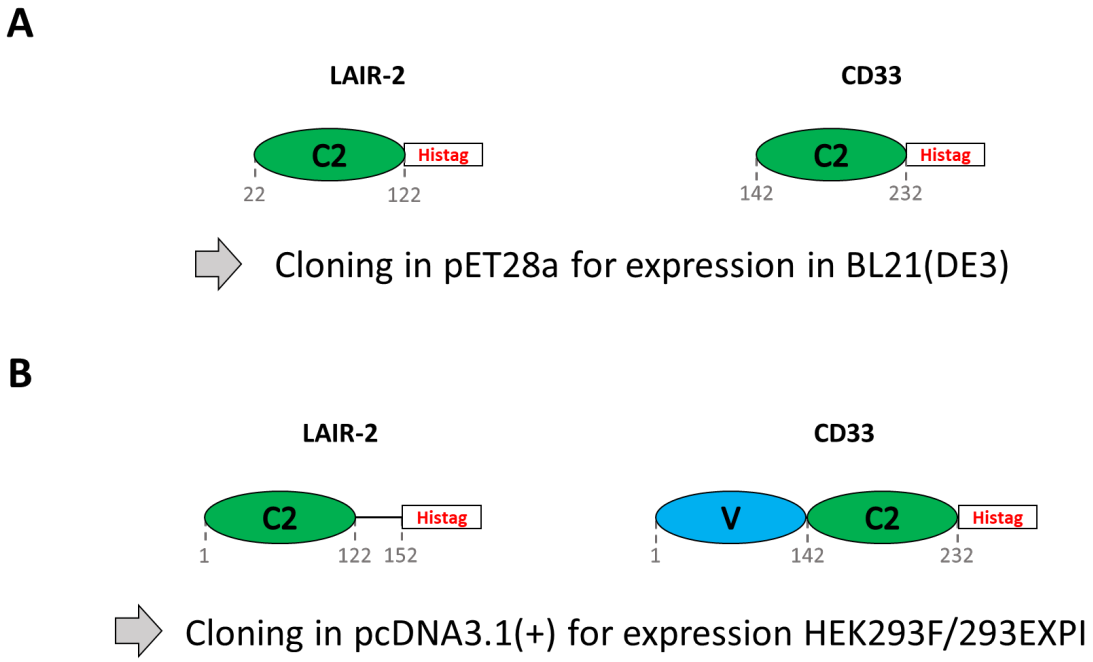

Figure 27: Schematic representation of the Ig-like receptors fragments expressed in bacterial (A) and eukaryotic expression systems (B). *The N- and C-terminal residues are indicated with grey numbers (immature protein amino acids numbering). The additional C-terminal polyhistidine tags (Histag) are labelled in red.*

2 Expression in bacteria: E. coli BL21(DE3)

We first tested the expression of the receptor constructs into *E. coli* BL21(DE3) cells. We tried the expression of LAIR-2 and CD33 using classical IPTG induction or an autoinduction medium (Appendix 1). As shown in Figure 16, none of the two tested induction procedures allowed the expression of the LAIR-2 Ig-like domain. Indeed, even if LAIR-1 and LAIR-2 Ig-like domain sequences are highly homologous (84% of homology), no protein band appeared after induction (Figure 28A).

Regarding the Ig-like domain of CD33, the expression was induced in BL21(DE3) but the produce protein was only present in the non-soluble fraction (Figure 28B). This was confirmed by western blot analysis using an HRP-coupled monoclonal antibody directed against the polyhistidine tag (not shown). As for LAIR-2 the expression of CD33 Ig-like domain in BL21(DE3) could not be achieved in these conditions.

Therefore, the bacterial expression system did not seem suitable for the expression of LAIR-2 and CD33 Ig-like domains in the conditions tested.

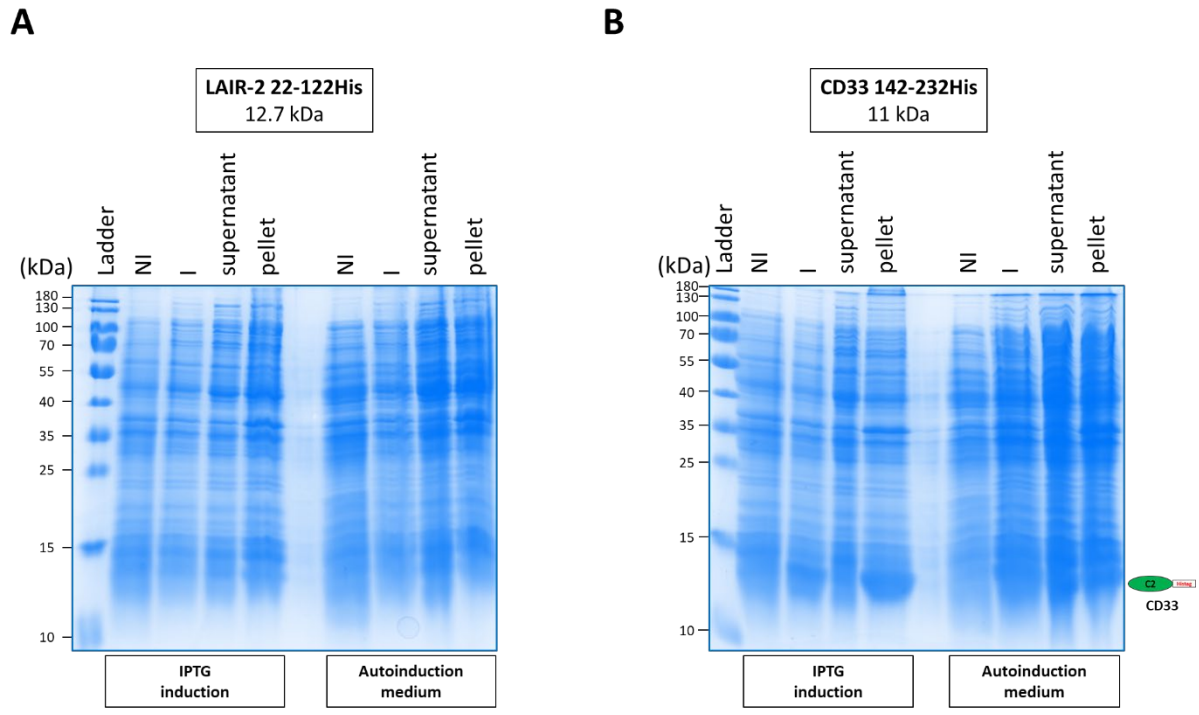

Figure 28: Expression tests of LAIR-2 and CD33 Ig-like domains in E. coli BL21(DE3). *SDS-PAGE analysis (14% acrylamide) of the different fractions of the expression tests of Ig-like domains of LAIR-2 (A) and CD33 (B). For each receptor Ig-like domain, the transformed cells were analyzed before (NI) and after (I) induction. The analyses of the supernatant and pellet fractions of the cells after lysis are also shown. The induction procedure (i.e. IPTG induction or autoinduction medium) is indicated at the bottom of the corresponding lanes. The theoretical molecular weight of each fragment is indicated in black at the top of each gel. The expected Mw of the Ig-like domains are indicated with its schematic representation on the right side of the gel. The molecular weights of the ladder bands (in kDa) are indicated in black on the left side of each gel.*

3 Expression in eukaryotic cells: HEK293F

In order to express the entire extracellular regions of LAIR-2 and CD33, we transfected HEK293F cells with the pcDNA3.1(+) vectors containing the corresponding coding sequences (Appendix 1). We then selected the stable transfectants using neomycin (400 µg/mL). The culture medium of stably expressing cells was analyzed by western blot using an HRP-coupled monoclonal antibody directed against the polyhistidine tag. The western blot analysis revealed that the stable cell lines expressed the three constructs in a soluble form. However, the expression levels are very different for the three receptor fragments: LAIR-2 was very poorly expressed whereas CD33 seemed to be expressed in reasonable quantities (Figure 29).

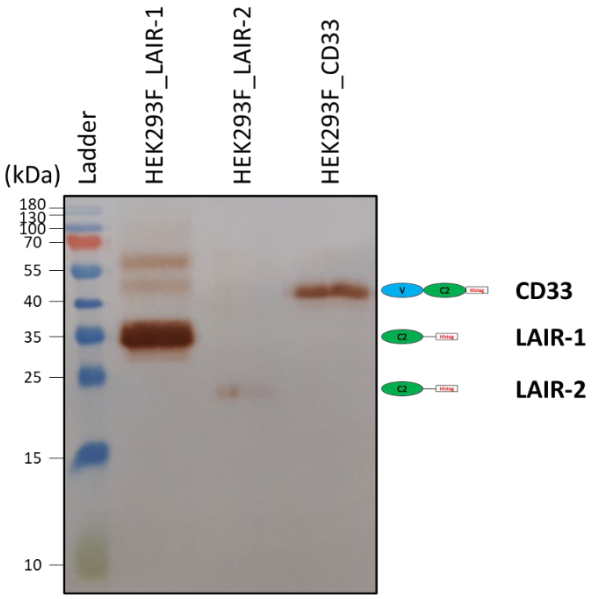

Figure 29: Expression of the extracellular domains of LAIR-1, LAIR-2 and CD33 in HEK293F cells. *Western blot analysis of the cell culture supernatants (1 mL of supernatant precipitated with trichloroacetic acid) of HEK293F transfected cells using an anti-polyhistidine antibody coupled with horseradish peroxidase. The schematic representation of the three constructs corresponding to the protein bands are shown on the right side of the membrane. The molecular weights of the ladder bands (in kDa) are indicated in black on the left side of the membrane.*

V. **Articles 3 and 4:** investigation of C1q interaction with CR1 and LRP1

During my PhD thesis, I had the opportunity to work on C1q interaction with two other receptors: CR1 and LRP1. These two receptors are large multimodular endocytic receptors that were shown to be involved in the C1q-mediated enhancement of immune complexes and apoptotic cells clearance. Briefly, we performed a molecular dissection strategy to identify which part of each receptor was engaged into C1q interaction. We managed to show that the CCP24-25 modules of CR1 and clusters II and IV of LRP1 interact with the collagen-like region of C1q through a binding site close to the one of the $C1r_2s_2$ tetramer, a behavior that is similar to what was observed in the case of LAIR-1 (Discussion & perspectives section). The following published papers report the results we obtained for the investigation of C1q interaction with CR1 (Article 3) and LRP1 (Article 4).

1 **Article 3:** C1q and mannose-binding lectin interact with CR1 in the same region on CCP24-25 modules

frontiers in Immunology

ORIGINAL RESEARCH
published: 07 March 2018
doi: 10.3389/fimmu.2018.00453

C1q and Mannose-Binding Lectin Interact with CR1 in the Same Region on CCP24-25 Modules

*Mickaël Jacquet, Gianluca Cioci, Guillaume Fouet, Isabelle Bally, Nicole M. Thielens, Christine Gaboriaud and Véronique Rossi**

Univ. Grenoble Alpes, CEA, CNRS, IBS, Grenoble, France

Complement receptor type 1 (CR1) is a multi modular membrane receptor composed of 30 homologous complement control protein modules (CCP) organized in four different functional regions called long homologous repeats (LHR A, B, C, and D). CR1 is a receptor for complement-opsonins C3b and C4b and specifically interacts through pairs of CCP modules located in LHR A, B, and C. Defense collagens such as mannose-binding lectin (MBL), ficolin-2, and C1q also act as opsonins and are involved in immune clearance through binding to the LHR-D region of CR1. Our previous results using deletion variants of CR1 mapped the interaction site for MBL and ficolin-2 on CCP24-25. The present work aimed at deciphering the interaction of C1q with CR1 using new CR1 variants concentrated around CCP24-25. CR1 bimodular fragment CCP24-25 and CR1 CCP22-30 deleted from CCP24-25 produced in eukaryotic cells enabled to highlight that the interaction site for both MBL and C1q is located on the same pair of modules CCP24-25. C1q binding to CR1 shares with MBL a main common interaction site on the collagen stalks but also subsidiary sites most probably located on C1q globular heads, contrarily to MBL.

Keywords: complement, C1q, CR1/CD35, CCP modules, protein engineering, interaction, surface plasmon resonance, receptor

OPEN ACCESS

Edited by:
Zvi Fishelson,
Tel Aviv University, Israel

Reviewed by:
Kenneth Reid,
University of Oxford,
United Kingdom
Teizo Fujita,
Fukushima Medical
University, Japan

****Correspondence:***
Véronique Rossi
veronique.rossi@ibs.fr

Specialty section:
This article was submitted to Molecular Innate Immunity, a section of the journal Frontiers in Immunology

Received: *16 January 2018*
Accepted: *20 February 2018*
Published: *07 March 2018*

Citation:
Jacquet M, Cioci G, Fouet G, Bally I, Thielens NM, Gaboriaud C and Rossi V (2018) C1q and Mannose-Binding Lectin Interact with CR1 in the Same Region on CCP24-25 Modules. Front. Immunol. 9:453. doi: 10.3389/fimmu.2018.00453

INTRODUCTION

C1q is a defense collagen that plays a crucial role in innate immunity. Beside its implication in the initiation of the classical pathway of complement, in association with its cognate C1r and C1s serine proteases, it is involved in a number of other non-complement functions, such as immune complex clearance, phagocytosis, cytokine regulation, and immune effector mechanisms mediation (1–4).

C1q is a complex molecule of 460 kDa, resembling a bunch of flowers made from the association of three different polypeptide chains, A, B, and C, organized into six heterotrimeric subunits. The overall molecule presents two distinct regions, with six globular heads (GR) on one end (flowers) and six collagenic stalks (CLF) assembled into a bundle of fibers, on the other end (5, 6). Because of

Abbreviations: GR, globular region of C1q; CLF, collagenic stalks of C1q; CR1, complement receptor type 1; sCR1, soluble CR1; CCP, complement control protein repeat; LRP1, LDL receptor related protein 1; RAGE, receptor for advanced glycation end products; Siglec-3, sialic-acid-binding immunoglobulin-like lectin-3; LAIR-1, leukocyte associated immunoglobulin-like receptor 1; CRT, calreticulin; MBL, mannose-binding lectin; MASP, MBL-associated serine protease; SPR, surface plasmon resonance; RU, resonance unit; TEA, triethanolamine-HCl; SAXS, small-angle X-ray scattering; ESRF, European Synchrotron Radiation Facility.

its multimeric organization, C1q acts as a multipattern recognition molecule, as well as other members of the defense collagens familly, mannose-binding lectin (MBL), and ficolins (7, 8). Their anchorage on some of their targets is made possible by this multimeric scaffold that can provide avidity and versatile interactions with the globular heads and/or the collagen stalks. Therefore, the diversity of ligands for C1q relates in part to its GR and C1q tail domains, which bind specific cell surface receptors to regulate innate immunity. Most receptors described for C1q GR and CLF are involved in the phagocytic uptake by macrophages of self and non self-products. They include LDL receptor-related protein 1 (LRP1/CD91), calreticulin (CRT), gC1qR, receptor for advanced glycation end products (RAGE), leukocyte associated immunoglobulin-like receptor 1 (LAIR-1/CD305), sialic-acid-binding immunoglobulin-like lectin-3 (Siglec-3/CD33), and complement receptor 1 (CR1/CD35) (9–14). Some of these receptors interact with C1q GRs (RAGE, CD33, gC1qR) or with C1q CLF (LAIR-1), or with both C1q regions (CRT). Nevertheless, most of these interactions are not completely characterized yet and might differ according to the physiological context. In the case of CR1, it has been proposed that the interaction is mediated by C1q CLF (15, 16).

Complement receptor 1 (CR1/CD35) is a large multimodular type 1 transmembrane glycoprotein exposed at the surface of a wide range of cells. It is predominantly expressed on erythrocytes and most peripheral blood leukocytes and is mainly involved in the clearance from the blood stream of complement opsonized components (17–20). CR1 has also a major role in controling the complement-mediated attack. It is implicated in the acceleration of complement convertases decay and cooperates as a cofactor of factor I in the cleavage of C3b and C4b. Its crucial role in the protection of renal epithelial cells by reducing the level of complement deposition triggered by the classical and lectin pathways has been reported recently (21).

The extracellular region of the most common polymorphic size variant of CR1 is composed of 30 independent folding units called complement control protein repeats (CCP) organized in four long homologous repeats (LHR) A, B, C, and D. CR1 binds opsonins C3b and C4b specifically through pairs or triplets of consecutive CCP modules, CCP8-9 and CCP15-17 in LHR-B and C (C3b) and CCP1-2 in LHR A (C4b) (22–25). CR1 also binds C1q, MBL, and ficolin-2, more recently shown to also act as CR1-interacting opsonins specific of the LHR-D region (15, 26). The binding of MBL to CR1 involves its collagen-like regions at a site that is located at, or close to the site that interacts with its associated serine proteases (26). The opsonic function of MBL might, therefore, implicate a protease-free molecule linked to a target through its recognition domains and to cell surface CR1 through its collagen stalks.

Results from our laboratory indicated using a range of size variants of CR1 LHR-D that MBL and ficolin-2 bind to CCP24-25 (26). In the present study, we extend our previous findings by investigating more precisely the site of interaction for MBL using purified CCP24-25 and we highlight that C1q interacts with the same pair of modules. Moreover, we provide evidence that C1q binds CR1 through its collagen stalks but also through subsidiary sites, most probably located in its globular regions.

MATERIALS AND METHODS

Proteins and Reagents

C1q was purified from human serum and quantified as previously described (27). Human serum was obtained from the Etablissement Français du Sang (EFS) Rhône-Alpes (agreement number 14-1940 regarding its use in research). C1q collagen stalks (CLF) and globular heads (GR) were prepared according to Tacnet-Delorme et al. (28). Recombinant MBL was provided by Natimmune (Copenhagen, Denmark) and quantified as previously described (29). Recombinant MBL-associated serine protease (MASP)-3 was obtained according to the procedure of Jacquet et al. (26). Recombinant soluble human CR1 (sCR1) was purchased from R&D Systems Europe. Oligonucleotides were from Eurogentec. Restriction and modification enzymes were from New England Biolabs. All CR1 variants constructs were engineered using site-directed mutagenesis with the QuickChange II XL kit (Agilent Technologies). For protein quantification, Mw and $A_{1\%,1\ cm}$ were, respectively, for C1q (459,300; 6.8), CLF (189,900; 2.1), GR (48,000; 9.3), dimeric MASP-3 (175,200; 13.5), and tetrameric MBL (305,400; 7.8).

Production of the CR1 CCP22-30 His_6 Variants in Insect Cells

The CR1 CCP22-30 His_6 fragment, its deletion variants ΔCCP22-23, ΔCCP26-30, ΔCCP25-26, and fragments CCP25-26 and CCP24-25 were produced in *Trichoplusia ni* insect cells, purified, characterized, and quantified as described in Ref. (26). The CCP24-25 His_6 plasmid was generated by site-directed mutagenesis (Quickchange XLII, Agilent) from the template pNT-Bac-CR1 CCP22-30 His_6, using an optimized procedure for large insertion/deletion (30). Purification of CCP24-25 on a Ni NTA column (His-select, Sigma Aldrich), was achieved as described previously (26). The concentration of the purified CR1 CCP24-25 variant was estimated using the absorption coefficient $A_{1\%,1\ cm}$ at 280 nm of 10.5 calculated using the PROTPARAM program on the Expasy Server[1], and an experimental molecular weight determined by MALDI mass spectrometry of 18,500 Da.

Production of CR1 CCP22-30 His_6 and CR1 CCP22-30 ΔCCP24-25 in Mammalian Cells

A 6 × His-Tag was inserted at the C-terminal end of CR1 CCP22-30 by site-directed mutagenesis using the pcDNA3.1 CR1 CCP22-30 construct as a template and the protocol described for CCP24-25 engineering. Using the same mutagenesis protocol, the ΔCCP24-25 deletion construct was then obtained by deletion of the CCP24-25 coding sequence from the pcDNA3.1 CR1 CCP22-30 His_6 template. Purification of the secreted CR1 fragments transiently produced in Freestyle 293-F cells (4 days) was achieved as described previously (26). The concentration of purified CR1 CCP22-30 and CR1 ΔCCP24-25 was determined using respective Mw obtained by MALDI mass spectrometry of 78,752 ± 78 and 57,550 ± 57 Da and calculated $A_{1\%,1\ cm}$ at 280 nm of, respectively, 13.5 and 14.1.

[1] http://web.expasy.org/protparam/.

Surface Plasmon Resonance (SPR) Analyses and Data Evaluation

Multiple cycle interaction analyses and competition experiments were performed on a BIAcore 3000 instrument (GE Healthcare). Recombinant soluble CR1 (sCR1), CR1 CCP22–30, and its size variants were covalently immobilized on CM5 sensor chips in 10 mM HEPES, 150 mM NaCl, 0.005% surfactant P20, pH 7.4 (HBS-P) using the amine coupling chemistry according to the manufacturer's instructions (GE Healthcare). The protein ligands were diluted in 10 mM sodium acetate, pH 4.2 at 25 µg/ml (sCR1), 20 µg/ml (CR1 CCP22-30), and 5 µg/ml (deletion variants and bimodular CCP fragments). Binding was measured at a flow rate of 20 µl/min in HBS-P containing 3 mM EDTA for MBL and in 50 mM triethanolamine-HCl (TEA), 150 mM NaCl, 1 mM $CaCl_2$, 0.005% surfactant P20, pH 7.4 for C1q. Sixty microliters of each soluble analyte at desired concentrations were injected over surfaces with immobilized sCR1 [9,500 resonance units (RU)], CR1 CCP22–30 or CR1 ΔCCP24-25 (1,500 to 4,500 RU) and CCP24-25 (1,000 RU). A flow cell submitted to the coupling steps without immobilized protein was used as blank, and the specific binding signal was obtained by subtracting the background signal over the blank surface. For competition assays, C1q was pre incubated for 20 min at room temperature with recombinant MASP-3 in 50 mM TEA, 150 mM NaCl, 1 mM $CaCl_2$ pH 7.4 before injection. Regeneration of the surfaces was achieved by 10 µl injections of 1 M NaCl, 10 mM EDTA. Kinetic data were analyzed by global fitting to a 1:1 Langmuir binding model of both the association and dissociation phases for at least five analyte concentrations simultaneously, using the BIAevaluation 3.2 software (GE Healthcare). Buffer blanks were subtracted from the data sets used for kinetic analysis (double referencing). The apparent equilibrium dissociation constants (K_D) were calculated from the ratio of the dissociation and association rate constants (k_d/k_a). Chi^2 values were below 7 in all cases.

Single cycle interaction analyses were performed on a T200 instrument (GE Healthcare). CR1 CCP22-30 and its deletion fragment ΔCCP24-25 were diluted to 20 µg/ml in 10 mM sodium acetate, pH 4.2, and immobilized on a CM5 (series S) sensor chip (GE Healthcare) in HBS-P using the amine coupling chemistry according to the manufacturer's instructions (GE Healthcare). The reference surface was prepared using the same procedure except that the protein solution was replaced by buffer. The immobilization levels for CR1 CCP22-30 and ΔCCP24-25 were, respectively, 3,000 and 2,200 RU. C1q and MBL binding was measured in 50 mM TEA, 150 mM NaCl, 0.05% surfactant P20 pH 7.4 containing 1 mM $CaCl_2$ for C1q or 3 mM EDTA for MBL at a flow rate of 20 µl/min. The signals recorded on the reference flow cell were subtracted from those obtained on immobilized CR1 fragments.

Interaction Studies Using Solid-Phase Binding Assays

96-well microtiter plates (Greiner Bio-One) were coated with 3.4 pmol of each CR1 variant in PBS, and incubated overnight at 4°C. Saturation was then performed by adding 250 µl of PBS containing 1% BSA and 0.05% tween 20 per well for 90 min at room temperature. Four washes were performed using 200 µl of PBS, 0.05% tween 20 (PBS-T). C1q (10 µg/ml in PBS-T) was added and incubated at room temperature for 90 min. After four washes, bound C1q was detected by successive incubations with an anti-C1q rabbit polyclonal antibody (1:1,000 dilution) and a horseradish peroxidase-conjugated anti-rabbit antibody (Sigma) (1:20,000 dilution). After extensive washes with PBS-T, 100 µl of tetramethylbenzidine solution (Tebu-Bio) was added to each well. The reaction was stopped by adding 100 µl of 1 M H_2SO_4 and the optical densiy at 450 nm of each well was measured using an ELISA plate reader (FLUOstar Optima; BMG Labtech).

Analysis of Small-Angle X-ray Scattering (SAXS)

Small-angle X-ray scattering experiments were performed at the European Synchrotron Radiation Facility (ESRF, Grenoble) beamline BM29, using a Pilatus 1M detector, and an X-ray energy of 12.5 keV. A gel filtration was performed immediately prior to the experiment using a S200 10/300 column (GE Healthcare), 10 mM TRIS, 150 mM NaCl, pH 8.0 in the presence of 1 mM dithiothreitol (DTT) to protect the sample from radiation damage and limit the aggregation. The distance between detector and sample was 2.87 m, covering a q-range of 0.025–5/nm and the sample temperature was set to 4°C. For each dataset, 10 measurements of 1 s exposure were recorded on a 50 µl sample injected into the capillary. Three concentrations of the CCP24-25 fragment were used (serial dilutions: 5, 2.5, 1.25 mg/ml). Images were radially integrated, averaged, and buffer subtracted using the beamline data processing pipeline (31). As some aggregation was observed in the highest concentration even in the presence of 1 mM DTT, the final SAXS curve has been obtained by merging the high angle and low angle regions from the 5 and 1.25 mg/ml, respectively, using the PRIMUS software from the ATSAS package (32). Low resolution *ab initio* envelopes were calculated using DAMMIF and also GASBOR, to make use of good data quality in the high angle region. An intitial model of CCP24-25 was obtained by homology modeling using the server ALLOSMOD (33) and the crystal structure of the CRRY complement receptor (2xrb) as starting template. Two N-glycans were modeled at positions Asn 1534 and Asn 1540 according to the prediction of the NetNGlyc server.[2] The program CORAL was used to fit the SAXS data by defining two rigid bodies (the CCP24 and CCP25 modules) and two flexible regions (the linker between the modules and the C-terminal His-tag).

RESULTS

The CR1 CCP22-30 Fragment Efficiently Binds C1q

The CR1 CCP22-30 fragment was originally produced in insect cells as detailed in Ref. (26). Its interaction properties with C1q

[2]http://www.cbs.dtu.dk/services/NetNGlyc/.

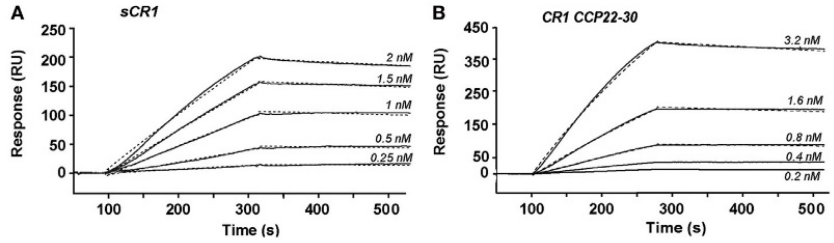

FIGURE 1 | Kinetic analysis of the interaction of C1q with immobilized soluble CR1 (sCR1) and CR1 CCP22-30. C1q was injected at the indicated concentrations over immobilized sCR1 (9,500 RU) **(A)** and CCP22-30 (1,500 RU) **(B)** in 50 mM triethanolamine-HCl (TEA), 145 mM NaCl, 1 mM $CaCl_2$, 0.005% surfactant P20, pH 7.4. Fits obtained by a global fitting of the data to a Langmuir 1:1 binding model are shown in dotted lines. The results shown are representative of three experiments (see **Table 1**).

TABLE 1 | Kinetic and equilibrium dissociation constants for the binding of C1q to immobilized soluble CR1 (sCR1) and CR1 CCP22-30.

	k_a (M^{-1} s^{-1})	k_d (s^{-1})	K_D (nM)	n^a
Immobilized sCR1	$1.30 \pm 0.22 \times 10^6$	$6.60 \pm 1.47 \times 10^{-4}$	0.49 ± 0.04	3
Immobilized CR1 CCP22-30	$1.63 \pm 0.70 \times 10^6$	$4.26 \pm 2.27 \times 10^{-4}$	0.26 ± 0.07	3

Values are expressed as means ± SE.
[a]Number of separate experiments on different sensorchips.

were analyzed by SPR spectroscopy and compared with those of sCR1. The slight sigmoidal shape of the curves in the association phase and the slow dissociation (**Figure 1**) suggest a complex interaction model involving multivalent interaction. However, the binding curves could be fitted using a 1:1 Langmuir model with satisfactory Chi^2 values (around 7) for both sCR1 and the CR1 CCP22-30 fragment. These results show that C1q binds to both sCR1 and CR1 CCP22-30 with comparable association and dissociation constants (k_a and k_d) resulting in apparent equilibrium dissociation constants (K_Ds) in the same nanomolar range of 0.49 and 0.26 nM, respectively (**Table 1**). This indicates that the CCP22-30 region of CR1 is sufficient for efficient C1q binding and most probably contains the main CR1 interaction sites for C1q.

Location of the C1q-Binding Site in CR1 CCP22-30 Using Deletion CR1 Variants

With a view to locate more precisely the modules of the CR1 CCP22-30 region involved in C1q interaction, we used various CR1 CCP22-30 fragments represented schematically in **Figure 2A**. Solid-phase binding assays with immobilized CR1 variants, lead to the results summarized in **Figure 2B**. Fragments ΔCCP22-23 and ΔCCP26-30 were still able to bind to C1q and their binding capacities were even increased by comparison with CR1 CCP22-30. These results indicate that modules CCP24-30 and CCP22-25 contain the determinants required for C1q binding, suggesting the involvement of the CCP24-25 segment common to both variants. The higher binding capacity of both variants could likely be explained by a better accessibility of the C1q binding site, expecially in the shorter fragment ΔCCP26-30. Furthermore, the importance of CCP24 and CCP25 in C1q binding was confirmed by the interaction capacities of both fragment ΔCCP25-26 and the bimodular fragment CCP25-26. Indeed, the decreased C1q

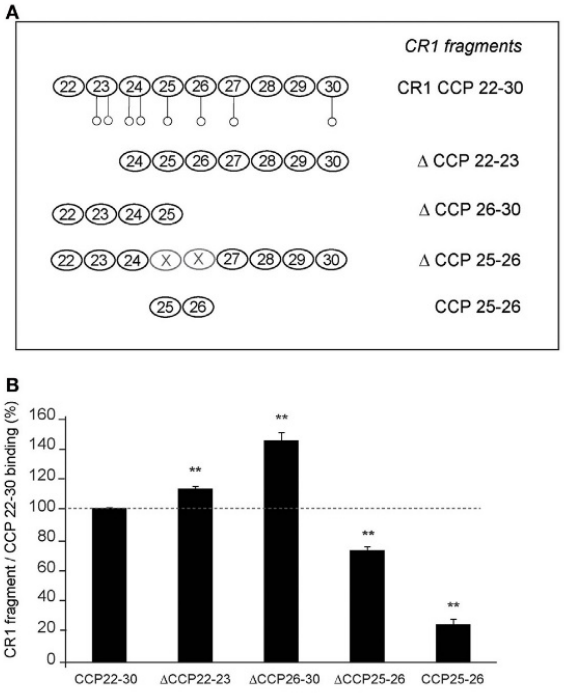

FIGURE 2 | Localization of the C1q binding sites in CR1 CCP22-30 using deletion fragments. **(A)** Schematic view of the different fragments of CR1 CCP22-30. Potential N-glycosylations are represented by open circles ○. **(B)** Interaction of C1q with immobilized CR1 CCP22-30 fragments analyzed by ELISA. C1q (10 µg/ml in PBS) was added to microtiter plate coated with 3.4 pmol of each CCP22-30 fragment as described in Section "Materials and Methods." After 1.5 h incubation at room temperature, bound C1q was detected with rabbit antibodies recognizing C1q and HRP secondary antibodies. Data are presented as the mean ± SE of four individual experiments. (**), Student's *t*-test values $p < 0.01$ of C1q binding to each fragment compared to CCP22-30.

binding observed with fragment ΔCCP25-26 (27%), where CR1 CCP25-26 are missing, supports the implication of CCP25 in C1q binding. In addition, the low binding (24%) of the CCP25-26 fragment points out the importance of CCP24 in C1q binding. Overall, these CR1 deletion variants highlight the importance of the CR1 module pair CCP24-CCP25 in C1q interaction.

C1q and MBL Both Interact with CR1 in the Same CCP24-25 Region

We have shown previously using a similar approach that the binding site of CR1 for MBL is most probably located as shown here for C1q, in the same pair of modules CCP24-25. However, none of the fragments used focused exclusively on the CCP24-25 modules. For that reason, we decided to produce two additional CR1 CCP22-30 fragments, one with a deletion of CCP24-25 called ΔCCP24-25 and the bimodular fragment CCP24-25 (**Figure 3A**). In order to improve the purification of CR1 CCP22-30 and ΔCCP24-25, a 6His-tag was introduced at the C-terminal end of the fragments as explained in Section "Materials and Methods." No interaction difference was noticed depending on the cellular expression system used (insect cells or mammalian FreeStyle 293-F cells) or on the presence or absence of the 6His-Tag (26). These observations imply that the sialic acid moiety present on the extremities of N-linked glycans in protein expressed in mammalian cells but not on insect cells has no impact on CR1 interaction properties with defense collagens. Both CR1 CCP22-30 and ΔCCP24-25 variants were purified using a one-step nickel-affinity chromatography. The mean yields of purified CCP24-25 and ΔCCP24-25 fragments from 1 l of expression supernatant were, respectively, around 3 and 4.5 mg. As observed by SDS-PAGE analysis (**Figure 3B**), each fragment was pure and migrated as a single band of apparent molecular weight in reducing conditions of, respectively, around 60 (ΔCCP24-25) and 21 kDa (CCP24-25). Mass spectrometry analysis yielded heterogeneous peaks centered on 57,034 ± 60 and 18,500 ± 20 Da for ΔCCP24-25 and CCP24-25, respectively, accounting for the polypeptide chains (49,918 and 15,388 Da) plus extra masses (7,116 and 3,112 Da) corresponding to N-linked carbohydrates. The interaction properties of both fragments for C1q and MBL were then assessed using SPR spectroscopy (**Figure 4**). CR1 CCP24-25 interacted with C1q and MBL with high affinity, as reflected by K_D values in the nM range (0.19 and 0.65 nM, respectively), the complex

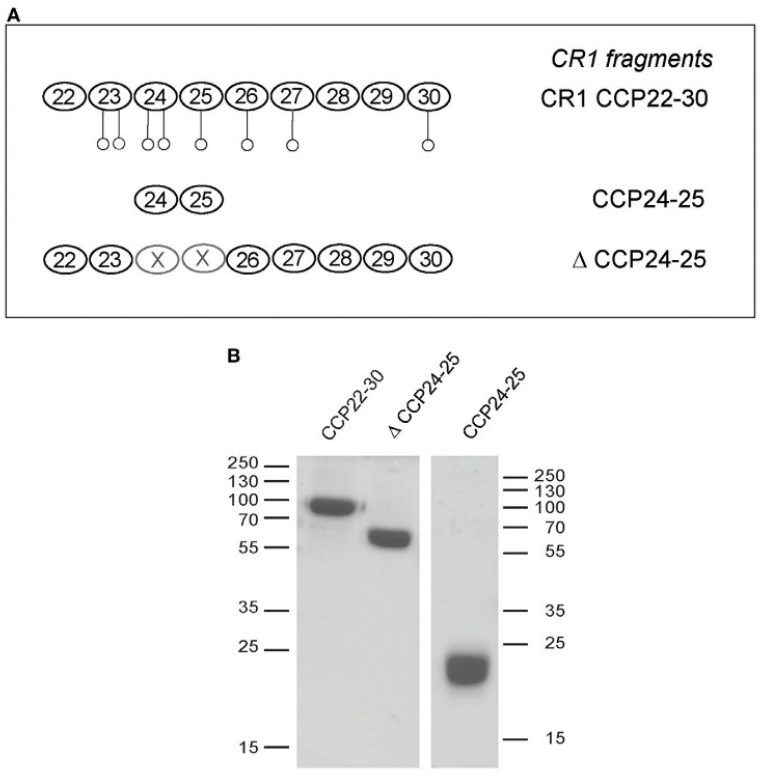

FIGURE 3 | Complement receptor type 1 (CR1) variants produced to study the CCP24-25 module pair interaction properties. **(A)** Schematic view of CCP24-25 variants produced in eukaryotic cells. Potential N-glycosylations are represented by open circles ○. **(B)** SDS-PAGE analysis of 4 µg of the CR1variants under reducing conditions. The positions of the molecular weight markers (expressed in kilodaltons) are indicated. *A full scan of the original gel is provided in Figure S1 in Supplementary Material.*

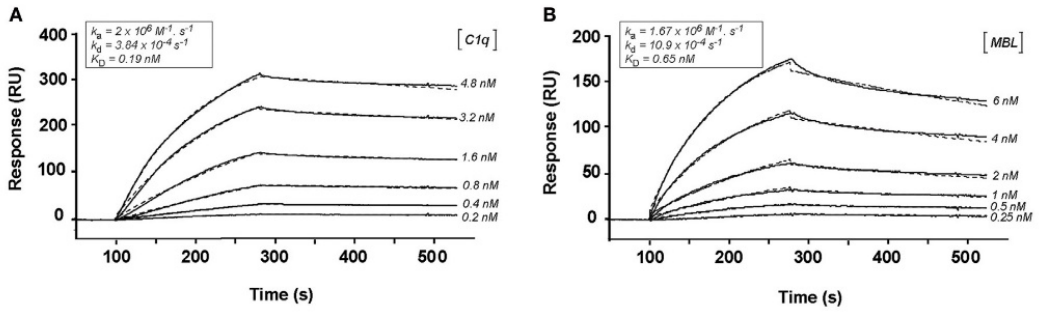

FIGURE 4 | Kinetic analysis of the interaction of C1q and mannose-binding lectin (MBL) with CR1 CCP24-25. C1q **(A)** and MBL **(B)**, at indicated concentrations, were injected in 50 mM triethanolamine-HCl (TEA), 145 mM NaCl, 0.05% surfactant P20, pH 7.4, on immobilized CR1 CCP24-25 (1,000 RU). The buffer was supplemented with 3 mM EDTA for MBL binding. Fits are shown as dotted lines and were obtained by global fitting of the data using a 1:1 Langmuir-binding model. The kinetic constants obtained are framed on the top of each sensorgramm.

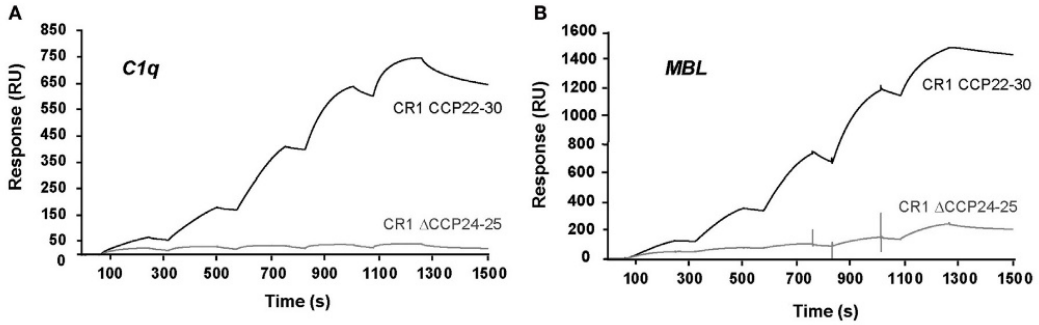

FIGURE 5 | Interaction of C1q and mannose-binding lectin (MBL) with immobilized CR1 CCP22-30 and CR1 ΔCCP24-25. The binding curves were obtained in single cycle mode by injecting increasing concentrations of C1q **(A)** or MBL **(B)** on immobilized CR1 CCP22-30 (3,000 RU) or CR1 ΔCCP24-25 (2,200 RU). C1q (0.25, 0.5, 1, 2, and 4 nM) was injected at 20 µl/min for 180 s in 50 mM triethanolamine-HCl (TEA), 150 mM NaCl, 1 mM $CaCl_2$, 0.05% surfractant P20, pH 7.4. MBL (1, 2, 4, 8, and 16 nM) was injected in the same conditions except that the buffer contained 3 mM EDTA instead of $CaCl_2$.

TABLE 2 | Overall small-angle X-ray scattering experimental parameters for the CCP24-25 fragment.

Conc (mg/ml)	Rg Guinier (nm)	Q*Rg limits	I(0)	Rg Gnom (nm)	Dmax (nm)	MW Gnom[a]	MW Dammif[a]
1.25	2.67 ± 0.19	0.47–1.19	27.4 ± 0.05	2.74	9.8	15.8	–
2.5	2.78 ± 0.12	0.52–1.12	28.7 ± 0.04	2.78	9.8	16.4	–
5.0	2.76 ± 0.53[b]	0.92–1.24	29.2 ± 0.07	2.84	9.8	16.4	–
Merged	2.67 ± 0.2	0.47–1.19	27.4 ± 0.04	2.74	9.8	15.6	18.1

[a]*The MW Gnom is calculated from the Porod volume. The MW Dammif is calculated from the ab initio envelope.*
[b]*Aggregation.*

with C1q being slightly more stable than the complex with MBL, as indicated by a 3.5-fold lower dissociation rate constant (3.84 10^{-4} s^{-1} versus 1.09 10^{-3} s^{-1}). The specificity of C1q and MBL binding for CR1 CCP24-25 was then controlled using the deletion fragment ΔCCP24-25. As shown in **Figure 5**, deletion of CCP24-25 abolished the interaction with C1q and strongly decreased binding of MBL. Taken together, these results unambigously restrain the main interaction sites of CR1 for both MBL and C1q to the same pair of modules CCP24-25.

The CCP24-25 Fragment Pair Adopts an Extended Conformation in Solution

Small-angle X-ray scattering analysis has been performed on the CCP24-25 fragment produced in insect cells at the ESRF BM29 beamline, as described in Section "Materials and Methods." The global parameters derived from the SAXS data (**Table 2**) characterize the CCP24-25 fragment as a monomeric protein having an Rg of about 2.7 nm. The pair distribution P(r) curve shows the typical aspect of an elongated multidomain protein with a

Dmax of ~9.8 nm (**Figure 6A**). Kratky analysis clearly shows flexibility with a maximum at q*Rg ~ 3.5 which is significantly higher than the theoretical value ($\sqrt{3}$) that is characteristic of well folded, globular proteins (34) (**Figure 6B**). Also the curve does not tend to 0 at high q*Rg indicating high local flexibility that could be mainly attributed to the presence of the glycans, but also to the C-terminal histidine tag and to the semi-flexible linker. The overall *ab initio* envelopes, calculated by the GASBOR software, show two elongated blobs with a global boomerang shape (**Figures 6D–E**). Temptatively, one could attribute the larger blob to the CCP24 which is slightly bigger in size and also bears two N-glycans. The molecular weight estimate from the *ab initio* envelope is ~18.1 kDa which is in good agreement with the experimental value (18.5 kDa). Rigid body modeling using the program CORAL resulted in an extended conformation with the bend point located between the two CCP modules and a good fit to the experimental data ($\chi = 1.2$) that could be superposed on the *ab initio* envelope (**Figures 6C–E**).

Location of the CR1-Binding Sites within C1q

In order to identify the region of C1q that is involved in CR1 interaction, the comparative binding of C1q collagen stalks (CLF), C1q globular heads (GR), and whole C1q to CR1 CCP22-30 was performed by SPR. The results shown in **Figure 7A** indicate that CR1 mostly interacts with C1q CLF although binding to C1q GR is also observed. Moreover, the competition with MASP-3, used as a competitor for the C1r/C1s serine protease interaction site on C1q (35) (**Figure 7B**), confirms that there is indeed a binding site on the collagen stalks of C1q likely located on or in close proximity of the C1r/C1s interaction site. Interestingly, the inhibition is not complete when MASP-3 occupies all the potential C1q sites (C1q:MASP-3 dimer molar ratio of 1:2) and does not decrease when MASP-3 is added in excess (1:4 and 1:8 ratios). The remaining interaction observed with maximal MASP-3 competition (around 50%) might be due to the contribution of other binding sites on the CLF and/or on the globular regions of C1q.

DISCUSSION

Previous studies have reported that CR1 is a binding platform for complement opsonins C3b, C4b and defense collagens, such as C1q, MBL, and ficolin-2 (15, 26, 36–39). The present work, based on a dissection strategy, highlights that the interaction region of CR1 with C1q and MBL on CR1-LHR-D is restricted to only two CCP modules, CCP24 and CCP25. We first confirmed

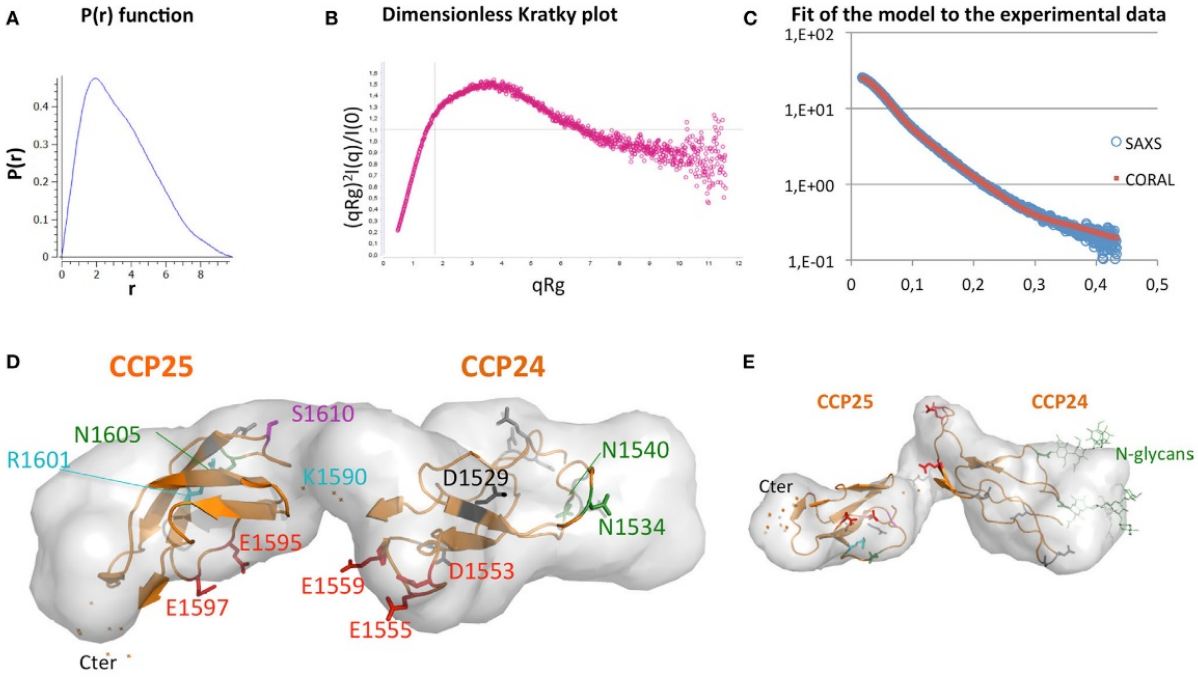

FIGURE 6 | Elongated shape of CCP24-25, associated to a possible interpretative model. **(A)** Small-angle X-ray scattering (SAXS) pair distance distribution, **(B)** SAXS dimensionless Kratky plot, which shows elongation and remaining flexibility. **(C)** Fit of the model [shown in panels **(D,E)**] to the experimental data. **(D)** Top and **(E)** side views of an *ab initio* envelope computed with GASBOR. A Coral-derived model of CCP24-25 is shown inside to illustrate how the shape corresponds to two CCP modules. This interpretative model is used to illustrate the positions on each module of glycosylation sites (green), rs 4844609 SNP (magenta), Knops groups variants (cyan), acidic clusters (red) initially suggested as potential MBL binding sites, and the other acidic residues (gray and black). D1529 is the homologous counterpart of D1076 in CR1 CCP17 (black). The two flexible carbohydrates included in the model are only illustrated in the side view.

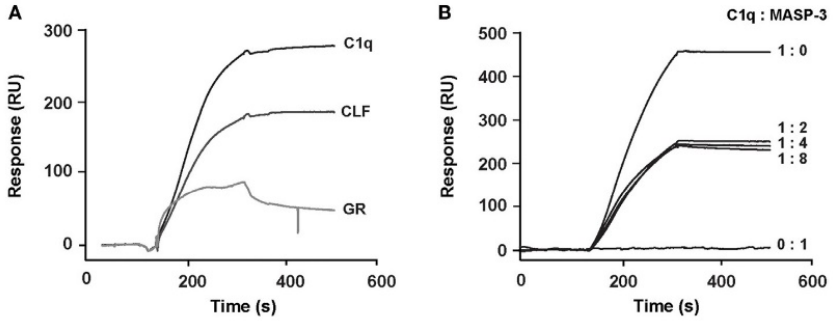

FIGURE 7 | Localization of the binding site of soluble CR1 on C1q. **(A)** Comparative binding of C1q and its CLF and GR on complement receptor type 1 (CR1) CCP22-30 analyzed by surface plasmon resonance (SPR). The CR1 CCP22-30 fragment was immobilized on CM5 sensor chips (4,500 RU) and 2 nM of C1q or CLF and 12 nM of GR were injected over the surfaces as described in Section "Materials and Methods." **(B)** MBL-associated serine protease (MASP)-3 competition of the binding of C1q to CR1 CCP22-30 analyzed by SPR. C1q (2 nM) was incubated at room temperature for 20 min in the absence or presence of recombinant MASP-3 at indicated molar ratios and injected over immobilized CR1 CCP22-30 (4,500 RU). No binding was observed when MASP-3 alone (20 nM) was injected.

in this study that CR1 fragment CCP22-30 encompassing the LHR-D plus two additional modules (CCP29-30) contains a site of interaction for C1q. This was previously shown using lysates of transfected Chinese hamster ovary cells (15) but is demonstrated here using purified recombinant CR1 fragments expressed in eukaryotic cells. For all CR1 fragments produced, the interaction could be only measured by SPR with immobilized CR1 as it was also the case for MBL (26). The explanation for that observation is probably due to the organization of CR1 on the cell membrane into clusters that would require a similar molecule presentation *in vitro* to allow the right positioning of multiple sites suitable for the binding of defense collagens (40, 41). The affinity of C1q for CR1 obtained by SPR was comparable to that previously found for MBL interaction (26) with K_Ds of 0.49 nM (MBL 0.76 nM) for sCR1 and 0.26 nM (MBL 0.37 nM) for CR1 CCP22-30. For both C1q and MBL, the CCP22-30 fragment had an affinity that was slightly higher than that of full-length sCR1, indicating that the site of interaction for the defense collagens is located mainly in this region with no or little implication of other LHRs. This is in accordance with the additive interaction of C3b, C4b, and C1q for CR1 observed by Tas et al. (16) and more recently with the results of Ref. (42) that the CR1 CCP15-25 fragment is able to interact with C1q. Using a panel of deletion fragments of CR1 CCP22-30 (26), we get an indirect indication of the CCP24-25 implication in CR1 interaction with C1q, as shown also for MBL and ficolin-2. The present work aimed at going deeper into the characterization of the interaction of CR1 CCP24-25 with C1q and MBL. Direct evidence for the involvement of the two CCP24 and CCP25 modules was provided by the production of two supplementary fragments, one consisting of the CCP24-25 bimodular fragment, and the second one corresponding to the CR1 CCP22-30 fragment deleted from the two CCP24-25 modules. The CCP24-25 bimodular fragment was shown to interact equally with C1q and MBL. In addition, the CCP24-25 specificity was also clearly demonstrated by binding assays on the truncated fragment ΔCCP24-25 that showed no binding for C1q and negligible binding to MBL compared to the entire CR1 CCP22-30. Taken together, these results clearly assign the binding specificity of CR1 for defense collagens C1q and MBL to its CCP24-25 module pair.

Although the whole CR1 molecule shows a partially folded back solution structure (43), we obtained SAXS data showing an extended conformation of the CCP24-25 module pair in solution, which is fully consistent with the elongated conformation mainly observed for other complement regulators interactions (25). From these data, we could propose an interpretative model (illustrated in **Figure 6D**), which can be used as a support for discussion. Two clusters of acidic residues were initially suggested as possible common interaction sites for the conserved lysine residues on the collagen stalks of MBL and ficolin-2 (26). They are shown in red in **Figure 6D** and correspond to Asp 1553, Glu, 1555 and Glu 1559 in CCP24 and Glu 1595 and Glu 1597 in CCP25. These acidic residues were selected because: (i) the interaction of CR1 with C1q or MBL is highly sensitive to ionic strength (15, 39); (ii) MASP-3 can compete with the interaction between CR1 and the defense collagens (MBL, ficolin-2, C1q), which suggests a common binding to the conserved lysine residues in the collagen stalks of these proteins (29, 35, 44); (iii) the proposed clusters are unique to the LHR-D, including at least one acidic residue which has no counterpart in the other LHR regions. We have tested the charge effect of these acidic residues by mild mutations into their corresponding amide residue (Asp/Asn and Glu/Gln), thus preserving their overall shape but not their charge. Unfortunately, the mutations do not significantly affect the binding of CR1 to MBL and C1q (data not shown). From this negative result, it can be deduced at least that the charge effect of these acidic clusters is not essential or might be compensated by the remaining acidic residues (5 on CCP24 and 1 in CCP25 in gray or black in **Figure 6D**). A recent study on CR1 isolated from homozygous and heterozygous donors for the rs 4844609 SNP (resulting in the change of Ser 1610 to Thr in module CCP25, in magenta in **Figure 6D**) showed a small but significant increase in C1q binding compared to CR1 without this SNP (45). Although we could not reproduce this observation with a CR1CCP22-30 Ser 1610 Thr mutant produced in our laboratory, this might indicate that

the C1q-binding site could be located nearby the Ser1610. On the other end, Knops blood groups variants are also in close proximity to the mutated acidic residues and it could be noticed that charge differences on Knops group variants (cyan) (42) have no effect on C1q binding. Moreover, sialic acids at the glycosylation extremities (glycosylation sites in dark green in **Figure 6D**) do not influence C1q binding either. Apparently, this is not a simple question and further investigations will be required to precisely define the collagen binding-site residues. Among possible directions, we might consider the hypothesis that the charge interaction involves an acidic residue which is conserved in all LHR regions, the selectivity for the collagen-like partners deriving from the evolution of its surrounding residues. Following this altenative hypothesis, one interesting candidate would be Asp1529, because Asp1076, its homologous counterpart in CCP17, provides the main ionic interaction of CCP17 with C3b, in direct interaction with C3b Arg1310 [PDB 5O9 (25)]. Overall, this might suggest that C1q interacts in between the two modules, possibly on the upper face (**Figure 6D**) including this Asp 1529, Ser 1610 and four other non-mutated acidic residues (in gray).

Finally, the other goal of the present work was to identify the regions on C1q that are responsible for the interaction with CR1. It was previously shown that C1q collagen tails interact with sCR1 and can also mediate C1q binding to erythrocytes CR1 (15, 16). We confirm the importance of C1q CLF in CR1 interaction using SPR but in addition our results also bring out the potential implication of subsidiary sites on C1q for CR1 binding. This conclusion arises from two different approaches: (i) the interaction of C1q CLF and C1q globular heads with immobilized CR1 CCP22-30 by SPR showing that there is a contribution of both C1q regions in CR1 binding (ii) the competition with MASP-3 that does not completely abolish C1q binding to CR1. Moreover, mutating the protease-binding site (LysB61A, LysC58A) in C1q (35) reduces without abolishing, the interaction with CR1 (Figure S2 in Supplementary Material). Overall these results point out that there are additionnal sites on C1q for CR1 interaction most probably located on C1q globular heads. In this respect it can not be excluded that the short overlapping sequences common to the CLF and the GR, due to the generation of both fragments by limited proteolysis of C1q (residues A85-97, B81-97, C78-94) might contribute to CR1 interactions (46, 47). In the case of MBL, our previous studies showed unambigously that the interaction with CR1 involves only its collagen stalks (26). However, eventhough MBL and C1q are homologous proteins, the case of C1q is more complex and might be of physiological relevance. Effectively, C1q has been reported to serve as a bridging molecule for membrane receptors involved in immune tolerance. This is the case for C1q interaction with CD91/CRT involved in the clearance of apoptotic cells (48) and also, as described more recently, for the inhibitory immunoreceptors implicating partnering of C1q/LAIR-1/RAGE and HMGB1 (49) or C1q/LAIR-1/CD33 (13). In all these bridging interactions, C1q engages both its collagen tails and globular heads. One can, therefore, postulate that since CR1 is a large receptor clustered on the cell membrane, it can present a multisite platform for an efficient interaction with C1q.

AUTHOR CONTRIBUTIONS

VR, NT, and CG designed the study; MJ, GC, GF, and IB performed the research; MJ, GC, VR, CG, and NT analyzed the data; VR, NT, and CG wrote the manuscript; all authors revised and approved the final version of the manuscript.

ACKNOWLEDGMENTS

This work used the platforms of the Grenoble Instruct-ERIC center (ISBG; UMS 3518 CNRS-CEA-UGA-EMBL) with support from FRISBI (ANR-10-INSB-05-02) and GRAL (ANR-10-LABX-49-01) within the Grenoble Partnership for Structural Biology (PSB). The authors thank Luca Signor for assistance and access to the mass spectrometry facility as well as Martha Brennich and other local contacts and staff for assistance and access to the ESRF BM29 beamline. This work was supported by grants from the French National Research Agency (ANR-09-PIRI-0021 and ANR16-CE11-0019).

SUPPLEMENTARY MATERIAL

The Supplementary Material for this article can be found online at http://www.frontiersin.org/articles/10.3389/fimmu.2018.00453/full#supplementary-material.

REFERENCES

1. Bobak DA, Washburn RG, Frank MM. C1q enhances the phagocytosis of *Cryptococcus neoformans* blastospores by human monocytes. *J Immunol* (1988) 141:592–7.
2. Webster SD, Galvan MD, Ferran E, Garzon-Rodriguez W, Glabe CG, Tenner AJ. Antibody-mediated phagocytosis of the amyloid beta-peptide in microglia is differentially modulated by C1q. *J Immunol* (2001) 166: 7496–503. doi:10.4049/jimmunol.166.12.7496
3. Nayak A, Pednekar L, Reid KB, Kishore U. Complement and non-complement activating functions of C1q: a prototypical innate immune molecule. *Innate Immun* (2012) 18:350–63. doi:10.1177/1753425910396252
4. Bohlson SS, O'Conner SD, Hulsebus HJ, Ho M-M, Fraser DA. Complement, C1q, and C1q-related molecules regulate macrophage polarization. *Front Immunol* (2014) 5:402. doi:10.3389/fimmu.2014.00402
5. Gaboriaud C, Frachet P, Thielens NM, Arlaud GJ. The human C1q globular domain: structure and recognition of non-immune self ligands. *Front Immunol* (2012) 2:92. doi:10.3389/fimmu.2011.00092
6. Kouser L, Madhukaran SP, Shastri A, Saraon A, Ferluga J, Al-Mozaini M, et al. Emerging and novel functions of complement protein C1q. *Front Immunol* (2015) 6:317. doi:10.3389/fimmu.2015.00317
7. Bohlson SS, Fraser DA, Tenner AJ. Complement proteins C1q and MBL are pattern recognition molecules that signal immediate and long-term protective immune functions. *Mol Immunol* (2007) 44:33–43. doi:10.1016/j.molimm.2006.06.021
8. Degn SE, Thiel S. Humoral pattern recognition and the complement system. *Scand J Immunol* (2013) 78:181–93. doi:10.1111/sji.12070
9. Ghebrehiwet B, Hosszu KK, Valentino A, Ji Y, Peerschke EIB. Monocyte expressed macromolecular C1 and C1q receptors as molecular sensors of danger: implications in SLE. *Front Immunol* (2014) 5:278. doi:10.3389/fimmu.2014.00278
10. Thielens NM, Tedesco F, Bohlson SS, Gaboriaud C, Tenner AJ. C1q: a fresh look upon an old molecule. *Mol Immunol* (2017) 89:73–83. doi:10.1016/j.molimm.2017.05.025
11. Paidassi H, Tacnet-Delorme P, Arlaud GJ, Frachet P. How phagocytes track down and respond to apoptotic cells. *Crit Rev Immunol* (2009) 29:111–30. doi:10.1615/CritRevImmunol.v29.i2.20

12. Son M, Santiago-Schwarz F, Al-Abed Y, Diamond B. C1q limits dendritic cell differentiation and activation by engaging LAIR-1. *Proc Natl Acad Sci U S A* (2012) 109:E3160–7. doi:10.1073/pnas.1212753109
13. Son M, Diamond B, Volpe BT, Aranow CB, Mackay MC, Santiago-Schwarz F. Evidence for C1q-mediated crosslinking of CD33/LAIR-1 inhibitory immunoreceptors and biological control of CD33/LAIR-1 expression. *Sci Rep* (2017) 7:270. doi:10.1038/s41598-017-00290-w
14. Eggleton P, Tenner AJ, Reid KBM. C1q receptors. *Clin Exp Immunol* (2000) 120:406–12. doi:10.1046/j.1365-2249.2000.01218.x
15. Klickstein LB, Barbashov SF, Liu T, Jack RM, Nicholson-Weller A. Complement receptor type 1 (CR1, CD35) is a receptor for C1q. *Immunity* (1997) 7:345–55. doi:10.1016/S1074-7613(00)80356-8
16. Tas SW, Klickstein LB, Barbashov SF, Nicholson-Weller A. C1q and C4b bind simultaneously to CR1 and additively support erythrocyte adhesion. *J Immunol* (1999) 163:5056–63.
17. Fearon D. Identification of the membrane glycoprotein that is the C3b receptor of the human erythrocyte, polymorphonuclear leukocyte, B lymphocyte, and monocyte. *J Exp Med* (1980) 152:20–30. doi:10.1084/jem.152.1.20
18. Ross GD, Yount WJ, Walport MJ, Winfield JB, Parker CJ, Fuller CR, et al. Disease-associated loss of erythrocyte complement receptors (CR1, C3b receptors) in patients with systemic lupus erythematosus and other diseases involving autoantibodies and/or complement activation. *J Immunol* (1985) 135:2005–14.
19. Fearon DT, Klickstein LB, Wong WW, Wilson JG, Moore FD, Weis JJ, et al. Immunoregulatory functions of complement: structural and functional studies of complement receptor type 1 (CR1; CD35) and type 2 (CR2; CD21). *Prog Clin Biol Res* (1989) 297:211–20.
20. Birmingham DJ, Hebert LA. CR1 and CR1-like: the primate immune adherence receptors. *Immunol Rev* (2001) 180:100–11. doi:10.1034/j.1600-065X.2001.1800109.x
21. Java A, Liszewski MK, Hourcade DE, Zhang F, Atkinson JP. Role of complement receptor 1 (CR1; CD35) on epithelial cells: a model for understanding complement-mediated damage in the kidney. *Mol Immunol* (2015) 67:584–95. doi:10.1016/j.molimm.2015.07.016
22. Krych-Goldberg M, Hauhart RE, Subramanian VB, Yurcisin BM, Crimmins DL, Hourcade DE, et al. Decay accelerating activity of complement receptor type 1 (CD35). Two active sites are required for dissociating C5 convertases. *J Biol Chem* (1999) 274:31160–8. doi:10.1074/jbc.274.44.31160
23. Krych-Goldberg M, Atkinson JP. Structure-function relationships of complement receptor type 1. *Immunol Rev* (2001) 180:112–22. doi:10.1034/j.1600-065X.2001.1800110.x
24. Smith BO, Mallin RL, Krych-Goldberg M, Wang X, Hauhart RE, Bromek K, et al. Structure of the C3b binding site of CR1 (CD35), the immune adherence receptor. *Cell* (2002) 108:769–80. doi:10.1016/S0092-8674(02)00672-4
25. Forneris F, Wu J, Xue X, Ricklin D, Lin Z, Sfyroera G, et al. Regulators of complement activity mediate inhibitory mechanisms through a common C3b-binding mode. *EMBO J* (2016) 35:1133–49. doi:10.15252/embj.201593673
26. Jacquet M, Lacroix M, Ancelet S, Gout E, Gaboriaud C, Thielens NM, et al. Deciphering complement receptor type 1 interactions with recognition proteins of the lectin complement pathway. *J Immunol* (2013) 190:3721–31. doi:10.4049/jimmunol.1202451
27. Arlaud GJ, Sim RB, Duplaa AM, Colomb MG. Differential elution of Clq, Clr and Cls from human Cl bound to immune aggregates. Use in the rapid purification of Cl subcomponents. *Mol Immunol* (1979) 16:445–50. doi:10.1016/0161-5890(79)90069-5
28. Tacnet-Delorme P, Chevallier S, Arlaud GJ. Amyloid fibrils activate the C1 complex of complement under physiological conditions: evidence for a binding site for A on the C1q globular regions. *J Immunol* (2001) 167:6374–81. doi:10.4049/jimmunol.167.11.6374
29. Teillet F, Lacroix M, Thiel S, Weilguny D, Agger T, Arlaud GJ, et al. Identification of the site of human Mannan-binding lectin involved in the interaction with its partner serine proteases: the essential role of Lys55. *J Immunol* (2007) 178:5710–6. doi:10.4049/jimmunol.178.9.5710
30. Wang W, Malcolm BA. Two-stage PCR protocol allowing introduction of multiple mutations, deletions and insertions using QuikChange Site-Directed Mutagenesis. *Biotechniques* (1999) 26:680–2.
31. Brennich ME, Kieffer J, Bonamis G, De Maria Antolinos A, Hutin S, Pernot P, et al. Online data analysis at the ESRF bioSAXS beamline, BM29. *J Appl Crystallogr* (2016) 49:203–12. doi:10.1107/S1600576715024462
32. Franke D, Petoukhov MV, Konarev PV, Panjkovich A, Tuukkanen A, Mertens HDT, et al. ATSAS 2.8: a comprehensive data analysis suite for small-angle scattering from macromolecular solutions. *J Appl Crystallogr* (2017) 50:1212–25. doi:10.1107/S1600576717007786
33. Weinkam P, Chen YC, Pons J, Sali A. Impact of mutations on the allosteric conformational equilibrium. *J Mol Biol* (2013) 425:647–61. doi:10.1016/j.jmb.2012.11.041
34. Durand D, Vivès C, Cannella D, Pérez J, Pebay-Peyroula E, Vachette P, et al. NADPH oxidase activator p67(phox) behaves in solution as a multidomain protein with semi-flexible linkers. *J Struct Biol* (2010) 169:45–53. doi:10.1016/j.jsb.2009.08.009
35. Bally I, Ancelet S, Moriscot C, Gonnet F, Mantovani A, Daniel R, et al. Expression of recombinant human complement C1q allows identification of the C1r/C1s-binding sites. *Proc Natl Acad Sci U S A* (2013) 110:8650–5. doi:10.1073/pnas.1304894110
36. Klickstein LB, Bartow TJ, Miletic V, Rabson LD, Smith JA, Fearon DT. Identification of distinct C3b and C4b recognition sites in the human C3b/C4b receptor (CR1, CD35) by deletion mutagenesis. *J Exp Med* (1988) 168:1699–717. doi:10.1084/jem.168.5.1699
37. Makrides SC, Scesney SM, Ford PJ, Evans KS, Carson GR, Marsh HC. Cell surface expression of the C3b/C4b receptor (CR1) protects Chinese hamster ovary cells from lysis by human complement. *J Biol Chem* (1992) 267:24754–61.
38. Krych M, Hourcade D, Atkinson JP. Sites within the complement C3b/C4b receptor important for the specificity of ligand binding. *Proc Natl Acad Sci U S A* (1991) 88:4353–7. doi:10.1073/pnas.88.10.4353
39. Ghiran I, Barbashov SF, Klickstein LB, Tas SW, Jensenius JC, Nicholson-Weller A. Complement receptor 1/CD35 is a receptor for Mannan-binding lectin. *J Exp Med* (2000) 192:1797–808. doi:10.1084/jem.192.12.1797
40. Chevalier J, Kazatchkine MD. Distribution in clusters of complement receptor type one (CR1) on human erythrocytes. *J Immunol* (1989) 142:2031–6.
41. Lapin ZJ, Höppener C, Gelbard HA, Novotny L. Near-field quantification of complement receptor 1 (CR1/CD35) protein clustering in human erythrocytes. *J Neuroimmune Pharmacol* (2012) 7:539–43. doi:10.1007/s11481-012-9346-3
42. Tetteh-Quarcoo PB, Schmidt CQ, Tham W-H, Hauhart R, Mertens HDT, Rowe A, et al. Lack of evidence from studies of soluble protein fragments that knops blood group polymorphisms in complement receptor-type 1 are driven by malaria. *PLoS One* (2012) 7:e34820. doi:10.1371/journal.pone.0034820
43. Furtado PB, Huang CY, Ihyembe D, Hammond RA, Marsh HC, Perkins SJ. The partly folded back solution structure arrangement of the 30 SCR domains in human complement receptor type 1 (CR1) permits access to its C3b and C4b ligands. *J Mol Biol* (2008) 375:102–18. doi:10.1016/j.jmb.2007.09.085
44. Lacroix M, Dumestre-Pérard C, Schoehn G, Houen G, Cesbron J-Y, Arlaud GJ, et al. Residue Lys57 in the collagen-like region of human L-ficolin and its counterpart Lys47 in H-ficolin play a key role in the interaction with the Mannan-binding lectin-associated serine proteases and the collectin receptor calreticulin. *J Immunol* (2009) 182:456–65. doi:10.4049/jimmunol.182.1.456
45. Fonseca MI, Chu S, Pierce AL, Brubaker WD, Hauhart RE, Mastroeni D, et al. Analysis of the putative role of CR1 in Alzheimer's disease: genetic association, expression and function. *PLoS One* (2016) 11:e0149792. doi:10.1371/journal.pone.0149792
46. Reid KBM. Isolation, by partial pepsin digestion, of the three collagen-like regions present in subcomponent Clq of the first component of human complement. *Biochem J* (1976) 155:5–17. doi:10.1042/bj1550005
47. Gaboriaud C, Juanhuix J, Gruez A, Lacroix M, Darnault C, Pignol D, et al. The crystal structure of the globular head of complement protein C1q provides a basis for its versatile recognition properties. *J Biol Chem* (2003) 278:46974–82. doi:10.1074/jbc.M307764200
48. Gardai SJ, Xiao Y-Q, Dickinson M, Nick JA, Voelker DR, Greene KE, et al. By binding SIRPα or calreticulin/CD91, lung collectins act as dual function surveillance molecules to suppress or enhance inflammation. *Cell* (2003) 115:13–23. doi:10.1016/S0092-8674(03)00758-X

49. Son M, Porat A, He M, Suurmond J, Santiago-Schwarz F, Andersson U, et al. C1q and HMGB1 reciprocally regulate human macrophage polarization. *Blood* (2016) 128:2218–28. doi:10.1182/blood-2016-05-719757

Conflict of Interest Statement: The authors declare that the research was conducted in the absence of any commercial or financial relationships that could be construed as a potential conflict of interest.

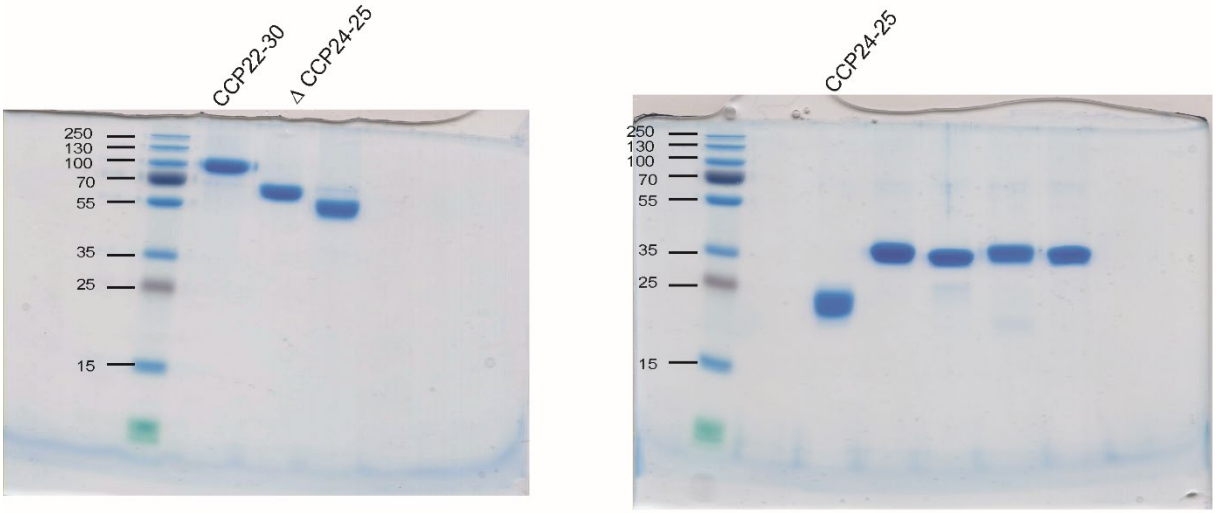

Figure S1 - full size gels corresponding to data shown in Figure 3

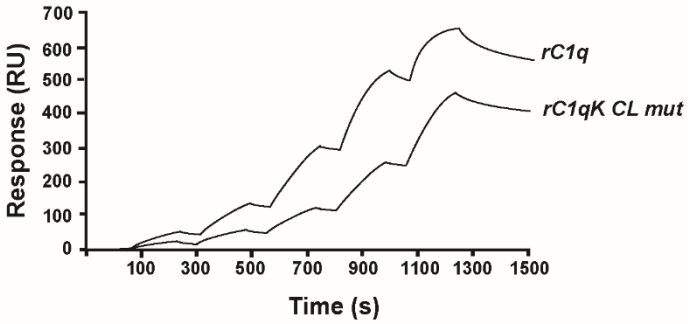

Figure S2

The Lysines of the CLF of C1q responsible for C1r2C1s2 interaction are partially involved in CR1 recognition. The binding curves were obtained in single cycle mode by injecting over immobilized CR1 CCP22-30 (3,000 RU), increasing concentrations of recombinant C1q (rC1q) or recombinant C1q LysA59Ala, LysB61Ala, LysC58Ala (rC1qK CL mut) prepared as described in (35). Both recombinant C1q variants were injected at concentrations of 0.25, 0.5, 1, 2 and 4 nM at 20 µl/min for 180 sec in a buffer containing 50 mM TEA, 150 mM NaCl, 1 mM $CaCl_2$, surfactant P20 0.05%, pH 7.4.

2 **Article 4:** Complement C1q interacts with LRP1 clusters II and IV through a site close but different from the binding site of its C1r and C1s-associated proteases

frontiers in Immunology

ORIGINAL RESEARCH
published: 21 October 2020
doi: 10.3389/fimmu.2020.583754

Complement C1q Interacts With LRP1 Clusters II and IV Through a Site Close but Different From the Binding Site of Its C1r and C1s-Associated Proteases

Guillaume Fouët[1†], Evelyne Gout[1†], Catherine Wicker-Planquart[1], Isabelle Bally[1], Camilla De Nardis[2], Stéphane Dedieu[3], Anne Chouquet[1], Christine Gaboriaud[1], Nicole M. Thielens[1], Jean-Philippe Kleman[1] and Véronique Rossi[1*]*

[1] Université Grenoble Alpes, CNRS, CEA, IBS, Grenoble, France, [2] Bijvoet Center for Biomolecular Research, Department of Chemistry, Faculty of Science, Utrecht University, Utrecht, Netherlands, [3] Université de Reims Champagne-Ardenne, UMR CNRS 7369 MEDyC, Reims, France

LRP1 is a large endocytic modular receptor that plays a crucial role in the scavenging of apoptotic material through binding to pattern-recognition molecules. It is a membrane anchored receptor of the LDL receptor family with 4 extracellular clusters of ligand binding modules called cysteine rich complement-type repeats that are involved in the interaction of LRP1 with its numerous ligands. Complement C1q was shown to interact with LRP1 and to be implicated in the phagocytosis of apoptotic cells. The present work aimed at exploring how these two large molecules interact at the molecular level using a dissection strategy. For that purpose, recombinant LRP1 clusters II, III and IV were produced in mammalian HEK293F cells and their binding properties were investigated. Clusters II and IV were found to interact specifically and efficiently with C1q with K_{Ds} in the nanomolar range. The use of truncated C1q fragments and recombinant mutated C1q allowed to localize more precisely the binding site for LRP1 on the collagen-like regions of C1q (CLRs), nearby the site that is implicated in the interaction with the cognate protease tetramer C1r2s2. This site could be a common anchorage for other ligands of C1q CLRs such as sulfated proteoglycans and Complement receptor type 1. The use of a cellular model, consisting in CHO LRP1-null cells transfected with full-length LRP1 or a cluster IV minireceptor (mini IV) confirmed that mini IV interacts with C1q at the cell membrane as well as full-length LRP1. Further cellular interaction studies finally highlighted that mini IV can endorse the full-length LRP1 binding efficiency for apoptotic cells and that C1q has no impact on this interaction.

Keywords: complement C1q, scavenger receptor, LRP1, CD91, interaction

OPEN ACCESS

Edited by:
Jagadeesh Bayry, Institut National de la Santé et de la Recherche Médicale (INSERM), France

Reviewed by:
Roberta Bulla, University of Trieste, Italy
Chiara Agostinis, IRCCS Materno Infantile Burlo Garofolo (IRCCS), Italy

***Correspondence:**
Véronique Rossi
veronique.rossi@ibs.fr
Jean-Philippe Kleman
Jean-Philippe.kleman@ibs.fr

†These authors have contributed equally to this work

Specialty section:
This article was submitted to Molecular Innate Immunity, a section of the journal Frontiers in Immunology

Received: *15 July 2020*
Accepted: *28 September 2020*
Published: *21 October 2020*

Citation:
Fouët G, Gout E, Wicker-Planquart C, Bally I, De Nardis C, Dedieu S, Chouquet A, Gaboriaud C, Thielens NM, Kleman J-P and Rossi V (2020) Complement C1q Interacts With LRP1 Clusters II and IV Through a Site Close but Different From the Binding Site of Its C1r and C1s-Associated Proteases. Front. Immunol. 11:583754. doi: 10.3389/fimmu.2020.583754

INTRODUCTION

C1q is a defense collagen that is known for decades for its implication in the elimination of pathogens or altered-self bodies through the classical cascade of complement. In this context C1q recognizes targets and triggers the complement cascade through activation of an associated protease tetramer C1r2s2. Nowadays, a large body of research also highlights some widely diverse, non-complement related functions of C1q. As examples, C1q can act as an opsonin bridging targets and membrane receptors, C1q is implicated in the modulation of immune cells differentiation and it has an essential role in the enhancement of apoptotic cells phagocytosis (1–3). C1q is a 450 kDa protein assembled from three different polypeptide chains into six stems forming a bouquet like scaffold. C1q exposes six identical globular heads (GR) on one end, extending in six collagen stems (Collagen-Like Regions, CLR) that associate into a bundle on the other end of the molecule. This particular structural arrangement is providing a wide diversity in C1q functions, with the globular heads recognizing targets that for most of them will trigger the classical complement cascade whereas the collagen regions are implicated in other non-complement functions. Removal of apoptotic cells has been described to involve a ternary complex on phagocytic cells that is composed of LRP1, a membrane scavenger receptor belonging to the LDL receptor family, and two soluble proteins, calreticulin (CRT) and defense collagens such as MBL, SP-A and SP-D, or C1q. The implication in efferocytosis of such a membrane complex is nevertheless controversial, such as its molecular arrangement. Some studies describe the beneficial C1q-dependent uptake of apoptotic cells through LRP1/CRT interaction (4, 5), but it also appeared lately, using LRP1 deficient macrophages, that LRP1 is not required in macrophage-mediated C1q-dependent phagocytosis (6). Moreover, it was also shown that C1q interacts in a binary way with LRP1 without the need of CRT (7). LRP1 is a large 600 kDa endocytic receptor that participates in several biological pathways and plays prominent role in endocytosis of a large number of unrelated ligands. It is the largest member of the scavenger receptor family with an extracellular polypeptide extension composed of numerous structurally homologous modules of three types, EGF repeats, β-propeller domains and cysteine-rich calcium dependent complement type repeats called CR or LA modules (**Figure 1**). Four different clusters, I, II, III and IV each composed of respectively 2, 8, 10 and 11 consecutive CR modules are the binding platforms for LRP1 extracellular ligands (8). Clusters II and IV are the targets for most of LRP1 ligands and display only minor differences in binding kinetics whereas few have been described for cluster III (9). When processed inside the cells, LRP1 is associated with a chaperone of 39 kDa called receptor-associated protein (RAP), that binds the three clusters (II, III and IV), and is then eliminated when mature LRP1 becomes exposed outside the cell membrane (10). Extensive studies on RAP binding to LRP1 and dissection of other ligand interactions highlight a common binding strategy of LRP1 CR modules to LRP1 ligands, including a calcium-dependent mode of electrostatic recognition, together with avidity effects resulting from the use of multiple sites. Ligand binding appears to involve the docking of two or more lysine residues into acidic pockets located within CR modules of the receptor referred as "acidic necklace" (11). There are still incomplete data about C1q interaction with LRP1. Duus et al. showed that C1q interacts with LRP1 in the absence of CRT, and that the binding interferes with interaction of ligands of both clusters II and IV (7). In this work we aimed at going further in deciphering this interaction using soluble and membrane clusters of LRP1. We provide evidence that C1q interacts specifically with clusters II and IV at a RAP-competing binding site. We also highlight that cluster IV plays a central role in both C1q and apoptotic cells binding. On C1q, this interaction involves mainly C1q CLR and mobilizes basic residues that are close but different from the protease C1r2s2 binding site. This site could constitute a common "anchor station" shared by other C1q ligands such as sulfated proteoglycans and CR1.

Abbreviations: GR, globular region of C1q; CLR, collagen like region of C1q; CR, complement-type repeat; LDL, low-density lipoprotein; LRP1, LDL receptor-related protein 1; rC1qABC, recombinant C1q mutant LysA59/LysB61/LysC58, SP-A, surfactant protein A; SP-D, surfactant protein D; CRT, calreticulin; CR1, complement receptor1; MBL, mannose-binding lectin; MASP, MBL-associated serine protease; SPR, surface plasmon resonance; RAP, receptor-associated protein; RU, resonance unit; EGF, epidermal growth factor.

MATERIALS AND METHODS

Proteins, Cells, and Reagents

C1q was purified from human serum and quantified as described (12). Human serum was obtained from the Etablissement Français du Sang (EFS) Rhône-Alpes (agreement number 14-1940 regarding its use in research). C1q collagen stalks (CLR) and C1q globular heads (GR) were prepared according to Tacnet-Delorme et al. (13). The recombinant protease tetramer C1r2s2 was produced and purified according to Bally et al. (14). Full-length LRP1 (soluble LRP1) was produced and purified according to De Nardis et al. (15). Recombinant C1q and C1q mutant LysA59Ala/LysB61Ala/LysC58Ala were produced and purified as described in Bally et al. (16). For protein quantification, Mw and $A_{1\%,\ 1\ cm}$ were respectively for C1q (459,300; 6.8) (12), CLR (189,900; 2.1), GR (48,000; 9.3) (17), C1r2s2 (330,000; 13.5) (18). Oligonucleotides were from Eurogentec. Restriction and modification enzymes were from New England Biolabs.

Full-length LRP1 Myc DDK clone (RC218369) was purchased from Origene. The pET22B-RAP plasmid was kindly provided by Søren Moestrup, Aahrus University, Denmark. pcDNA3.1 mini IV HA-tag was cloned as previously indicated (19).

Cloning of LRP1 Clusters II, III, and IV in pcDNA3.1 for Soluble Expression

The DNA sequence encoding the signal peptide for human LRP1 was inserted in pcDNA3.1/Neo by site directed mutagenesis using the QuickChange II XL kit (Agilent Technologies) according to an optimized procedure (20). A nucleotide

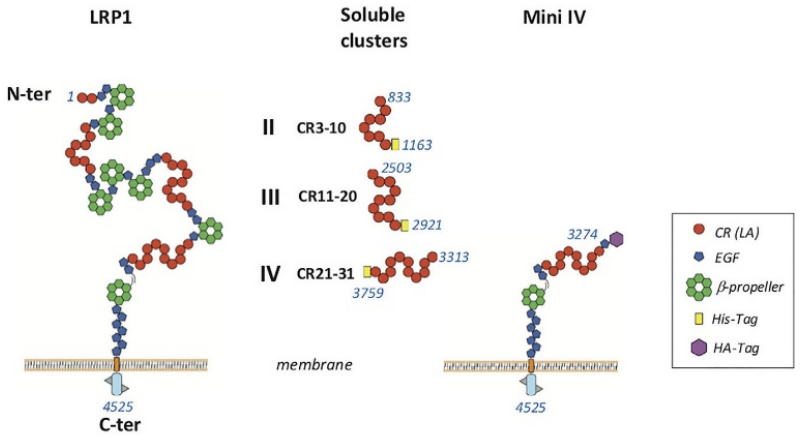

FIGURE 1 | Schematic representation of LRP1 fragments used in this study LRP1 clusters II, III and IV were produced in 293-F mammalian cells with a His-Tag at the C-terminal extremity. Membrane full-length LRP1 and minireceptor IV (mini IV) were used for cellular interaction studies. CR, complement repeat; LA, LDL receptor class A; HA, hemaglutinin; EGF, epidermal growth factor. Amino acid numbering of mature LRP1 is indicated in blue.

sequence encoding the four amino acids, AIDA, located after the signal peptide cleavage site of LRP1 (10) plus a *BamHI* restriction site were introduced on the 3′-end of the sequence coding for the signal peptide in order to subclone soluble cluster sequences between *BamHI* and *XhoI* sites.

The cDNA for each cluster II, III and IV corresponding respectively to the mature LRP1 amino acid fragments 833-1163 (II), 2503-2921 (III), and 3313-3759 (IV) with a supplementary sequence coding for a 7 (cluster III) or 8 His-TAG (cluster II and IV) on the 5′ end, was generated by PCR amplification of full-length LRP1 Myc DDK and cloned in pcDNA3.1/LRP1 signal peptide vector as mentioned above.

Production of LRP1 Soluble Clusters II, III, and IV in HEK293F Cells and Purification

pcDNA 3.1 plasmids coding for each cluster II, III and IV were transfected in Freestyle HEK293F (293-F) cells using 293fectin, according to the manufacturer's protocol (Invitrogen) and stabilized by G418 selection (400 µg/ml). Around 500 ml of expression medium were harvested and submitted to two-step purification. First, the medium was dialyzed in 20 mM Tris, 150 mM NaCl, pH 7.5 and loaded on a HiTrap™ Chelating HP column (5 ml, GE Healthcare Life sciences). The fractions containing the clusters were then concentrated/diluted in 50 mM sodium acetate, 50 mM NaCl, 10 mM EDTA, pH 6 before loading on an anion exchange column Mono Q® 5/50 GL (GE Healthcare Life sciences) and elution was achieved through a NaCl gradient (50 - 500 mM). Concentration was finally carried out to reach around 0.5 mg/ml and the buffer changed into 20 mM Tris, 150 mM NaCl, pH 7.5.

The concentration of the purified soluble LRP1 clusters was estimated using the absorption coefficient $A_{1\%,\ 1\ cm}$ at 280 nm calculated using the PROTPARAM program on the Expasy server, and an experimental molecular weight determined by MALDI mass spectrometry. Their $A_{1\%,\ 1\ cm}$ at 280 nm and molecular weight were respectively 11.78 and 50,372 for cluster II, 9.96 and 63,734 for cluster III and 10.16 and 62,528 for cluster IV.

Mass spectrometry analyses were performed on a Matrix Assisted Laser Desorption Ionization-Time of Flight (MALDI-TOF) mass spectrometer (Autoflex, Bruker Daltonics), operated in linear positive mode. The proteins (1 mg/ml) were diluted 1:2 to 1:10 in SA matrix [sinapinic acid (Sigma-Aldrich) 10 mg/ml in acetonitrile/water/trifluoroacetic acid [50/50/0.1 (v/v/v)] and 2 µL were deposited directly on the target.

RAP Expression and Purification

RAP was overexpressed by pET22B-RAP transformed *Escherichia coli* BL21(DE3) using conventional IPTG induction (1 mM) in LB medium for 3 h at 37°C. Bacteria were lysed by sonication in 100 mM NaCl, 20 mM Tris, 10 mM $MgCl_2$, pH 8.5 supplemented with Complete® protease inhibitor cocktail (Roche Diagnostics). The lysate was then purified by nickel-affinity chromatography (Hiis-select, Sigma-Aldrich) followed by gel filtration on Superdex®S75 10/300 (GE Healthcare Life sciences). Purification was performed in 100 mM NaCl, 20 mM Tris, pH 8.0. For concentration determination, a molecular mass of 36,440 Da corresponding to the RAP amino acid sequence preceded by a thrombin cleavage site and a 6His-Tag (MHHHHHHLVPRGS ... Y) and $A_{1\%,\ 1\ cm}$ at 280 nm of 9.26 were calculated by the PROTPARAM program.

Soluble LRP1 Clusters and RAP Interaction Experiments by SPR

For all surface plasmon resonance experiments, protein ligands were immobilized on CM5 sensor chips using the amine coupling chemistry according to the manufacturer's instructions (GE Healthcare). Immobilizations were performed at 10 µl/min in 10 mM HEPES, 150 mM NaCl, 3 mM EDTA, 0.005%, surfactant P20, pH 7.4 (HBSEP, for BIAcore 3000) or the same buffer supplemented with 0.05% surfactant P20 (HBSEP+,

for T200 instrument). Regeneration of the surfaces was achieved by 15 µL injections of 1 M NaCl, 10 mM EDTA.

RAP interaction with full-length LRP1 and clusters II, III, and IV was determined on a BIAcore 3000 instrument (GE Healthcare). Full-length LRP1 was diluted at 50 µg/ml in 10 mM sodium acetate pH 3.5 to get an immobilization level of 7,400 RU. Clusters were diluted at 10 µg/ml in 10 mM sodium acetate pH 4.0 (clusters II and III) and 4.5 (cluster IV). For interaction measurements, RAP (ranging from 0.25 to 16 nM) was injected over immobilized clusters II (2,967 RU), III (3,460 RU) and IV (3,396 RU) in 50 mM triethanolamine-HCl (TEA), 150 mM NaCl, 1 mM $CaCl_2$, 0.005% P20, pH 7.4 at 20 µl/min. Kinetic data were analyzed by global fitting to a 1:1 Langmuir binding model of both the association and dissociation phases using the BIAevaluation 3.2 software (GE Healthcare).

Interaction of soluble clusters II, III, and IV with immobilized C1q was also performed on a BIAcore 3000. For that, serum C1q was diluted in 10 mM sodium acetate, pH 5.5 at 23 µg/ml and injected over the CM5 chip to get the immobilization level of 17,500 RU. Cluster II, III and IV (500 nM) interaction was done in 50 mM TEA, 150 mM NaCl, 1 mM $CaCl_2$, 0.005% P20 pH 7.4 at 20 µl/min.

Serum C1q, C1q GR, and CLR binding to immobilized clusters II and IV and C1r2s2 competition was performed on a T200 instrument. Both clusters were diluted at 50 µg/ml in 10 mM sodium acetate, pH 4 for immobilization. The interaction of C1q or CLR or GR on immobilized LRP1 cluster II (1,230 RU) or cluster IV (1,270 RU) was measured in 50 mM Tris, 150 mM NaCl, 2 mM $CaCl_2$, 0.05% P20, pH 7.4 at 30 µl/min with association and dissociation of 180 s. For C1r2s2 competition, C1q was pre-incubated (15 min at 25°C) with C1r2s2 before injection. The equilibrium dissociation constants (K_D) for serum C1q binding to clusters II and IV were determined by injection of concentrations ranging from 0.125 nM to 8 nM. The K_{Ds} were calculated from measured binding levels at equilibrium (Req) by fitting plots of Req versus concentration using steady state analysis (Biaevaluation software).

Determination of the K_{Ds} for the interaction of clusters II and IV with immobilized serum C1q, rC1q WT, and rC1q ABC was performed on a T200 instrument on immobilized serum C1q (14,000 RU), recombinant C1q (11,000 RU) and C1q mutant LysA59Ala/LysB61Ala/LysC58Ala (rC1qABC, 12,300 RU). All C1q samples were diluted in 10 mM sodium acetate, pH 5. The interaction of clusters II and IV was measured by injection of indicated concentrations (see **Figure 7**) in 50 mM Tris, 150 mM NaCl, 2 mM $CaCl_2$, 0.05% P20, pH 7.4, for 180 s at 30 µl/min. The equilibrium dissociation constants (K_D) were calculated as mentioned above for serum C1q interaction with immobilized clusters.

Transfection and Expression of Full-Length LRP1 and Mini IV Receptor in LRP1-Null CHO Cells

Cell Culture and Culture Conditions

LRP1-deficient CHO cells called in this study CHO-null cells (21) were obtained from Kanekiyo Takahisa from the Department of Neuroscience, Mayo Clinic, Jacksonville, Florida, USA. Unless otherwise stated, all reagents are from Gibco®. CHO-null and Jurkat cells were respectively cultured in DMEM-F12 (Dulbecco's modified Eagle's medium), or in RPMI (Roswell Park Memorial Institute medium), supplemented with 10% (v/v) Fetal Bovine Serum (FBS) at 37°C with an humidified atmosphere and 5% CO_2. For CHO clones expressing LRP1 receptors (full-length or mini IV), the media were supplemented with G418 (geneticin sulfate) at 400 µg/ml.

Transfection of Full-Length and Mini IV LRP1 Receptors in CHO-Null Cells and Analysis of Receptors Expression

Plasmid DNAs were transfected into CHO-null cells by lipofectamine 2000 following manufacturer's instructions (Invitrogen™). Briefly, 24 h before transfection, cells were plated in 35 mm dishes (or 6-well plates) at 0.5 10^6 cells per dish, in 1.5 ml of culture medium without G418, to reach 70% confluency at transfection. Four µg of plasmid DNA and 10 µl of lipofectamine 2000 were separately diluted in 250 µl of OptiMEM and mixed. After 15 min incubation, the mix was added to each well, and the cells were further incubated for 72 h at 37°C before adding 400 µg/ml of G418 for selection.

Monoclonal cell populations were isolated and amplified after a series of 3 limit dilutions. Briefly, transfected cells were counted and diluted to inoculate unique cells into a 96-well plate. After 10 to 12 days in culture, full-length LRP1 or cluster IV mini-receptor expression and cell population homogeneity were tested by flow cytometry and immunofluorescence microscopy as detailed below.

Flow Cytometry

Adherent CHO-K1 transfected cells were recovered using Gibco® Versene buffer and further washed in PBS (Phosphate-Buffered Saline) supplemented with 1% BSA (Bovine Serum Albumin; Sigma-Aldrich). For each sample, 1×10^6 cells were incubated on ice for 45 min in 100 µl of anti-CD91-PE (BD Biosciences; dilution 1/5 in PBS 1% BSA) for full-length LRP1 receptor, or 100 µl of anti-HA-PE (Miltenyi biotech, Bergish Gladbach, Germany; dilution 1/20 in PBS 1% BSA) for mini IV LRP1 truncated receptor. Cells were then washed twice in PBS 1% BSA before analysis (MACSQuant VYB flow cytometer - Miltenyi Biotech, Bergish Gladbach, Germany) using the 561 nm excitation and 586(15) nm emission channel (Y1). PE positive populations were estimated after forward scatter (FSC) and side scatter (SSC) gating on the cells. For each condition, at least 20,000 events were analyzed.

Immunofluorescence Microscopy

Naïve or transfected CHO-null cells cultured on coverslip were fixed in 4% (w/v) paraformaldehyde (PFA) and processed for immunofluorescence using LRP1 full-length or mini IV receptors labeling respectively with anti-CD91-PE (BD Biosciences; dilution 1/5 in PBS 1% BSA) or anti-HA-PE (Miltenyi biotech, dilution 1/20 in PBS 1% BSA). Alternatively, secondary labeling with Cy3-conjugated anti-mouse antibody (dilution 1/250 in PBS 1% BSA) of anti-CD91 (BD Biosciences;

dilution 1/250 in PBS 1% BSA) and of anti-HA (anti-HA.11 Biolegend 1/1000 in PBS 1% BSA) were used for LRP1 and mini IV receptors, respectively. Coverslips were mounted on slides using Vectashield with DAPI (Vector laboratory). Pictures were acquired with IQ software (Andor™), using a spinning disk confocal microscope (Yokogawa CSU-X1–IX81 Olympus) with an iXon EMCCD camera (Andor™), and the appropriate channels for PE and DAPI visualization.

Interaction of C1q with Transfected Cells

CHO-null, or expressing either full-length LRP1 or mini IV LRP1 truncated receptors were detached using Versene, washed once in PBS 1% BSA and resuspended in the same buffer. For each condition, 1×10^6 cells were incubated 30 min on ice with 8 µg of C1q in 100 µl PBS 1% BSA. After 2 washes with 1 ml of PBS 1% BSA, bound C1q was detected by immunostaining using a monoclonal anti C1q antibody (mAB A201 Quidel Corporation, dilution 1/100 in PBS 1% BSA) for 45 min on ice, followed by Cy3-conjugated goat anti-mouse antibody (dilution 1/250 in PBS 1% BSA for 30 min on ice). Flow cytometry analyses were performed on a MACSQuant VYB cytometer as already described, using the 561/586(15) nm Y1 channel for Cy3.

Interaction of Jurkat Cells With LRP1 Receptors Expressing CHO Cells and C1q Impact Determination

The cell-cell interaction assay was performed using flow cytometry of differentially labeled Jurkat and CHO-null cells expressing either none, full-length LRP1, or mini IV receptors. In brief, 24 h before the assay, cells were harvested and labeled using PKH26 for CHO clones or PKH67 for Jurkat cells, according to manufacturer instructions (Sigma-Aldrich). The labeling reaction was stopped after 5 min incubation in the dark by adding pure FBS. After washing, CHO control and clones expressing LRP1 constructs were plated at 2×10^5 cells per ml culture medium in 12-well plate. PKH67 labeled Jurkat cells were resuspended in complete RPMI medium at 1×10^6 cells per ml and when required, apoptosis was induced by UVB irradiation at 312 nm for 5 min (500 mJ/cm^2) in 60 *mm* cell culture dish (5 ml/dish). 16 h after labeling healthy or late apoptotic Jurkat cells were centrifuged and counted. This treatment yields around 74% of apoptotic Jurkat cells. When required, Jurkat cells (2×10^6 cells) were incubated with 15 µg of C1q in 100 µl DPBS (Dulbecco's PBS in the presence of calcium and magnesium, 3% BSA) for 1 h on ice. For interaction tests, 2×10^6 PKH67 labeled Jurkat cells were washed in 1 ml DPBS, resuspended in 1 ml of complete DMEM-F12 and added to the monolayer of CHO-K1 cells labeled with PKH26 in the 12-well plates. After incubation at 37°C (typically 2 h), the CHO-K1 cells in a monolayer were washed with 1 ml DPBS to remove the non-attached Jurkat cells. PKH26-labeled CHO-K1 cells decorated with PKH67 labeled Jurkat cell were recovered by gentle scraping or using 100 ml of trypsin solution (Trypsin EDTA, Gibco®) before analysis by flow cytometry as described above, using the 561/586(15) nm Y1 channel for PKH26 and the 488/525(50) nm B1 channel for PKH67.

RESULTS

Production and Purification of Soluble LRP1 Clusters From Mammalian Cells in Culture

Soluble LRP1 clusters II, III, and IV were produced in 293-F cells and purified from the culture supernatant by nickel affinity and anion exchange chromatography as described in *Materials and Methods*. These clusters were designed to get soluble fragments restricted to the CR modules described as functional interacting LRP1 regions. In our study, clusters II, III and IV are therefore respectively composed of 8, 10, and 11 CR modules (CR3-10, CR11-20, and CR21-31) (**Figure 1**). To ensure proper cleavage of the LRP1 signal peptide upon secretion, we chose the strategy of Bu and colleagues (10) with the insertion of 4 amino acids (AIDA), naturally located in full-length LRP1 after the cleavage site of the signal peptide. The resulting protein fragments for each cluster have all 6 additional N-terminal amino acids, AIDA plus a GS introduced by the cloning process, and carry also a C-terminal 7 or 8 His-TAG (8 for II and IV and 7 for III). The amount of cluster secreted in the 293-F culture medium was two to three times higher for cluster III than for clusters II and IV, with purification yields of respectively around 0.25 mg/L (II), 0.90 mg/L (III) and 0.40 mg/L (IV). As suggested by Bu and colleagues (10), attempts to improve the production yield were carried in the presence of co-expressed RAP, but no expression increase could be achieved (*data not shown*). Nevertheless, the purification procedure leads to pure secreted fragments as observed by SDS-PAGE analysis (**Figure 2A**). MALDI mass spectrometry analyses (**Figure 2B**), gave for each cluster a mass increase when compared to the calculated polypeptide mass, resulting from post-translational modifications, such as N-linked oligosaccharides, which is consistent with the apparent molecular weights observed on the gel.

Validation of RAP and LRP1 Clusters as Tools for Deciphering LRP1 Ligand Interaction Properties

RAP was expressed in *E. coli* and purified using a two-step chromatography protocol (section 2.4 M&M). The apparent molecular mass of purified RAP observed by SDS-PAGE analysis (**Figure 3**) is as expected around 40 kDa (22, 23). For functional validation, we tested its interaction with soluble full-length LRP1 (also called ecto-LRP1 by De Nardis and colleagues) (15) using surface plasmon resonance. The kinetic constants gave a K_D value of 0.76 ± 0.08 nM, and association and dissociation constants of respectively $1.41 \pm 0.17 \times 10^6$ M^{-1} s^{-1} and $1.05 \pm 0.07 \times 10^{-3}$ s^{-1} (**Figure 3**, **Table 1**). The interaction of RAP with purified clusters II, III and IV was also investigated and gave K_D values in the same nanomolar range of respectively 1.09 ± 0.31 nM (II), 1.06 ± 0.1 nM (III) and 1.28 ± 0.12 nM (IV) (**Figure 3**, **Table 1**). These results are in agreement with previous studies (24–26) indicating that RAP interaction with LRP1 is strong and that the affinity of RAP for each individual cluster is in the same range. In the present study, RAP interaction allowed the validation of the functional integrity of the expressed LRP1 clusters.

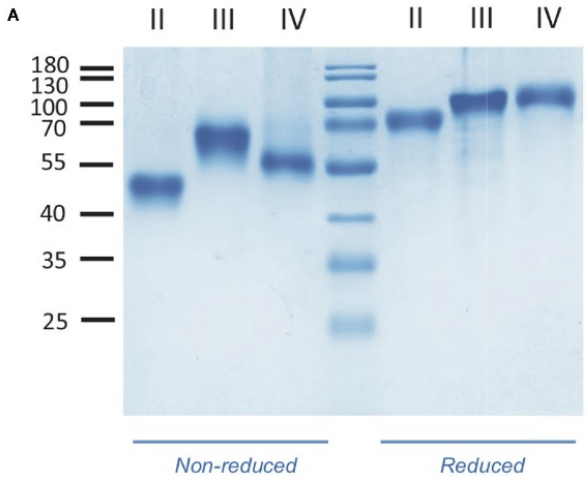

B

	Cluster II	Cluster III	Cluster IV
M (Da) *calculated from the amino acid sequence*	37 724	47 295	51 579
MS M (Da)	50 372	63 734	62 528
Predicted N-Glycosylations	4	6	3

FIGURE 2 | Characterization of LRP1 clusters. **(A)** SDS-PAGE analysis of LRP1 clusters. Clusters II, III and IV in non-reducing (left) and reducing conditions (right), molecular weight markers are indicated in kDa. **(B)**, MALDI mass spectrometry analysis of LRP1 clusters. M, molecular weight; MS, Mass spectrometry.

The Interaction of C1q With LRP1 Is Involving Clusters II and IV

Several studies highlighted that most LRP1 ligands are interacting specifically with clusters II and IV (25, 27, 28). The location of LRP1 sites for C1q interaction was one of the questions we aimed at answering first. For that, SPR analyses were performed with clusters II, III and IV injection over immobilized serum C1q. Clusters II and IV interacted similarly with C1q whereas cluster III did not (**Figure 4A**). Moreover, the interaction was efficiently overcome by RAP competition in an equimolar ratio indicating that RAP interaction sites on LRP1 might be shared for C1q interaction or be positioned in a neighbouring region close enough to get competition (**Figures 4B, C**). SPR kinetic analysis shown in **Figure 5**, also pointed out that serum C1q has affinities for both clusters II and IV that are in the same range. With immobilized serum C1q, clusters II or IV interaction had both K_{Ds} in a sub-micromolar range (**Figure 5**, **Table 2**). Interestingly, in the reverse configuration, when serum C1q was injected over immobilized clusters II and IV they had an affinity increase of around 100 fold with respectively 3.49 ± 0.45 nM for cluster II and 0.69 ± 0.1 nM for cluster IV (**Figure 5**, **Table 2**). This increased affinity when the clusters are immobilized compared to the reverse orientation might be explained by the known avidity of C1q for surface bound ligands. From these results, even though in the same range, the affinities of C1q for cluster IV appeared to be higher than for cluster II.

The Interaction Site on C1q for LRP1 Clusters II and IV Is Different From the Proteases Binding Site but Is Located in Close Proximity

To decipher the interaction of LRP1 with C1q, both clusters II and IV were first tested for their binding to two separate regions, the globular heads (GR) or collagen regions (CLR) obtained from purified serum C1q. The results of **Figure 6** indicate that the CLRs contribute to almost all the interaction of C1q with both clusters, with a small contribution from the GRs. That

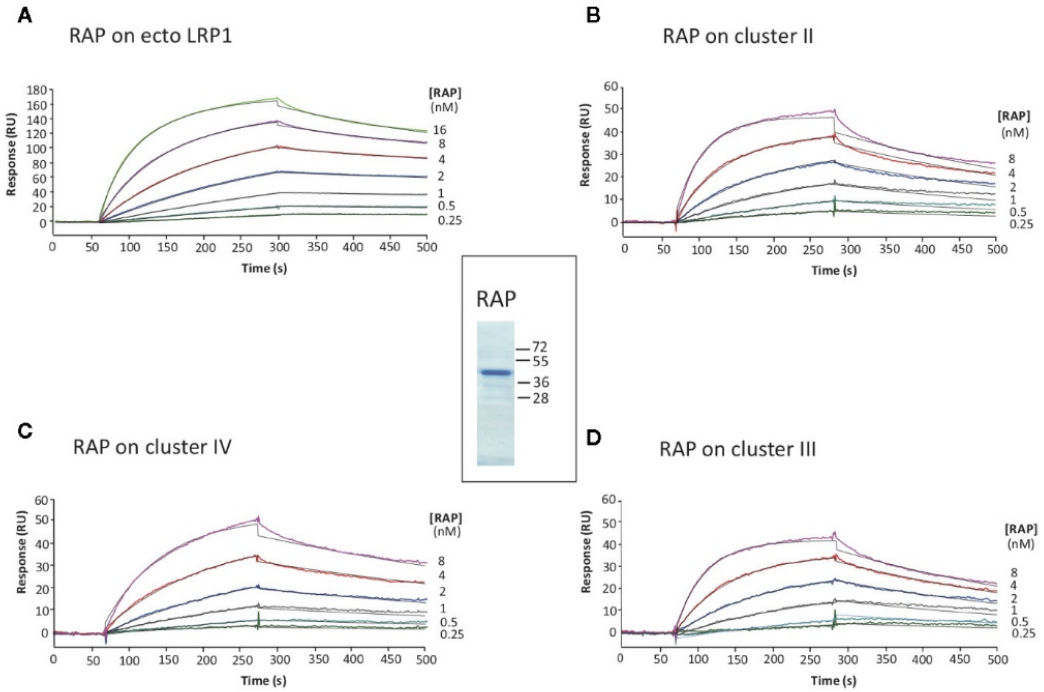

FIGURE 3 | Kinetic analysis of RAP interaction with immobilized full-length LRP1 and clusters II, III and IV. SDS-PAGE of RAP in reducing conditions, molecular weight markers are indicated in kDa (center panel). SPR analysis of RAP interaction with full-length LRP1: RAP was injected at indicated concentrations over immobilized full-length LRP1 (**A**, 7,400 RU), and LRP1 clusters II (**B**, 2,967 RU), III (**D**, 3,460 RU) and IV (**C**, 3,396 RU) in 50 mM triethanolamine-HCl (TEA), 145 mM NaCl, 1 mM $CaCl_2$, 0.005% surfactant P20, pH 7.4. The fitting obtained using a Langmuir 1:1 binding model is shown in black lines. Kinetic constants are summarized in **Table 1**.

TABLE 1 | Kinetic and equilibrium dissociation constants for the binding of RAP to immobilized ecto-LRP1 and clusters II, III, and IV.

	ka (M^{-1} s^{-1})	*kd* (s^{-1})	K_D (nM)	n^a
Immobilized ecto LRP1	$1.41 \pm 0.17 \times 10^6$	$1.05 \pm 0.07 \times 10^{-3}$	0.76 ± 0.08	4
Immobilized cluster II	$2.20 \pm 1.42 \times 10^6$	$1.96 \pm 0.86 \times 10^{-3}$	1.09 ± 0.31	2
Immobilized cluster III	$2.95 \pm 0.37 \times 10^6$	$3.08 \pm 0.09 \times 10^{-3}$	1.06 ± 0.10	2
Immobilized cluster IV	$1.18 \pm 0.40 \times 10^6$	$1.47 \pm 0.37 \times 10^{-3}$	1.28 ± 0.12	2

Values are expressed as means ± SE.
n^a Number of separate experiments.

observation then raised the question of defining more precisely the location of the binding site of LRP1 on the CLR. For that purpose, an equimolar amount of C1r2s2, whose binding site has been previously identified on C1q CLR (16) was added to C1q prior to its injection on immobilized clusters. The large decrease observed for C1q interaction with cluster II and cluster IV in the presence of C1r2s2 indicates that the protease tetramer competes with LRP1 for binding to C1q (**Figure 6**). The remaining signal can be explained by the contribution of the GRs that are not interacting with the protease tetramer and therefore remain free for binding. These results suggest that the interaction site of C1q for LRP1 may be the same as the C1q binding site for the serine protease tetramer. To go further in the location of the site interacting with LRP1, we used a recombinant variant of C1q, carrying mutations of LysA59, LysB61, and LysC58 (called rC1qABC) and devoid of the C1r2s2 binding capacity (16). Unexpectedly, the results of **Figure 7** highlight that wild-type and mutated C1q interact with both clusters II and IV in the same manner. Indeed, kinetic analyses for all C1q proteins tested yielded affinities ranging from 2.75 to 5.14×10^{-7} M for cluster II and 1.58 to 2.2×10^{-7} M for cluster IV interactions (**Table 2**). Overall, these data reveal that LRP1 binding to C1q involves one or some site(s) located in close proximity but distinct from the tetramer binding site.

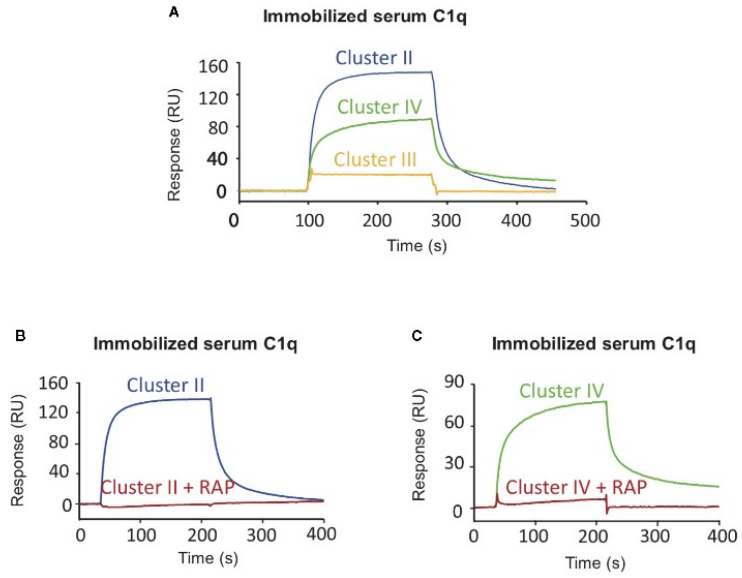

FIGURE 4 | LRP1 clusters II and IV interact with C1q. SPR analysis of LRP1 clusters II (blue curves), III (yellow curves) and IV (green curves) interactions over immobilized C1q, in the presence or absence of RAP. Clusters II, III and IV (500 nM in 50 mM TEA, 150 mM NaCl, 2 mM CaCl2, 0.005% P20, pH 7.4) were injected over immobilized serum C1q (17,500 RU) with or without RAP (500 nM). **(A)** comparison of the interaction curves in the absence of RAP for clusters II, III and IV. **(B, C)** Comparison of the binding of Cluster II **(B)** and Cluster IV **(C)** in the presence or in the absence of RAP.

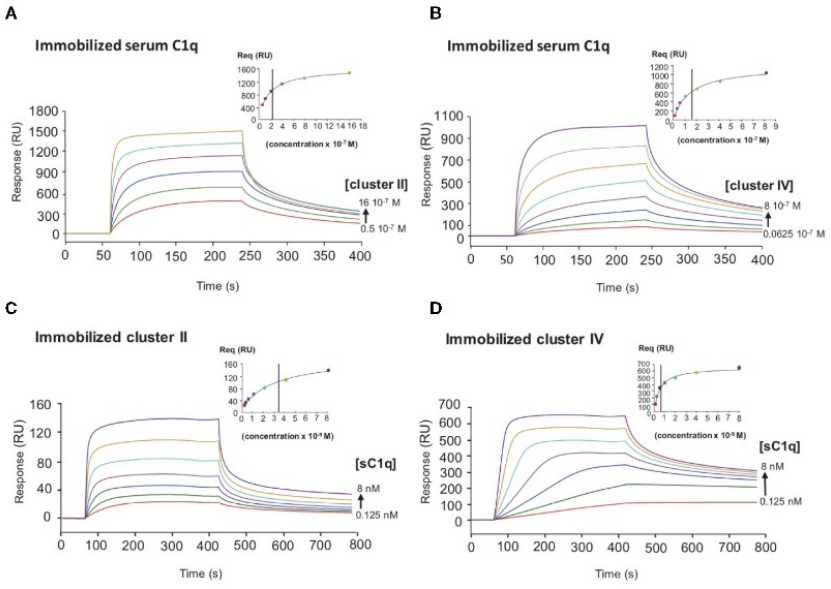

FIGURE 5 | Comparative kinetic analysis of the interaction of serum C1q with LRP1 clusters II and IV. SPR analysis of LRP1 clusters II and IV interactions with serum C1q in two configurations. Top panels, clusters II and IV were injected over immobilized serum C1q (14,000 RU), **(A, B)** respectively. Bottom panels, serum C1q was injected over immobilized clusters II (1,230 RU) and IV (1,270 RU), **(C, D)** respectively. All injection were performed in 50 mM Tris, 150 mM NaCl, 2 mM $CaCl_2$, 0.05% P20, pH 7.4. The concentration of soluble ligands is indicated on each curve. The Req versus concentration plots of steady state fittings are shown on the top right of the SPR curves. K_D values (means ± SD) for each kinetics are summarized in **Table 2**.

TABLE 2 | Equilibrium dissociation constants for the binding of clusters II and IV to C1q.

Immobilized protein	Injected protein	K_D (M)
cluster II	sC1q	$3.49 \pm 0.45 \times 10^{-9}$
cluster IV	sC1q	$0.69 \pm 0.11 \times 10^{-9}$
sC1q	cluster II	$2.75 \pm 0.55 \times 10^{-7}$
sC1q	cluster IV	$1.58 \pm 0.02 \times 10^{-7}$
rC1q WT	cluster II	$3.18 \pm 0.67 \times 10^{-7}$
rC1q WT	cluster IV	$1.83 \pm 0.02 \times 10^{-7}$
rC1q ABC	cluster II	$5.14 \pm 0.55 \times 10^{-7}$
rC1q ABC	cluster IV	$2.22 \pm 0.11 \times 10^{-7}$

Values are expressed as means ± SE of two separate experiments.

C1q Interacts With Full-Length LRP1 and Mini Receptor IV at the Surface of Transfected CHO Cells

In order to confirm at the cell surface the results obtained with purified proteins, we expressed full-length LRP1 or the minireceptor IV (mini IV) at the surface of LRP1-null CHO cells and monitored their ability to bind C1q. CHO-null cells were chosen for their non-phagocytic properties in order to get a simple adsorption cellular model (29). LRP1 mini IV consists in the N-terminal truncation of the extracellular portion of LRP1 until the EGF module preceding cluster IV CR21. It therefore contains the full native LRP1 C-terminal region from amino acid 3274 to 4525 (mature protein numbering). A N-terminal HA-Tag has also been added to facilitate LRP1 mini IV immunolabeling (**Figure 1**). The ectopic expression of LRP1 full-length or LRP1 mini IV constructs in LRP1-null CHO cells was confirmed by immunofluorescence (**Figure 8A**). In comparison with the LRP1-null CHO control cells, a clear labeling of the transfected constructs reveals, as expected, the expression of both LRP1 constructs at the plasma membrane. The transiently transfected CHO cells were further selected as described in the Materials and Methods section to obtain enriched populations for LRP1 constructs expression, as probed by flow cytometry (**Figure 8A**). We obtained consistently more than 95% of the cells expressing the receptor constructs and controlled regularly the stable expression of these constructs by flow cytometry to conduct reproducible experiments throughout the present study.

We next used the stable cell populations to study C1q interaction with LRP1 or its truncated counterpart at the cell surface. In brief, LRP1-null, full-length and mini IV cells were preincubated with C1q before being harvested and labeled using anti-C1q antibody. The mean fluorescence intensity of C1q labeling was measured for each cell population and compared

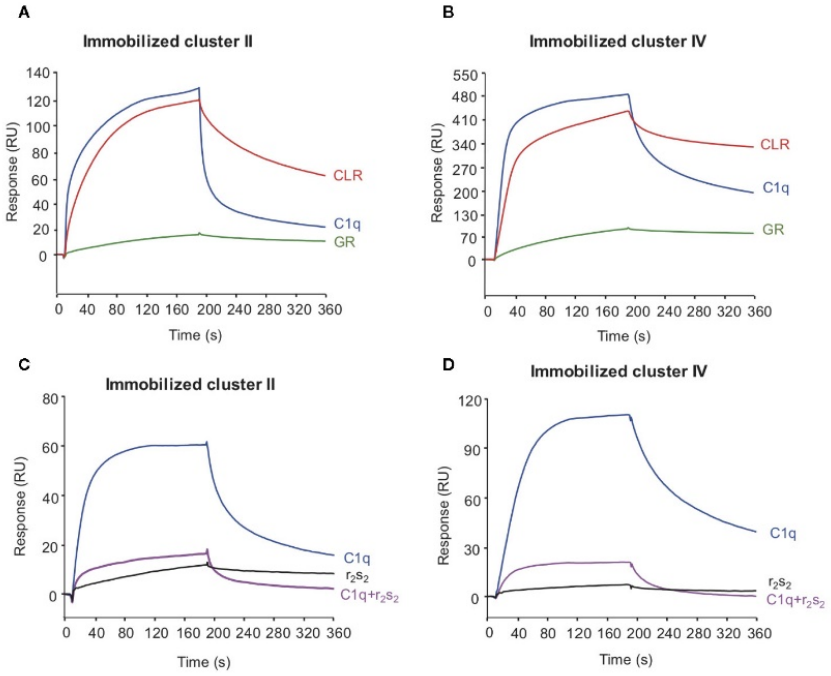

FIGURE 6 | The interaction site of LRP1 clusters II and IV on C1q is located on the collagen stalks at or close to the site interacting with C1r2s2 tetramer. C1q (10 nM, blue curves), CLR (10 nM, red curves) and GR (60 nM, green curves) were injected over immobilized LRP1 cluster II (1,230 RU, **A** panel) or LRP1 cluster IV (1,270 RU, **B** panel), in 50 mM Tris, 150 mM NaCl, 2 mM $CaCl_2$, 0.05% P20, pH 7.4. C1q (1 nM) was injected on the same amount of clusters II and IV (bottom **C, D**) with (pink curves) or without (blue curves) C1r2s2 (1 nM). r2s2 was also injected alone (1 nM) as a reference (black curves).

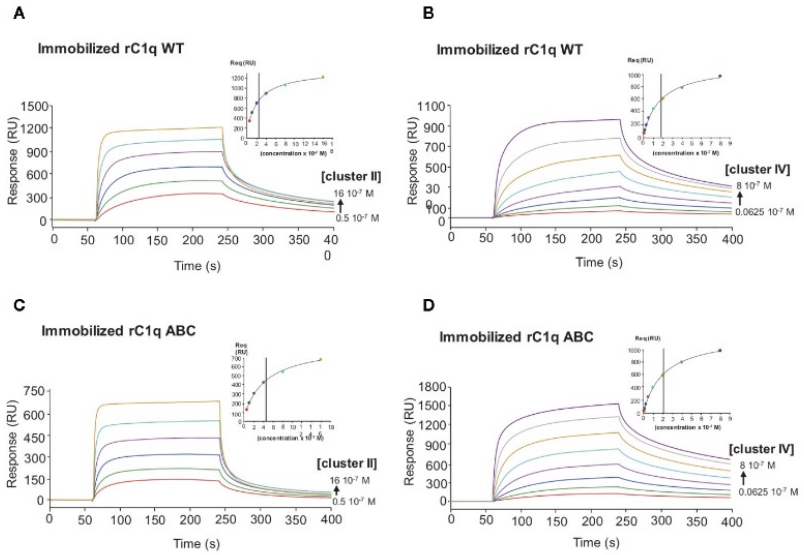

FIGURE 7 | Comparative kinetic analysis of the interaction of LRP1 clusters II and IV with immobilized recombinant C1q variants. LRP1 clusters II (left panels) and IV (right panels) were injected at indicated concentrations over immobilized recombinant C1q (rC1q WT, 11,000 RU, **A**, **B** panels) or C1q mutant LysA59Ala/LysB61Ala/LysC58Ala (rC1q ABC, 12,300 RU, **C**, **D** panels) in 50 mM Tris, 150 mM NaCl, 2 mM $CaCl_2$, 0.05% P20, pH 7.4. The Req versus concentration plots of steady state fittings are shown on the top right of the SPR curves. K_D values (means ± SD) for each kinetics are summarized in **Table 2**.

to control labeling (**Figure 8B**). The comparison of the measurements from 6 independent experiments, corrected for the secondary antibody only control labeling, underlines the specific increase of C1q binding to LRP1 full-length and mini IV expressing CHO cells in comparison to the mean values obtained on null cells (**Figure 8B**). The binding background observed on null-cells likely arises from the wide variety of C1q cell surface targets (2, 3). Taken together, these results and our data obtained *in vitro* (**Figure 4**) confirm the interaction of C1q with LRP1 and strongly support a role for cluster IV in mediating this interaction both *in vitro* and at the cell surface.

LRP1 and Cluster IV Are Implicated in the Recognition of Apoptotic Cells

The implication of C1q in apoptotic cell clearance driven by LRP1 has been described in two publications (4, 5). We therefore took benefit of our cell model system to study the differential implication of LRP1 and its cluster IV-containing domain in LRP1-dependent apoptotic cell recognition, using late apoptotic Jurkat cells as baits. Using the membrane-specific vital dyes PKH26 and PKH67 to respectively label CHO and Jurkat cells, respectively. We measured by flow cytometry the binding of PKH67 (Jurkat) to the PKH26 positive cell population (**Figure 9A**). As illustrated in the dot-plot diagram in a representative experiment (**Figure 9A**), the decoration of CHO cells by Jurkat cells is estimated from the percentage of double labeled PKH26 cells among the entire PKH26 population (upper right quadrant; **Figure 9A**). We compared the decoration efficiency of healthy or late apoptotic Jurkat after incubation at 37°C with CHO cells expressing or not the LRP1 full-length (FL) or mini IV constructs. The mean values from 13 independent experiments in each condition and their respective standard deviations are shown in **Figure 9B**. The expression of LRP1 or its truncated form are both enhancing the decoration of CHO cells by late apoptotic Jurkat cells but not by healthy Jurkat cells, suggesting that LRP1 is implicated in the specific recognition of apoptotic cells. A representative specific binding of apoptotic Jurkat cells to LRP1 expressing CHO cells is also shown by time lapse immunofluorescence (**Supplementary Figure S1**). In these experimental conditions as expected from non-phagocytic CHO cells, recognition of the apoptotic Jurkat cells accounts entirely for the adsorption of Jurkat cells as confirmed by a treatment with trypsin before flow cytometry that is reverting the adsorption to the level of the control experiments (**Supplementary Figure S2**).

As demonstrated herein, LRP1 expression in CHO-null cells promotes C1q binding (**Figure 8B**). We thus wondered whether C1q could modulate the specific recognition of the late apoptotic Jurkat cells. Using the same experimental set-up, we measured the adsorption of Jurkat cells in the absence or in the presence of 10 μg/ml of C1q purified from serum (**Figure 10**). In these conditions, the recognition of apoptotic cells by CHO cells was not modified by the presence of C1q, even for the cells expressing ectopic full-length LRP1, that have been used for the C1q decoration experiments shown in **Figure 8**. Our data suggest that the specific binding of C1q to LRP1 is not enhancing the LRP1-dependent apoptotic cell recognition in a simplified cellular context.

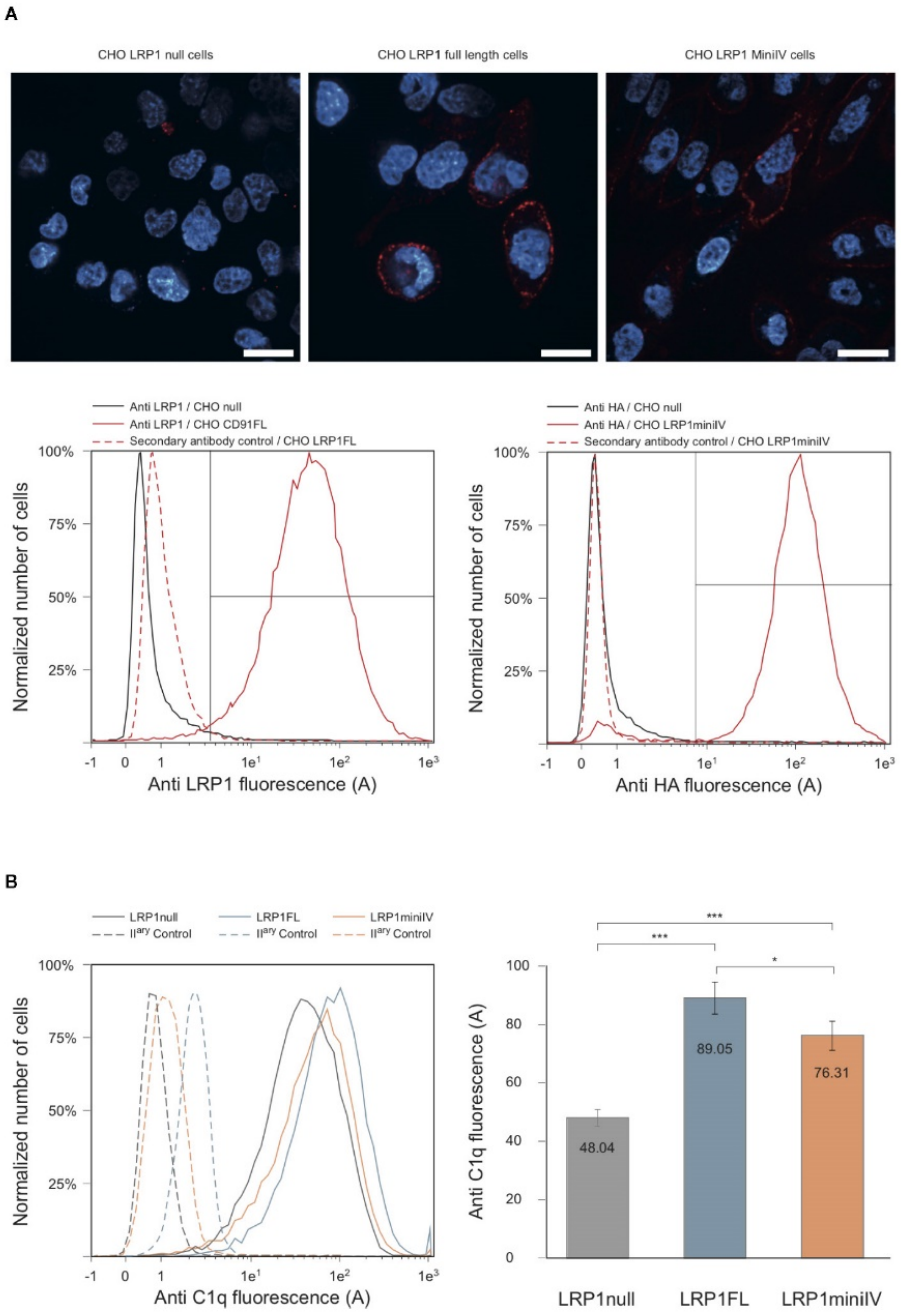

FIGURE 8 | C1q interacts with full-length LRP1 and mini IV at the surface of transfected CHO cells. **(A)** Antibody labeling of LRP1-null CHO cells and CHO cells transfected with full-length LRP1 or mini IV. Top panels, confocal sectioning of LRP1-null, full-length LRP1 and mini IV (red) DAPI counterstained (blue) adherent CHO cells (bars = 20 µm). Bottom panels, histogram overlays of the corresponding cell populations analyzed by flow cytometry. Left, control LRP1-null cells (black) and LRP1 full-length transfected CHO cells (red) labeled with anti LRP1 antibody. Right panel, control LRP1-null CHO cells (black) and mini IV transfected CHO cells (red) labeled with anti HA antibody. Red dotted histograms correspond to secondary antibodies controls. The region for positive cells is shown (brackets) and represents more than 95% of the total cell population. **(B)** Flow cytometric histograms of a typical C1q decoration experiment. Plain lines correspond to C1q binding to LRP1-null cells (grey), full-length LRP1 (blue) and mini IV (red) CHO cells. Dashed lines are the corresponding controls with only secondary antibody only. Right panel, mean C1q fluorescence intensities (corrected from the controls) of six independent experiments. *** Student bilateral unpaired $<1 \times 10^{-4}$. * Student bilateral unpaired $>4 \times 10^{-2}$.

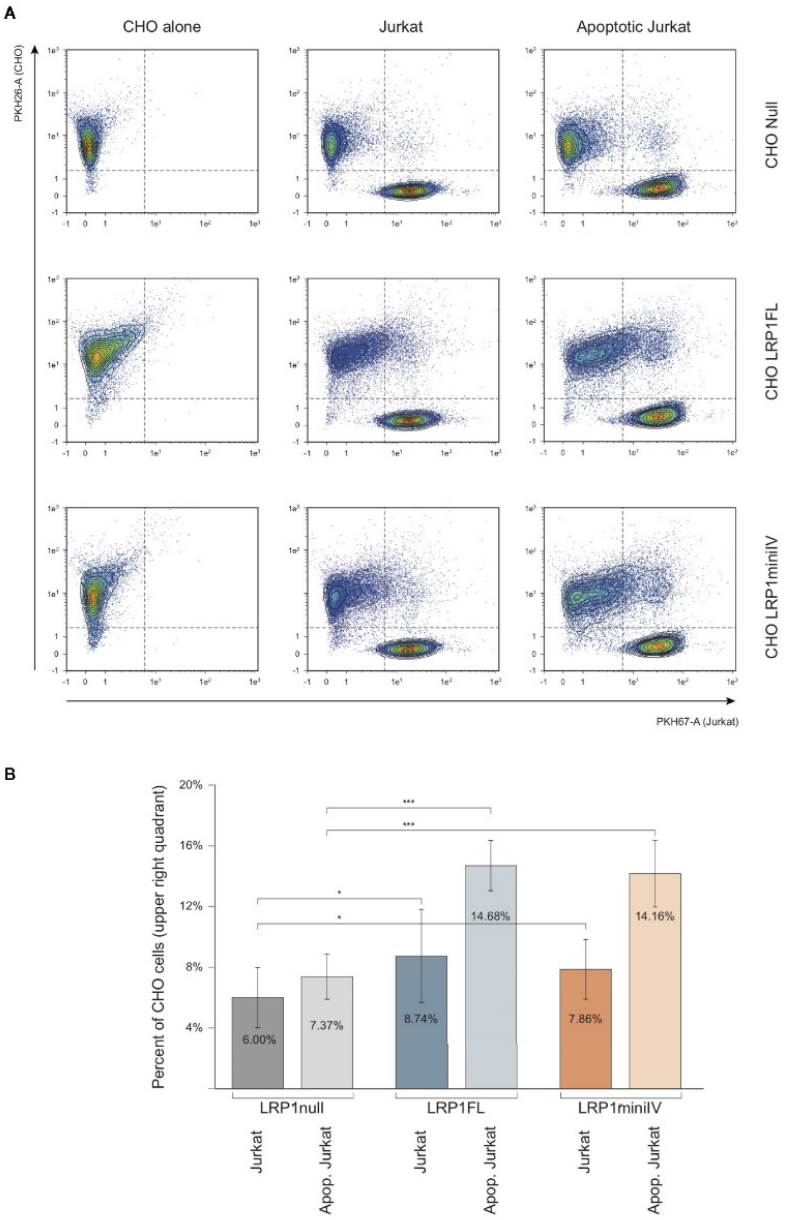

FIGURE 9 | Flow cytometry analysis of the interaction of Jurkat apoptotic cells with LRP1 full-length and mini IV CHO cells. **(A)** Dot plots of the analysis of PKH26 fluorescent CHO cells (red, Y4-A channel) decorated by PKH67 fluorescent Jurkat cells (green, B1-A channel). Decoration efficiency is calculated in the upper quadrant of the region drawn, as the percentage of PKH26 positive events **(B)** Histograms obtained from 13 independent experiments. Student T test relevance is shown above the histograms. *** Student bilateral unpaired $<1 \times 10^{-2}$, * Student bilateral unpaired $<2 \times 10^{-1}$.

DISCUSSION

In this study we demonstrate that the interaction of C1q with LRP1 is involving clusters II and cluster IV, two regions that have been described as interacting with most of LRP1 ligands (25, 27). This complements the study of Duus et al. (7) that proposed from competition experiments with diverse LRP1 ligands that clusters II and IV might be the regions recognized by C1q. We add here undoubtful confirmation, using soluble purified recombinant clusters, that the binding site for C1q is located on the CRs

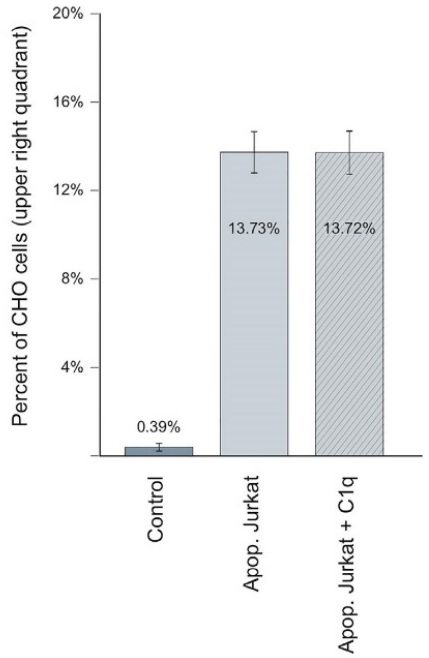

FIGURE 10 | C1q is not implicated in LRP1-dependent adsorption of Jurkat apoptotic cells Flow cytometry analysis of CHO cells stably expressing full-length LRP1, incubated with apoptotic Jurkat cells in the presence (dashed) or absence (plain) of C1q. Histograms representing the percentage of CHO-associated Jurkat cells from 4 independent experiments.

modular region of both clusters II and IV and that this interaction is in the same range of affinity although slightly higher for cluster IV than cluster II (around two to five fold). RAP, used as a tool to validate the functional integrity of the recombinant clusters and for competition for C1q binding to LRP1 *in vitro*, was found to compete very efficiently for the interaction of C1q with the LRP1 clusters. Indeed, an equimolar amount of RAP was sufficient to completely inhibit C1q binding to both clusters. This therefore revealed that, as also observed for other LRP1 ligands, the C1q interaction site might be located on both clusters at the same sites as RAP or involve overlapping sites (25, 27). On C1q side, our CLR and GR fragments binding experiments indicated that the interaction with LRP1 mobilizes mainly the collagen stalks and is involving sites that are buried by the C1r2s2 tetramer binding. Even though C1r2s2 competes with LRP1 for C1q binding in SPR conditions for which LRP1 clusters are immobilized, no LRP1 competition for C1 activation could be observed in a C1q reconstituted serum assay (**Figure S3**). This observation is probably not reflecting what would happen at the cell surface. Indeed, in our complement activation experimental conditions, the competition could only be done with soluble C1q and LRP1 clusters, which is not a typical physiological context. Moreover, the affinity of the C1r2s2 interaction with C1q is stronger than the one of soluble LRP1 clusters which is in favor of the C1 formation in this experimental setting [**Table 2**, (16)].

A common feature of most of LDL-receptors ligands is their ability to bind to heparin, suggesting the implication of one or more highly positively charged regions in the recognition of the receptor. Indeed, a "Lysine ligand mode" of interaction with tandem CR modules has been described for the binding of LRP1 with its ligands, such as RAP (30), α2Macroglobulin (31), ApoE (32), and factor VIII (33). These interactions are calcium dependent and salt sensitive. LRP1 binding to C1q is inhibited by high salt concentration (0.65 M NaCl) (7) which suggests that it is driven by electrostatic interactions. We also verified that the interaction of C1q with LRP1 clusters II and IV is inhibited by 5 mM EDTA, as expected (*data not shown*). Since C1r2s2 binding to C1q involves ionic, calcium-dependent interactions with C1q lysine residues, one could easily assume these lysines to serve as ligands for LRP1 clusters. To our surprise, a recombinant mutant of C1q lacking these specific lysines still retained its full-binding abilities for both clusters with an affinity in the same nanomolar range as for wild type C1q. These findings suggest that other basic residues in the surrounding could be potential candidates for LRP1 interaction. Contrarily to C1q, in the case of the interaction of LRP1 with MBL, Duus and collaborators observed that the K55 lysine that is implicated in the interaction with the MBL associated proteases MASPs is also responsible for the interaction with LRP1 (34). Moreover, this interaction might involve a single lysine since it is completely abolished by the point mutation K55A of the MBL. The same difference between C1q and MBL behavior was also highlighted in the case of CR1 receptor binding, that was still efficiently interacting with the rC1qABC mutant and no longer with the K55A mutant of the MBL (17, 20). To our knowledge, C1q binds sulfated proteoglycans through its GRs (35) and also even more efficiently through its CLRs (36–38). These studies also evidenced that sulfated proteoglycans inhibit the first step of complement activation by impairing the association of C1r and C1s with C1q. Moreover, through chemical modification using TNBS (2,4,6 trinitrobenzenesulfonate), lysine residues on C1q CLR were shown to be involved in the interaction with fucoidan (39). All together these findings suggest an interaction site on C1q CLR for proteoglycans that could be shared also for LRP1 interaction and that is located nearby the C1r2s2 site. The basic residues in C1q collagen stalks are shown on the model of **Figure 11**. Most of the lysines are modified by O-glycosylation (40), except a proximal lysine 65 of the B C1q chain (K_B65), 15 Å distal to the lysine 61 (K_B61) that is crucial for C1r2s2 binding (16). This K_B65 could be a good candidate for LRP1 interaction. Most of LRP1 ligands have been shown to involve the docking of two or more lysine residues into the acidic pocket of CR modules, which raises the question of a second (or more) basic residue(s) in the interaction of C1q. One possibility could be the interaction with R_C51 which is 56 Å far away from K_B65, on the same molecular face, which remains in the possible range of reported distances between CR acidic pockets (11, 32, 41). Of note even though most of LRP1 ligands involve lysines for interaction with the receptor, arginine can be a possible basic partner of CR module interaction (42). The interaction of LRP1 clusters with C1q at this K_B65 position does not exclude that in the absence

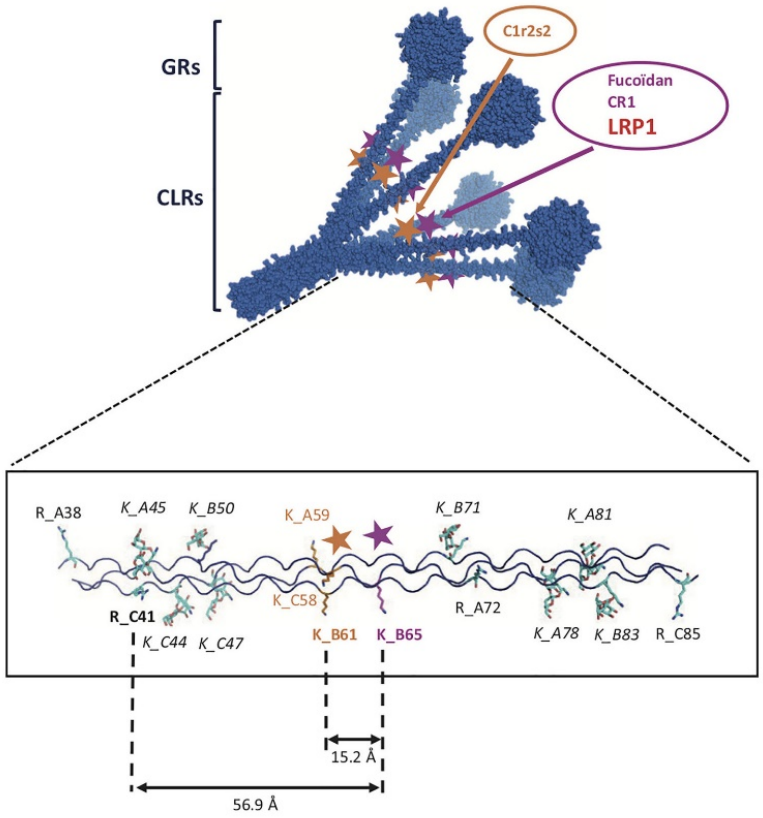

FIGURE 11 | Detailed model of C1q CLRs interaction sites. Upper part: 3-D model of C1q representing a bouquet-like scaffold formed by 6 collagen stalks (CLRs) expending into 6 globular regions (GRs). The two interaction sites for C1r2s2 and for CLR ligands such as LRP1, fucoidan and CR1 are indicated by orange and pink stars, respectively. Bottom part: detailed localization of basic amino acids on one C1q CLR. Lysines or arginines are labeled by R or K letters, followed by the name of the C1q chain, A, B or C and amino acid position. Italics are indicating glycosylated lysines. Bold characters represent residues potentially involved in the binding of LRP1.

of C1r2s2, C1q could interact synergically with both K_B65 and K_B61 and behave differently in our C1q mutant involving other residues, as it was described for RAP multiple lysine mutants (43). It is also not excluded that the single lysine K_B65 could be the only actor of the interaction as it is the case for the K55 of the MBL (34). Taken together our results on LRP1 and similar results obtained in our team for another C1q receptor, CR1 (17), lead us to propose a common site on C1q CLR for receptor interaction involving basic residues distinct but close to the C1r2s2 site.

The comparable affinity of LRP1 ligands for cluster II and IV binding is explained in some studies by a cluster replication that is specific to LRP1. LRP1 is the largest receptor of the LDL-receptor family with multiple biological functions. Since LRP1 such as C1q is a highly flexible protein that interacts with a wide variety of structurally unrelated ligands, in a multivalent manner, it is difficult to imagine a simple model for C1q interaction. Nevertheless, if C1q, like many other ligands, shares affinities for clusters II and IV, it is not evidenced in our study that they interact on both clusters synergically. This might be difficult if we consider that the potential residues for LRP1 interaction are oriented towards the center of the C1q cone (**Figure 11**). Some LRP1 ligands have been described to interact better with cluster IV than with cluster II which is also what we observe in our study (33, 44). From that observation, one could hypothesize that the LRP1 ligands bind first to the cluster that is more distant from the membrane (cluster II) and then interact with cluster IV. Interestingly, MBL and L-ficolin were found to interact with LRP1 (34) and we also localized the interaction site for MBL on cluster II and IV as it is the case for C1q (*data not shown*). Taken all together these data could indicate that the interaction mode of LRP1 could be enlarged to other members of the defense collagen family.

We then aimed at confirming that C1q interaction was also happening at the cell surface using a simple non-phagocytic cellular model. For that purpose, LRP1-null cells were

transfected with DNA coding for full-length LRP1 and a mini receptor IV that was chosen preferentially because of its natural location close to the membrane. Our results show that C1q interacts indeed with both LRP1 and minireceptor IV and that the interaction of mini IV receptor is nearly as important as that of full-length LRP1 (85% of the binding compared to LRP1). These results also suggest that other sites might contribute (but to a lesser extent) to LRP1 binding to C1q that could possibly be located on cluster II, the second site identified by our *in vitro* experiments. Since C1q and LRP1 were reported to be important in efferocytosis (1) we naturally addressed the question of apoptotic cells interaction with LRP1 and the implication of C1q in their initial recognition step. Our results indicate that LRP1 full-length and LRP1 mini IV are involved in late apoptotic cells binding in the absence of C1q, with a 100% increase compared to LRP1-null cells. The interaction is increased in the same proportions for full-length and mini IV LRP1 indicating that the binding capacity of the whole LRP1 molecule for late apoptotic cells could be fully endorsed by cluster IV. No LRP1 dependent difference could be observed on the binding of early apoptotic cells (*data not shown*).

The implication of C1q in the removal of apoptotic cells through binding to LRP1 is controversial. While Ogden and Vanvidier et al. (4, 5) observed that a ternary complex including C1q/LRP1 and CRT participates in the phagocytosis of apoptotic cells, Lillis et al. (45) found that the apoptosis enhancement by C1q is independent of LRP1 uptake of apoptotic cells and clearance. In our cell surface model, we focused on the first step of this removing process by looking at the role of C1q in LRP1 adsorption of apoptotic cells and could show that C1q has no enhancing effect on that binding. This observation tends to validate the data of Lillis and collaborators and implies that C1q binding to LRP1 might have another biological role than that of a bridging molecule in a C1q/LRP1/CRT complex.

Overall our data indicate that similarly to many other LRP1 ligands, C1q binds to both clusters II and IV. The site responsible for LRP1 binding on C1q is located on its CLR, nearby the interaction site of the cognate protease tetramer C1r2s2. We propose a common canonical site for other C1q receptors and ligands, such as fucoidan and CR1. From a functional point of view, we show that C1q binds to both full-length and mini IV LRP1 receptors but that the first step of the uptake of late apoptotic cells by LRP1 is not influenced by C1q. Our results also highlight that cluster IV receptor can endorse most of LRP1 full-length binding capacities.

DATA AVAILABILITY STATEMENT

The datasets generated for this study are available on request to the corresponding authors.

AUTHOR CONTRIBUTIONS

JPK, VR, and NT designed the study. GF, EG, CW-P, IB, AC, JPK, and VR performed the research. GF, EG, CW-P, IB, JPK, VR, and NT analyzed the data. CDN and SD contributed key reagents. CG contributed to discussions and structural implements. VR, JPK, EG, and NT wrote the manuscript draft. All authors contributed to the article and approved the submitted version.

FUNDING

This work has been supported by the French National Research Agency (grant ANR-16-CE11-0019) and by the University Grenoble Alpes (grant AGIR). This work used the platforms of the Grenoble Instruct-ERIC Center (ISBG; UMS 3518 CNRS CEA-UGA-EMBL) with support from the French Infrastructure for Integrated Structural Biology (FRISBI; ANR-10-INSB-05-02) and GRAL, a project of the University Grenoble Alpes graduate school (Ecoles Universitaires de Recherche) CBH-EUR-GS (ANR-17-EURE-0003) within the Grenoble Partnership for Structural Biology.

ACKNOWLEDGMENTS

We thank Jean-Baptiste Reiser for access to the SPR platform, Luca Signor for mass spectrometry analyses, Rose-Laure Revel-Goyet and Françoise Lacroix for the support and access to the M4D Cell imaging Platform. We thank Pascale Tacnet-Delorme and Philippe Frachet for scientific discussions and technical advices. IBS acknowledges integration into the Interdisciplinary Research Institute of Grenoble (IRIG, CEA).

SUPPLEMENTARY MATERIAL

The Supplementary Material for this article can be found online at: https://www.frontiersin.org/articles/10.3389/fimmu.2020.583754/full#supplementary-material

REFERENCES

1. Galvan MD, Greenlee-Wacker MC, Bohlson SS. C1q and phagocytosis: the perfect complement to a good meal. *J Leukoc Biol* (2012) 92:489–97. doi: 10.1189/jlb.0212099
2. Kouser L, Madhukaran SP, Shastri A, Saraon A, Ferluga J, Al-Mozaini M, et al. Emerging and Novel Functions of Complement Protein C1q. *Front Immunol* (2015) 6:317. doi: 10.3389/fimmu.2015.00317
3. Thielens NM, Tedesco F, Bohlson SS, Gaboriaud C, Tenner AJ. C1q: A fresh look upon an old molecule. *Mol Immunol* (2017) 89:73–83. doi: 10.1016/j.molimm.2017.05.025
4. Ogden CA, deCathelineau A, Hoffmann PR, Bratton D, Ghebrehiwet B, Fadok VA, et al. C1q and Mannose Binding Lectin Engagement of Cell Surface Calreticulin and Cd91 Initiates Macropinocytosis and Uptake of Apoptotic Cells. *J Exp Med* (2001) 194:781–96. doi: 10.1084/jem.194.6.781
5. Vandivier RW, Ogden CA, Fadok VA, Hoffmann PR, Brown KK, Botto M, et al. Role of Surfactant Proteins A, D, and C1q in the Clearance of Apoptotic Cells In Vivo and In Vitro: Calreticulin and CD91 as a Common Collectin Receptor Complex. *J Immunol* (2002) 169:3978–86. doi: 10.4049/jimmunol.169.7.3978
6. Lillis AP, Van Duyn LB, Murphy-Ullrich JE, Strickland DK. LDL Receptor-Related Protein 1: Unique Tissue-Specific Functions Revealed by Selective

Gene Knockout Studies. *Physiol Rev* (2008) 88:887–918. doi: 10.1152/physrev.00033.2007

7. Duus K, Hansen EW, Tacnet P, Frachet P, Arlaud GJ, Thielens NM, et al. Direct interaction between CD91 and C1q: Direct interaction between CD91 and C1q. *FEBS J* (2010) 277:3526–37. doi: 10.1111/j.1742-4658.2010.07762.x
8. Strickland DK, Ranganathan S. Diverse role of LDL receptor-related protein in the clearance of proteases and in signaling. *J Thromb Haemost* (2003) 1:1663–70. doi: 10.1046/j.1538-7836.2003.00330.x
9. Croy JE, Shin WD, Knauer MF, Knauer DJ, Komives EA. All Three LDL Receptor Homology Regions of the LDL Receptor-Related Protein Bind Multiple Ligands †. *Biochemistry* (2003) 42:13049–57. doi: 10.1021/bi034752s
10. Bu G, Rennke S. Receptor-associated protein is a folding chaperone for low density lipoprotein receptor-related protein. *J Biol Chem* (1996) 271:22218–24. doi: 10.1074/jbc.271.36.22218
11. Fisher C, Beglova N, Blacklow SC. Structure of an LDLR-RAP Complex Reveals a General Mode for Ligand Recognition by Lipoprotein Receptors. *Mol Cell* (2006) 22:277–83. doi: 10.1016/j.molcel.2006.02.021
12. Arlaud GJ, Sim RB, Duplaa AM, Colomb MG. Differential elution of Clq, Clr and Cls from human Cl bound to immune aggregates. Use in the rapid purification of Cl subcomponents. *Mol Immunol* (1979) 16:445–50. doi: 10.1016/0161-5890(79)90069-5
13. Tacnet-Delorme P, Chevallier S, Arlaud GJ. -Amyloid Fibrils Activate the C1 Complex of Complement Under Physiological Conditions: Evidence for a Binding Site for A on the C1q Globular Regions. *J Immunol* (2001) 167:6374–81. doi: 10.4049/jimmunol.167.11.6374
14. Bally I, Inforzato A, Dalonneau F, Stravalaci M, Bottazzi B, Gaboriaud C, et al. Interaction of C1q With Pentraxin 3 and IgM Revisited: Mutational Studies With Recombinant C1q Variants. *Front Immunol* (2019) 10:461. doi: 10.3389/fimmu.2019.00461
15. De Nardis C, Lössl P, van den Biggelaar M, Madoori PK, Leloup N, Mertens K, et al. Recombinant Expression of the Full-length Ectodomain of LDL Receptor-related Protein 1 (LRP1) Unravels pH-dependent Conformational Changes and the Stoichiometry of Binding with Receptor-associated Protein (RAP). *J Biol Chem* (2016) 292(3):912–24. doi: 10.1074/jbc.M116.758862. jbc.M116.758862.
16. Bally I, Ancelet S, Moriscot C, Gonnet F, Mantovani A, Daniel R, et al. Expression of recombinant human complement C1q allows identification of the C1r/C1s-binding sites. *Proc Natl Acad Sci* (2013) 110:8650–5. doi: 10.1073/pnas.1304894110
17. Jacquet M, Cioci G, Fouet G, Bally I, Thielens NM, Gaboriaud C, et al. C1q and Mannose-Binding Lectin Interact with CR1 in the Same Region on CCP24-25 Modules. *Front Immunol* (2018) 9:453. doi: 10.3389/fimmu.2018.00453
18. Arlaud GJ, Thielens NM. Human complement serine proteases C1r and C1s and their proenzymes. *Methods Enzymol* (1993) 223:61–82. doi: 10.1016/0076-6879(93)23038-o
19. Obermoeller-McCormick LM, Li Y, Osaka H, FitzGerald DJ, Schwartz AL, Bu G. Dissection of receptor folding and ligand-binding property with functional minireceptors of LDL receptor-related protein. *J Cell Sci* (2001) 114:899–908.
20. Jacquet M, Lacroix M, Ancelet S, Gout E, Gaboriaud C, Thielens NM, et al. Deciphering Complement Receptor Type 1 Interactions with Recognition Proteins of the Lectin Complement Pathway. *J Immunol* (2013) 190:3721–31. doi: 10.4049/jimmunol.1202451
21. FitzGerald DJ, Fryling CM, Zdanovsky A, Saelinger CB, Kounnas M, Winkles JA, et al. Pseudomonas Exotoxin-mediated Selection Yields Cells with Altered Expression of Low-Density Lipoprotein Receptor-related Protein.9. *J Biol Chem* (1995) 129(6):1533–41. doi: 10.1083/jcb.129.6.1533
22. Bu G, Williams S, Strickland DK, Schwartz AL. Low density lipoprotein receptor-related protein/alpha 2-macroglobulin receptor is an hepatic receptor for tissue-type plasminogen activator. *Proc Natl Acad Sci U S A* (1992) 89:7427–31. doi: 10.1073/pnas.89.16.7427
23. Williams SE, Ashcom JD, Argraves WS, Strickland DK. A novel mechanism for controlling the activity of alpha 2-macroglobulin receptor/low density lipoprotein receptor-related protein. Multiple regulatory sites for 39-kDa receptor-associated protein. *J Biol Chem* (1992) 267:9035–40.
24. Horn IR, van den Berg BM, van der Meijden PZ, Pannekoek H, van Zonneveld A-J. Molecular Analysis of Ligand Binding to the Second Cluster of Complement-type Repeats of the Low Density Lipoprotein Receptor-related Protein Evidence for an allosteric component in receptor-associated protein-mediated inhibition of ligand binding. *J Biol Chem* (1997) 272:13608–13. doi: 10.1074/jbc.272.21.13608
25. Neels JG, van den Berg BM, Lookene A, Olivecrona G, Pannekoek H, van Zonneveld A-J. The second and fourth cluster of class A cysteine-rich repeats of the low density lipoprotein receptor-related protein share ligand-binding properties. *J Biol Chem* (1999) 274:31305–11. doi: 10.1074/jbc.274.44.31305
26. Sarafanov AG, Makogonenko EM, Andersen OM, Mikhailenko IA, Ananyeva NM, Khrenov AV, et al. Localization of the low-density lipoprotein receptor-related protein regions involved in binding to the A2 domain of coagulation factor VIII. *Thromb Haemost* (2007) 98:1170–81. doi: 10.1160/TH07-05-0353
27. Willnow TE, Orth K, Herz J. Molecular dissection of ligand binding sites on the low density lipoprotein receptor-related protein. *J Biol Chem* (1994) 269:15827–32.
28. Moestrup SK, Holtet TL, Etzerodt M, Thøgersen HC, Nykjaer A, Andreasen PA, et al. Alpha 2-macroglobulin-proteinase complexes, plasminogen activator inhibitor type-1-plasminogen activator complexes, and receptor-associated protein bind to a region of the alpha 2-macroglobulin receptor containing a cluster of eight complement-type repeats. *J Biol Chem* (1993) 268:13691–6.
29. Downey GP, Botelho RJ, Butler JR, Moltyaner Y, Chien P, Schreiber AD, et al. Phagosomal Maturation, Acidification, and Inhibition of Bacterial Growth in Nonphagocytic Cells Transfected with FcgRIIA Receptors.10. *J Biol Chem* (1999) 274:28436–44. doi: 10.1074/jbc.274.40.28436
30. Migliorini MM, Behre EH, Brew S, Ingham KC, Strickland DK. Allosteric Modulation of Ligand Binding to Low Density Lipoprotein Receptor-related Protein by the Receptor-associated Protein Requires Critical Lysine Residues within Its Carboxyl-terminal Domain. *J Biol Chem* (2003) 278:17986–92. doi: 10.1074/jbc.M212592200
31. Nielsen KL, Holtet TL, Etzerodt M, Moestrup SK, Gliemann J, Sottrup-Jensen L, et al. Identification of Residues in α-Macroglobulins Important for Binding to the α_2 -Macroglobulin Receptor/Low Density Lipoprotein Receptor-related Protein. *J Biol Chem* (1996) 271:12909–12. doi: 10.1074/jbc.271.22.12909
32. Guttman M, Prieto JH, Handel TM, Domaille PJ, Komives EA. Structure of the Minimal Interface Between ApoE and LRP. *J Mol Biol* (2010) 398:306–19. doi: 10.1016/j.jmb.2010.03.022
33. Young PA, Migliorini M, Strickland DK. Evidence That Factor VIII Forms a Bivalent Complex with the Low Density Lipoprotein (LDL) Receptor-related Protein 1 (LRP1):Identification of Cluster IV on LRP1 as the major binding site. *J Biol Chem* (2016) 291:26035–44. doi: 10.1074/jbc.M116.754622
34. Duus K, Thielens NM, Lacroix M, Tacnet P, Frachet P, Holmskov U, et al. CD91 interacts with mannan-binding lectin (MBL) through the MBL-associated serine protease-binding site: CD91 interacts with mannan-binding lectin. *FEBS J* (2010) 277:4956–64. doi: 10.1111/j.1742-4658.2010.07901.x
35. Garlatti V, Chouquet A, Lunardi T, Vives R, Paidassi H, Lortat-Jacob H, et al. Cutting Edge: C1q Binds Deoxyribose and Heparan Sulfate through Neighboring Sites of Its Recognition Domain. *J Immunol* (2010) 185:808–12. doi: 10.4049/jimmunol.1000184
36. Almeda S, Rosenberg RD, Bing DH. The binding properties of human complement component C1q. Interaction with mucopolysaccharides. *J Biol Chem* (1983) 258:785–91.
37. Kirschfink M, Blase L, Engelmann S, Schwartz-Albiez R. Secreted chondroitin sulfate proteoglycan of human B cell lines binds to the complement protein C1q and inhibits complex formation of C1. *J Immunol* (1997) 158:1324–31.
38. Tissot B, Daniel R, Place C. Interaction of the C1 complex of Complement with sulfated polysaccharide and DNA probed by single molecule fluorescence microscopy. *Eur J Biochem* (2003) 270:4714–20. doi: 10.1046/j.1432-1033.2003.03870.x
39. Tissot B, Montdargent B, Chevolot L, Varenne A, Descroix S, Gareil P, et al. Interaction of fucoidan with the proteins of the complement classical pathway. *Biochim Biophys Acta BBA - Proteins Proteomics* (2003) 1651:5–16. doi: 10.1016/S1570-9639(03)00230-9
40. Pflieger D, Przybylski C, Gonnet F, Le Caer JP, Lunardi T, Arlaud GJ, et al. Analysis of Human C1q by Combined Bottom-up and Top-down Mass Spectrometry: detailed mapping of post-translational modifications and insights into C1r/C1s binding sites. *Mol Cell Proteomics* (2010) 9:593–610. doi: 10.1074/mcp.M900350-MCP200
41. Jensen GA, Andersen OM, Bonvin AMJJ, Bjerrum-Bohr I, Etzerodt M, Thøgersen HC, et al. Binding Site Structure of One LRP–RAP Complex:

Implications for a Common Ligand–Receptor Binding Motif. *J Mol Biol* (2006) 362:700–16. doi: 10.1016/j.jmb.2006.07.013

42. Nikolic J, Belot L, Raux H, Legrand P, Gaudin Y, A. Albertini A. Structural basis for the recognition of LDL-receptor family members by VSV glycoprotein. *Nat Commun* (2018) 9:1029. doi: 10.1038/s41467-018-03432-4
43. Dolmer K, Campos A, Gettins PGW. Quantitative Dissection of the Binding Contributions of Ligand Lysines of the Receptor-associated Protein (RAP) to the Low Density Lipoprotein Receptor-related Protein (LRP1). *J Biol Chem* (2013) 288:24081–90. doi: 10.1074/jbc.M113.473728
44. Migliorini M, Li S-H, Zhou A, Emal CD, Lawrence DA, Strickland DK. High-affinity binding of plasminogen-activator inhibitor 1 complexes to LDL receptor-related protein 1 requires lysines 80, 88, and 207. *J Biol Chem* (2020) 295:212–22. doi: 10.1074/jbc.RA119.010449
45. Lillis AP, Greenlee MC, Mikhailenko I, Pizzo SV, Tenner AJ, Strickland DK, et al. Murine Low-Density Lipoprotein Receptor-Related Protein 1 (LRP) Is Required for Phagocytosis of Targets Bearing LRP Ligands but Is Not Required for C1q-Triggered Enhancement of Phagocytosis. *J Immunol* (2008) 181:364–73. doi: 10.4049/jimmunol.181.1.364

Conflict of Interest: The authors declare that the research was conducted in the absence of any commercial or financial relationships that could be construed as a potential conflict of interest.

Supplementary Material

Complement C1q interacts with LRP1 clusters II and IV through a site close but different from the binding site of its C1r and C1s associated proteases

Guillaume Fouët[1†], Evelyne Gout[1†], Catherine Wicker-Planquart[1], Isabelle Bally[1], Camilla de Nardis[2], Stéphane Dedieu[3], Anne Chouquet[1], Christine Gaboriaud[1], Nicole M. Thielens[1], Jean Philippe Kleman[1*], Véronique Rossi[1*].

***Correspondence:**
Corresponding Authors
veronique.rossi@ibs.fr; jean-philippe.kleman@ibs.fr

Supplementary Figures S1, S3 and S3

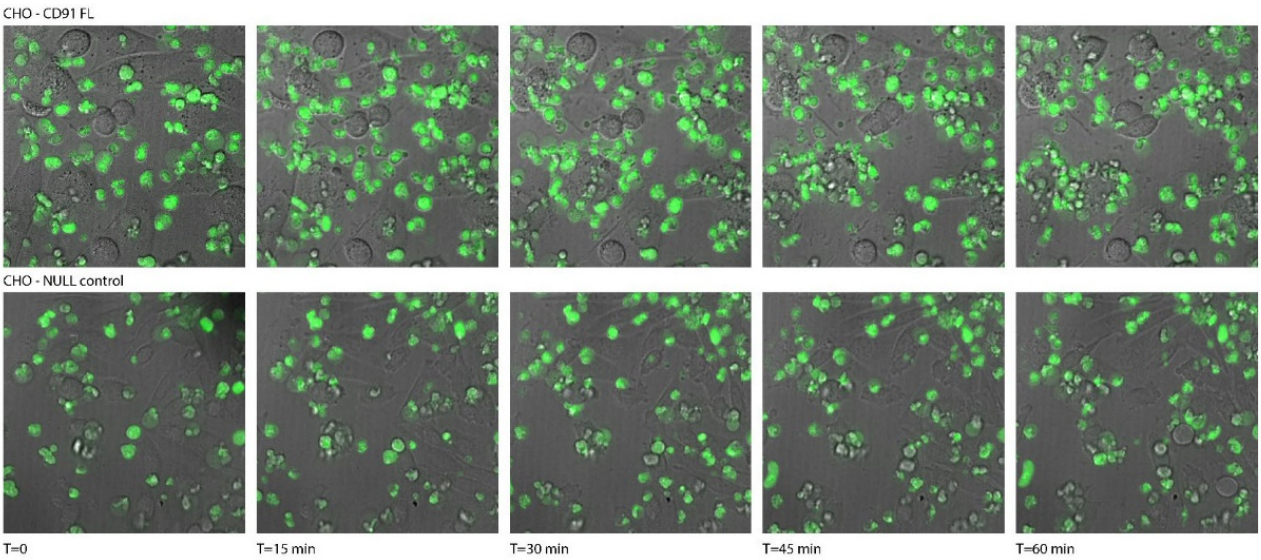

Supplementary S1 – Time Lapse Immunofluorescence analysis of the interaction of apoptotic Jurkat cells with CHO expressing full-length LRP1

Control NULL and LRP1 FL CHO cells were plated in 35mm glass bottom dishes the day before analysis. Labeled apoptotic cells (green fluorescence) were added in the medium over the spread CHO cells (visible in the transmission light channel, gray) and subsequently imaged every 3 minutes using spinning disk confocal microscopy, maintaining the 488 excitation laser at a minimal value of 1% of its nominal power. The figure (1 timepoint shown every 15 min) illustrates the typical redistribution of the apoptotic cells around the CHO LRP1 FL cells but not around control NULL cells.

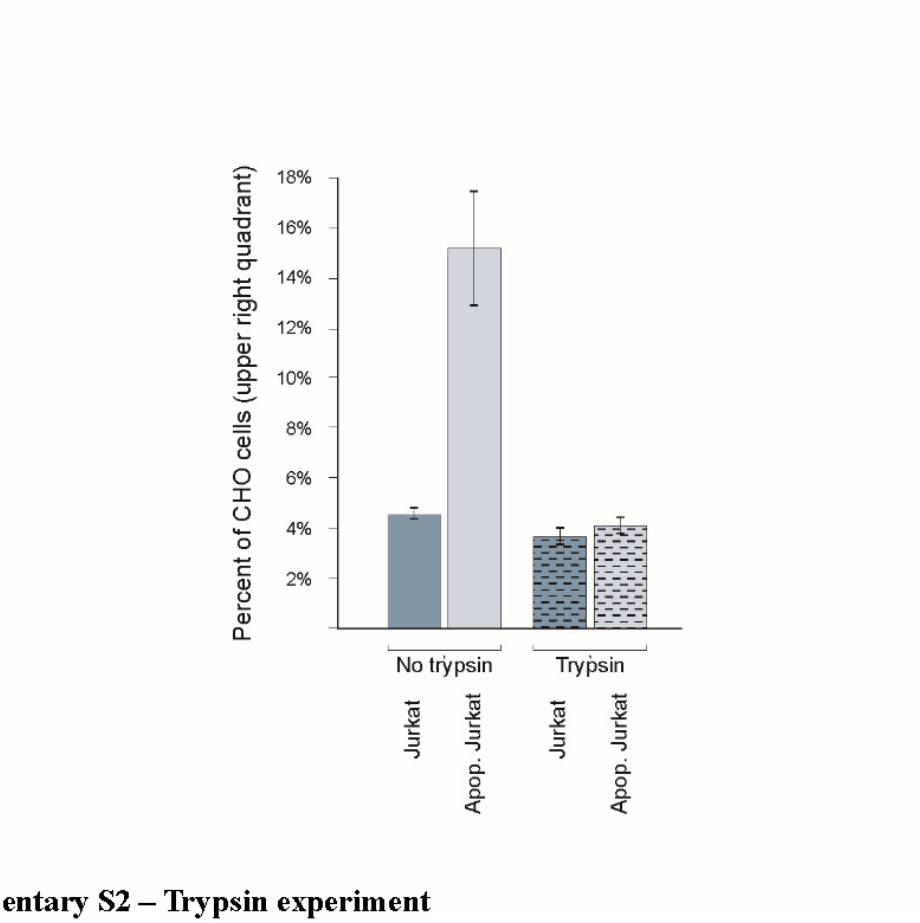

Supplementary S2 – Trypsin experiment

Flow cytometry analysis after trypsin treatment of CHO cells in contact with healthy or apoptotic Jurkat cells. CHO cells expressing full-length LRP1 were incubated with Jurkat cells before being harvested and post-treated by trypsin.

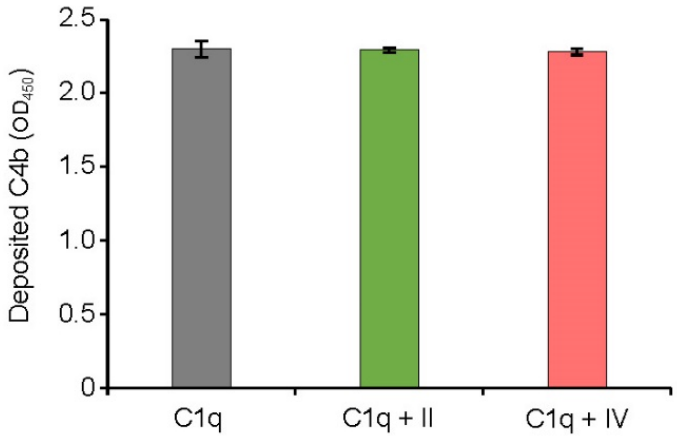

Supplementary S3 – Complement activation in the presence of LRP1 clusters II and IV

C1q-depleted serum (CompTech, 1:25 dilution) was reconstituted with purified serum C1q (4 µg/mL) or C1q (4 µg/mL) that had been preincubated 15 min at room temperature with cluster II or IV at a 100-fold molar excess. This mixture was added to microwells coated with 2 µg/mL IgM. The resulting C1-cleaving activity was measured by C4b deposition assay as described in (14). Deposited C4b was detected with an anti-human polyclonal antibody, and results are expressed as absorbance at 450 nm (OD_{450}), following background subtraction [mean ± SEM of two and three independent experiments for cluster II and IV respectively]. Normal human serum was used as a positive control (OD_{450} = 2.32 ± 0.03).

DISCUSSION & PERSPECTIVES

I. LAIR-1 and GPVI homologs share a common collagen backbone recognition mechanism

During this PhD thesis, we were interested in the deciphering of the immune Ig-like receptors (RAGE, CD33, LAIR-1 and LAIR-2) interaction with the defense collagen C1q. Due to limitations inherent to the protein production, we mainly focused on the receptor LAIR-1 for which we managed to produce a soluble form of the extracellular Ig-like domain. As expected, we showed that LAIR-1 Ig-like domain specifically interacts with the C1q CLR with the essential contribution of LAIR-1 R59 and E61 residues. These residues have already been described for their critical role for membrane LAIR-1 interaction with collagens I, III and IV peptides (Brondijk et al. 2010a). Therefore, this suggests that LAIR-1 recognition of the C1q CLR collagen backbone shares some specificity with other collagens through its R59 and E61 residues. Interestingly, these two residues are conserved in GPVI, a collagen receptor homologous to LAIR-1 (Figure 13). Therefore, LAIR-1 and GPVI interaction with collagens might engage similar mechanisms. This hypothesis was first suggested by Tomlinson et al., who showed that LAIR-1 co expression with GPVI inhibits the collagen-induced GPVI signaling (Tomlinson et al. 2007). Unfortunately, there are no studies in the literature reporting the engagement of these two arginine and glutamate residues (R38 and E40, in GPVI sequence) in the GPVI interaction with collagen. However, a crystal structure of the GPVI Ig-like domain in complex with a collagen peptide has been deposited in the PDB in 2017 with no associated publication (PDB code: 5OU8). This structure unambiguously demonstrates that the R38 and E40 residues of GPVI are critical for collagen recognition with a central position at the interaction surface (Figures 14B and 22). As for GPVI, LAIR-1 interaction with collagen is dependent on the presence of hydroxyproline residues. Consistently, R38 and E40 residues in the GPVI/collagen crystal structure mainly interact with hydroxyproline residues and, extended to LAIR-1 by homology, this strongly suggests that LAIR-1 R59 and E61 residues recognize hydroxyproline residues (Figure 22). Based on that assumption, we identified putative LAIR-1 binding motifs on C1q and, thanks to additional data from our experiments, we proposed a model for LAIR-1 interaction with a C1q collagen stem (Article 2). This model allowed us to identify LAIR-1 residues involved in the specific recognition of C1q collagen chains. This highlights that the interaction of C1q with LAIR-1 isn't just based on generic collagen backbone recognition, but is more specific with the accurate recognition of C1q CLR amino acids by LAIR-1 distal residues in addition to the central R59 and E61.

II. LAIR-1 dimerization and C1q interaction

We wanted to explore the question about the LAIR-1 dimerization associated to its signaling function, and more precisely in the context of its interaction with C1q. Indeed, LAIR-1 dimerization is required in order to trigger signal transduction and inhibitory responses. Generally, studies of receptors dimerization use Fc region fusion proteins and there are many examples in the literature of studies using soluble Fc-fused LAIR-1 Ig-like domains (Lebbink et al. 2006, 2009; Rygiel et al. 2011; Olde Nordkamp et al. 2014a; Agashe et al. 2018; Kumawat et al. 2019). The use of such fusion proteins could be delicate in the case of C1q interaction study because it is now well established that Fc regions of immunoglobulins are high affinity ligands for the C1q globular regions (Marqués et al. 1993; Ugurlar et al. 2018). Therefore, the use of Fc-fused proteins could likely introduce additional interaction properties independent of the LAIR-1 Ig-like domain. Based on available structural data, we managed to produce a dimeric variant of our LAIR-1 Ig-like domain construct by introducing an intermolecular disulfide bond instead of using Fc fusion (Results part, section III). First SPR experiments revealed that the S92C dimeric LAIR-1 variant interacts with higher affinity than wild-type LAIR-1 over immobilized C1q. Even if this result needs to be replicated, it indicates that we now have soluble LAIR-1 variants (exclusively monomeric or dimeric) to test the *in vitro* effects of LAIR-1 dimerization on C1q interaction.

Moreover, we used X-ray crystallography to solve the structure of LAIR-1 S92C dimer. This structure did not match with the one that we were expecting. Indeed, the two Ig-like domains were elongated in our crystal structure. We then performed SAXS experiments and showed that this covalently linked LAIR-1 dimeric variant displays a free rotation around the disulfide bond, likely introducing dynamic feature of the dimer in solution. These results support the idea that LAIR-1 dimerization on a cell surface should be induced by ligand interaction (Figure 30A).

In order to limit the free rotation of the two LAIR-1 Ig-like domains, CHO cells were transfected with full-length LAIR-1 containing the S92C mutation. Indeed, on the cell surface, the orientation of the C-terminal extremity of the Ig-like domain will also be constrained by the transmembrane domain, therefore possibly limiting the rotation around the disulfide bond (Figure 30B). This cellular aspect of the study is part of a collaboration with the team of Yves Delneste at the Centre de Recherche en Cancérologie et Immunologie Nantes Angers (CRCINA).

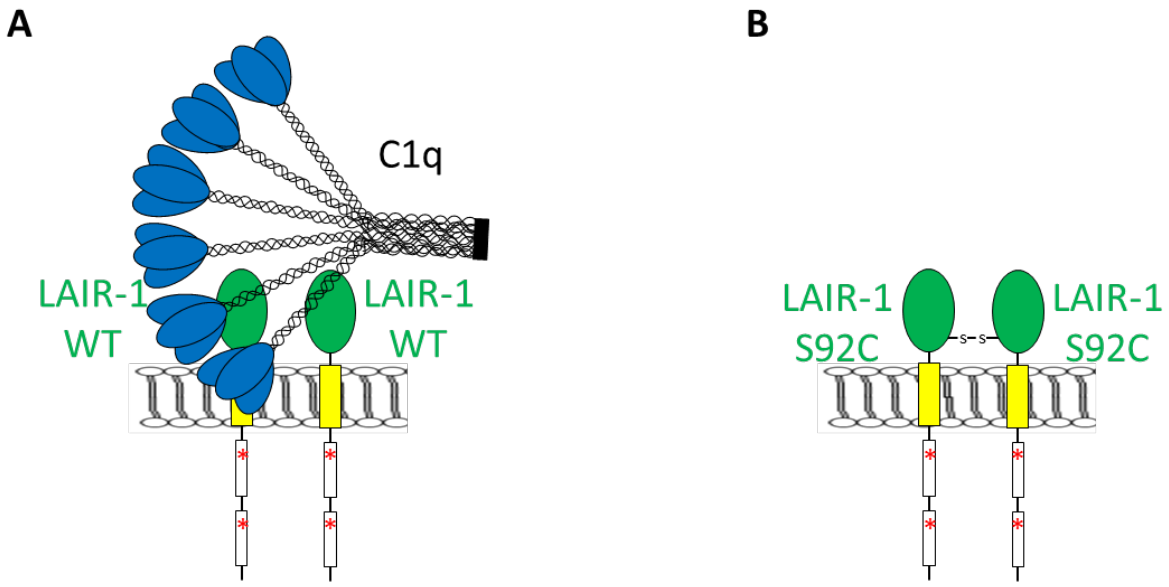

Figure 30: Schematic representation of LAIR-1 WT and S92C dimerization on cell surface. ***A****. LAIR-1 WT dimerization of the cell surface requires the binding of a ligand.* ***B****. LAIR-1 S92C dimer on the cell surface is blocked by the formation of the disulfide bond between the two monomers. The Ig-like domains are represented in green, the transmembrane domain in yellow and the intracellular ITIMs are represented with red asterisks. The disulfide bond between the two Ig-like domains of LAIR-1 S92C is shown in black.*

Furthermore, Olde Nordkamp and colleagues reported that the soluble Fc-fused Ig-like domain of LAIR-2 was able to efficiently inhibit both the classical and lectin complement pathways (Olde Nordkamp et al. 2014a). Therefore, it would be interesting to test if the dimeric LAIR-1 S92C Ig-like domain could also inhibit complement activation through the classical and lectin pathways.

III. CLR_nc2 fusion protein: a promising tool to investigate the functions associated to C1q collagen-like regions

In order to investigate the interaction of LAIR-1 with the collagen-like regions of C1q, we engineered the first recombinant C1q CLR (Article 1). The most delicate issue of the recombinant production of heterotrimeric C1q CLR is to preserve its specific trimerization and registering of the three different collagen chains. Indeed, this registering function is achieved by the C1q GR and their removal could result in random association of the C1q collagen chains. We fixed this issue by replacing the C1q GR by the second non-collagenous trimerization domain of collagen IX (nc2). Such substitution results in the production of a chimeric C1q called CLR_nc2 consisting in an N-terminal C1q collagen-like region with 6 C-terminal nc2 domains instead of the GR. We showed that the CLR_nc2 protein is well assembled and folded using different biochemical and biophysical methods and SPR experiments revealed that this chimeric “headless C1q” retains its functional interaction properties towards C1q CLR ligands.

We used this newly developed tool to investigate the interaction of LAIR-1 with the collagen-like region of C1q, especially by taking advantage of the recombinant production to introduce point mutations into the CLR sequence. Therefore, based on our model of LAIR-1 interaction with C1q, we produced two C1qCLR_nc2 variants comprising the mutation of R72 or K65 residues of C1q A and B chains into a glutamate. We tested these two variants for their interaction with C1q using SPR and showed that the C1q A_R72 and B_K65 are not essential for LAIR-1 binding but are likely involved in the specificity of the interaction.

Before use, the CLR_nc2 variants were tested for their interaction with $C1r_2s_2$ in order to check their functionality. Interestingly, one CLR_nc2 variant containing the mutation of lysine 65 on CLR B chain into a glutamate residue (B_K65E) exhibited a reduced binding capacity for $C1r_2s_2$ compared to the wild type (Appendix 3). Therefore, we unexpectedly revealed the importance of this particular residue, in the interaction with the $C1r_2s_2$ tetramer. This highlights the potential use of the CLR_nc2 protein to investigate C1q interaction with $C1r_2s_2$ and therefore may help in the understanding of complement classical pathway activation.

One additional interesting application of the newly generated CLR_nc2 protein lies in the development of an ELISA for detection of autoantibodies directed against C1q in patients suffering from autoimmune diseases. Indeed, the anti-C1q autoantibodies found in patients suffering from SLE are mainly directed against its collagen-like regions (Uwatoko et al. 1984, 1987). Moreover, the principal issue in the development of such ELISA development is the intrinsic ability of C1q to interact with the serum immune complexes present in patients with SLE, thus perturbating the detection process. Therefore, to prevent this nonspecific interaction, two solutions are reported in the literature: the use of high ionic strength (0.5-1 M NaCl) or the replacement of C1q by the CLR (Antes et al. 1988; Wener et al. 1989; Kohro-Kawata et al. 2002). However, the production of C1q CLR by enzymatic digestion is a hard and expensive process. Therefore, the recombinant CLR_nc2 protein provides an easier way to rapidly generate high quality antigen for ELISA purpose.

In addition, the CLR_nc2 protein could constitute an important tool to deconvolute the contribution of C1q functional regions (i.e., CLR and GR) in the interaction with its receptors. For example, we showed that CR1 and LRP1 interaction with C1q mostly involves its CLR but a contribution of the GR was also observed (Articles 3 and 4). This suggests that the possible shared sequence between the C1q CLR and GR fragments (Figure 19), could contain a binding site for these receptors or that secondary binding to C1q GR may take place. Therefore, the use

of the CLR_nc2 protein, for which the extremities can be user-defined, should unambiguously answer this question.

Aside from *in vitro* interaction studies the CLR_nc2 protein could be used in cellular investigations. In this context, we plan to study the effects of CLR_nc2 binding on the cytokines expression profile by macrophages. This work was initially proposed as a part of the collaboration with the team of Yves Delneste at the Centre de Recherche en Cancérologie et Immunologie Nantes Angers (CRCINA). Such analysis could provide insights into the contribution of the CLR in the C1q-mediated macrophage polarization.

Moreover, we generated a truncated fragment of the CLR_nc2 protein by deleting the N-terminal sequence corresponding to the collagen bundle until the hinge region of each C1q chain. This results in the generation of a single heterotrimeric collagen stem with a C-terminal nc2 domain. The interaction of LAIR-1 with this fragment was similar to the one with C1q, supporting the presence of the LAIR-1 binding site in the collagen cone.

Furthermore, this smaller fragment of the CLR_nc2 (C1qstem_nc2) was initially developed for structural studies purpose. The recombinant production of user-defined small heterotrimeric C1q CLR fragments will likely open the way towards the structural characterization of C1q interaction with its CLR ligands/receptors. For instance, a previous study reports the crystal structure of the CUB_1-EGF-CUB_2 domains of C1s in complex with a synthetic collagen peptide (Venkatraman Girija et al. 2013). In this study, the authors used a homotrimeric collagen peptide corresponding to a MBL-like sequence. The MBL and C1q sequences in the binding region of $C1r_2s_2$ and MASPs share similar amino acids and allowed the authors to extrapolate and discuss about C1s interaction with C1q. The C1qstem_nc2 fragment containing the “real” heterotrimeric collagen helix of C1q could be used to solve the structure of C1r and/or C1s in complex with a C1q CLR fragment. In the context of my PhD, and especially the investigation of LAIR-1 interaction with C1q, we performed crystallization trials of the C1qstem_nc2 alone and with the Ig-like domain of LAIR-1. We tested several conditions using the Classics Suite and PEGs I (Qiagen) screens available at the HTX lab platform of EMBL Grenoble. None of the tested conditions gave promising results with mostly clear drops. These unsuccessful trials could be explained by the certainly too long and too flexible C1qstem_nc2 protein. Indeed, the C1qstem_nc2 contains 16 Gly-X-Y collagen triplets in addition to the nc2 domain, which results in a quite long molecule certainly presenting intrinsic flexibility. Therefore, the collagen part should be reduced in size and optimized to help crystallization. For example, the structural study of Wallis laboratory used a 9-triplets long collagen peptide and the collagen I guest

fragment used for the nc2 domain crystal structure contains only 11 collagen triplets (Venkatraman Girija et al. 2013; Boudko and Bächinger 2016). Therefore, the C1qstem_nc2 protein needs to be shortened in order to have an optimal collagen triple helix size, containing the LAIR-1 binding site. In addition, the many post-translational modifications undergone by the collagen region constrains the use of eukaryotic expression systems (in our case, 293EXPI cells) to produce the C1qstem_nc2. Unfortunately, only weak purification yields have been obtained (around 300 µg per liter of cell culture). These low purification yields limited the crystallization assays and further expression/purification steps optimization would be required to improve the purification yields and try higher protein concentrations.

IV. The duality of C1q complement-dependent and independent functions

As mentioned above, the molecular dissection of C1q showed that LAIR-1 interaction with C1q exclusively involves its CLR. To more precisely identify the LAIR-1 binding site on the C1q CLR, we performed a competition assay with $C1r_2s_2$, the canonical C1q CLR ligand and showed that LAIR-1 is no more able to interact with C1q when it is associated with $C1r_2s_2$ in the C1 complex. This inhibitory effect of $C1r_2s_2$ on C1q recognition by LAIR-1 demonstrates that the LAIR-1 binding site is not located on the N-terminal collagen bundle of C1q as previously suggested (Liu et al. 2019) but in the collagen cone, close to the binding site of the $C1r_2s_2$ tetramer. The location of LAIR-1 binding site into the collagen cone of C1q instead of its N-terminal collagen bundle is somehow consistent with the better accessibility of the isolated collagen stems. Importantly, the C-terminal half of the C1q collagen stem of the cone is rich in basic residues that could constitute an environment prone to receptors binding. Moreover, we also reported the ability of $C1r_2s_2$ to prevent the binding of two C1q CLR receptors: CR1 and LRP1 (Articles 3 and 4). Interestingly, we showed that none of LAIR-1, CR1 or LRP1 binding to C1q involved the same binding site as $C1r_2s_2$, namely C1q A_K59, B_K61 and C_K58 residues (Bally et al. 2013). Exclusive interaction of C1q with the $C1r_2s_2$ tetramer or its CLR receptors highlights the intrinsic distinction of C1q CLR functions. On one hand, when associated with the $C1r_2s_2$ tetramer, C1q triggers pathogens and damage-self elimination through complement classical pathway activation. On the other hand, when C1q is devoid of its cognate proteases, it is able to interact with several membrane receptors through its collagen-like region (LAIR-1, CR1 and LRP1) and trigger complement-independent functions such as phagocytosis enhancement or immune response modulation.

This PhD thesis aimed at deciphering the molecular mechanisms underlying the immune tolerance and modulation functions of C1q, especially, through its interaction with the immune Ig-like receptor LAIR-1. We provided the first detailed investigation of C1q interaction with LAIR-1 Ig-like domain from a structural and molecular point of view. This work will contribute to the understanding of the C1q immune tolerogenic properties mediated through LAIR-1 interaction. However, it is important here to keep in mind that immune cells also possess receptors for the globular regions of C1q at their surface such as the two Ig-like receptors CD33 and RAGE that have distinct activities regarding inflammatory signals. Therefore, the characterization of C1q GR interaction with these receptors is needed in order to further decipher the mechanisms underlying C1q-mediated immune modulation.

APPENDICES

I. Appendix 1: Material and methods for protein expression

1 Molecular biology: Design of the expression vectors

The DNA coding the full-length sequences of human LAIR-1, LAIR-2 and CD33 were purchased from OriGene (product numbers RG206439, RC210108 and SC122608, respectively). The sequences of interest were amplified by polymerase chain reaction (PCR) using oligonucleotides designed in order to insert specific restriction enzymes cleavage sites for cloning purposes. When needed, additional polyhistidine tag (Histag) and a stop codon were also inserted at the 3'end.

1.1 Design of the pET28a vectors for expression of LAIR-1, LAIR-2 or CD33 in bacteria

The coding sequences of the Ig-like domain of LAIR-1 (22-122), LAIR-2 (22-122) and CD33 (142-232) (immature protein amino acids numbering for all constructs) were amplified using the oligonucleotides listed in Table 3. The oligonucleotides were designed in order to insert flanking *NcoI* and *XhoI* restriction sites at the 5' and 3' extremities, respectively. The pET28a vector (Novagen, product number 69864-3) contains a polyhistidine tag (6 His) followed by a stop codon, we therefore inserted a *XhoI* restriction site just after the coding sequence of the protein so that we did not have to insert also the tag by PCR (Figure 31).

Name	Sequence (5'→3')	Modification
pET_LR1_22-122_For	CAT CAT **CCA TGG** GCC AGG AGG AAG ATC TGC CCA G	5' insertion of ***NcoI***
pET_LR1_22-122_Rev	CCG CCG **CTC GAG** ACC TTC TTT CAC CAG CAG CTC CAG	3' insertion of ***XhoI***
pET_LR2_22-122_For	CAT CAT **CCA TGG** GCC AGG AGG GGG CCC TTC	5' insertion of ***NcoI***
pET_LR2_22-122_Rev	CCG CCG **CTC GAG** ACC TTC TTT CAC CAG CAG CTC CAG	3' insertion of ***XhoI***
pET_CD33_142-232_For	CAT CAT **CCA TGG** GCA CCC ACA GGC CCA AAA TCC	5' insertion of ***NcoI***
pET_CD33_142-232_Rev	CCG CCG **CTC GAG** ACC GGT GAC GTT GAG CTG GAT GG	3' insertion of ***XhoI***

Table 3: List of the oligonucleotides used for the design of the pET28a vectors. *All primers were purchased from Eurogentec.*

The PCR experiments were performed with the Phusion High-fidelity PCR Master mix following the manufacturer's protocol (ThermoFisher Scientific, product number F532S) (Table 4).

PCR REACTION MIX			
Template DNA		**1 ng** (2 µL at 0.5 ng/µL)	
Phusion Master Mix 2X		**25 µL**	
Forward primer (final concentration)		**0.5 µM** (2.5 µL at 10 µM)	
Reverse primer (final concentration)		**0.5 µM** (2.5 µL at 10 µM)	
Sterile H_2O		**18 µL** (add to 50 µL)	
PCR CYCLES			
Steps	**Temperature**	**Time**	**Number of cycles**
Initial denaturation	98 °C	60 s	1
Denaturation	98 °C	30 s	10
Annealing	55 °C	30 s	
Extension	72 °C	30 s	
Denaturation	98 °C	30 s	20
Annealing	60 °C	30 s	
Extension	72 °C	30 s	
Final extension	72 °C	5 min	1
Hold	15°C	∞	

Table 4: Conditions of the PCR experiments.

The PCR products were loaded on a 1% agarose gel and purified using the NucleoSpin gel and PCR clean-up kit following the manufacturer's protocol (Macherey-Nagel, product number 740609). Then the PCR products and the pET28a vector were digested with both *NcoI* and *XhoI* restriction enzymes (New England Biolabs, product numbers FD0573 and FD0694, respectively) and the digested products were purified using the NucleoSpin gel and PCR clean-up kit.

The digested vector and inserts were ligated using the T4 DNA ligase using the manufacturer's protocol (ThermoFisher Scientific, product number EL0011) (Table 5).

LIGATION REACTION MIX	
NcoI/*XhoI* digested pET28a	**50 ng** (2 µL at 25 ng/µL)
NcoI/*XhoI* digested insert (5:1 insert:vector molar ratio)	**15 ng** (0.5µL at 30 ng/µL)
10X ligation buffer	**2 µL**
T4 DNA ligase	**1 µL** (5 U)
Sterile H_2O	**14.5 µL** (add to 20 µL)
Incubation 1 hour at room temperature	

Table 5: Conditions of the ligation experiments.

DH5α competent cells were transformed using the ligation products and selected on kanamycin (50 µg/mL) LB-Agar petri dishes following the manufacturer's protocol (ThermoFisher Scientific, product number 18265017).

Plasmid DNA of growing colonies was extracted and purified using the NucleoSpin plasmid mini kit (Macherey-Nagel, product number 740588). The sequence of the purified DNA was controlled by Sanger sequencing (Eurofins Genomics).

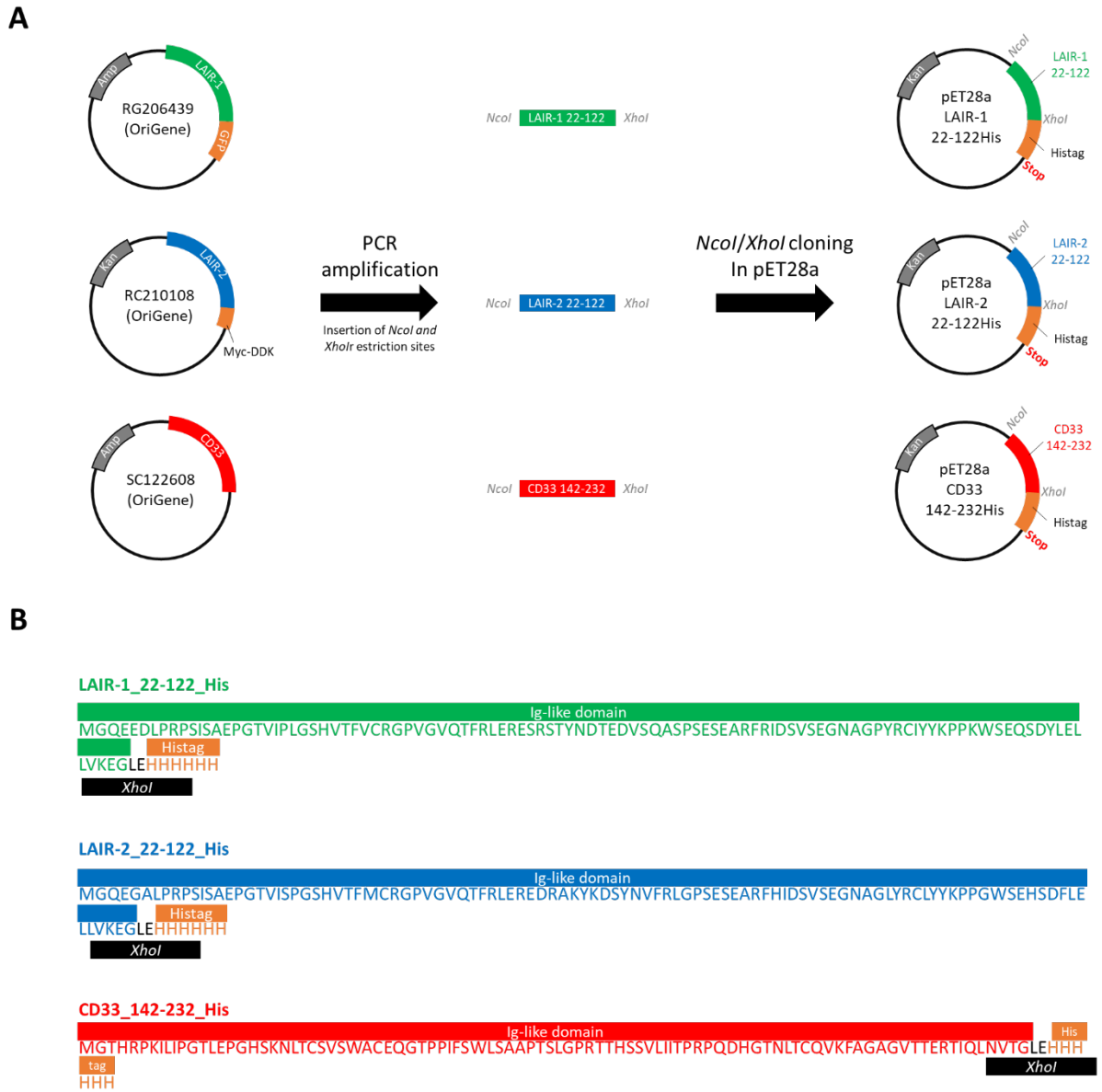

Figure 31: Design of pET28a(+) vectors containing the coding sequence of LAIR-1, LAIR-2 and CD33 Ig-like domains. *A. Schematic representation of the cloning procedure.* ***B****. Amino acids sequences of the LAIR-1, LAIR-2 and CD33 constructs cloned in pET28a(+) for bacterial expression. The additional leucine and glutamate residues due to the presence of the XhoI restriction site are indicated in black. The polyhistidine tags (Histag) of pET28a(+) vectors are shown in orange.*

1.2 Design of the pcDNA3.1(+) vectors for expression of LAIR-1, LAIR-2 or CD33 in mammalian cells

The coding sequences of the entire extracellular regions with the N-terminal signal peptide of LAIR-1 (1-163), LAIR-2 (1-152) or CD33 (1-232), (immature protein amino acids numbering for all constructs) were amplified by PCR using the oligonucleotides listed in Table 6. The oligonucleotides were designed in order to amplify the sequence coding the desired protein and insert the coding sequence for a polyhistidine tag followed by a stop codon at the 3' extremity and two flanking *NheI* and *XhoI* restriction sites at the 5' and 3'end, respectively.

Name	Sequence (5'→3')	Modification
pcDNA_LR1_1-163_For	CTA CTA **GCT AGC** ATG TCT CCC CAC CCC ACC	5'insertion of ***NheI***
pcDNA_LR1_1-163_Rev	CCG CCG **CTC GAG TCA GTG GTG GTG GTG GTG GTG** ATG CTC AGC CAG GCC	3'insertion of **Histag**, **stop** and ***XhoI***
pcDNA_LR2_1-152_For	CTA CTA **GCT AGC** ATG TCT CCA CAC CTC ACT GC	5' insertion of ***NheI***
pcDNA_LR2_1-152_Rev	CCG CCG **CTC GAG TCA GTG GTG GTG GTG GTG GTG** ACC TGG TGC ATC AAA TCC GGA GG	3' insertion of **Histag**, **stop** and ***XhoI***
pcDNA_CD33_1-232_For	CTA CTA **GCT AGC** ATG CCG CTG CTG CTA CTG	5' insertion of ***NheI*** in 5'
pcDNA_CD33_1-232_For	CCG CCG **CTC GAG TCA GTG GTG GTG GTG GTG GTG** ACC GGT GAC GTT GAG CTG GAT GG	3' insertion of **Histag**, **stop** and ***XhoI***

Table 6: List of the oligonucleotides used for the design of the pcDNA3.1(+) vectors. *All primers were purchased from Eurogentec.*

The PCR experiments were performed in the same conditions as described in Table 4. The rest of the cloning procedure was similar to the one used for the design of the pET28a vectors with the differences that *NcoI* restriction enzyme was replaced by *NheI* (New England Biolabs, product number FD0973) and the insert was cloned in a pcDNA3.1(+) vector (ThermoFisher Scientific, product number V79020) (Figure 32).

Figure 32: Design of pcDNA3.1(+) vectors containing the coding sequence of LAIR-1, LAIR-2 and CD33 extracellular regions. ***A****. Schematic representation of the cloning procedure.* ***B****. Amino acid sequences of LAIR-1 (green), LAIR-2 (blue) and CD33 (red) Ig-like domains. The native signal peptides and the polyhistidine tags (Histag) are shown in yellow and orange, respectively.*

2 Expression tests

2.1 Bacterial expression system: BL21(DE3)

The expression tests in *E. coli* BL21(DE3) were performed with two different induction methods: (i) IPTG (1 mM) or (ii) auto induction medium.

2.1.1 IPTG induction

BL21(DE3) competent cells (Sigma-Aldrich, product number CMC0014) were transformed with the pET28a vector containing the coding sequence of LAIR-1, LAIR-2 and CD33 Ig-like domain and selected on kanamycin (50 µg/mL) LB-Agar petri dishes following the manufacturer's recommendations. Positive colonies were cultured overnight in 10 mL of LB medium containing kanamycin (50 µg/mL) at 37°C, 180 rpm agitation speed.

Then, 100 mL of LB medium containing kanamycin (50 µg/mL) were inoculated at 0.1 of OD_{600} with the overnight preculture and incubated at 37°C, 180 rpm. Once the bacterial culture raised an OD_{600} value of 0.8, IPTG at a final concentration of 1 mM was added to the culture before incubation for 3 hours, at 37°C, 180 rpm. To get a control of expression before IPTG addition, a 1 mL sample of culture was taken and centrifuged at 11,000 g for 5 minutes. After centrifugation, the supernatant was removed and the pellet was resuspended in 4X Laemmli reducing buffer (Homemade: Tris 125 mM, β-mercaptoethanol 1.4 M, glycerol 20%, bromophenol blue 0.1%, pH 6.8) for SDS-PAGE analysis (NI lanes; Figure 28). For the control after induction, a 500 µL sample of culture was taken and treated as described for the NI control (I lanes; Figures 28). The analyses of the supernatant and pellet fractions of the cells after lysis were performed as follows. 2 mL of the 100 mL culture were centrifuged 30 minutes at 4,000 g, 4°C. The supernatant was removed and the cells were resuspended in buffer A (Tris 25 mM, NaCL 150 mM, pH 8.2) before lysis by sonication (2 min, 10 sec ON, 20 sec OFF). The lysate was then centrifuged 30 minutes at 11,000 g, 4°C. 75 µL of supernatant were sampled and mixed with 25 µL of 4X Laemmli reducing buffer for SDS-PAGE analysis (Figure 28). The pellet was resuspended in 2 mL of Buffer A and 75 µL were sampled and mixed with 25 µL of 4X Laemmli reducing buffer for SDS-PAGE analysis (Figure 28).

2.1.2 Autoinduction medium

The transformed BL21(DE3) cells were cultured in 30 mL of LB containing kanamycin (50 µg/mL) for 8 hours at 37°C, 180 rpm. After incubation, a 250 µL sample was taken and cells were harvested (11,000 g, 5 min) and resuspended in 4X Laemmli reducing buffer for SDS-PAGE analysis (NI lanes; Figure 28). One liter of autoinduction medium (Table 7) was then inoculated with 25 mL of preculture and submitted to incubation at 37°C, 180 rpm. After 2 hours of incubation, the temperature was decreased to 27°C and the culture was grown overnight.

Solutions Preparation	
$MgSO_4$ 1M	$MgSO_4$-$7H_2O$: 24.65 g H_2O: add to 100 mL
50X 5052	Glycerol: 25 g Glucose: 2.5 g α-Lactose: 10 g H_2O: add to 100 mL
20X NPS	$(NH_4)2SO_4$: 2.6 g KH_2PO_4: 13.6 g Na_2HPO_4: 14.2 g H_2O: add to 100 mL
TY	Tryptone: 10 g Yeast extract: 5 g H_2O: add to 1 L
Auto induction medium composition	
Solutions	**Volume**
$MgSO_4$ 1M	1 mL
50X 5052	20 mL
20X NPS	50 mL
Antibiotic	1 mL of 1000X stock solution
TY	Add to 1 L

Table 7: Composition of the auto induction medium.

After the overnight incubation, a 250 µL sample was taken and the cells were harvested (11,000 g, 5 min) and resuspended in 4X Laemmli reducing buffer for SDS-PAGE analysis (I lanes; Figure 28).

The analyses of the supernatant and pellet fractions of the cells after lysis were performed as follows. Two mL of the 1 L culture were centrifuged 30 minutes at 4,000 g, 4°C. The supernatant was removed and the cells were resuspended in buffer A (Tris 25 mM, NaCL 150 mM, pH 8.2) before lysis by sonication (2 min, 10 sec ON, 20 sec OFF). The lysate was then centrifuged for 30 minutes at 11,000 g, 4°C. 75 µL of supernatant were sampled and mixed with 25 µL of 4X Laemmli reducing buffer for SDS-PAGE analysis (Figure 28). The pellet was resuspended in 2 mL of Buffer A and 75 µL were sampled and mixed with 25 µL of 4X Laemmli reducing buffer for SDS-PAGE analysis (Figure 28).

2.2 Eukaryotic expression system: HEK293F

The production of LAIR-1, LAIR-2 and CD33 extracellular domains was performed using the HEK293F expression system. HEK293F cells were transfected with the pcDNA3.1(+) vectors containing the coding sequence of LAIR-1, LAIR-2 or CD33 extracellular region following the manufacturer's protocol (ThermoFisher Scientific, product number R79007). After transfection, the cells expressing the protein of interest were selected using neomycin (also known as geneticin or G418) at a concentration of 400 µg/mL (ThermoFisher Scientific, product number 10131027). The culture supernatant was harvested and replaced every 72 or 96 h of growth during the selection process to get stable cell lines. The mortality (number of dead cells over total number of cells) was determined at each cells dilution and is shown in Figure 33.

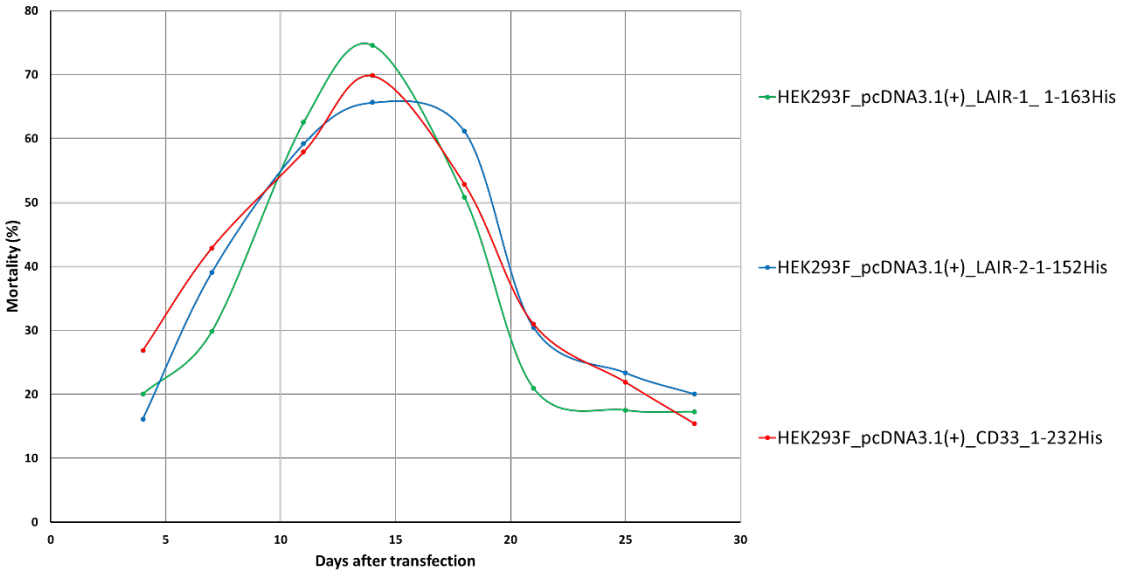

Figure 33: Selection of HEK293F cells after transfection with pcDNA3.1(+) vectors containing the coding sequences of LAIR-1, LAIR-2 or CD33 extracellular region.

After the selection, the culture supernatant was tested for the presence of the constructs of interest by western blot using an HRP-coupled monoclonal anti-Histag antibody according to the manufacturer's recommendations (Sigma-Aldrich, product number A7058).

One mL of cell culture was centrifuged at 1,000 g for 5 minutes and the supernatant was harvested and mixed with 1 mL of trichloroacetic acid (TCA) 50% and kept at 4°C to induce proteins precipitation. After 1 night at 4°C, the sample was centrifuged 30 minutes at 11,000 g, 4°C, the supernatant was discarded and the pellet was washed with 1 mL of acetone 100% and centrifuged 30 minutes at 11,000 g, 4°C. The supernatant was removed and the pellet was dried and resuspended in 2X Laemmli reducing buffer. Samples were loaded on a 14% acrylamide gel for SDS-PAGE and western blot analyses (Figure 29).

II. Appendix 2: Material and methods for unpublished data: LAIR-1 dimerization effects on C1q interaction

1 Production of LAIR-1 S92K variant and S92C covalent dimer

The pET28a vectors containing the coding sequences of LAIR-1 Ig-like domain S92K and S92C variants were generated by site directed mutagenesis of the pET28a_LAIR-1_22-122His vector (Appendix 1). The mutagenesis was performed using the Quikchange II XL kit (Agilent, product number 200522) and the oligonucleotides used are listed in Table 8.

NAME	Sequence (5'→3')	Modification
LAIR-1_S92K_For	gcc aga ttc cgc att gac tca gta **aag** gaa gga aat gcc gg	Insertion of **S92K** mutation
LAIR-1_S92K_Rev	cc ggc att tcc ttc **ctt** tac tga gtc aat gcg gaa tct ggc	
LAIR-1_S92C_For	gcc aga ttc cgc att gac tca gta **tgt** gaa gga aat gc	Insertion of **S92C** mutation
LAIR-1_S92C_Rev	gc att tcc ttc **aca** tac tga gtc aat gcg gaa tct ggc	

Table 8: Oligonucleotides used for the mutagenesis of pET28a_LAIR-1_22-122His. The mutated codons are colored

The two LAIR-1 variants were expressed and purified as described for the wild-type. In the particular case of the S92C variant, it was purified in a monomeric form and concentrated up to 5 mg/mL. The concentrated sample was kept at 4°C for at least 1 week in order to trigger the spontaneous formation of the disulfide bond formation between two LAIR-1 S92C monomers. Then, the sample was loaded back on a Superdex 75 column in 25 mM Tris, 150 mM NaCl, pH 8.2 in order to separate the dimers from the remaining monomers (generally, the dimeric portion represents 60% of the total proteins). The dimeric fraction was collected and concentrated up to 2 mg/mL.

2 Size-exclusion chromatography - multi angle laser light scattering (SEC-MALLS)

SEC combined with online detection by MALLS and refractometry was used to measure the absolute molecular mass of LAIR-1 WT, S92K and S92C. The SEC run was performed on a Superdex 75 10*300 gel filtration column (GE Healthcare) equilibrated in 25 mM Tris, 150 mM NaCl, pH 8.2. Separation was performed at room temperature and 50 µL of protein samples

at 5 mg/mL (WT), 4 mg/mL (S92K) or 4.5 mg/mL (S92C) were injected with a constant flow rate of 0.5 mL/min. Online MALLS detection was performed with a DAWN-HELEOS II detector (Wyatt Technology Corp.) using a laser emitting at 690 nm. Protein concentration was determined by measuring the differential refractive index online using an Optilab T-rEX detector (Wyatt Technology Corp.) with a refractive increment *dn*/*dc* of 0.185 mL^{-1} g^{-1}. Weight-averaged molecular weight determination was done with the ASTRA6 software (Wyatt Technologies).

3 Crystallization and structure determination of LAIR-1 S92C dimer

3.1 Crystallization

A first automated screening of the crystallization conditions of LAIR-1 S92C was performed by vapor diffusion using the sitting drop method at 293 K (HTXLab, CRIMS©). The protein, at a concentration of 23 mg/mL was tested with 4 screens: Classics-Suite (Qiagen), PACT (Molecular Dimensions), Wizard_I+II (Rigaku Reagents) and Morpheus (Molecular Dimensions). For each screen, we used a 1:1 ratio for the mixed protein and reservoir solution volumes, respectively.

Based on these 4 screens, we refined the crystallization condition for which the best crystals were obtained (i.e. 0.1 M MES, 0.2 M NaCl, 20 % (w/v) PEG 6000, pH 6). To do so, we varied the PEG 6000 concentrations, the salt and the pH of the reservoir solutions (Table 9). For this crystallization assay, we used the hanging drop method by mixing 1 µL of protein sample concentrated at 21.5 mg/mL with 0.9 µL of reservoir solution. The crystals were harvested directly from the drops (B1, C1, C2 and D2) and flash-frozen in liquid nitrogen. The crystal structure presented in the results section was solved using the diffraction data obtained from the crystals grown in C1 conditions (MES 0.1 M, $LiCl_2$ 0.2 M, PEG 6000 15 %, pH 6).

PEG 6000	15%	17%	19%	20%	21%	23%
Glycerol						8%
0.1 M MES, pH6 0.2 M NaCl	1	2	3	4	5	6
	A ○	○	○	○	○	○
PEG 6000	15%	17%	19%	20%	21%	23%
Glycerol						8%
0.1 M MES, pH6.5 0.2 M NaCl	1	2	3	4	5	6
	B ○	○	○	○	○	○
PEG 6000	15%	17%	19%	20%	21%	23%
Glycerol						8%
0.1 M MES, pH6 0.2 M $LiCl_2$	1	2	3	4	5	6
	C ○	○	○	○	○	○
PEG 6000	15%	17%	19%	20%	21%	23%
Glycerol						8%
0.1 M MES, pH6.5 0.2 M LiCl2	1	2	3	4	5	6
	D ○	○	○	○	○	○

Table 9: Plan of the crystallization plate used for the refinement of the LAIR-1 S92C crystallization conditions.

3.2 Data collection and structure determination

LAIR-1 S92C data were collected at the European Synchrotron radiation Facility (ESRF) on the ID30-A3 beamline.

Diffraction data collected on ID30-A3 beamline	
Space group	H3
Cell parameters	a=b=143.133Å c=72.404 Å, α=β=90° γ=120°
Wavelength (Å)	0.96770
Resolution limits (Å)	2.7-47

Outer shell (Å)	2.70 – 2.746
R_{merge}	0.033 (0.417)
Total observations	44680 (2343)
Unique observations	14887 (748)
Completeness (%)	98.0 (99.6)
Multiplicity	3.0 (3.1)
CC (1/2)	0.999 (0.882)
Outer resolution shell values are indicated in parentheses.	
Structure refinement statistics	
Resolution limits	2.7-72
R_{work}	0.193
R_{free}	0.257
RMSD bond lengths (Å)	0.009
RMSD bond angles (°)	1.705

Table 10: LAIR-1 S92C diffraction data and structure refinement statistics.

The collected data were automatically processed using the EDNA autoprocessing available at the ESRF. Molecular replacement was then performed with the CCP4 suite using Molrep. The model used for molecular replacement was the structure of the monomeric LAIR-1 Ig-like domain (PDB code: 3KGR). The structure was refined with multiple cycles of manual building using COOT (Emsley et al. 2010) and of refinement using Refmac5 (CCP4 suite). The refinement statistics (Table 10) were obtained using the last refmac5 refinement cycle.

Other diffraction data have been collected for the S92C LAIR-1 obtained in different conditions, but the same crystal packing as above has always been obtained.

4 Small angle X-ray scattering (SAXS)

SAXS experiments on LAIR-1 S92C (3.5 mg/mL) were performed at the European Synchrotron radiation Facility (ESRF) on the BM29 “BioSAXS” beamline using an X-ray energy of 12.5 keV. To prevent radiation damage, the measurement was performed 10 times and then averaged. Samples scattering curves were obtained after subtraction of the average buffer signals using standard protocols with PRIMUS (Konarev et al. 2003). The theoretical SAXS curve was generated from the PDB files of our model and solved structures using the FoXS online server (Schneidman-Duhovny et al. 2010).

5 Surface plasmon resonance (SPR)

The SPR experiments were performed at 25°C on a BIAcore T200 instrument (GE Healthcare). Serum-derived C1q (35 µg/mL in 10 mM sodium acetate, pH5) was immobilized on a CM5 sensor chip using the amine coupling chemistry at a flowrate of 10 µL/min in 10 mM HEPES, 150 mM NaCl, 3 mM EDTA, 0.05% (v/v) surfactant P20, pH 7.4. The interaction experiments were performed at a flowrate of 30 µL/min in 50 mM Tris, 150 mM NaCl, 2 mM $CaCl_2$, 0.05% surfactant P20 (pH 7.5). All data were analyzed using the T200 Biaevaluation 3.1 software (GE Healthcare).

LAIR-1 S92C was injected at increasing concentration (1-32 µM) over immobilized serum-derived C1q (14,000 RU) with association and dissociation steps of 360 s. The equilibrium dissociation constant (K_D) values were calculated from measured responses at equilibrium (Req) by fitting plots Req versus concentration using steady state analysis (Biaevaluation software).

LAIR-1 WT and S92K were injected at a concentration of 10 µM over immobilized serum-derived C1q (14,000 RU) with association and dissociation steps of 180 s.

6 Crystallization assays of LAIR-1 S92C with a synthetic collagen peptide or the C1qstem_nc2 construct

Automated screenings of the crystallization conditions of LAIR-1 S92C in the presence of a synthetic collagen peptide (Ac-GPOGPOGPOGPKGEQGPOGPO-NH2) or the C1qstem_nc2 at a molar ratio of 1:1 (LAIR-1 S92C:collagen) were performed in each case by vapor diffusion using the sitting drop method at 293 K (HTXLab, CRIMS©).

For the assays with the synthetic collagen peptide, LAIR-1 S92C was at a concentration of 15 mg/mL and four screens were tested: Classics-Suite (Qiagen), PACT (Molecular Dimensions), Midas-plus (Molecular Dimensions) and Morpheus (Molecular Dimensions).

For the assays with the C1stem_nc2 construct, LAIR-1 S92C was at a concentration of 5 mg/mL and two screens were tested: Classics-Suite (Qiagen) and PEGs-I (Qiagen).

III. **Appendix 3:** Kinetic analysis of $C1r_2s_2$ interaction with immobilized C1qCLR_nc2 WT and B_K65E

A

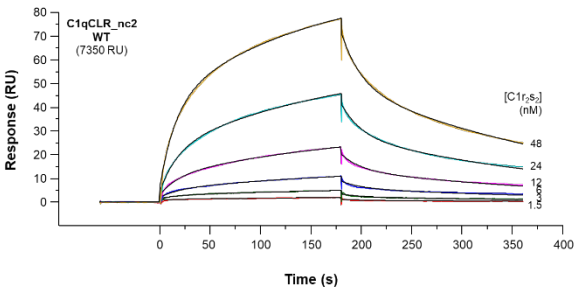

B

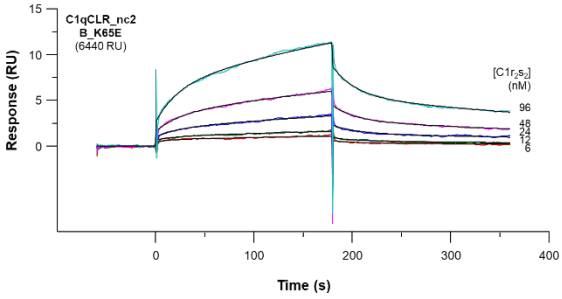

C

Ligand	$C1r_2s_2$				
	k_{a1}	k_{d1}	k_{a2}	k_{d2}	K_D
	$M^{-1}.s^{-1}$ (x 10^5)	s^{-1} (x 10^{-2})	$M^{-1}.s^{-1}$ (x 10^{-3})	s^{-1} (x 10^{-3})	nM
C1qCLR_nc2 WT	3.6 ± 0.4	4.4 ± 0.1	10.2 ± 0.3	5.1 ± 0.1	**41.3 ± 4.9**
C1qCLR_nc2 B_K65E	0.6 ± 0.3	3.5 ± 0.1	7.6 ± 0.1	2.9 ± 0.4	**177.5 ± 59.0**

Values are mean ± SD of 3 (WT) and 2 (B_k65E) separate experiments. The association (*ka*) and dissociation (*kd*) rate constants were determined by global fitting of the data using two state reaction binding model. The resulting dissociation constate K_D was determined byfrom the rate constants: $K_D = 1/[(k_{a1}/k_{d1})(1 + k_{a2}/k_{d2})]$.

Figure 34: Kinetic analysis of $C1r_2s_2$ interaction with C1qCLR_nc2 WT and B_K65E. *A. $C1r_2s_2$ was injected at increasing concentrations over immobilized C1qCLR_nc2 WT (**A**) or B_K65E (**B**). The quantities of immobilized C1qCLR_nc2 variants are indicated. Fits obtained by a global fitting of the data with a two-state reaction binding model are shown in black. **C.** Summary table of the kinetic constants.*

BIBLIOGRAPHY

Adachi H, Tsujimoto M, Arai H, Inoue K (1997) Expression cloning of a novel scavenger receptor from human endothelial cells. J Biol Chem 272:31217–31220. https://doi.org/10.1074/jbc.272.50.31217

Agashe VV, Jankowska-Gan E, Keller M, et al (2018) Leukocyte-Associated Ig-like Receptor 1 Inhibits T $_{h}$ 1 Responses but Is Required for Natural and Induced Monocyte-Dependent T $_{h}$ 17 Responses. The Journal of Immunology ji1701753. https://doi.org/10.4049/jimmunol.1701753

Alcorlo M, Tortajada A, Rodríguez de Córdoba S, Llorca O (2013) Structural basis for the stabilization of the complement alternative pathway C3 convertase by properdin. Proc Natl Acad Sci U S A 110:13504–13509. https://doi.org/10.1073/pnas.1309618110

Almitairi JOM, Venkatraman Girija U, Furze CM, et al (2018) Structure of the C1r-C1s interaction of the C1 complex of complement activation. Proc Natl Acad Sci USA 115:768–773. https://doi.org/10.1073/pnas.1718709115

Antes U, Heinz HP, Loos M (1988) Evidence for the presence of autoantibodies to the collagen-like portion of C1q in systemic lupus erythematosus. Arthritis Rheum 31:457–464. https://doi.org/10.1002/art.1780310401

Bally I, Ancelet S, Moriscot C, et al (2013) Expression of recombinant human complement C1q allows identification of the C1r/C1s-binding sites. PNAS 110:8650–8655. https://doi.org/10.1073/pnas.1304894110

Bally I, Inforzato A, Dalonneau F, et al (2019) Interaction of C1q With Pentraxin 3 and IgM Revisited: Mutational Studies With Recombinant C1q Variants. Front Immunol 10:. https://doi.org/10.3389/fimmu.2019.00461

Bally I, Rossi V, Lunardi T, et al (2009) Identification of the C1q-binding Sites of Human C1r and C1s: a refined three-dimensional model of the C1 complex of complement. J Biol Chem 284:19340–19348. https://doi.org/10.1074/jbc.M109.004473

Barrow AD, Trowsdale J (2008) The extended human leukocyte receptor complex: diverse ways of modulating immune responses. Immunol Rev 224:98–123. https://doi.org/10.1111/j.1600-065X.2008.00653.x

Baruah P, Dumitriu IE, Malik TH, et al (2009) C1q enhances IFN-gamma production by antigen-specific T cells via the CD40 costimulatory pathway on dendritic cells. Blood 113:3485–3493. https://doi.org/10.1182/blood-2008-06-164392

Baruah P, Dumitriu IE, Peri G, et al (2006) The tissue pentraxin PTX3 limits C1q-mediated complement activation and phagocytosis of apoptotic cells by dendritic cells. J Leukoc Biol 80:87–95. https://doi.org/10.1189/jlb.0805445

Bengtsson AA, Sturfelt G, Truedsson L, et al (2000) Activation of type I interferon system in systemic lupus erythematosus correlates with disease activity but not with antiretroviral antibodies. Lupus 9:664–671. https://doi.org/10.1191/096120300674499064

Berisio R, Vitagliano L, Mazzarella L, Zagari A (2002) Crystal structure of the collagen triple helix model [(Pro-Pro-Gly)(10)](3). Protein Sci 11:262–270. https://doi.org/10.1110/ps.32602

Berwin B, Delneste Y, Lovingood RV, et al (2004) SREC-I, a type F scavenger receptor, is an endocytic receptor for calreticulin. J Biol Chem 279:51250–51257. https://doi.org/10.1074/jbc.M406202200

Bode GH, Losen M, Buurman WA, et al (2014) Complement activation by ceramide transporter proteins. J Immunol 192:1154–1161. https://doi.org/10.4049/jimmunol.1301673

Bogin O, Kvansakul M, Rom E, et al (2002) Insight into Schmid metaphyseal chondrodysplasia from the crystal structure of the collagen X NC1 domain trimer. Structure 10:165–173. https://doi.org/10.1016/s0969-2126(02)00697-4

Bonaccorsi I, Cantoni C, Carrega P, et al (2010) The immune inhibitory receptor LAIR-1 is highly expressed by plasmacytoid dendritic cells and acts complementary with NKp44 to control IFNα production. PLoS ONE 5:e15080. https://doi.org/10.1371/journal.pone.0015080

Botto M, Dell'Agnola C, Bygrave AE, et al (1998) Homozygous C1q deficiency causes glomerulonephritis associated with multiple apoptotic bodies. Nat Genet 19:56–59. https://doi.org/10.1038/ng0598-56

Botto M, Walport MJ (2002) C1q, Autoimmunity and Apoptosis. Immunobiology 205:395–406. https://doi.org/10.1078/0171-2985-00141

Boudko SP, Bächinger HP (2012) The NC2 Domain of Type IX Collagen Determines the Chain Register of the Triple Helix. J Biol Chem 287:44536–44545. https://doi.org/10.1074/jbc.M112.417543

Boudko SP, Bächinger HP (2016) Structural insight for chain selection and stagger control in collagen. Sci Rep 6:. https://doi.org/10.1038/srep37831

Boudko SP, Engel J, Bächinger HP (2012) The crucial role of trimerization domains in collagen folding. The International Journal of Biochemistry & Cell Biology 44:21–32. https://doi.org/10.1016/j.biocel.2011.09.009

Boudko SP, Sasaki T, Engel J, et al (2009) Crystal structure of human collagen XVIII trimerization domain: A novel collagen trimerization Fold. J Mol Biol 392:787–802. https://doi.org/10.1016/j.jmb.2009.07.057

Boudko SP, Zientek KD, Vance J, et al (2010) The NC2 Domain of Collagen IX Provides Chain Selection and Heterotrimerization. J Biol Chem 285:23721–23731. https://doi.org/10.1074/jbc.M110.128405

Bourhis J-M, Mariano N, Zhao Y, et al (2012) Structural Basis of Fibrillar Collagen Trimerization and Related Genetic Disorders. Nat Struct Mol Biol 19:1031–1036. https://doi.org/10.1038/nsmb.2389

Brodsky-Doyle B, Leonard KR, Reid KB (1976) Circular-dichroism and electron-microscopy studies of human subcomponent C1q before and after limited proteolysis by pepsin. Biochem J 159:279–286

Brondijk THC, Bihan D, Farndale RW, Huizinga EG (2012) Implications for collagen I chain registry from the structure of the collagen von Willebrand factor A3 domain complex. Proc Natl Acad Sci U S A 109:5253–5258. https://doi.org/10.1073/pnas.1112388109

Brondijk THC, de Ruiter T, Ballering J, et al (2010a) Crystal structure and collagen-binding site of immune inhibitory receptor LAIR-1: unexpected implications for collagen binding by platelet receptor GPVI. Blood 115:1364–1373

Brondijk THC, Ruiter T de, Ballering J, et al (2010b) Crystal structure and collagen-binding site of immune inhibitory receptor LAIR-1: unexpected implications for collagen binding by platelet receptor GPVI. Blood 115:1364–1373. https://doi.org/10.1182/blood-2009-10-246322

Bruckner P (2010) Suprastructures of extracellular matrices: paradigms of functions controlled by aggregates rather than molecules. Cell Tissue Res 339:7–18. https://doi.org/10.1007/s00441-009-0864-0

Bulla R, Tripodo C, Rami D, et al (2016) C1q acts in the tumour microenvironment as a cancer-promoting factor independently of complement activation. Nature Communications 7:10346. https://doi.org/10.1038/ncomms10346

Cao Q, Fu A, The People's Liberation Army 107 Hospital AH of BZMU, et al (2015) Leukocyte-associated immunoglobulin-like receptor-1 expressed in epithelial ovarian cancer cells and involved in cell proliferation and invasion. Biochemical and Biophysical Research Communications 458:. https://doi.org/10.1016/J.BBRC.2015.01.127

Carvalheiro T, Garcia S, Pascoal Ramos MI, et al (2020) Leukocyte Associated Immunoglobulin Like Receptor 1 Regulation and Function on Monocytes and Dendritic Cells During Inflammation. Front Immunol 11:. https://doi.org/10.3389/fimmu.2020.01793

Casals C, García-Fojeda B, Minutti CM (2019) Soluble defense collagens: Sweeping up immune threats. Mol Immunol 112:291–304. https://doi.org/10.1016/j.molimm.2019.06.007

Castellano G, Woltman AM, Nauta AJ, et al (2004) Maturation of dendritic cells abrogates C1q production in vivo and in vitro. Blood 103:3813–3820. https://doi.org/10.1182/blood-2003-09-3046

Colonna M, Trinchieri G, Liu Y-J (2004) Plasmacytoid dendritic cells in immunity. Nat Immunol 5:1219–1226. https://doi.org/10.1038/ni1141

Crocker PR, Paulson JC, Varki A (2007) Siglecs and their roles in the immune system. Nat Rev Immunol 7:255–266. https://doi.org/10.1038/nri2056

Csomor E, Bajtay Z, Sándor N, et al (2007) Complement protein C1q induces maturation of human dendritic cells. Mol Immunol 44:3389–3397. https://doi.org/10.1016/j.molimm.2007.02.014

Cutler AJ, Botto M, van Essen D, et al (1998) T cell-dependent immune response in C1q-deficient mice: defective interferon gamma production by antigen-specific T cells. J Exp Med 187:1789–1797. https://doi.org/10.1084/jem.187.11.1789

Davis AE, Mejia P, Lu F (2008) BIOLOGICAL ACTIVITIES OF C1 INHIBITOR. Mol Immunol 45:4057–4063. https://doi.org/10.1016/j.molimm.2008.06.028

Defendi F, Thielens NM, Clavarino G, et al (2020) The Immunopathology of Complement Proteins and Innate Immunity in Autoimmune Disease. Clin Rev Allergy Immunol 58:229–251. https://doi.org/10.1007/s12016-019-08774-5

Dembitzer FR, Kinoshita Y, Burstein D, et al (2012) gC1qR expression in normal and pathologic human tissues: differential expression in tissues of epithelial and mesenchymal origin. J Histochem Cytochem 60:467–474. https://doi.org/10.1369/0022155412440882

Dombkowski AA, Sultana KZ, Craig DB (2014) Protein disulfide engineering. FEBS Lett 588:206–212. https://doi.org/10.1016/j.febslet.2013.11.024

Eggleton P, Tenner AJ, Reid KBM (2000) C1q receptors. Clin Exp Immunol 120:406–412. https://doi.org/10.1046/j.1365-2249.2000.01218.x

Ehrengruber MU, Geiser T, Deranleau DA (1994) Activation of human neutrophils by C3a and C5A. Comparison of the effects on shape changes, chemotaxis, secretion, and respiratory burst. FEBS letters 346:181–184. https://doi.org/10.1016/0014-5793(94)00463-3

Elsner J, Oppermann M, Czech W, et al (1994a) C3a activates reactive oxygen radical species production and intracellular calcium transients in human eosinophils. European Journal of Immunology 24:518–522. https://doi.org/10.1002/eji.1830240304

Elsner J, Oppermann M, Czech W, Kapp A (1994b) C3a activates the respiratory burst in human polymorphonuclear neutrophilic leukocytes via pertussis toxin-sensitive G-proteins. Blood 83:3324–3331

Emsley P, Lohkamp B, Scott WG, Cowtan K (2010) Features and development of Coot. Acta Cryst D 66:486–501. https://doi.org/10.1107/S0907444910007493

Engel J, Prockop DJ (1991) The zipper-like folding of collagen triple helices and the effects of mutations that disrupt the zipper. Annu Rev Biophys Biophys Chem 20:137–152. https://doi.org/10.1146/annurev.bb.20.060191.001033

Farkas I, Baranyi L, Ishikawa Y, et al (2002) CD59 blocks not only the insertion of C9 into MAC but inhibits ion channel formation by homologous C5b-8 as well as C5b-9. Journal of Physiology 539:537–545. https://doi.org/10.1113/jphysiol.2001.013381

Farndale RW, Sixma JJ, Barnes MJ, de Groot PG (2004) The role of collagen in thrombosis and hemostasis. J Thromb Haemost 2:561–573. https://doi.org/10.1111/j.1538-7836.2004.00665.x

Fearon DT (1980) Identification of the membrane glycoprotein that is the C3b receptor of the human erythrocyte, polymorphonuclear leukocyte, B lymphocyte, and monocyte. J Exp Med 152:20–30. https://doi.org/10.1084/jem.152.1.20

Fearon DT (1979) Regulation of the amplification C3 convertase of human complement by an inhibitory protein isolated from human erythrocyte membrane. Proc Natl Acad Sci U S A 76:5867–5871. https://doi.org/10.1073/pnas.76.11.5867

Fearon DT, Klickstein LB, Wong WW, et al (1989) Immunoregulatory functions of complement: structural and functional studies of complement receptor type 1 (CR1; CD35) and type 2 (CR2; CD21). Prog Clin Biol Res 297:211–220

Ferry H, Potter PK, Crockford TL, et al (2007) Increased positive selection of B1 cells and reduced B cell tolerance to intracellular antigens in c1q-deficient mice. J Immunol 178:2916–2922. https://doi.org/10.4049/jimmunol.178.5.2916

Florian S, Sonneck K, Czerny M, et al (2006) Detection of novel leukocyte differentiation antigens on basophils and mast cells by HLDA8 antibodies. Allergy 61:1054–1062. https://doi.org/10.1111/j.1398-9995.2006.01171.x

Fouët G, Bally I, Signor L, et al (2020a) Headless C1q: a new molecular tool to decipher its collagen-like functions. FEBS J. https://doi.org/10.1111/febs.15543

Fouët G, Gout E, Wicker-Planquart C, et al (2020b) Complement C1q Interacts With LRP1 Clusters II and IV Through a Site Close but Different From the Binding Site of Its C1r and C1s-Associated Proteases. Front Immunol 11:. https://doi.org/10.3389/fimmu.2020.583754

Frantz C, Stewart KM, Weaver VM (2010) The extracellular matrix at a glance. J Cell Sci 123:4195–4200. https://doi.org/10.1242/jcs.023820

Fraser DA, Bohlson SS, Jasinskiene N, et al (2006) C1q and MBL, components of the innate immune system, influence monocyte cytokine expression. Journal of Leukocyte Biology 80:107–116. https://doi.org/10.1189/jlb.1105683

Fraser DA, Tenner AJ (2008) Directing an appropriate immune response: the role of defense collagens and other soluble pattern recognition molecules. Curr Drug Targets 9:113–122. https://doi.org/10.2174/138945008783502476

Fujita T (2002) Evolution of the lectin-complement pathway and its role in innate immunity. Nature Reviews Immunology 2:346–353. https://doi.org/10.1038/nri800

Fujita T, Gigli I, Nussenzweig V (1978) Human C4-binding protein. II. Role in proteolysis of C4b by C3b-inactivator. J Exp Med 148:1044–1051. https://doi.org/10.1084/jem.148.4.1044

Gaboriaud C, Frachet P, Thielens NM, Arlaud GJ (2011) The human c1q globular domain: structure and recognition of non-immune self ligands. Front Immunol 2:92. https://doi.org/10.3389/fimmu.2011.00092

Gaboriaud C, Juanhuix J, Gruez A, et al (2003) The crystal structure of the globular head of complement protein C1q provides a basis for its versatile recognition properties. J Biol Chem 278:46974–46982. https://doi.org/10.1074/jbc.M307764200

Gaboriaud C, Ling WL, Thielens NM, et al (2014) Deciphering the fine details of c1 assembly and activation mechanisms: "mission impossible"? Front Immunol 5:565. https://doi.org/10.3389/fimmu.2014.00565

Gaboriaud C, Teillet F, Gregory LA, et al (2007) Assembly of C1 and the MBL– and ficolin–MASP complexes: Structural insights. Immunobiology 212:279–288. https://doi.org/10.1016/j.imbio.2006.11.007

Gadjeva MG, Rouseva MM, Zlatarova AS, et al (2008) Interaction of Human C1q with IgG and IgM: Revisited. Biochemistry 47:13093–13102. https://doi.org/10.1021/bi801131h

Galvan MD, Foreman DB, Zeng E, et al (2012a) Complement component C1q regulates macrophage expression of Mer tyrosine kinase to promote clearance of apoptotic cells. J Immunol 188:3716–3723. https://doi.org/10.4049/jimmunol.1102920

Galvan MD, Greenlee-Wacker MC, Bohlson SS (2012b) C1q and phagocytosis: the perfect complement to a good meal. Journal of Leukocyte Biology 92:489–497. https://doi.org/10.1189/jlb.0212099

Ghebrehiwet B, Lim BL, Peerschke EI, et al (1994) Isolation, cDNA cloning, and overexpression of a 33-kD cell surface glycoprotein that binds to the globular "heads" of C1q. J Exp Med 179:1809–1821. https://doi.org/10.1084/jem.179.6.1809

Hadders MA, Bubeck D, Roversi P, et al (2012) Assembly and Regulation of the Membrane Attack Complex Based on Structures of C5b6 and sC5b9. Cell Rep 1:200–207

Harrison TE, Mørch AM, Felce JH, et al (2020) Structural basis for RIFIN-mediated activation of LILRB1 in malaria. Nature. https://doi.org/10.1038/s41586-020-2530-3

Haywood J, Qi J, Chen C-C, et al (2016) Structural basis of collagen recognition by human osteoclast-associated receptor and design of osteoclastogenesis inhibitors. Proc Natl Acad Sci USA 113:1038–1043. https://doi.org/10.1073/pnas.1522572113

He M, Kubo H, Morimoto K, et al (2011) Receptor for advanced glycation end products binds to phosphatidylserine and assists in the clearance of apoptotic cells. EMBO Rep 12:358–364. https://doi.org/10.1038/embor.2011.28

Hooks JJ, Moutsopoulos HM, Geis SA, et al (1979) Immune interferon in the circulation of patients with autoimmune disease. N Engl J Med 301:5–8. https://doi.org/10.1056/NEJM197907053010102

Horii K (2006) Structural basis for platelet collagen responses by the immune-type receptor glycoprotein VI. Blood 108:936–942. https://doi.org/10.1182/blood-2006-01-010215

Hourcade DE, Mitchell L, Kuttner-Kondo LA, et al (2002) Decay-accelerating factor (DAF), complement receptor 1 (CR1), and factor H dissociate the complement AP C3 convertase (C3bBb) via sites on the type A domain of Bb. J Biol Chem 277:1107–1112. https://doi.org/10.1074/jbc.M109322200

Hsieh F-L, Higgins MK (2017) The structure of a LAIR1-containing human antibody reveals a novel mechanism of antigen recognition. Elife 6:. https://doi.org/10.7554/eLife.27311

Hughes-Jones NC, Gardner B (1979) Reaction between the isolated globular sub-units of the complement component C1q and IgG-complexes. Mol Immunol 16:697–701. https://doi.org/10.1016/0161-5890(79)90010-5

Huijbers IJ, Iravani M, Popov S, et al (2010) A role for fibrillar collagen deposition and the collagen internalization receptor endo180 in glioma invasion. PLoS ONE 5:e9808. https://doi.org/10.1371/journal.pone.0009808

Iida K, Nussenzweig V (1981) Complement receptor is an inhibitor of the complement cascade. J Exp Med 153:1138–1150. https://doi.org/10.1084/jem.153.5.1138

Jacquet M, Cioci G, Fouet G, et al (2018) C1q and Mannose-Binding Lectin Interact with CR1 in the Same Region on CCP24-25 Modules. Front Immunol 9:. https://doi.org/10.3389/fimmu.2018.00453

Jalan AA, Sammon D, Hartgerink JD, et al (2020) Chain alignment of collagen I deciphered using computationally designed heterotrimers. Nat Chem Biol 16:423–429. https://doi.org/10.1038/s41589-019-0435-y

Jansen CA, Cruijsen CWA, de Ruiter T, et al (2007) Regulated expression of the inhibitory receptor LAIR-1 on human peripheral T cells during T cell activation and differentiation. European Journal of Immunology 37:914–924. https://doi.org/10.1002/eji.200636678

Jiang H, Cooper B, Robey FA, Gewurz H (1992) DNA binds and activates complement via residues 14-26 of the human C1q A chain. J Biol Chem 267:25597–25601

Jin J, Wang Y, Ma Q, et al (2018) LAIR-1 activation inhibits inflammatory macrophage phenotype in vitro. Cell Immunol 331:78–84. https://doi.org/10.1016/j.cellimm.2018.05.011

Kadowaki N, Antonenko S, Liu YJ (2001) Distinct CpG DNA and polyinosinic-polycytidylic acid double-stranded RNA, respectively, stimulate CD11c- type 2 dendritic cell precursors and CD11c+ dendritic cells to produce type I IFN. J Immunol 166:2291–2295. https://doi.org/10.4049/jimmunol.166.4.2291

Kanakoudi-Tsakalidou F, Farmaki E, Tzimouli V, et al (2014) Simultaneous changes in serum HMGB1 and IFN-α levels and in LAIR-1 expression on plasmatoid dendritic cells of patients with juvenile SLE. New therapeutic options? Lupus 23:305–312. https://doi.org/10.1177/0961203313519157

Kang HJ, Lee S-M, Lee H-H, et al (2007) Mannose-binding lectin without the aid of its associated serine proteases alters lipopolysaccharide-mediated cytokine/chemokine secretion from human endothelial cells. Immunology 122:335–342. https://doi.org/10.1111/j.1365-2567.2007.02644.x

Kang X, Lu Z, Cui C, et al (2015) The ITIM-containing receptor LAIR1 is essential for acute myeloid leukaemia development. Nature Cell Biology 17:665–677. https://doi.org/10.1038/ncb3158

Kauppila S, Stenbäck F, Risteli J, et al (1998) Aberrant type I and type III collagen gene expression in human breast cancer in vivo. J Pathol 186:262–268. https://doi.org/10.1002/(SICI)1096-9896(1998110)186:3<262::AID-PATH191>3.0.CO;2-3

Kirou KA, Lee C, George S, et al (2004) Coordinate overexpression of interferon-alpha-induced genes in systemic lupus erythematosus. Arthritis Rheum 50:3958–3967. https://doi.org/10.1002/art.20798

Kishore U, Ghai R, Greenhough TJ, et al (2004) Structural and functional anatomy of the globular domain of complement protein C1q. Immunol Lett 95:. https://doi.org/10.1016/j.imlet.2004.06.015

Kishore U, Reid KB (1999) Modular organization of proteins containing C1q-like globular domain. Immunopharmacology 42:15–21. https://doi.org/10.1016/s0162-3109(99)00011-9

Klickstein LB, Barbashov SF, Liu T, et al (1997) Complement receptor type 1 (CR1, CD35) is a receptor for C1q. Immunity 7:345–355. https://doi.org/10.1016/s1074-7613(00)80356-8

Knight CG, Morton LF, Onley DJ, et al (1999) Collagen-platelet interaction: Gly-Pro-Hyp is uniquely specific for platelet Gp VI and mediates platelet activation by collagen. Cardiovasc Res 41:450–457. https://doi.org/10.1016/s0008-6363(98)00306-x

Kohro-Kawata J, Wener MH, Mannik M (2002) The effect of high salt concentration on detection of serum immune complexes and autoantibodies to C1q in patients with systemic lupus erythematosus. J Rheumatol 29:84–89

Kojouharova MS, Gadjeva MG, Tsacheva IG, et al (2004) Mutational analyses of the recombinant globular regions of human C1q A, B, and C chains suggest an essential role for arginine and histidine residues in the C1q-IgG interaction. J Immunol 172:4351–4358. https://doi.org/10.4049/jimmunol.172.7.4351

Kojouharova MS, Tsacheva IG, Tchorbadjieva MI, et al (2003) Localization of ligand-binding sites on human C1q globular head region using recombinant globular head fragments and single-chain antibodies. Biochim Biophys Acta 1652:64–74. https://doi.org/10.1016/j.bbapap.2003.08.003

Konarev PV, Volkov VV, Sokolova AV, et al (2003) PRIMUS: A Windows PC-based system for small-angle scattering data analysis. Journal of Applied Crystallography 36:1277–1282. https://doi.org/10.1107/S0021889803012779

Krissinel E, Henrick K (2007) Inference of Macromolecular Assemblies from Crystalline State. Journal of Molecular Biology 372:774–797. https://doi.org/10.1016/j.jmb.2007.05.022

Kumawat K, Geerdink RJ, Hennus MP, et al (2019) LAIR-1 Limits Neutrophilic Airway Inflammation. Front Immunol 10:842. https://doi.org/10.3389/fimmu.2019.00842

Kvansakul M, Bogin O, Hohenester E, Yayon A (2003) Crystal structure of the collagen alpha1(VIII) NC1 trimer. Matrix Biol 22:145–152. https://doi.org/10.1016/s0945-053x(02)00119-1

La Cava A (2010) Targeting B cells with biologics in SLE. Expert Opin Biol Ther 10:1555–1561. https://doi.org/10.1517/14712598.2010.524923

Lanzavecchia A (2018) Dissecting human antibody responses: useful, basic and surprising findings. EMBO Molecular Medicine 10:e8879. https://doi.org/10.15252/emmm.201808879

Lebbink RJ, de Ruiter T, Adelmeijer J, et al (2006) Collagens are functional, high affinity ligands for the inhibitory immune receptor LAIR-1. J Exp Med 203:1419–1425. https://doi.org/10.1084/jem.20052554

Lebbink RJ, Raynal N, de Ruiter T, et al (2009) Identification of multiple potent binding sites for human leukocyte associated Ig-like receptor LAIR on collagens II and III. Matrix Biol 28:202–210. https://doi.org/10.1016/j.matbio.2009.03.005

Lebbink RJ, van den Berg MCW, de Ruiter T, et al (2008) The soluble leukocyte-associated Ig-like receptor (LAIR)-2 antagonizes the collagen/LAIR-1 inhibitory immune interaction. J Immunol 180:1662–1669

Leffler J, Herbert AP, Norström E, et al (2010) Annexin-II, DNA, and histones serve as factor H ligands on the surface of apoptotic cells. J Biol Chem 285:3766–3776. https://doi.org/10.1074/jbc.M109.045427

Leitinger B, Hohenester E (2007) Mammalian collagen receptors. Matrix Biol 26:146–155. https://doi.org/10.1016/j.matbio.2006.10.007

Lillis AP, Greenlee MC, Mikhailenko I, et al (2008) Murine low-density lipoprotein receptor-related protein 1 (LRP) is required for phagocytosis of targets bearing LRP ligands but is not required for C1q-triggered enhancement of phagocytosis. J Immunol 181:364–373. https://doi.org/10.4049/jimmunol.181.1.364

Ling GS, Crawford G, Buang N, et al (2018) C1q restrains autoimmunity and viral infection by regulating CD8+ T-cell metabolism. Science 360:558–563. https://doi.org/10.1126/science.aao4555

Liu T, Xiang A, Peng T, et al (2019) HMGB1-C1q complexes regulate macrophage function by switching between leukotriene and specialized proresolving mediator biosynthesis. Proc Natl Acad Sci USA 116:23254–23263. https://doi.org/10.1073/pnas.1907490116

Loos M, Euteneuer B, Clas F (1990) Interaction of bacterial endotoxin (LPS) with fluid phase and macrophage membrane associated C1Q. The FC-recognizing component of the complement system. Adv Exp Med Biol 256:301–317. https://doi.org/10.1007/978-1-4757-5140-6_26

Lu JH, Teh BK, Wang L da, et al (2008) The classical and regulatory functions of C1q in immunity and autoimmunity. Cell Mol Immunol 5:9–21. https://doi.org/10.1038/cmi.2008.2

Lubbers R, van Essen MF, van Kooten C, Trouw LA (2017) Production of complement components by cells of the immune system. Clin Exp Immunol 188:183–194. https://doi.org/10.1111/cei.12952

Ma W, Rai V, Hudson BI, et al (2012) RAGE binds C1q and enhances C1q-mediated phagocytosis. Cellular Immunology 274:72–82. https://doi.org/10.1016/j.cellimm.2012.02.001

Mangogna A, Agostinis C, Bonazza D, et al (2019) Is the Complement Protein C1q a Pro- or Anti-tumorigenic Factor? Bioinformatics Analysis Involving Human Carcinomas. Front Immunol 10:. https://doi.org/10.3389/fimmu.2019.00865

Marqués G, Antón LC, Barrio E, et al (1993) Arginine residues of the globular regions of human C1q involved in the interaction with immunoglobulin G. J Biol Chem 268:10393–10402

Martin M, Leffler J, Blom AM (2012) Annexin A2 and A5 serve as new ligands for C1q on apoptotic cells. J Biol Chem 287:33733–33744. https://doi.org/10.1074/jbc.M112.341339

Masaki T, Matsumoto M, Nakanishi I, et al (1992) Factor I-dependent inactivation of human complement C4b of the classical pathway by C3b/C4b receptor (CR1, CD35) and membrane cofactor protein (MCP, CD46). J Biochem 111:573–578. https://doi.org/10.1093/oxfordjournals.jbchem.a123799

Merle NS, Church SE, Fremeaux-Bacchi V, Roumenina LT (2015a) Complement System Part I – Molecular Mechanisms of Activation and Regulation. Front Immunol 6:. https://doi.org/10.3389/fimmu.2015.00262

Merle NS, Noe R, Halbwachs-Mecarelli L, et al (2015b) Complement System Part II: Role in Immunity. Front Immunol 6:. https://doi.org/10.3389/fimmu.2015.00257

Mevorach D, Mascarenhas JO, Gershov D, Elkon KB (1998) Complement-dependent clearance of apoptotic cells by human macrophages. J Exp Med 188:2313–2320. https://doi.org/10.1084/jem.188.12.2313

Meyaard L, Adema GJ, Chang C, et al (1997) LAIR-1, a novel inhibitory receptor expressed on human mononuclear leukocytes. Immunity 7:283–290

Meyaard L, Hurenkamp J, Clevers H, et al (1999) Leukocyte-associated Ig-like receptor-1 functions as an inhibitory receptor on cytotoxic T cells. J Immunol 162:5800–5804

Moreau C, Bally I, Chouquet A, et al (2016) Structural and Functional Characterization of a Single-Chain Form of the Recognition Domain of Complement Protein C1q. Front Immunol 7:79. https://doi.org/10.3389/fimmu.2016.00079

Myllyharju J, Kivirikko KI (2004) Collagens, modifying enzymes and their mutations in humans, flies and worms. Trends in Genetics 20:33–43. https://doi.org/10.1016/j.tig.2003.11.004

Nauta AJ, Bottazzi B, Mantovani A, et al (2003) Biochemical and functional characterization of the interaction between pentraxin 3 and C1q. Eur J Immunol 33:465–473. https://doi.org/10.1002/immu.200310022

Nauta AJ, Castellano G, Xu W, et al (2004) Opsonization with C1q and Mannose-Binding Lectin Targets Apoptotic Cells to Dendritic Cells. The Journal of Immunology 173:3044–3050. https://doi.org/10.4049/jimmunol.173.5.3044

Navratil JS, Watkins SC, Wisnieski JJ, Ahearn JM (2001) The globular heads of C1q specifically recognize surface blebs of apoptotic vascular endothelial cells. J Immunol 166:3231–3239. https://doi.org/10.4049/jimmunol.166.5.3231

Nayak A, Pednekar L, Reid KB, Kishore U (2012) Complement and non-complement activating functions of C1q: A prototypical innate immune molecule. Innate Immun 18:350–363. https://doi.org/10.1177/1753425910396252

Nemerow GR, Yamamoto KI, Lint TF (1979) Restriction of complement-mediated membrane damage by the eighth component of complement: a dual role for C8 in the complement attack sequence. J Immunol 123:1245–1252

Niewold TB, Clark DN, Salloum R, Poole BD (2010) Interferon Alpha in Systemic Lupus Erythematosus. J Biomed Biotechnol 2010:. https://doi.org/10.1155/2010/948364

Nordkamp MJMO, Roon JAG van, Douwes M, et al (2011) Enhanced secretion of leukocyte-associated immunoglobulin-like receptor 2 (LAIR-2) and soluble LAIR-1 in rheumatoid arthritis: LAIR-2 is a more efficient antagonist of the LAIR-1–collagen inhibitory interaction than is soluble LAIR-1. Arthritis & Rheumatism 63:3749–3757. https://doi.org/10.1002/art.30612

Ogden CA, deCathelineau A, Hoffmann PR, et al (2001) C1q and Mannose Binding Lectin Engagement of Cell Surface Calreticulin and Cd91 Initiates Macropinocytosis and Uptake of Apoptotic Cells. J Exp Med 194:781–796

Olde Nordkamp MJM, Boross P, Yildiz C, et al (2014a) Inhibition of the classical and lectin pathway of the complement system by recombinant LAIR-2. J Innate Immun 6:284–292. https://doi.org/10.1159/000354976

Olde Nordkamp MJM, van Eijk M, Urbanus RT, et al (2014b) Leukocyte-associated Ig-like receptor-1 is a novel inhibitory receptor for surfactant protein D. J Leukoc Biol 96:105–111. https://doi.org/10.1189/jlb.3AB0213-092RR

Ouyang W, Xue J, Liu J, et al (2004) Establishment of an ELISA system for determining soluble LAIR-1 levels in sera of patients with HFRS and kidney transplant. J Immunol Methods 292:109–117. https://doi.org/10.1016/j.jim.2004.06.005

Païdassi H, Tacnet-Delorme P, Garlatti V, et al (2008) C1q Binds Phosphatidylserine and Likely Acts as a Multiligand-Bridging Molecule in Apoptotic Cell Recognition. J Immunol 180:2329–2338

Païdassi H, Tacnet-Delorme P, Verneret M, et al (2011) Investigations on the C1q–Calreticulin–Phosphatidylserine Interactions Yield New Insights into Apoptotic Cell Recognition. Journal of Molecular Biology 408:277–290. https://doi.org/10.1016/j.jmb.2011.02.029

Pangburn MK, Rawal N (2002) Structure and function of complement C5 convertase enzymes. Biochemical Society Transactions 30:1006–1010. https://doi.org/10.1042/bst0301006

Patten DA (2018) SCARF1: a multifaceted, yet largely understudied, scavenger receptor. Inflamm Res 67:627–632. https://doi.org/10.1007/s00011-018-1154-7

Pednekar L, Pandit H, Paudyal B, et al (2016) Complement Protein C1q Interacts with DC-SIGN via Its Globular Domain and Thus May Interfere with HIV-1 Transmission. Front Immunol 7:600. https://doi.org/10.3389/fimmu.2016.00600

Peng Q, Li K, Sacks SH, Zhou W (2009) The role of anaphylatoxins C3a and C5a in regulating innate and adaptive immune responses. Inflammation & Allergy Drug Targets 8:236–246. https://doi.org/10.2174/187152809788681038

Pflieger D, Przybylski C, Gonnet F, et al (2010) Analysis of Human C1q by Combined Bottom-up and Top-down Mass Spectrometry. Mol Cell Proteomics 9:593–610. https://doi.org/10.1074/mcp.M900350-MCP200

Pieper K, Tan J, Piccoli L, et al (2017) Public antibodies to malaria antigens generated by two LAIR1 insertion modalities. Nature 548:597–601. https://doi.org/10.1038/nature23670

Pieterse E, van der Vlag J (2014) Breaking Immunological Tolerance in Systemic Lupus Erythematosus. Front Immunol 5:. https://doi.org/10.3389/fimmu.2014.00164

Podack ER (1984) Molecular composition of the tubular structure of the membrane attack complex of complement. The Journal of Biological Chemistry 259:8641–8647

Poggi A, Catellani S, Bruzzone A, et al (2008) Lack of the leukocyte-associated Ig-like receptor-1 expression in high-risk chronic lymphocytic leukaemia results in the absence of a negative signal regulating kinase activation and cell division. Leukemia 22:980–988. https://doi.org/10.1038/leu.2008.21

Poggi A, Pellegatta F, Leone BE, et al (2000) Engagement of the leukocyte-associated Ig-like receptor-1 induces programmed cell death and prevents NF-kappaB nuclear translocation in human myeloid leukemias. Eur J Immunol 30:2751–2758. https://doi.org/10.1002/1521-4141(200010)30:10<2751::AID-IMMU2751>3.0.CO;2-L

Preissner KP, Podack ER, Müller-Eberhard HJ (1989) SC5b-7, SC5b-8 and SC5b-9 complexes of complement: ultrastructure and localization of the S-protein (vitronectin) within the macromolecules. Eur J Immunol 19:69–75. https://doi.org/10.1002/eji.1830190112

Rahman A, Isenberg DA (2008) Systemic lupus erythematosus. N Engl J Med 358:929–939. https://doi.org/10.1056/NEJMra071297

Ramirez-Ortiz ZG, Pendergraft WF, Prasad A, et al (2013) The scavenger receptor SCARF1 mediates apoptotic cell clearance and prevents autoimmunity. Nat Immunol 14:917–926. https://doi.org/10.1038/ni.2670

Rawal N, Pangburn MK (2003) Formation of high affinity C5 convertase of the classical pathway of complement. The Journal of Biological Chemistry 278:38476–38483. https://doi.org/10.1074/jbc.M307017200

Reid KB (1979) Complete amino acid sequences of the three collagen-like regions present in subcomponent C1q of the first component of human complement. Biochem J 179:367–371

Reid KBM (1976) Isolation, by partial pepsin digestion, of the three collagen-like regions present in subcomponent Clq of the first component of human complement. Biochemical Journal 155:5–17. https://doi.org/10.1042/bj1550005

Reid KBM (2018) Complement Component C1q: Historical Perspective of a Functionally Versatile, and Structurally Unusual, Serum Protein. Front Immunol 9:. https://doi.org/10.3389/fimmu.2018.00764

Ricard-Blum S (2011) The Collagen Family. Cold Spring Harb Perspect Biol 3:. https://doi.org/10.1101/cshperspect.a004978

Ricklin D, Hajishengallis G, Yang K, Lambris JD (2010) Complement: a key system for immune surveillance and homeostasis. Nat Immunol 11:785–797. https://doi.org/10.1038/ni.1923

Rollins SA, Sims PJ (1990) The complement-inhibitory activity of CD59 resides in its capacity to block incorporation of C9 into membrane C5b-9. Journal of Immunology 144:3478–3483

Roumenina LT, Popov KT, Bureeva SV, et al (2008) Interaction of the globular domain of human C1q with Salmonella typhimurium lipopolysaccharide. Biochim Biophys Acta 1784:1271–1276. https://doi.org/10.1016/j.bbapap.2008.04.029

Roumenina LT, Sène D, Radanova M, et al (2011) Functional complement C1q abnormality leads to impaired immune complexes and apoptotic cell clearance. J Immunol 187:4369–4373. https://doi.org/10.4049/jimmunol.1101749

Rygiel TP, Stolte EH, de Ruiter T, et al (2011) Tumor-expressed collagens can modulate immune cell function through the inhibitory collagen receptor LAIR-1. Mol Immunol 49:402–406. https://doi.org/10.1016/j.molimm.2011.09.006

Saito F, Hirayasu K, Satoh T, et al (2017) Immune evasion of Plasmodium falciparum by RIFIN via inhibitory receptors. Nature. https://doi.org/10.1038/nature24994

Sathish JG, Johnson KG, Fuller KJ, et al (2001) Constitutive Association of SHP-1 with Leukocyte-Associated Ig-Like Receptor-1 in Human T Cells. The Journal of Immunology 166:1763–1770. https://doi.org/10.4049/jimmunol.166.3.1763

Saverino D, Fabbi M, Merlo A, et al (2002) Surface density expression of the leukocyte-associated Ig-like receptor-1 is directly related to inhibition of human T-cell functions. Hum Immunol 63:534–546. https://doi.org/10.1016/s0198-8859(02)00409-3

Schneidman-Duhovny D, Hammel M, Sali A (2010) FoXS: a web server for rapid computation and fitting of SAXS profiles. Nucleic Acids Research 38:W540–W544. https://doi.org/10.1093/nar/gkq461

Schraufstatter IU, Trieu K, Sikora L, et al (2002) Complement c3a and c5a induce different signal transduction cascades in endothelial cells. Journal of Immunology (Baltimore, Md: 1950) 169:2102–2110. https://doi.org/10.4049/jimmunol.169.4.2102

Schumaker VN, Zavodszky P, Poon PH (1987) Activation of the First Component of Complement. Annual Review of Immunology 5:21–42. https://doi.org/10.1146/annurev.iy.05.040187.000321

Sharp TH, Boyle AL, Diebolder CA, et al (2019) Insights into IgM-mediated complement activation based on in situ structures of IgM-C1-C4b. PNAS 116:11900–11905. https://doi.org/10.1073/pnas.1901841116

Shaw LM, Olsen BR (1991) FACIT collagens: diverse molecular bridges in extracellular matrices. Trends in Biochemical Sciences 16:191–194. https://doi.org/10.1016/0968-0004(91)90074-6

Siegel RC, Schumaker VN (1983) Measurement of the association constants of the complexes formed between intact C1q or pepsin-treated C1q stalks and the unactivated or activated C1r2C1s2 tetramers. Mol Immunol 20:53–66

Sim RB, Reboul A, Arlaud GJ, et al (1979) Interaction of 125I-labelled complement subcomponents Cr and Cs with protease inhibitors in plasma. FEBS Letters 97:111–115. https://doi.org/10.1016/0014-5793(79)80063-0

Smethurst PA, Joutsi-Korhonen L, O'Connor MN, et al (2004) Identification of the primary collagen-binding surface on human glycoprotein VI by site-directed mutagenesis and by a blocking phage antibody. Blood 103:903–911. https://doi.org/10.1182/blood-2003-01-0308

Smethurst PA, Onley DJ, Jarvis GE, et al (2007) Structural basis for the platelet-collagen interaction: the smallest motif within collagen that recognizes and activates platelet Glycoprotein VI contains two glycine-proline-hydroxyproline triplets. J Biol Chem 282:1296–1304. https://doi.org/10.1074/jbc.M606479200

Son M, Diamond B (2015) C1q-Mediated Repression of Human Monocytes Is Regulated by Leukocyte-Associated Ig-Like Receptor 1 (LAIR-1). Mol Med 20:559–568. https://doi.org/10.2119/molmed.2014.00185

Son M, Diamond B, Santiago-Schwarz F (2015) Fundamental role of C1q in autoimmunity and inflammation. Immunol Res 63:101–106. https://doi.org/10.1007/s12026-015-8705-6

Son M, Diamond B, Volpe BT, et al (2017) Evidence for C1q-mediated crosslinking of CD33/LAIR-1 inhibitory immunoreceptors and biological control of CD33/LAIR-1 expression. Scientific Reports 7:. https://doi.org/10.1038/s41598-017-00290-w

Son M, Porat A, He M, et al (2016) C1q and HMGB1 reciprocally regulate human macrophage polarization. Blood 128:2218–2228

Son M, Santiago-Schwarz F, Al-Abed Y, Diamond B (2012) C1q limits dendritic cell differentiation and activation by engaging LAIR-1. Proc Natl Acad Sci USA 109:E3160-3167. https://doi.org/10.1073/pnas.1212753109

Sorci G, Riuzzi F, Giambanco I, Donato R (2013) RAGE in tissue homeostasis, repair and regeneration. Biochimica et Biophysica Acta (BBA) - Molecular Cell Research 1833:101–109. https://doi.org/10.1016/j.bbamcr.2012.10.021

Sundaramoorthy M, Meiyappan M, Todd P, Hudson BG (2002) Crystal structure of NC1 domains. Structural basis for type IV collagen assembly in basement membranes. J Biol Chem 277:31142–31153. https://doi.org/10.1074/jbc.M201740200

Tacnet-Delorme P, Chevallier S, Arlaud GJ (2001) β-Amyloid Fibrils Activate the C1 Complex of Complement Under Physiological Conditions: Evidence for a Binding Site for Aβ on the C1q Globular Regions. The Journal of Immunology 167:6374–6381. https://doi.org/10.4049/jimmunol.167.11.6374

Takayanagi H, Oda H, Yamamoto S, et al (1997) A new mechanism of bone destruction in rheumatoid arthritis: synovial fibroblasts induce osteoclastogenesis. Biochem Biophys Res Commun 240:279–286. https://doi.org/10.1006/bbrc.1997.7404

Tan J, Pieper K, Piccoli L, et al (2016) A LAIR-1 insertion generates broadly reactive antibodies against malaria variant antigens. Nature 529:105–109. https://doi.org/10.1038/nature16450

Tang X, Narayanan S, Peruzzi G, et al (2009) A single residue, arginine 65, is critical for the functional interaction of leukocyte associated inhibitory receptor (LAIR)-1 with collagens. J Immunol 182:5446–5452. https://doi.org/10.4049/jimmunol.0804052

Tas SW, Klickstein LB, Barbashov SF, Nicholson-Weller A (1999) C1q and C4b bind simultaneously to CR1 and additively support erythrocyte adhesion. J Immunol 163:5056–5063

Tegla CA, Cudrici C, Patel S, et al (2011) Membrane attack by complement: the assembly and biology of terminal complement complexes. Immunologic Research 51:45–60. https://doi.org/10.1007/s12026-011-8239-5

Terrasse R, Tacnet-Delorme P, Moriscot C, et al (2012) Human and pneumococcal cell surface glyceraldehyde-3-phosphate dehydrogenase (GAPDH) proteins are both ligands of human C1q protein. J Biol Chem 287:42620–42633. https://doi.org/10.1074/jbc.M112.423731

Tettey R, Ayeh-Kumi P, Tettey P, et al (2015) Severity of malaria in relation to a complement receptor 1 polymorphism: a case–control study. Pathog Glob Health 109:247–252. https://doi.org/10.1179/2047773215Y.0000000011

Than ME, Henrich S, Huber R, et al (2002) The 1.9-A crystal structure of the noncollagenous (NC1) domain of human placenta collagen IV shows stabilization via a novel type of covalent Met-Lys cross-link. Proc Natl Acad Sci U S A 99:6607–6612. https://doi.org/10.1073/pnas.062183499

Thangudu RR, Vinayagam A, Pugalenthi G, et al (2005) Native and modeled disulfide bonds in proteins: knowledge-based approaches toward structure prediction of disulfide-rich polypeptides. Proteins 58:866–879. https://doi.org/10.1002/prot.20369

Thielens NM, Bally IM, Ebenbichler CF, et al (1993) Further characterization of the interaction between the C1q subcomponent of human C1 and the transmembrane envelope glycoprotein gp41 of HIV-1. J Immunol 151:6583–6592

Tissot B, Daniel R, Place C (2003) Interaction of the C1 complex of complement with sulfated polysaccharide and DNA probed by single molecule fluorescence microscopy. Eur J Biochem 270:4714–4720. https://doi.org/10.1046/j.1432-1033.2003.03870.x

Tomlinson MG, Calaminus SD, Berlanga O, et al (2007) Collagen promotes sustained glycoprotein VI signaling in platelets and cell lines. J Thromb Haemost 5:2274–2283. https://doi.org/10.1111/j.1538-7836.2007.02746.x

Tsai F, Perlman H, Cuda CM (2017) The contribution of the programmed cell death machinery in innate immune cells to lupus nephritis. Clin Immunol 185:74–85. https://doi.org/10.1016/j.clim.2016.10.007

Tschopp J, Chonn A, Hertig S, French LE (1993) Clusterin, the human apolipoprotein and complement inhibitor, binds to complement C7, C8 beta, and the b domain of C9. J Immunol 151:2159–2165

Ugurlar D, Howes SC, de Kreuk B-J, et al (2018) Structures of C1-IgG1 provide insights into how danger pattern recognition activates complement. Science 359:794–797

Uwatoko S, Aotsuka S, Okawa M, et al (1984) Characterization of C1q-binding IgG complexes in systemic lupus erythematosus. Clin Immunol Immunopathol 30:104–116. https://doi.org/10.1016/0090-1229(84)90011-4

Uwatoko S, Aotsuka S, Okawa M, et al (1987) C1q solid-phase radioimmunoassay: evidence for detection of antibody directed against the collagen-like region of C1q in sera from patients with systemic lupus erythematosus. Clin Exp Immunol 69:98–106

van den Berg RH, Faber-Krol MC, Sim RB, Daha MR (1998) The first subcomponent of complement, C1q, triggers the production of IL-8, IL-6, and monocyte chemoattractant peptide-1 by human umbilical vein endothelial cells. J Immunol 161:6924–6930

van der Vuurst de Vries AR, Clevers H, Logtenberg T, Meyaard L (1999) Leukocyte-associated immunoglobulin-like receptor-1 (LAIR-1) is differentially expressed during human B cell differentiation and inhibits B cell receptor-mediated signaling. Eur J Immunol 29:3160–3167. https://doi.org/10.1002/(SICI)1521-4141(199910)29:10<3160::AID-IMMU3160>3.0.CO;2-S

Vanacore RM, Shanmugasundararaj S, Friedman DB, et al (2004) The alpha1.alpha2 network of collagen IV. Reinforced stabilization of the noncollagenous domain-1 by noncovalent forces and the absence of Met-Lys cross-links. J Biol Chem 279:44723–44730. https://doi.org/10.1074/jbc.M406344200

Vandivier RW, Ogden CA, Fadok VA, et al (2002) Role of Surfactant Proteins A, D, and C1q in the Clearance of Apoptotic Cells In Vivo and In Vitro: Calreticulin and CD91 as a Common Collectin Receptor Complex. The Journal of Immunology 169:3978–3986. https://doi.org/10.4049/jimmunol.169.7.3978

Vegh Z, Kew RR, Gruber BL, Ghebrehiwet B (2006) Chemotaxis of human monocyte-derived dendritic cells to complement component C1q is mediated by the receptors gC1qR and cC1qR. Mol Immunol 43:1402–1407. https://doi.org/10.1016/j.molimm.2005.07.030

Venkatraman Girija U, Gingras AR, Marshall JE, et al (2013) Structural basis of the C1q/C1s interaction and its central role in assembly of the C1 complex of complement activation. Proc Natl Acad Sci USA 110:13916–13920. https://doi.org/10.1073/pnas.1311113110

Verbrugge A, de Ruiter T, Geest C, et al (2006) Differential expression of leukocyte-associated Ig-like receptor-1 during neutrophil differentiation and activation. J Leukoc Biol 79:828–836. https://doi.org/10.1189/jlb.0705370

Walker DG (1998) Expression and regulation of complement C1q by human THP-1-derived macrophages. Mol Chem Neuropathol 34:197–218. https://doi.org/10.1007/BF02815080

Walport MJ (2001a) Complement. First of two parts. The New England Journal of Medicine 344:1058–1066. https://doi.org/10.1056/NEJM200104053441406

Walport MJ (2001b) Complement. Second of two parts. The New England Journal of Medicine 344:1140–1144. https://doi.org/10.1056/NEJM200104123441506

Walport MJ, Davies KA, Botto M (1998) C1q and Systemic Lupus Erythematosus. Immunobiology 199:265–285. https://doi.org/10.1016/S0171-2985(98)80032-6

Wang L, Wu J, Guo X, et al (2017) RAGE Plays a Role in LPS-Induced NF-κB Activation and Endothelial Hyperpermeability. Sensors (Basel) 17:. https://doi.org/10.3390/s17040722

Wang Y, Zhang X, Miao F, et al (2016) Clinical significance of leukocyte-associated immunoglobulin-like receptor-1 expression in human cervical cancer. Exp Ther Med 12:3699–3705. https://doi.org/10.3892/etm.2016.3842

Wener MH, Uwatoko S, Mannik M (1989) Antibodies to the collagen-like region of C1q in sera of patients with autoimmune rheumatic diseases. Arthritis Rheum 32:544–551. https://doi.org/10.1002/anr.1780320506

Whaley K, Ruddy S (1976) Modulation of the alternative complement pathways by beta 1 H globulin. J Exp Med 144:1147–1163. https://doi.org/10.1084/jem.144.5.1147

Wicker-Planquart C, Dufour S, Tacnet-Delorme P, et al (2020) Molecular and Cellular Interactions of Scavenger Receptor SR-F1 With Complement C1q Provide Insights Into Its Role in the Clearance of Apoptotic Cells. Front Immunol 11:. https://doi.org/10.3389/fimmu.2020.00544

Wirz JA, Boudko SP, Lerch TF, et al (2011) Crystal structure of the human collagen XV trimerization domain: a potent trimerizing unit common to multiplexin collagens. Matrix Biol 30:9–15. https://doi.org/10.1016/j.matbio.2010.09.005

Wu J-J, Weis MA, Kim LS, Eyre DR (2010) Type III Collagen, a Fibril Network Modifier in Articular Cartilage. The Journal of Biological Chemistry 285:18537. https://doi.org/10.1074/jbc.M110.112904

Wu X, Zhang L, Zhou J, et al (2019) Clinicopathologic significance of LAIR-1 expression in hepatocellular carcinoma. Current Problems in Cancer 43:18–26. https://doi.org/10.1016/j.currproblcancer.2018.04.005

Xu M j, Zhao R, Zhao ZJ (2000) Identification and characterization of leukocyte-associated Ig-like receptor-1 as a major anchor protein of tyrosine phosphatase SHP-1 in hematopoietic cells. J Biol Chem 275:17440–17446. https://doi.org/10.1074/jbc.M001313200

Yamada M, Oritani K, Kaisho T, et al (2004) Complement C1q regulates LPS-induced cytokine production in bone marrow-derived dendritic cells. Eur J Immunol 34:221–230. https://doi.org/10.1002/eji.200324026

Young KR, Ambrus JL, Malbran A, et al (1991) Complement subcomponent C1q stimulates Ig production by human B lymphocytes. J Immunol 146:3356–3364

Ytterberg SR, Schnitzer TJ (1982) Serum interferon levels in patients with systemic lupus erythematosus. Arthritis Rheum 25:401–406. https://doi.org/10.1002/art.1780250407

Zhang J, Zhang Y, Cheng S, et al (2020) LAIR-1 overexpression inhibits epithelial–mesenchymal transition in osteosarcoma via GLUT1-related energy metabolism. World J Surg Oncol 18:. https://doi.org/10.1186/s12957-020-01896-7

Zhang Y, Ding Y, Huang Y, et al (2013) Expression of leukocyte-associated immunoglobulin-like receptor-1 (LAIR-1) on osteoclasts and its potential role in rheumatoid arthritis. Clinics (Sao Paulo) 68:475–481. https://doi.org/10.6061/clinics/2013(04)07

Zhang Y, Lv K, Zhang CM, et al (2014) The role of LAIR-1 (CD305) in T cells and monocytes/macrophages in patients with rheumatoid arthritis. Cell Immunol 287:46–52. https://doi.org/10.1016/j.cellimm.2013.12.005

Zhang Y, Wang S, Dong H, et al (2018) LAIR-1 shedding from human fibroblast-like synoviocytes in rheumatoid arthritis following TNF-α stimulation. Clin Exp Immunol 192:193–205. https://doi.org/10.1111/cei.13100

Zhou Z, Xu M-J, Gao B (2016) Hepatocytes: a key cell type for innate immunity. Cellular & Molecular Immunology 13:301–315. https://doi.org/10.1038/cmi.2015.97

Zipfel PF, Skerka C (2009) Complement regulators and inhibitory proteins. Nat Rev Immunol 9:729–740. https://doi.org/10.1038/nri2620

Zocchi MR, Pellegatta F, Pierri I, et al (2001) Leukocyte-associated Ig-like receptor-1 prevents granulocyte-monocyte colony stimulating factor-dependent proliferation and Akt1/PKB alpha activation in primary acute myeloid leukemia cells. Eur J Immunol 31:3667–3675. https://doi.org/10.1002/1521-4141(200112)31:12<3667::aid-immu3667>3.0.co;2-g

Zutter MM, Edelson BT (2007) The α2β1 integrin: A novel collectin/C1q receptor. Immunobiology 212:343–353. https://doi.org/10.1016/j.imbio.2006.11.013

Résumé

La molécule C1q a longtemps été étudiée pour son rôle majeur dans l'activation de la voie classique du complément. C1q peut reconnaître de nombreux motifs à la surface des pathogènes ou du soi altéré, via ses six régions globulaires C-terminales (GR). L'autre partie de la protéine, les régions collagéniques (CLR) de C1q, sont généralement associées au tétramère de protéases C1r et C1s ($C1r_2s_2$), responsable de l'initiation de la cascade du complément. Ces dernières années, des interactions de C1q avec de nombreux récepteurs membranaires ont été mises en évidence. Parmi ces fonctions indépendantes du complément, un rôle de modulation de la réponse immune par C1q est médié par son interaction avec des récepteurs à domaines de type immunoglobuline (Ig-like) : RAGE (receptor for advanced glycation end-products), CD33, LAIR-1 (leukocyte-associated Ig-like receptor 1) et LAIR-2. Ces récepteurs ont des activités opposées sur les signaux inflammatoires : RAGE induit des signaux pro-inflammatoires alors que CD33 et LAIR-1 sont des récepteurs anti-inflammatoires. Les signaux induits par l'interaction de C1q dépendent donc des récepteurs mis en jeu. Des études récentes suggèrent que RAGE et CD33 interagissent avec les GR alors que LAIR-1 reconnaît les CLR de C1q, ce qui génère un réseau d'interactions complexe qui module la réponse immune en regroupant des signaux pro- et anti-inflammatoires. Cette thèse a pour but d'élucider les détails moléculaires de l'interaction de C1q avec ces récepteurs afin d'aider à la compréhension de la modulation de la réponse immune par C1q. Nous nous sommes principalement intéressés à l'interaction de C1q avec LAIR-1. Une stratégie de dissection moléculaire de C1q, couplée à des expériences de compétition ainsi que l'utilisation de variants de C1q nous ont permis de localiser le site d'interaction de LAIR-1 proche mais différent de celui de $C1r_2s_2$ sur les CLR de C1q. Du côté de LAIR-1, une analyse par mutagénèse dirigée nous a permis d'identifier les acides aminés impliqués dans l'interaction avec C1q. Ces résultats suggèrent un modèle d'interaction de C1q avec le domaine Ig-like de LAIR-1. De plus, l'interaction spécifique de LAIR-1 avec les CLR de C1q nous a incité à développer la première production recombinante de cette région de C1q (CLR_nc2). Le remplacement des GR de C1q par le deuxième domaine non collagénique du collagène IX nous a permis de contrôler la mise en registre spécifique des chaînes collagéniques de C1q. La protéine CLR_nc2 a constitué un outil important dans le cadre de cette thèse et le sera certainement également pour l'étude future de l'interaction de C1q avec ses nombreux récepteurs.

Abstract

C1q has long been studied and described for its central role in the activation of the complement classical pathway. This C1q molecule is able to recognize and interact with a large number of molecular patterns on pathogens or altered-self surfaces through its six C-terminal globular regions (GR). On the other side of the protein, the collagen-like regions (CLR) of C1q are generally associated with the soluble tetramer of C1r and C1s proteases ($C1r_2s_2$) that is responsible for the initiation of the complement cascade. Over the last years, several complement-independent functions were shown to be held by C1q through its interaction with various membrane receptors present on cell surfaces. Among these functions, the immune modulation properties of C1q have been recently described and were shown to engage immune receptors from the immunoglobulin-like (Ig-like) family: receptor for advanced glycation end-products (RAGE), CD33, leukocyte-associated Ig-like receptor 1 (LAIR-1) and LAIR-2. These receptors have opposite activities towards inflammation: RAGE triggers pro-inflammatory pathways whereas LAIR-1 and CD33 are immune inhibitory receptors. The C1q-mediated signaling differs whether C1q interacts with one or several of these receptors simultaneously. Recent studies suggest that RAGE and CD33 interact with C1q GR while LAIR-1 binds the C1q CLR, leading to a complex interaction network that congregates pro and anti-inflammatory signals, thus modulating the immune response. This PhD thesis aims at deciphering the fine details of C1q interaction with these receptors in order to provide fundamental insights into the C1q-mediated immune modulation. We mainly focused on the interaction of C1q with the collagen receptor LAIR-1. Thanks to the molecular dissection of C1q associated with competition assays and use of recombinant C1q variants, we showed that LAIR-1 binding site is located in close proximity to but is different from the one of $C1r_2s_2$ on C1q CLR. On the LAIR-1 side, we performed a mutational analysis based on literature and structural data to identify the key residues involved in C1q binding. These results led us to propose a model of C1q CLR interaction with the Ig-like domain of LAIR-1. Moreover, the specific recognition of C1q CLR by LAIR-1 led us to develop and generate the first recombinant production of C1q CLR (CLR_nc2). The replacement of the C1q GR by the second non-collagenous domain of collagen IX allowed the preservation of the specific C1q collagen chains registering. The CLR_nc2 was an important tool in the context of this PhD thesis and it will certainly also be useful for the future studies on C1q interaction with its many receptors.